Nanomaterials for Biodiagnostic

- Nucleic Acid
  - Genetic information for identification
  - Diseases, bacterium, virus, pathogen
  - PCR with molecular fluorophore, State of the Art
  - Expansive, Non-portable, Non-multiplexing
- Proteins
  - Cancers and diseases, unusual high concentration of marker
  - ELISA (~pM) with molecular fluorophore
  - No PCR version

Colorimetric Detection of DNA

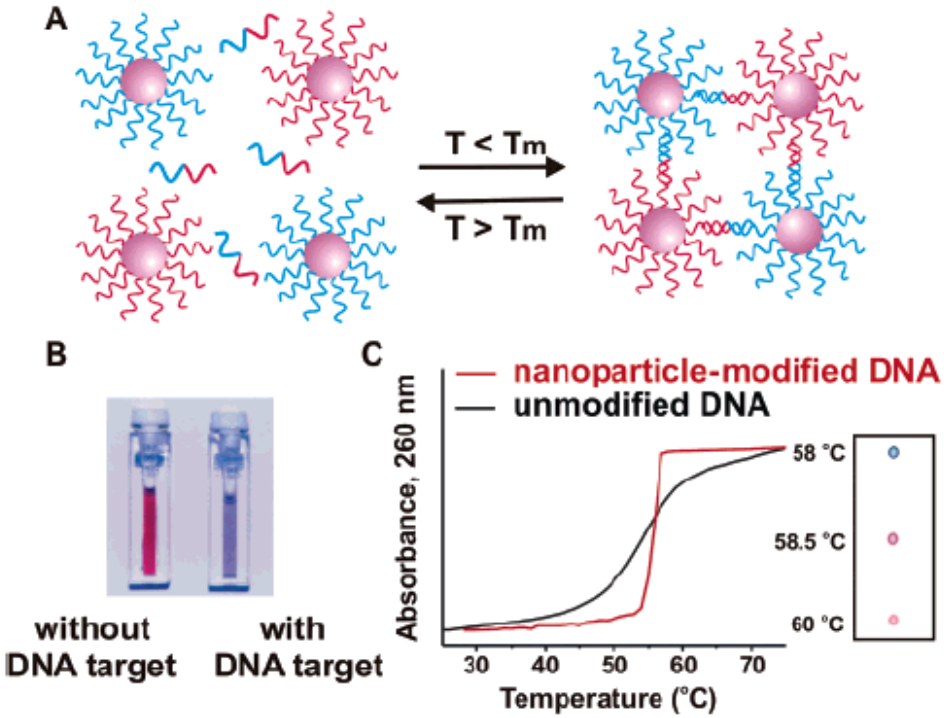

Figure 2. In the presence of complementary target DNA, oligonucleotide-functionalized gold nanoparticles will aggregate (A), resulting in a change of solution color from red to blue (B). The aggregation process can be monitored using UV−vis spectroscopy or simply by spotting the solution on a silica support (C). (Reprinted with permission from *Science* (http://www.aaas.org), ref 29. Copyright 1997 American Association for the Advancement of Science.)

A DNA-based method for rationally assembling nanoparticles into macroscopic materials

Chad A. Mirkin, Robert L. Letsinger, Robert C. Mucic & James J. Storhoff

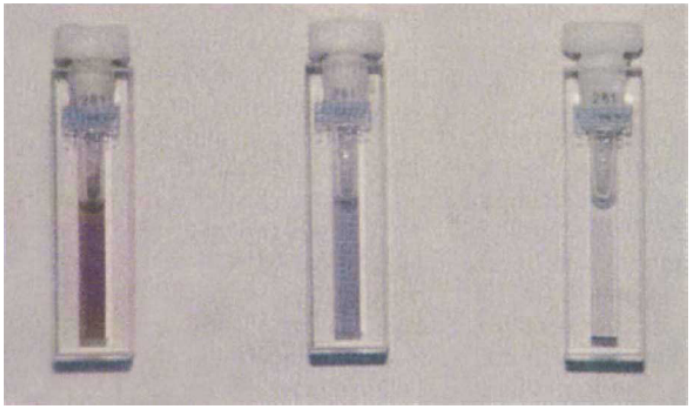

FIG. 2 Cuvettes with the Au colloids and the four DNA strands responsible for the assembly process. Left cuvette, at 80 °C with DNA-modified colloids in the unhybridized state; centre, after cooling to room temperature but before the precipitate settles; and right, after the polymeric precipitate settles to the bottom of the cuvette. Heating either of these cool solutions results in the reformation of the DNA-modified colloids in the unhybridized state (shown in the left cuvette).

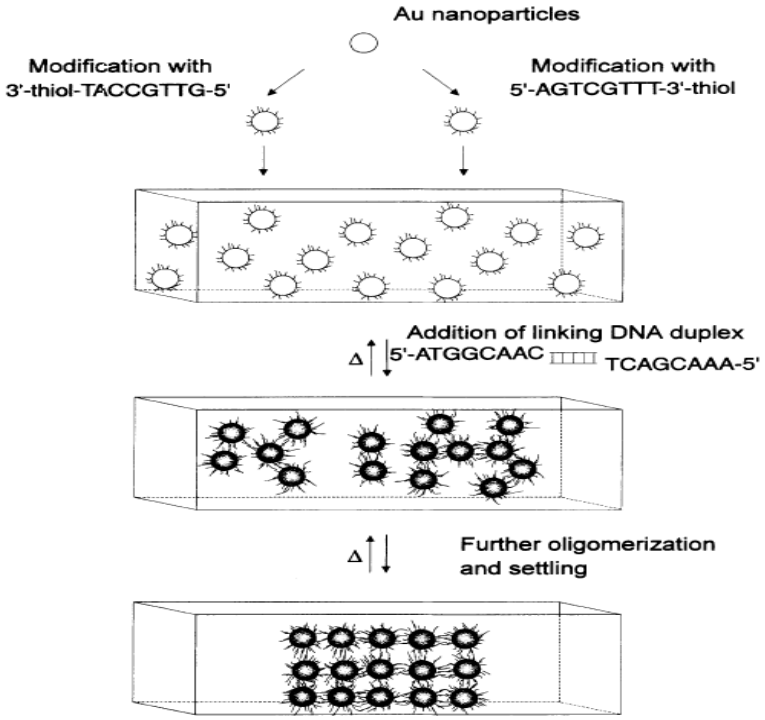

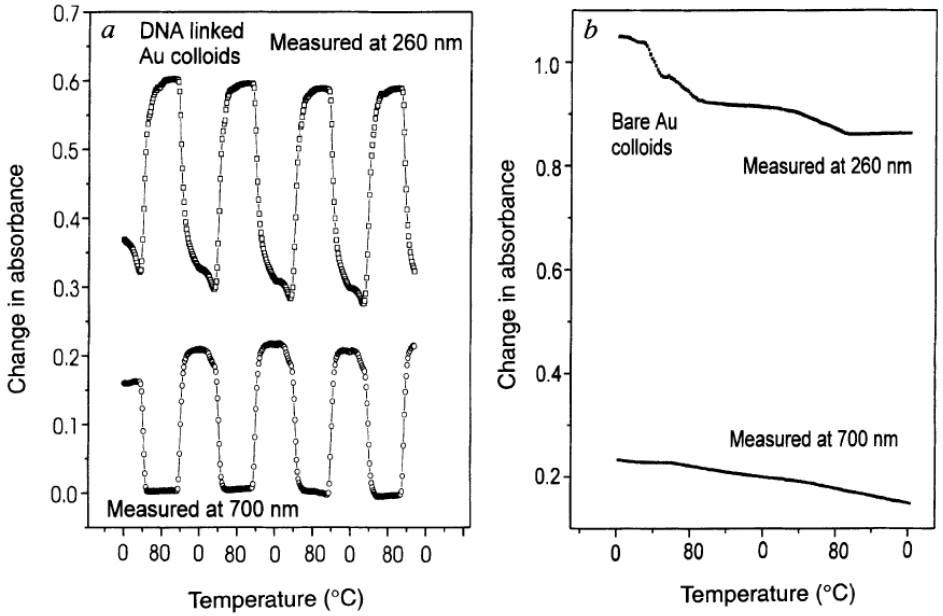

Nature, 1996, 382, 607

Selective Colorimetric Detection of Polynucleotides Based on the Distance-Dependent Optical Properties of Gold Nanoparticles

Robert Elghanian, James J. Storhoff, Robert C. Mucic,
Robert L. Letsinger,* Chad A. Mirkin*

SCIENCE • VOL. 277 • 22 AUGUST 1997

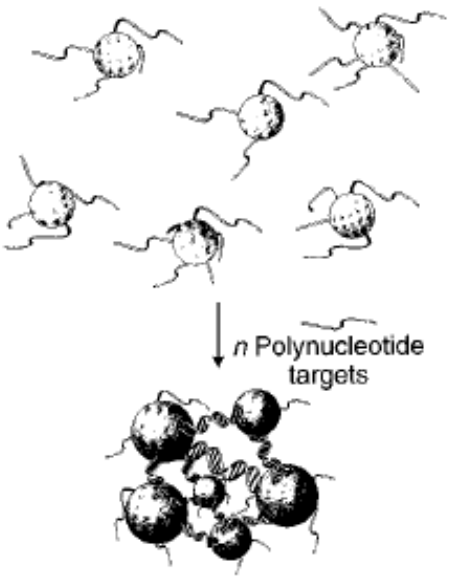

Fig. 1. Schematic representation of the concept for generating aggregates signaling hybridization of nanoparticle-oligonucleotide conjugates with oligonucleotide target molecules. The nanoparticles and the oligonucleotide interconnects are not drawn to scale, and the number of oligomers per particle is believed to be much larger than depicted.

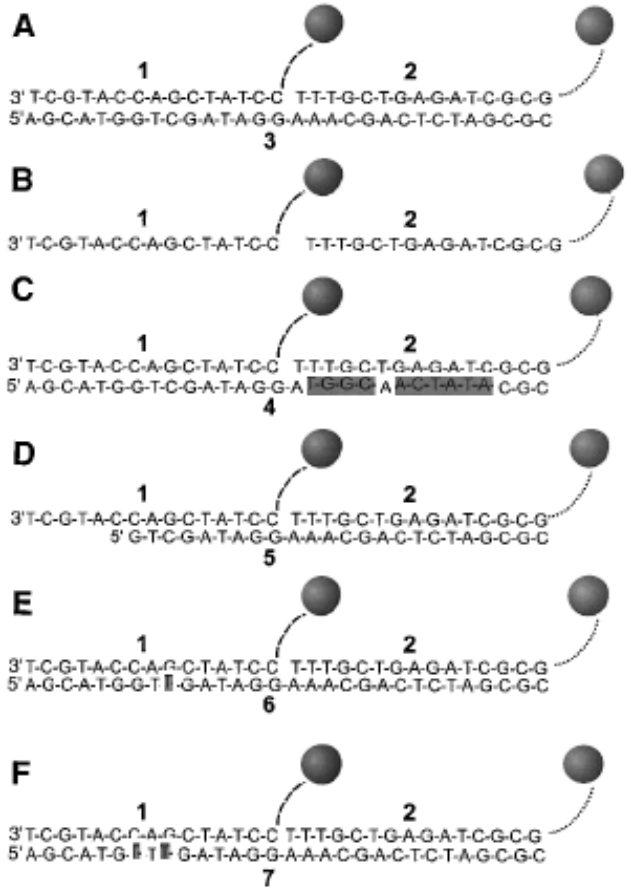

Fig. 2. Mercaptoalkyloligonucleotide-modified 13-nm Au particles and polynucleotide targets used for examining the selectivity of the nanoparticle-based colorimetric polynucleotide detection system. (**A**) Complementary target; (**B**) probes without the target; (**C**) a half-complementary target; (**D**) a 6-bp deletion; (**E**) a 1-bp mismatch; and (**F**) a 2-bp mismatch. For the sake of clarity, only two particles are shown; in reality a polymeric aggregate with many particles is formed. Dashed lines represent flexible spacer portions of the mercaptoalkyloligonucleotide strands bound to the nanoparticles; note that these spacers, because of their noncomplementary nature, do not participate in hybridization. The full sequences for the two probes, **1** and **2**, which bind to targets **3** through **7**, are

1-5′SH-$(CH_2)_6$- [CTA-ATC-CGC-ACA-G]
spacer

[CC-TAT-CGA-CCA-TGC-T]
probe

2-5′SH-$(CH_2)_6$-[ATG-GCA-ACT-ATA-C]
spacer

[GC-GCT-AGA-GTC-GTT-T]
probe

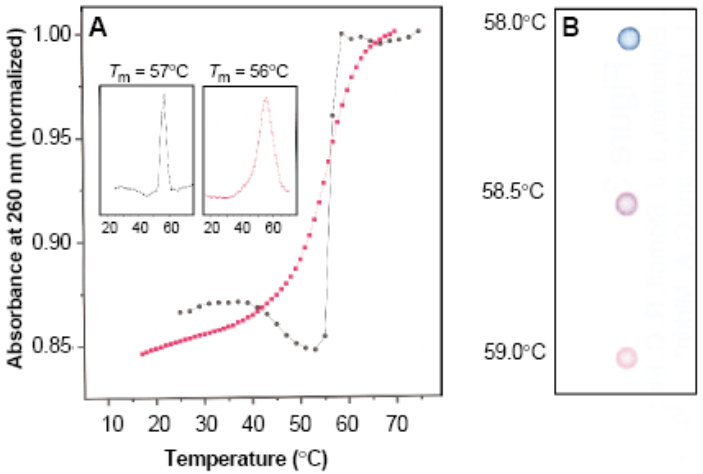

Fig. 3. (**A**) Comparison of the thermal dissociation curves for complexes of mercaptoalkyloligonucleotide-modified Au nanoparticles (black circles) and mercaptoalkyloligonucleotides without Au nanoparticles (red squares) with the complementary target, **3**, in hybridization buffer (0.1 M NaCl, 10 mM phosphate buffer, pH 7.0). For the first set (black circles), a mixture of 150 μl of each colloid conjugate and 3 μl of the target oligonucleotide in hybridization buffer (0.1 M NaCl, 10 mM phosphate, pH 7.0) was frozen at the temperature of dry ice, kept for 5 min, thawed over a period of 15 min, and diluted to 1.0 ml with buffer (final target concentration, 0.02 μM). The absorbance was measured at 1-min intervals with a temperature increase of 1°C per minute. The increase in absorption at 260 nm (A_{260}) was ~0.3 absorption units (AU). In the absence of the oligonucleotide targets, the absorbance of the nanoparticles did not increase with increasing temperature. For the second set, the mercaptoalkyloligonucleotides and complementary target (each 0.33 μM) were equilibrated at room temperature in 1 ml of buffer, and the changes in absorbance with temperature were monitored as before. The increase in A_{260} was 0.08 AU. (**Insets**) Derivative curves for each set (*15*). (**B**) Spot test showing T_c (thermal transition associated with the color change) for the Au nanoparticle probes hybridized with complementary target. A solution prepared from 150 μl of each probe and 3 μl of the target (0.06 μM final target concentration) was frozen for 5 min, allowed to thaw for 10 min, transferred to a 1-ml cuvette, and warmed at 58°C for 5 min in the thermally regulated cuvette chamber of the spectrophotometer. Samples (3 μl) were transferred to a C_{18} reverse phase plate with an Eppendorf pipette as the temperature of the solution was increased incrementally 0.5°C at 5-min intervals.

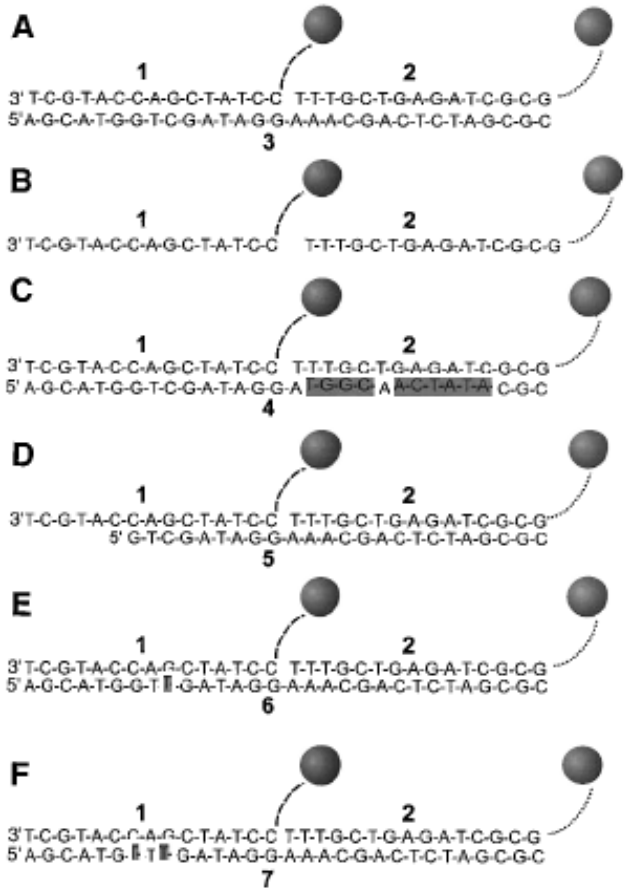

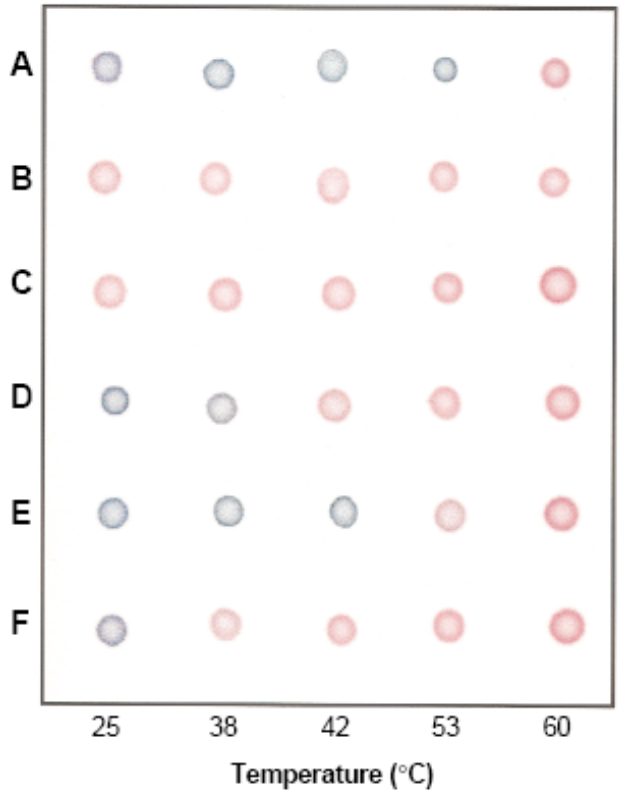

Fig. 4. Selective polynucleotide detection for the target probes shown in Fig. 2: (**A**) complementary target; (**B**) no target; (**C**) complementary to one probe; (**D**) a 6-bp deletion; (**E**) a 1-bp mismatch; and (**F**) a 2-bp mismatch. Nanoparticle aggregates were prepared in a 600-μl thin-walled Eppendorf tube by addition of 1 μl of a 6.6 μM oligonucleotide target to a mixture containing 50 μl of each probe (0.06 μM final target concentration). The mixture was frozen (5 min) in a bath of dry ice and isopropyl alcohol and allowed to warm to room temperature. Samples were then transferred to a temperature-controlled water bath, and 3-μl aliquots were removed at the indicated temperatures and spotted on a C_{18} reverse phase plate.

J. Am. Chem. Soc. **2000,** *122,* 9071−9077

Colloidal Au-Enhanced Surface Plasmon Resonance for Ultrasensitive Detection of DNA Hybridization

Lin He, Michael D. Musick, Sheila R. Nicewarner, Frank G. Salinas, Stephen J. Benkovic, Michael J. Natan, and Christine D. Keating*

Scheme 1. SPR Surface Assembly

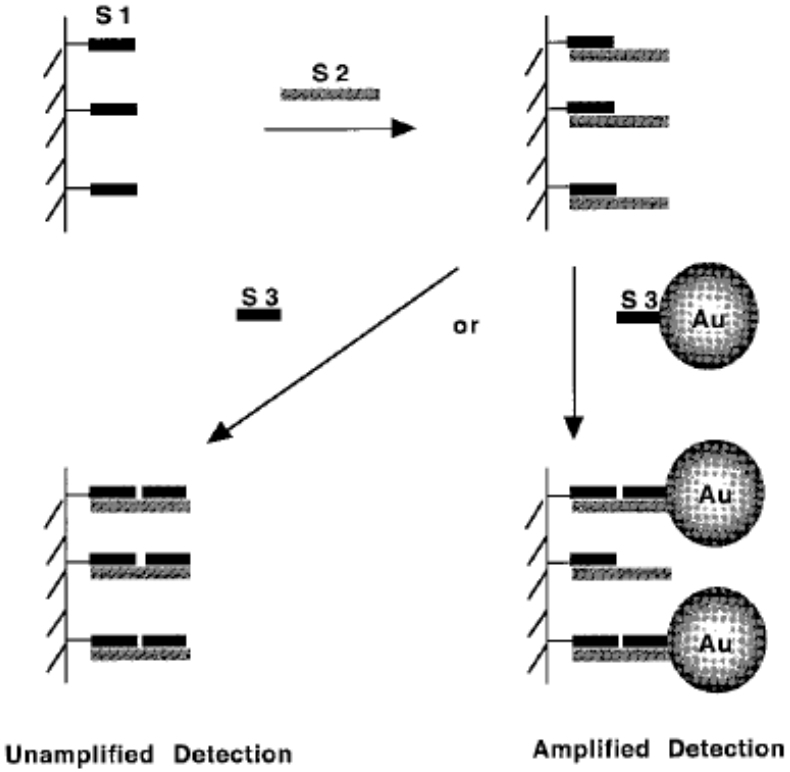

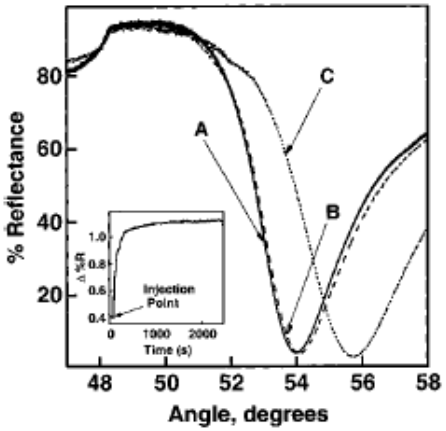

Figure 1. SPR curves of surfaces prepared in sequential steps as illustrated in Scheme 1: a MHA-coated Au film modified with a 12-mer oligonucleotide S1(A), after hybridization with its complementary 24-mer target S2 (B), and followed by introduction of S3:Au conjugate (C) to the surface. Inset: surface plasmon reflectance changes at 53.2° for the oligonucleotide-coated Au film measured during a 60-min exposure to S3:Au conjugates.

Scheme 2. SPR Surface Assembly in the Digestion Experiment

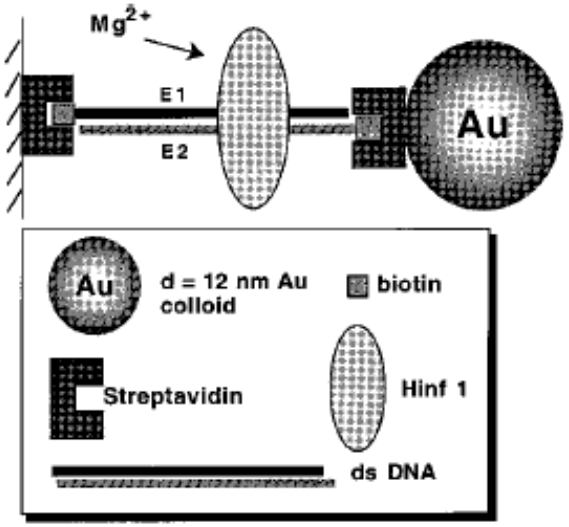

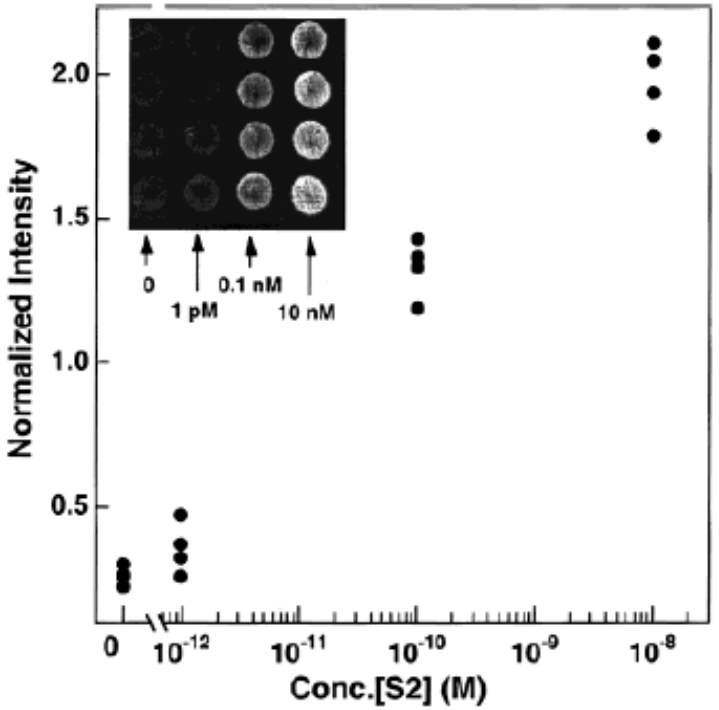

Figure 5. Plot of normalized intensity of SPR reflectance as a function of logarithmic concentration of the analyte 24-mer oligo (S2). Each spot represents one data point at the corresponding concentration. CCD parameters: exposure time = 0.3 s, 16 bit resolution, spot size = 4.5 mm in diameter. Inset: a 2-D SPR image of a Au surface derivatized with 20 μL of buffer blank, 1 pM, 0.1 nM, and 10 nM S2 oligos (from left to right, respectively).

Self-Assembled Nanoparticle Probes for Recognition and Detection of Biomolecules

Dustin J. Maxwell, Jason R. Taylor, and Shuming Nie*,†

9606 ■ J. AM. CHEM. SOC. 2002, *124*, 9606−9612

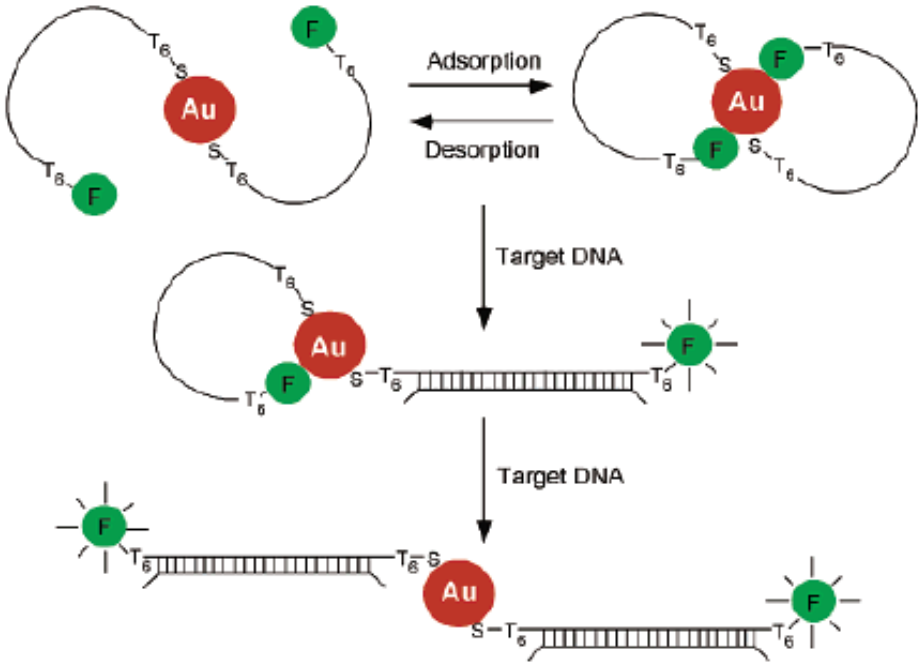

Figure 1. Nanoparticle-based probes and their operating principles. Two oligonucleotide molecules (oligos) are shown to self-assemble into a constrained conformation on each gold particle (2.5 nm diameter). A T_6 spacer (six thymines) is inserted at both the 3′- and 5′-ends to reduce steric hindrance. Single-stranded DNA is represented by a single line and double-stranded DNA by a cross-linked double line. In the assembled (closed) state, the fluorophore is quenched by the nanoparticle. Upon target binding, the constrained conformation opens, the fluorophore leaves the surface because of the structural rigidity of the hybridized DNA (double-stranded), and fluorescence is restored. In the open state, the fluorophore is separated from the particle surface by about 10 nm. See text for detailed explanation. Au, gold particle; F, fluorophore; S, sulfur atom.

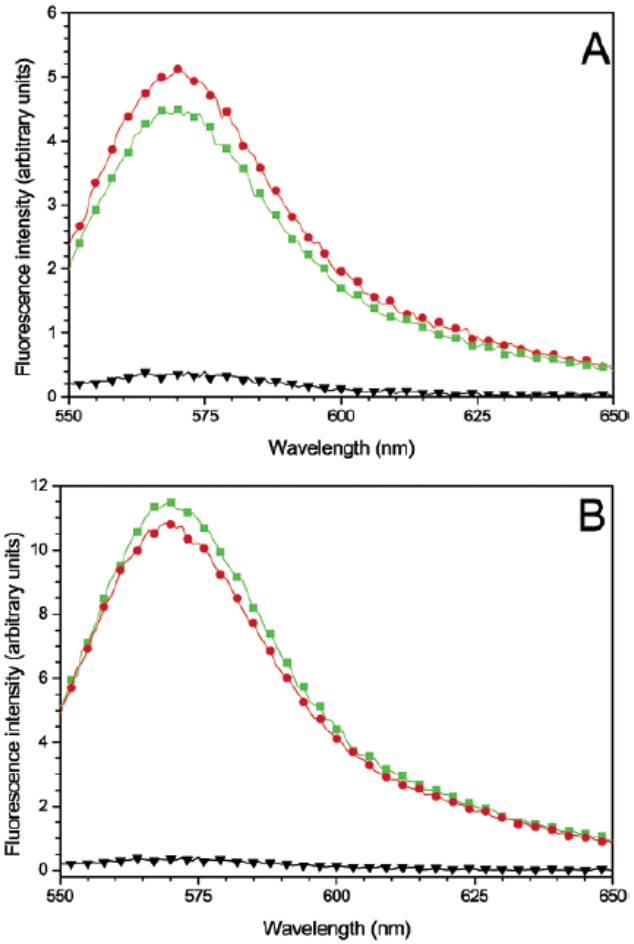

Figure 5. Fluorescence responses and the lack of sequence recognition abilities observed for nonthiolated nanoparticle probes. (A) Fluorescence spectra of nonthiolated probes generated by a complementary target (red curve), a noncomplementary target (green curve), and no target (black curve). These probes are considered nonfunctional because they do not recognize specific DNA sequences. (B) Fluorescence signals obtained from the supernatant solution when the probes were treated with a complementary target (red curve) or a noncomplementary target (green curve). The result revealed that the oligos were released into solution by nonspecific adsorption of the target on the particle surface. With a thiol group, this release was not observed (little or no signal in solution, black curve in B). The nonfunctional probes were prepared in the same way as the functional probes, except that the 3′-end thiol group was deleted. The intensity differences for the red and green curves were within experimental errors and had no particular significance.

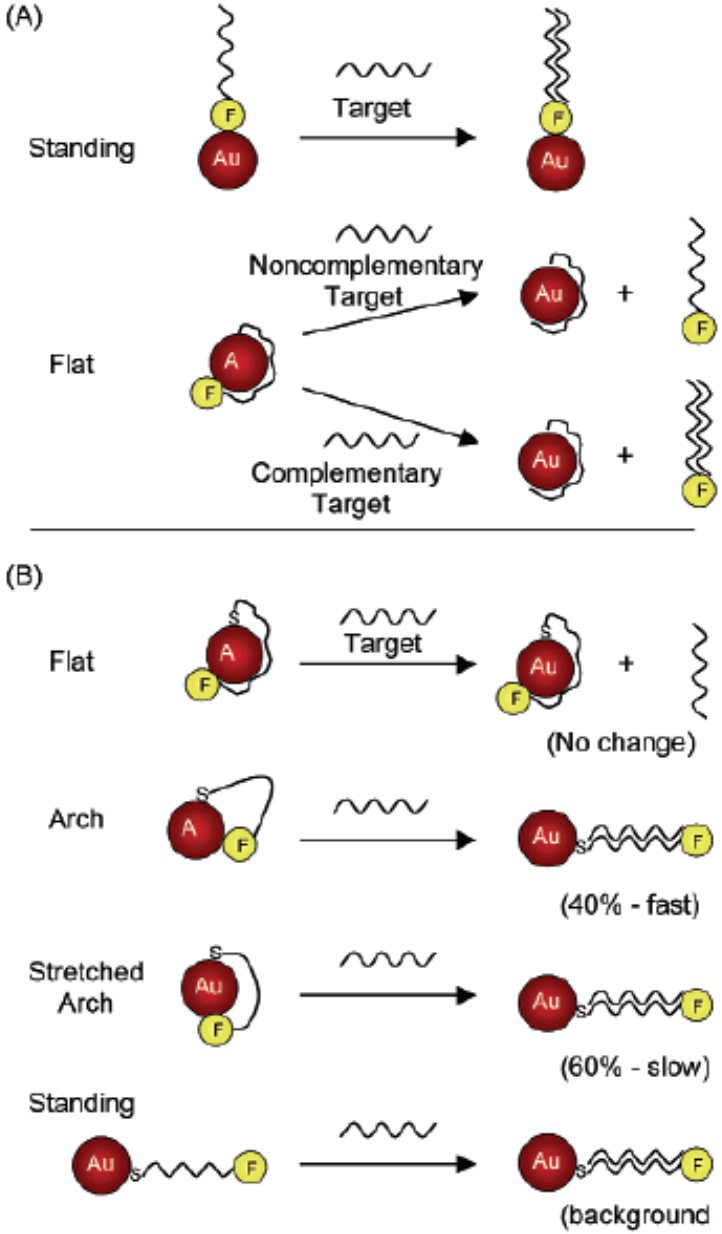

Figure 6. Schematic illustration of possible configurations for (a) nonthiolated and (b) thiolated oligonucleotides adsorbed on colloidal gold nanocrystals. Detailed discussion in text.

Scanometric DNA Array Detection with Nanoparticle Probes

SCIENCE VOL 289 8 SEPTEMBER 2000

T. Andrew Taton,[1,2] Chad A. Mirkin,[1,2]* Robert L. Letsinger[1]*

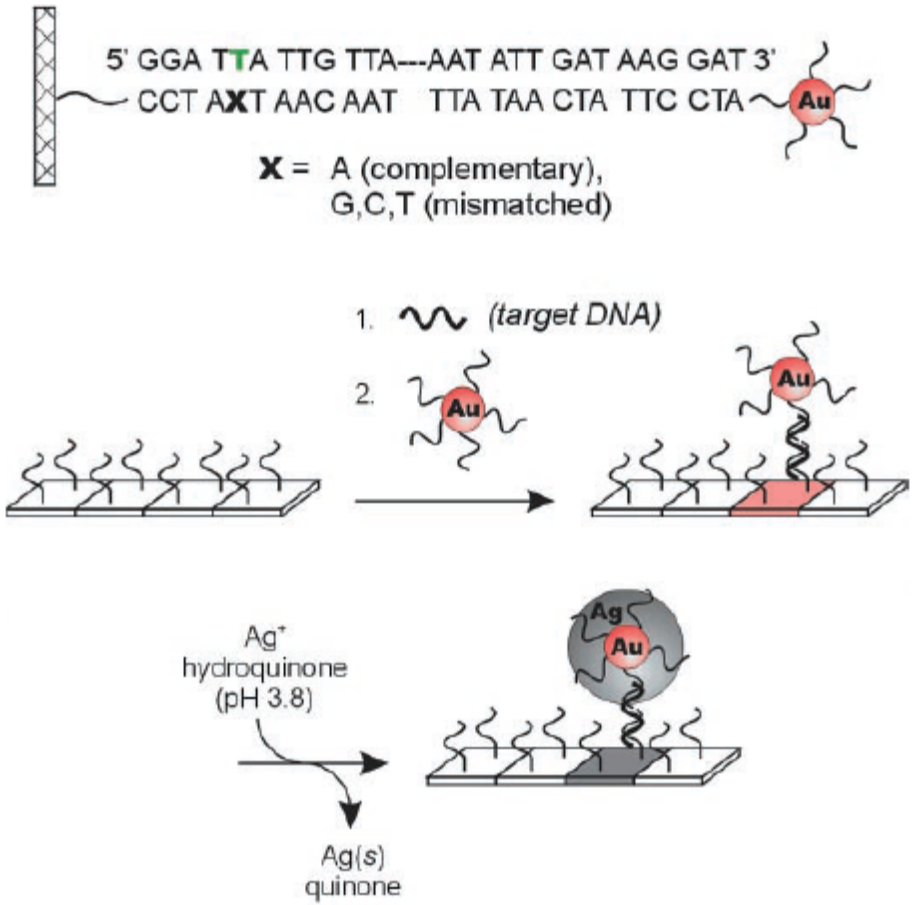

50 fM => 0.2 fM

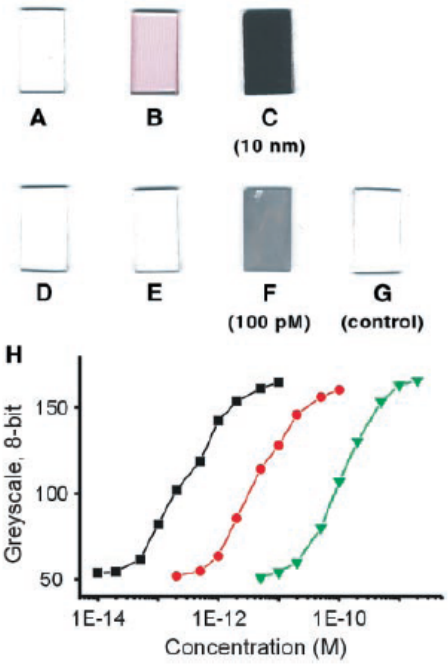

Fig. 1. Images of 7 mm by 13 mm, oligonucleotide-functionalized, float glass slides, obtained with a flatbed scanner. (**A**) Slide before hybridization of target and nanoparticle probe. (**B**) A slide identical to (A) after hybridization with oligonucleotide target (10 nM) and then nanoparticle probes (5 nM in particles). The pink color derives from the Au nanoparticle probes. (**C**) A slide identical to (B) after exposure to silver amplification solution for 5 min. (**D**) Slide before hybridization of target and nanoparticle probe. (**E**) A slide identical to (D) after hybridization with target (100 pM) and then nanoparticle probe (5 nM). The extinction of the submonolayer of nanoparticles is too low to be observed visually or with a flatbed scanner. (**F**) A slide identical to (E) after exposure to silver amplification solution for 5 min. Slide (F) is lighter than slide (C), indicating a lower concentration of target. (**G**) A control slide exposed to 5 nM nanoparticle probe and then exposed to silver amplification solution for 5 min. No darkening of the slide is observed. (**H**) Graph of 8-bit gray scale values as a function of target concentration. The gray scale values were taken from flatbed scanner images of oligonucleotide-functionalized glass surfaces that had been exposed to varying concentrations of oligonucleotide target, labeled with 5 nM oligonucleotide probe and immersed in silver amplification solution. For any given amplification time, the grayscale range is limited by surface saturation at high grayscale values and the sensitivity of the scanner at low values. Therefore, the dynamic range of this system can be adjusted by means of hybridization and amplification conditions (that is, lower target concentrations require longer amplification periods). Squares: 18-base capture-target overlap (*5*), 8× PBS hybridization buffer [1.2 M NaCl and 10 mM NaH_2PO_4/Na_2HPO_4 buffer (pH 7)], 15 min amplification time. Circles: 12-base capture-target overlap, 8× PBS hybridization buffer, 10 min amplification time. Triangles: 12-base capture-target overlap, 2× PBS hybridization buffer [0.3 M NaCl, 10 mM NaH_2PO_4/Na_2HPO_4 buffer (pH 7)], 5 min amplification time. The lowest target concentration that can be effectively distinguished from the background baseline is 50 fM.

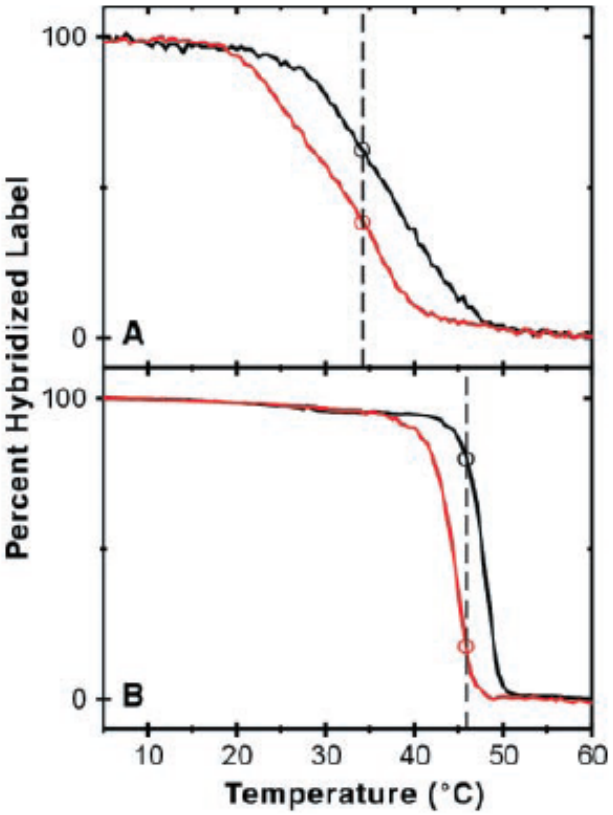

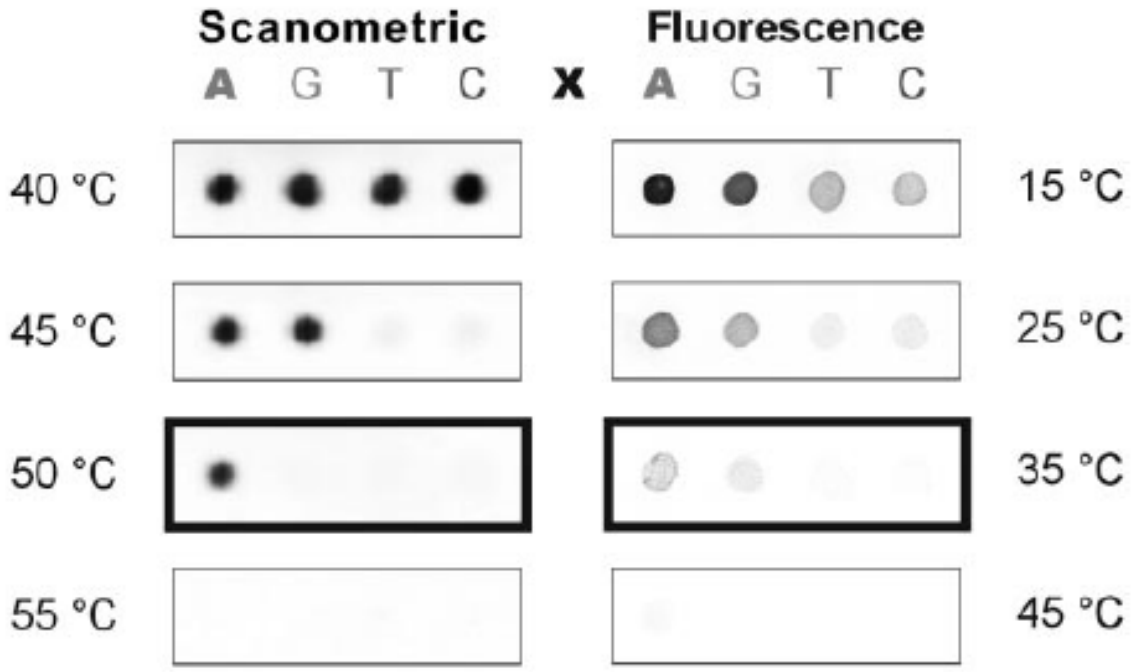

Fig. 3. (**Left**) Nanoparticle-labeled arrays developed at different stringency temperatures. Model oligonucleotide arrays (with the capture sequences shown in Scheme 1) were treated with oligonucleotide target and nanoparticle probes, followed by a 2-min buffer wash at the temperatures shown and subsequent silver amplification (*13*). Images were obtained with an Epson Expression 636 (600 dots per inch) flatbed scanner (Epson America, Long Beach, California). The darkened border indicates the array that showed optimum selectivity for the perfectly complementary target; at this temperature, the ratio of background-subtracted, 8-bit gray scale values for elements A:G:T:C, obtained from histogram averages in Adobe Photoshop (Adobe Systems, San Jose, California), is 96:9:7:6. (**Right**) Fluorophore-labeled arrays washed at different stringency temperatures. Model oligonucleotide arrays identical to those shown at left were treated with oligonucleotide target and Cy3-labeled oligonucleotide probes, followed by a 2-min buffer wash at the temperatures shown. Images were obtained with a ScanArray Confocal Microarray Scanner (GSI Lumonics, Billerica, Massachusetts). The darkened border indicates the array that showed the highest selectivity for the perfectly complementary target, as calculated by the QuantArray Analysis software package (GSI Lumonics); at this temperature, the intensity ratio (in percent, with the intensity of the X = A element at 15°C set to 100%) for elements A:G:T:C is 18:7:1:1.

Nanoparticles with Raman Spectroscopic Fingerprints for DNA and RNA Detection

YunWei Charles Cao, Rongchao Jin, Chad A. Mirkin*

30 AUGUST 2002 VOL 297 SCIENCE

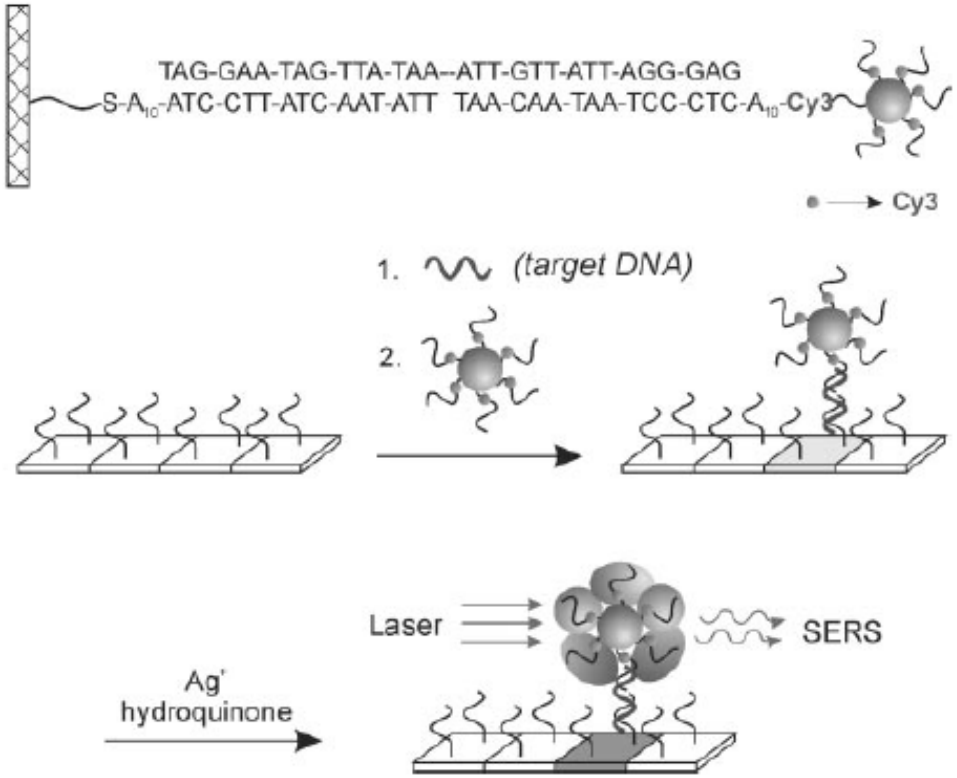

1 fM

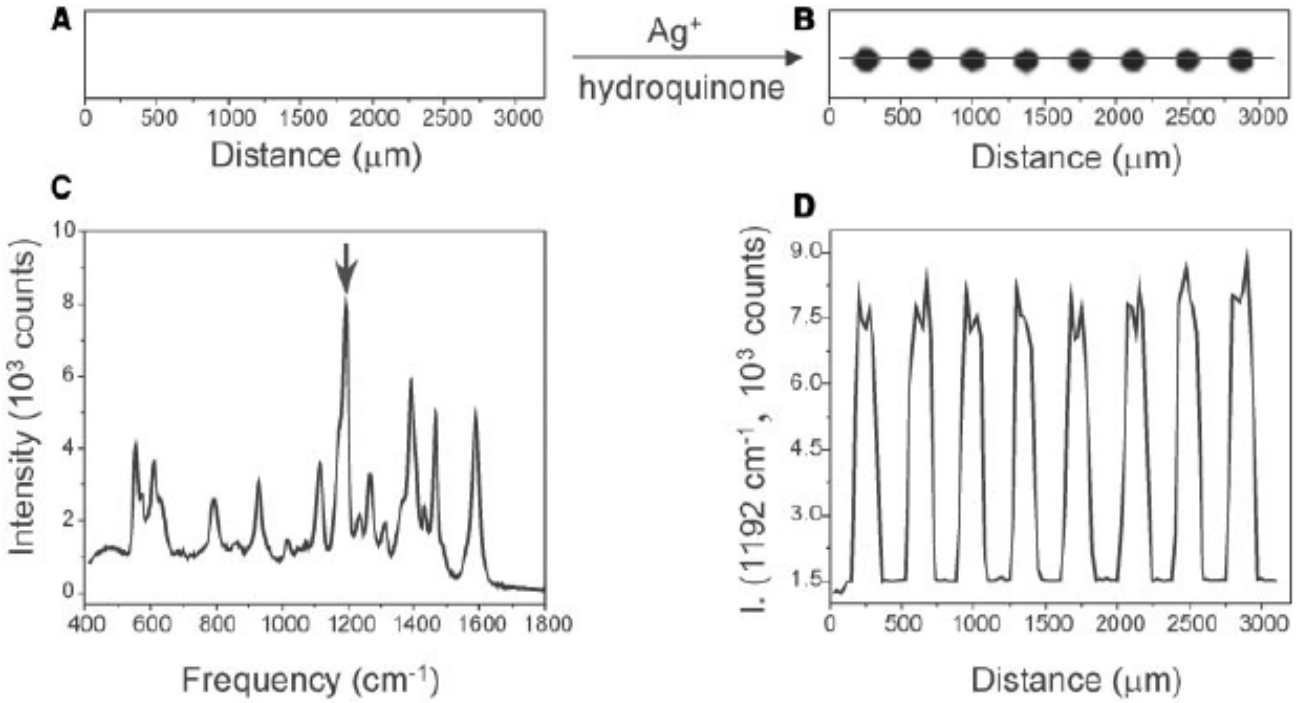

Fig. 1. Flatbed scanner images of microarrays hybridized with nanoparticles (**A**) before and (**B**) after Ag enhancing. (**C**) A typical Raman spectrum acquired from one of the Ag spots. (**D**) A profile of Raman intensity at 1192 cm^{-1} as a function of position on the chip; the laser beam from the Raman instrument is moved over the chip from left to right as defined by the line in (B).

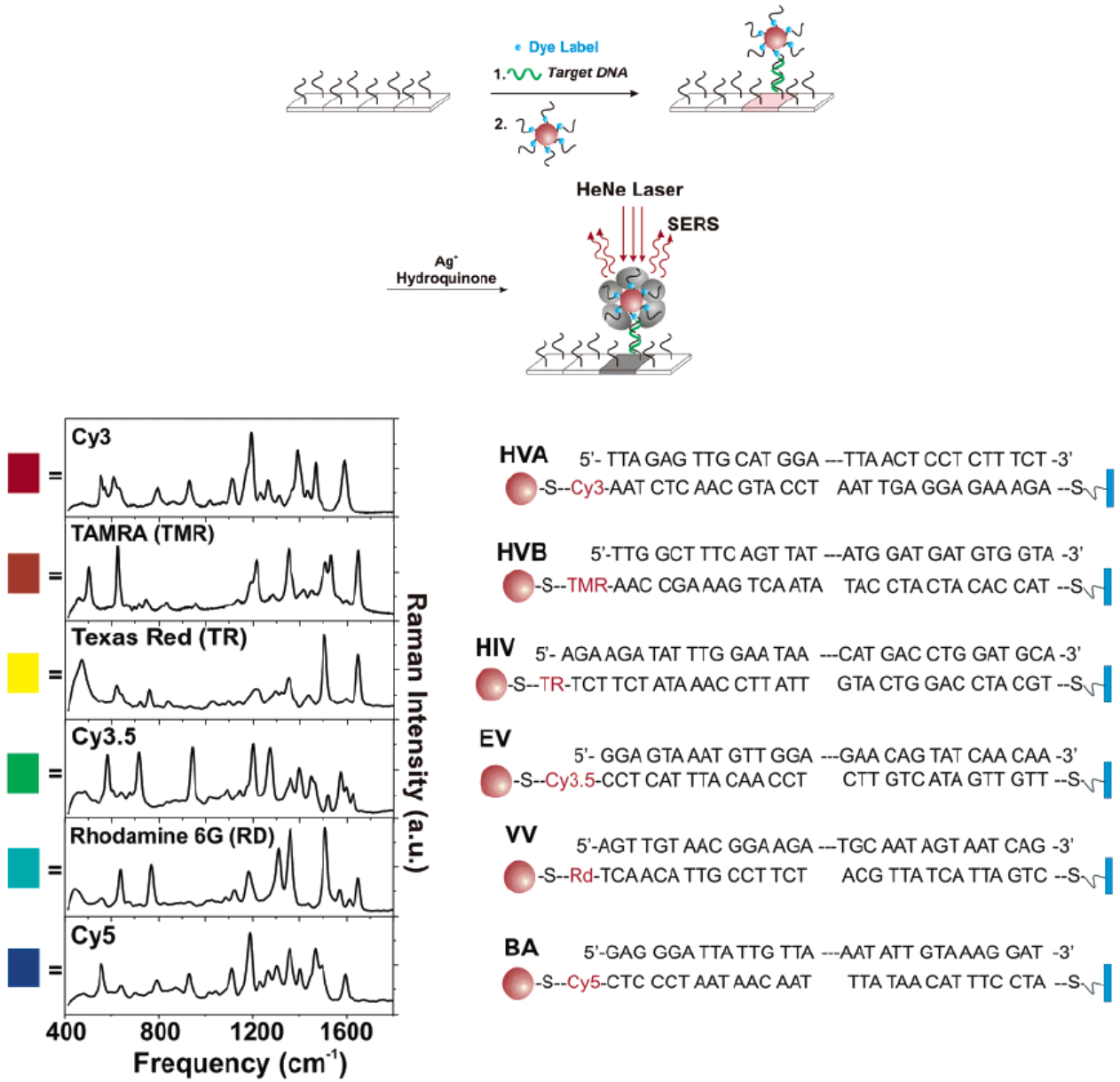

Figure 5. If Raman dyes (blue spheres) are attached to the labeling probe in the scanometric assay, the targets can be encoded and detected via the Raman signal of their labels. (Reprinted with permission from *Science* (http://www.aaas.org), ref 68. Copyright 2002 American Association for the Advancement of Science.)

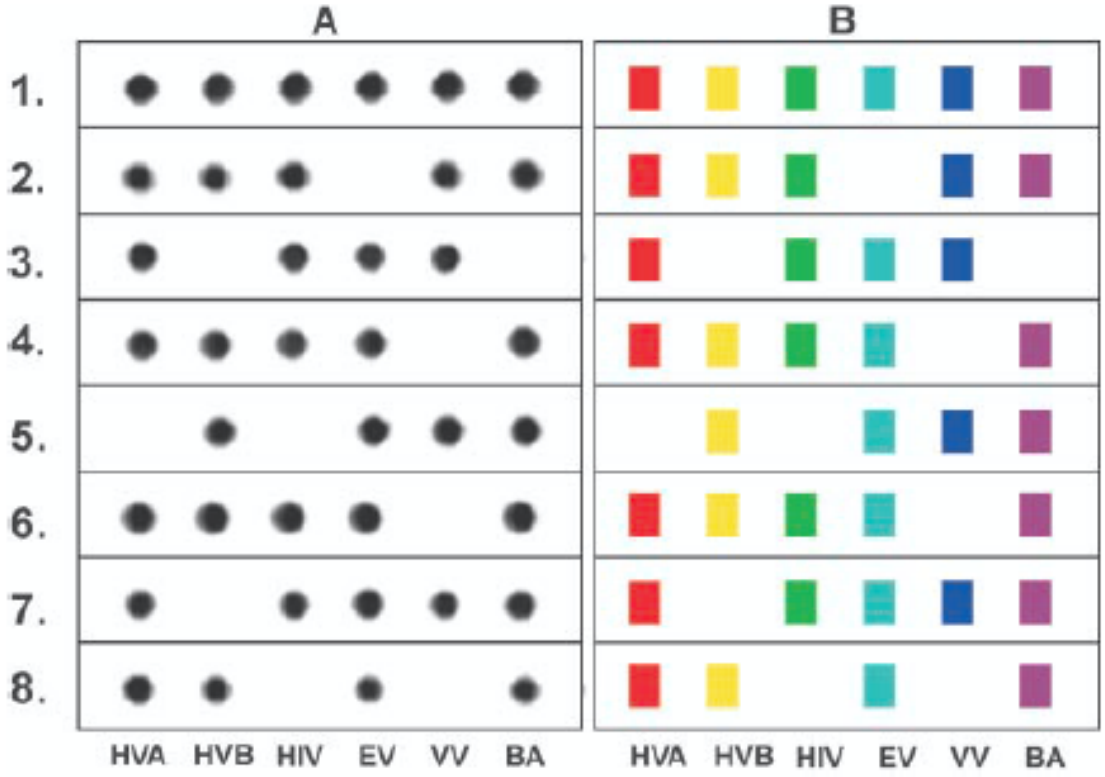

Fig. 3. (**A**) Flatbed scanner images of Ag-enhanced microarrays and (**B**) corresponding Raman spectra. The colored boxes correlate with the color-coded Raman spectra in Fig. 2. No false-positives or false-negatives were observed.

Bio-Bar-Code-Based DNA Detection with PCR-like Sensitivity

Jwa-Min Nam, Savka I. Stoeva, and Chad A. Mirkin*

J. AM. CHEM. SOC. 2004, *126*, 5932−5933

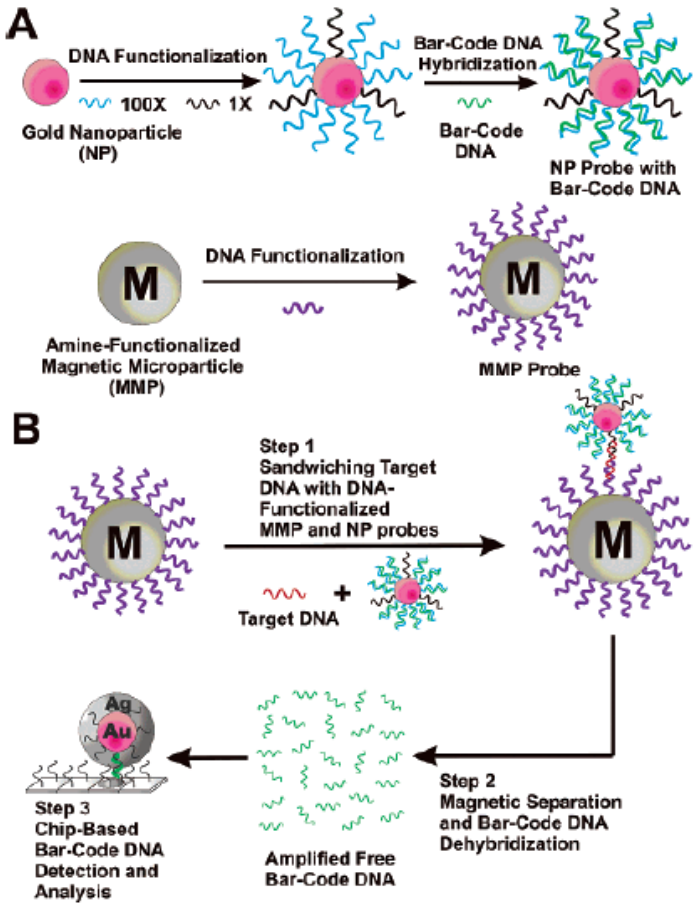

Figure 1. The DNA-BCA assay. (A) Nanoparticle and magnetic microparticle probe preparation. (B) Nanoparticle-based PCR-less DNA amplification scheme.

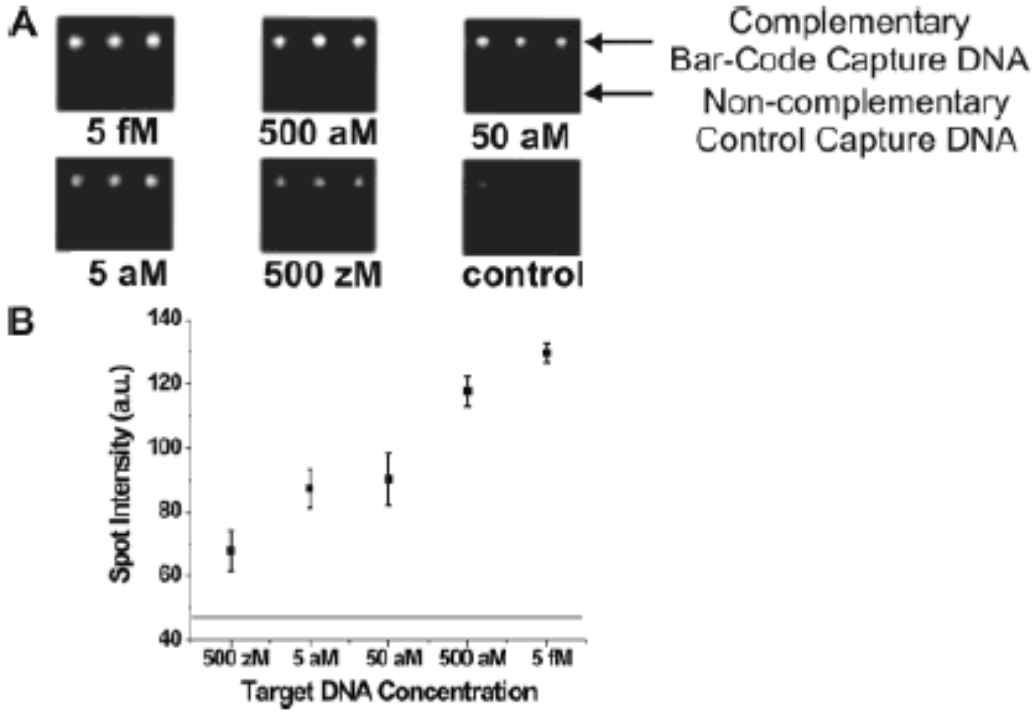

Figure 2. Amplified anthrax bar-code DNA detection with the Verigene ID system. (A) Anthrax bar-code DNA detection with 30 nm NP probes. (B) Quantitative data of spot intensities with 30 nm NP probes (Adobe Photoshop, Adobe Systems, Inc., San Jose, CA). The horizontal line represents control signal intensity (47 ± 2).

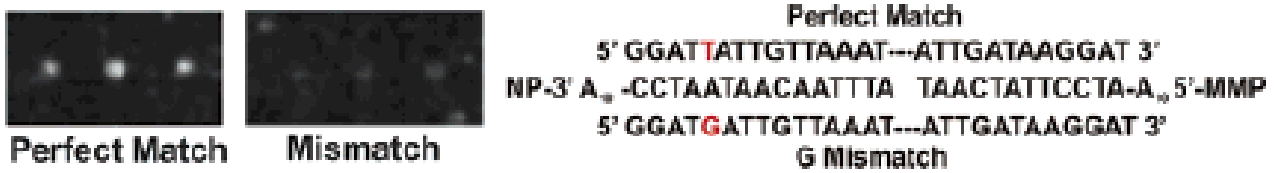

Figure 3. Single base mismatch experiment.

Nanoparticle-Based Bio–Bar Codes for the Ultrasensitive Detection of Proteins

26 SEPTEMBER 2003 VOL 301 SCIENCE

Jwa-Min Nam,* C. Shad Thaxton,* Chad A. Mirkin†

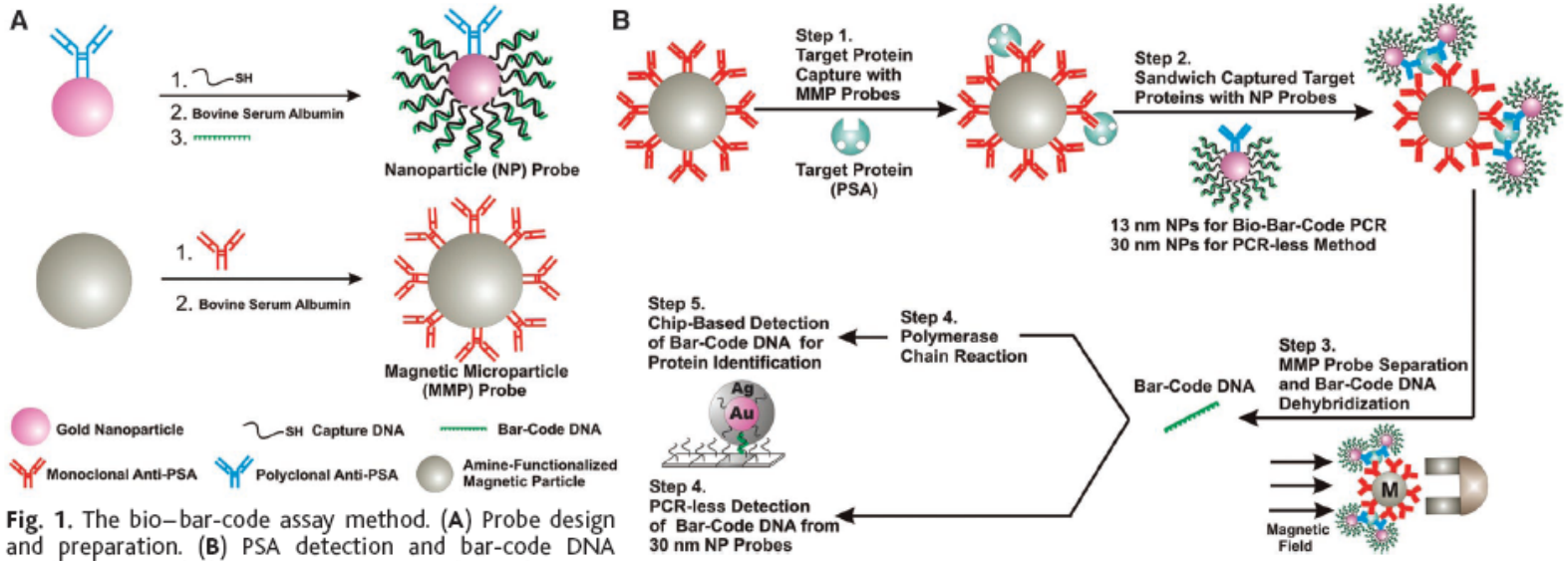

Fig. 1. The bio–bar-code assay method. (**A**) Probe design and preparation. (**B**) PSA detection and bar-code DNA amplification and identification. In a typical PSA-detection experiment, an aqueous dispersion of MMP probes functionalized with mAbs to PSA (50 μl of 3 mg/ml magnetic probe solution) was mixed with an aqueous solution of free PSA (10 μl of PSA) and stirred at 37°C for 30 min (Step 1). A 1.5-ml tube containing the assay solution was placed in a BioMag microcentrifuge tube separator (Polysciences, Incorporated, Warrington, PA) at room temperature. After 15 s, the MMP-PSA hybrids were concentrated on the wall of the tube. The supernatant (solution of unbound PSA molecules) was removed, and the MMPs were resuspended in 50 μl of 0.1 M phosphate-buffered saline (PBS) (repeated twice). The NP probes (for 13-nm NP probes, 50 μl at 1 nM; for 30-nm NP probes, 50 μl at 200 pM), functionalized with polyclonal Abs to PSA and hybridized bar-code DNA strands, were then added to the assay solution. The NPs reacted with the PSA immobilized on the MMPs and provided DNA strands for signal amplification and protein identification (Step 2). This solution was vigorously stirred at 37°C for 30 min. The MMPs were then washed with 0.1 M PBS with the magnetic separator to isolate the magnetic particles. This step was repeated four times, each time for 1 min, to remove everything but the MMPs (along with the PSA-bound NP probes). After the final wash step, the MMP probes were resuspended in NANOpure water (50 μl) for 2 min to dehybridize bar-code DNA strands from the nanoparticle probe surface. Dehybridized bar-code DNA was then easily separated and collected from the probes with the use of the magnetic separator (Step 3). For bar-code DNA amplification (Step 4), isolated bar-code DNA was added to a PCR reaction mixture (20-μl final volume) containing the appropriate primers, and the solution was then thermally cycled (*20*). The bar-code DNA amplicon was stained with ethidium bromide and mixed with gel-loading dye (*20*). Gel electrophoresis or scanometric DNA detection (*24*) was then performed to determine whether amplification had taken place. Primer amplification was ruled out with appropriate control experiments (*20*). Notice that the number of bound NP probes for each PSA is unknown and will depend upon target protein concentration.

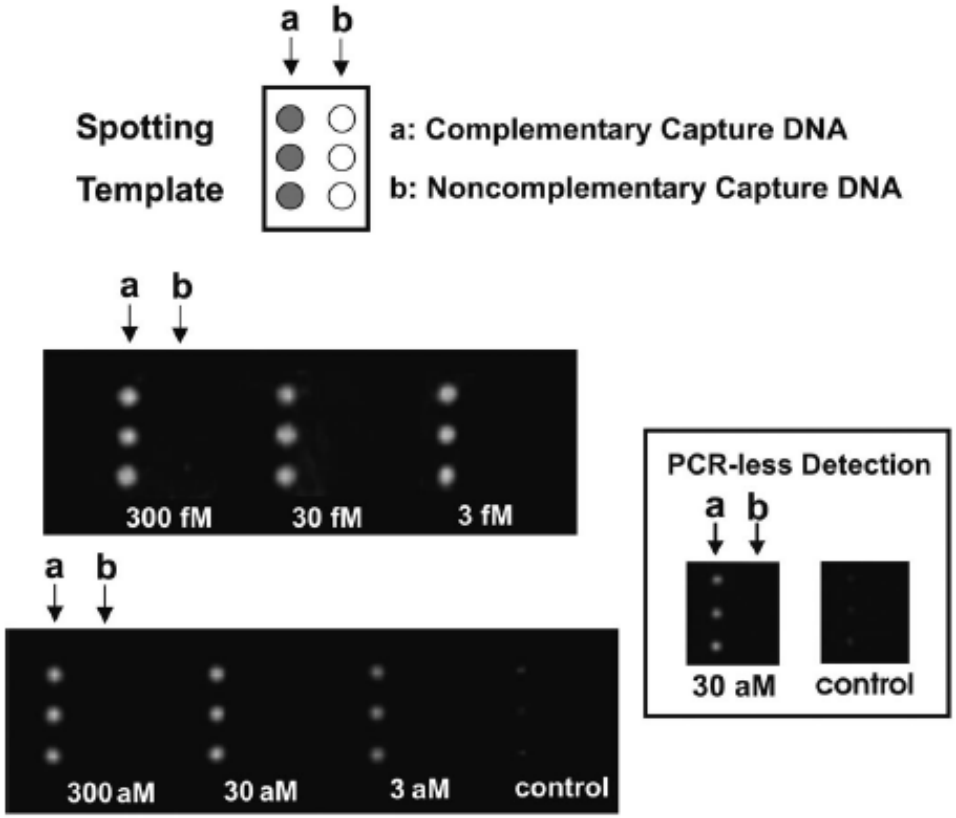

Fig. 2. Scanometric detection of PSA-specific bar-code DNA. PSA concentration (sample volume of 10 μl) was varied from 300 fM to 3 aM and a negative control sample where no PSA was added (control) is shown. For all seven samples, 2 μl of antidinitrophenyl (10 pM) and 2 μl of β-galactosidase (10 pM) were added as background proteins. Also shown is PCR-less detection of PSA (30 aM and control) with 30 nm NP probes (inset). Chips were imaged with the Verigene ID system (*20*).

Table 1. Detection Limits of Nucleic Acid Assays[a]

	assay	ss DNA	PCR products	genomic DNA
nanostructure-based methods	colorimetric[29] (cross-linked Au nanoparticles)	~10 nM		
	colorimetric[36] (non-cross-linked Au nanoparticles)	60 nM		
	magnetic relaxation[97] (iron oxide nanoparticles)	20 pM		
	electrochemical[96] (nanoparticles)	270 pM		
	scanometric[35,66,67] (Au nanoparticles with Ag amplification)	50 fM	100 aM[b]	200 fM
	Raman spectroscopy[68] (Au nanoparticles with Ag amplification)	~1 fM		
	electrical[93] (Au nanoparticles with Ag amplification)	500 fM		
	electrical[99] (Si nanowire)	10 fM		
	electrical[103] (carbon nanotube)	54 aM		
	resonant light-scattering[61–66] (metal nanoparticles)	170 fM[b]		33 fM
	fluorescence[56] (ZnS and CdSe quantum dots)	2 nM		
	surface plasmon resonance[41] (Au nanoparticles)	10 pM		
	quartz crystal microbalance[94] (Au nanoparticles)	~1 fM		
	laser diffraction[42] (Au nanoparticles)	~50 fM		
	fluorescence[45] (fluorescent nanoparticles)	~1 fM		
	bio-bar-code amplification[71] (Au nanoparticles with Ag amplification)	500 zM		
other non-enzymatic based methods	fluorescence[35] (molecular fluorophores)		~600 fM[b]	
	fluorescence (dendrimer amplification)[134]		2.5 μg	
	electrochemical amplification[136] (electroactive reporter molecules)	100 aM		

[a] Detection limits can vary based on target length and sequence; therefore, it is difficult to compare assays without testing them using identical targets and conditions. [b] Values taken from ref 34.

Table 2. Detection Limits of Protein Assays

	assay	target	protein in saline	protein in serum
nanostructure-based methods	optical[72] (Au nanoshells)	rabbit IgG	0.88 ng/mL (~4.4 pM)[a]	0.88 ng/mL (~4.4 pM)[c]
	optical[74] (Au nanoparticles)	IgE and IgG1	~20 nM	
	magnetic relaxation[98] (iron oxide nanoparticles)	adenovirus (ADV) and herpes simplex virus (HSV)	100 ADV/ 100μL	50 HSV/ 100 μL
	scanometric[79] (Au nanoparticles with Ag amplification)	mouse IgG	200 pM	
	Raman[82] (Au nanoparticles with Raman labels)	prostate-specific antigen		30 fM
	surface plasmon resonance[83,84] (triangular Ag particles on surfaces)	streptavidin(S A) and anti-biotin (AB)	~1 pM SA and ~700 pM AB	
	electrical[110] (single-walled carbon nanotubes)	10E3 antibody to U1A RNA splicing factor	~1 nM	
	electrical[20] (Si nanowires)	streptavidin	10 pM	
	bio-bar-code amplification[75] (Au nanoparticles with Ag amplification)	prostate-specific antigen	30 aM (3 aM)[b]	(30 aM)[b]
molecular fluorophore methods	enzyme-linked immunosorbent assay	various	pM range	pM range
electrochemical methods	electrochemical amplification[137] (oligonucleotide reporter molecules)	IgG	13 fM	
enzyme-based amplification methods	immuno-PCR[76]	bovine serum albumin	2 fM	
	rolling circle amplification[77]	prostate-specific antigen	3 fM	

[a] Reported in ng/mL; authors converted to molar concentration for ease of comparison. [b] These values are the lower limits when PCR is used to amplify the bar-code DNA prior to scanometric detection of bar codes.

Surface Plasmon

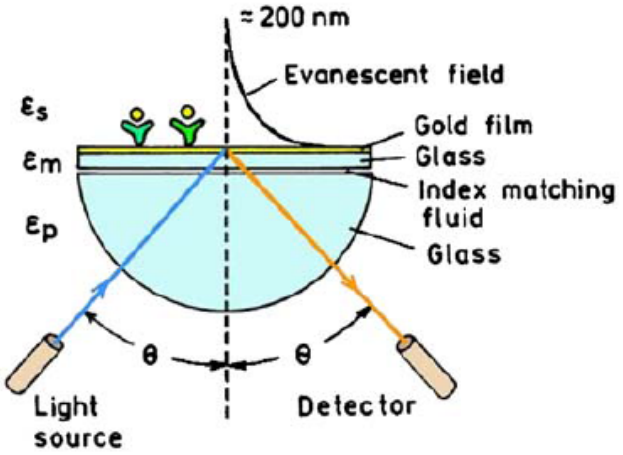

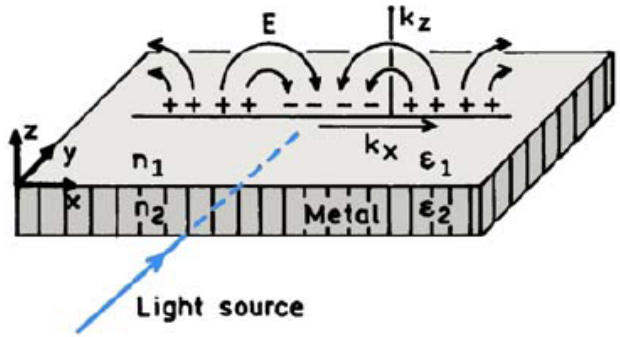

Figure 3. Schematics of an SPR experiment (top) and of the light-induced surface plasmons (bottom).

(b)

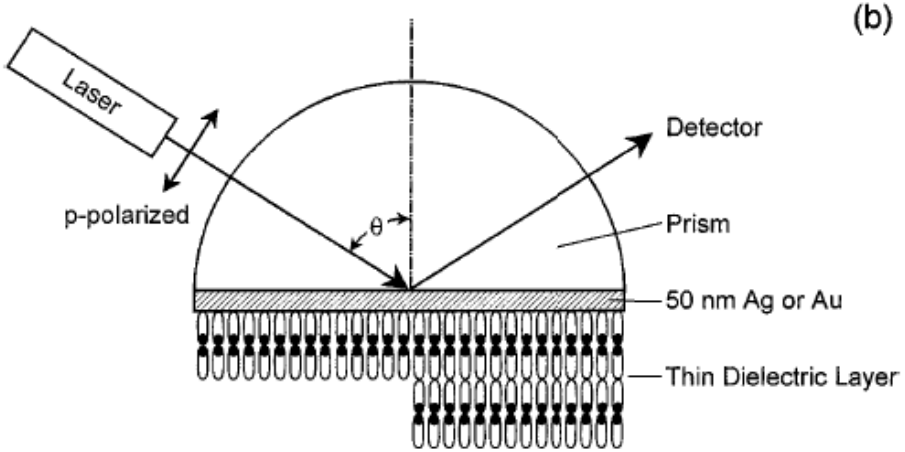

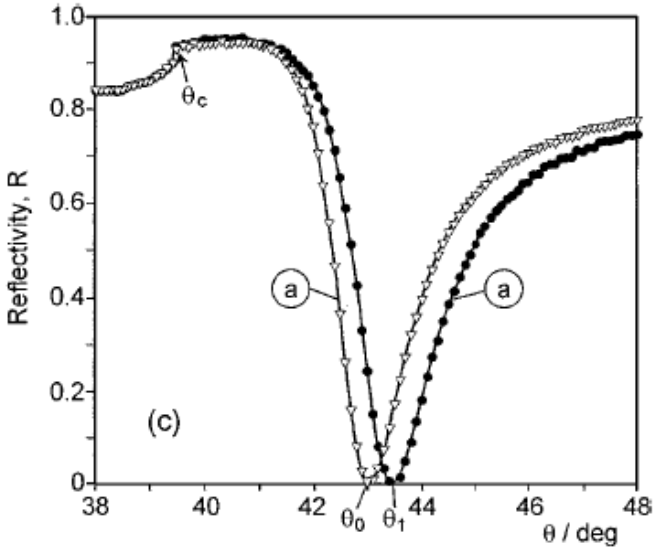

Drift: Drude model

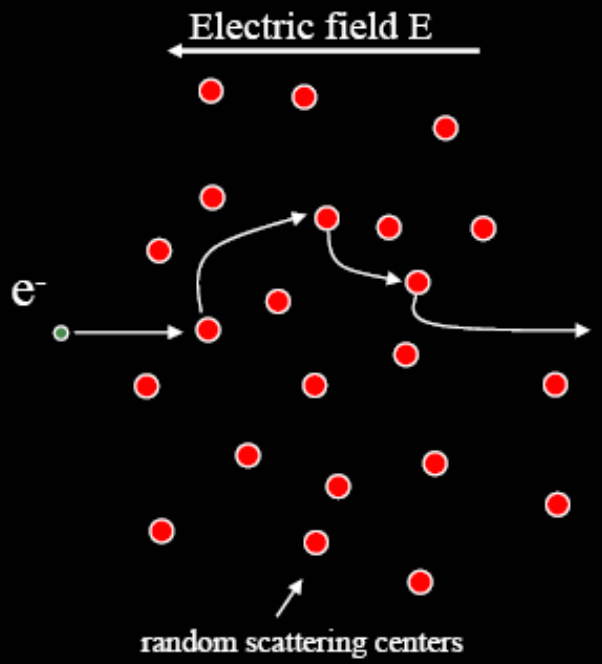

$$F = ma$$

$$eE = m\frac{\partial v}{\partial t}$$

$$v_{avg} = \underbrace{\frac{e\tau}{m}}_{\mu} E$$

$$j = nev_{avg} = \underbrace{\frac{ne^2\tau}{m}}_{\sigma} E$$

$$m\frac{\partial}{\partial t}\langle\vec{v}\rangle = q\vec{E} - \gamma\langle\vec{v}\rangle$$

$$\sigma(\omega) = \frac{\sigma_0}{1 + i\omega\tau}$$

AC Dielectric Response

$$\varepsilon_m = 1 - \frac{\omega_p^2}{\omega^2}$$

Plasma frequency

polarizability of a small metal sphere with dielectric function $\varepsilon(\lambda)$

$$\alpha = R^3 \frac{\varepsilon - 1}{\varepsilon + 2}.$$

$$\varepsilon = \varepsilon_\mathrm{b} + 1 - \frac{\omega_\mathrm{P}^2}{\omega^2 + \mathrm{i}\omega\gamma},$$

$$\alpha = \frac{R^3(\varepsilon_\mathrm{b}\omega^2 - \omega_\mathrm{P}^2) + i\omega\gamma\varepsilon_\mathrm{b}}{[(\varepsilon_\mathrm{b} + 3)\omega^2 - \omega_\mathrm{P}^2] + i\omega\gamma(\varepsilon_\mathrm{b} + 3)}.$$

$\omega_\mathrm{R} = \frac{\omega_\mathrm{P}}{\sqrt{\varepsilon_\mathrm{b}+3}}$ $\gamma(\varepsilon_\mathrm{b} + 3)$.

Biomolecular Binding in Real Time

Principle of Detection - SPR (Surface Plasmon Resonance)

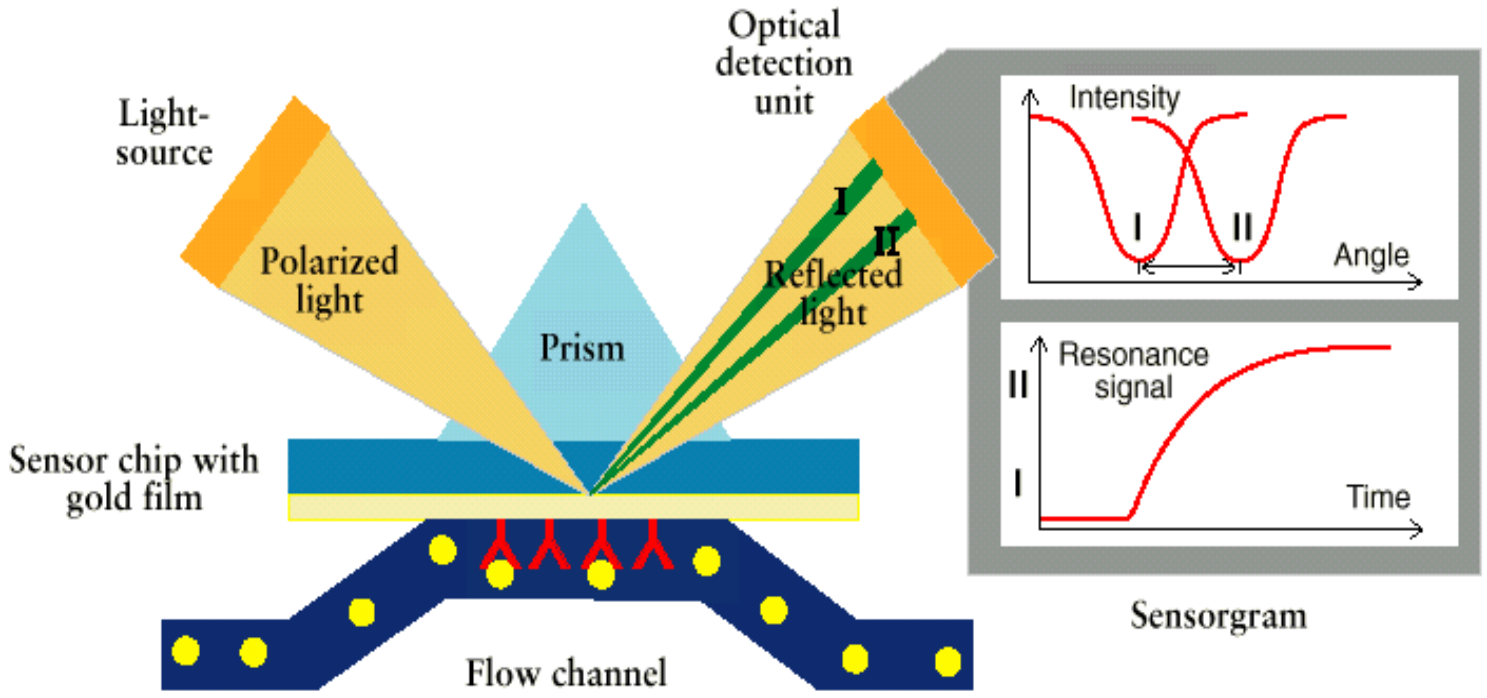

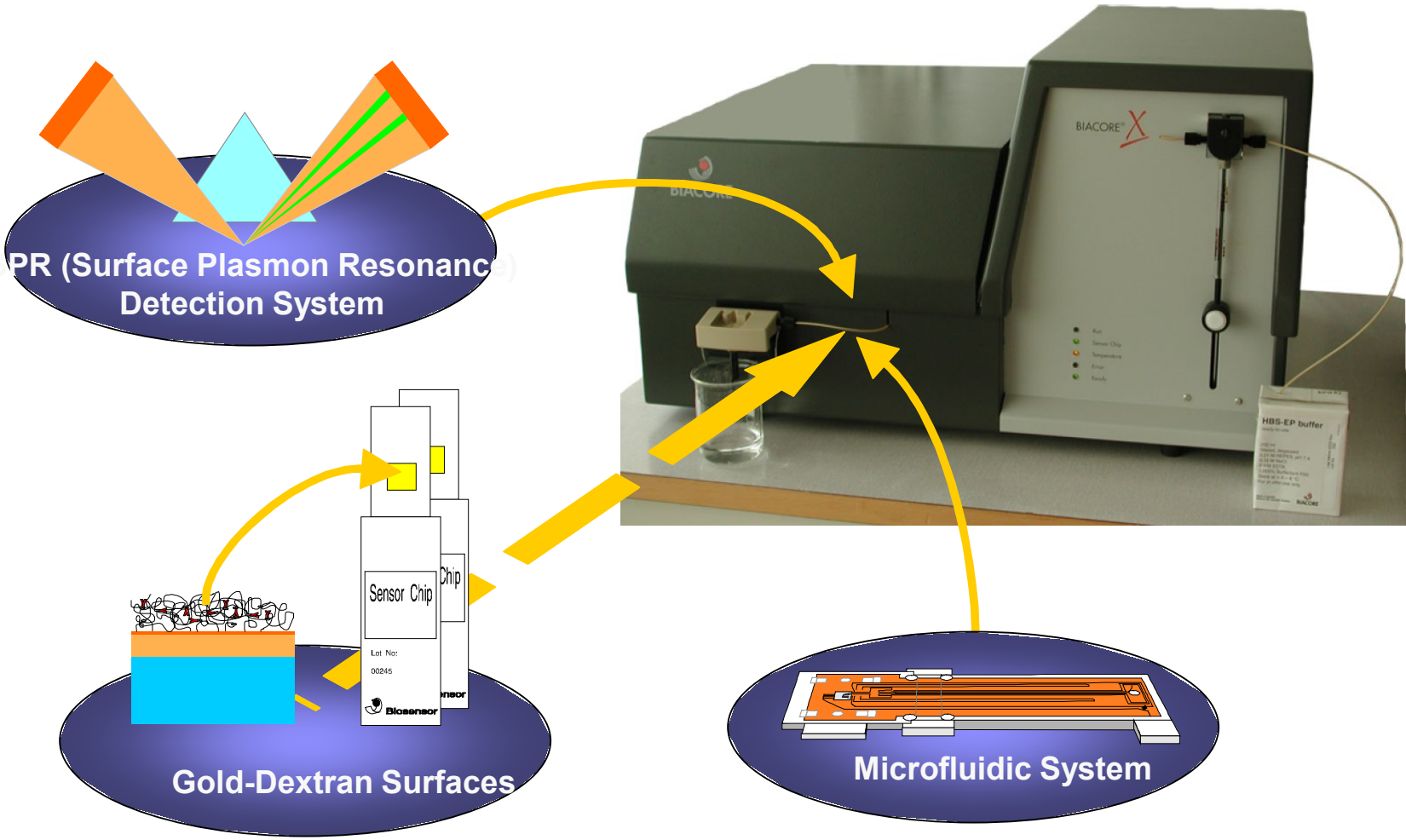
SPR (Surface Plasmon Resonance)
Detection System
BIACORE X
HBS-EP buffer
Sensor Chip
Lot No:
00245
Biosensor
Gold-Dextran Surfaces
Microfluidic System

SPR Imaging Apparatus

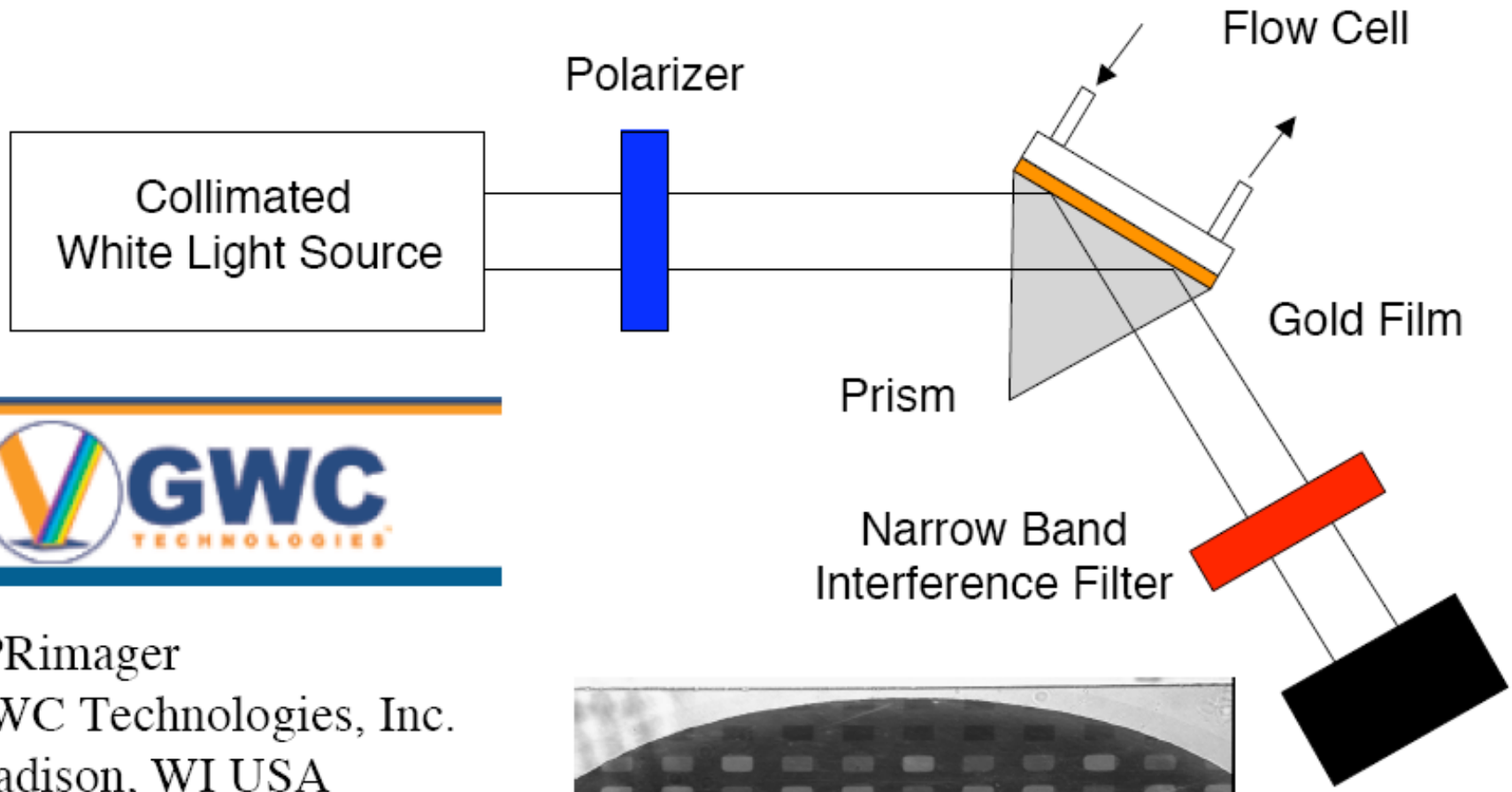

SPRimager
GWC Technologies, Inc.
Madison, WI USA

www.gwctechnologies.com

Raw Image

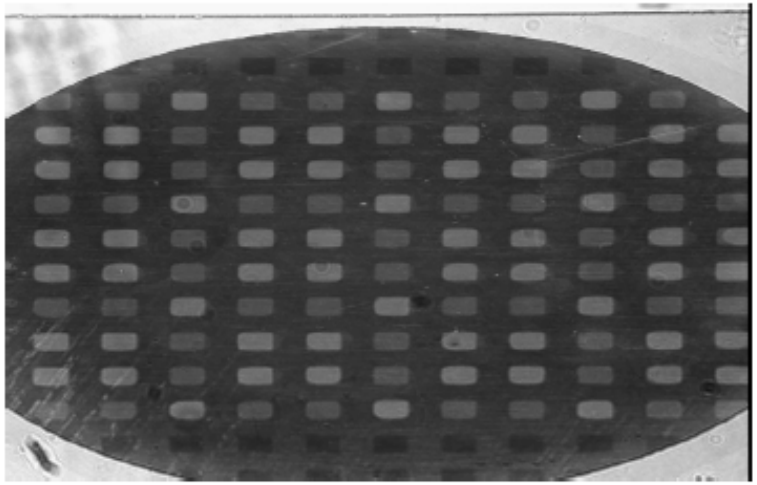

UCIrvin
University of California, Ir

Localized Plasmon

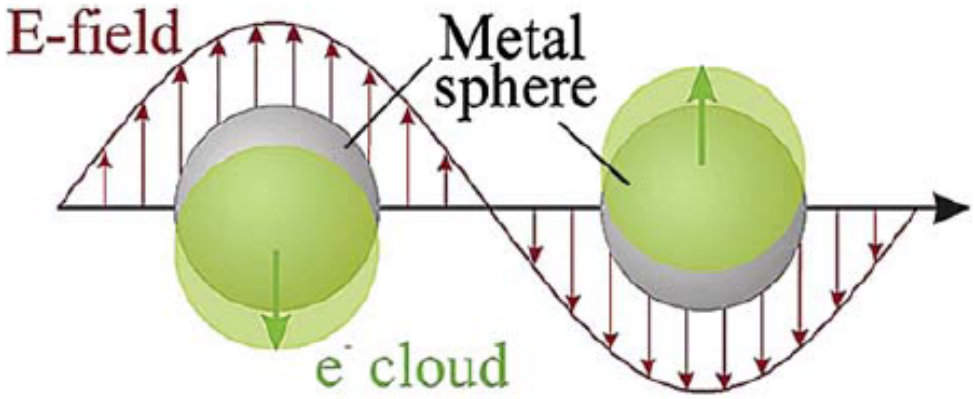

Figure 6. Schematic of plasmon oscillation for a sphere. From [39].

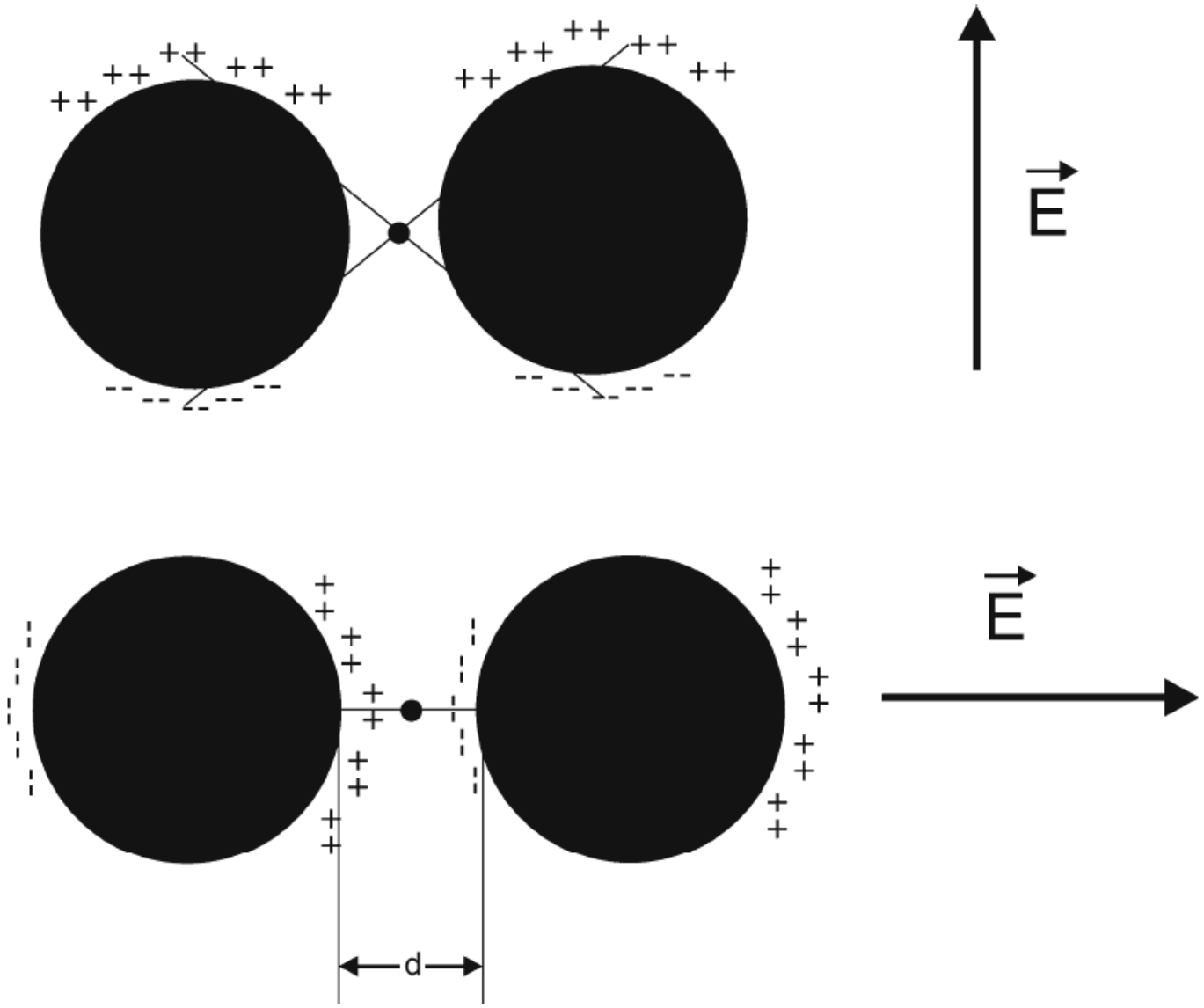
E
E
d

field enhancement

$E_s = gE_0$, where E_0 is the magnitude of the incident field

$$E_R \propto \alpha_R E_s \propto \alpha_R g E_0$$

$$E_{SERS} \propto \alpha_R g g' E_0$$

$$I_{SERS} \propto |\alpha_R|^2 |gg'|^2 I_0$$

$$g \cong g'$$

$$|E_L|^4 = |g|^4.$$

Probing Single Molecules and Single Nanoparticles by Surface-Enhanced Raman Scattering

SCIENCE • VOL. 275 • 21 FEBRUARY 1997

Shuming Nie* and Steven R. Emory

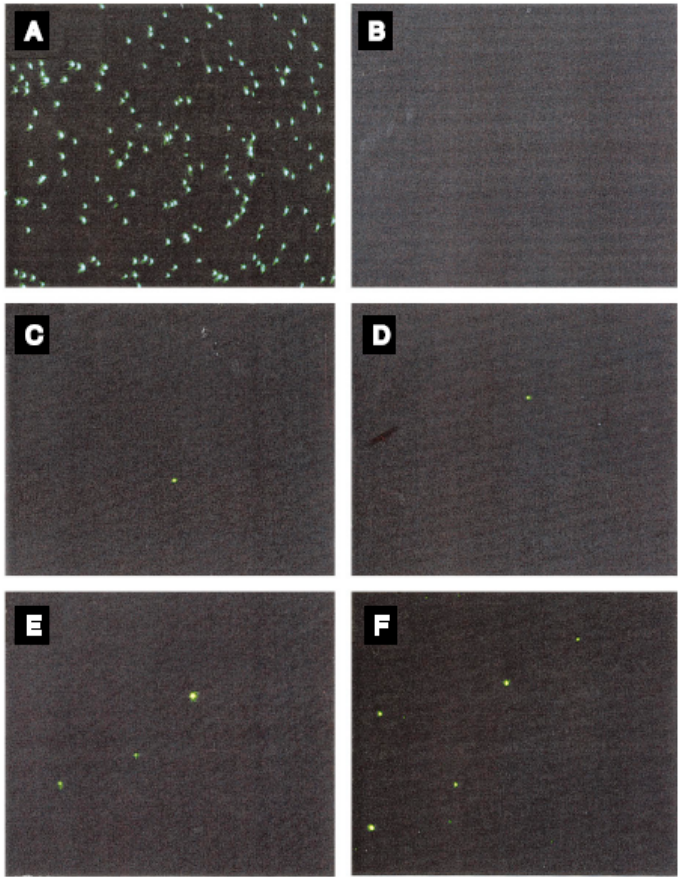

Fig. 1. Single Ag nanoparticles imaged with evanescent-wave excitation. Total internal reflection of the laser beam at the glass-liquid interface was used to reduce the laser scattering background. The instrument setup for evanescent-wave microscopy was adapted from Funatsu *et al.* (*11*). The images were directly recorded on color photographic film (ASA-1600) with a 30-s exposure by a Nikon 35-mm camera attached to the microscope. (**A**) Unfiltered photograph showing scattered laser light from all particles immobilized on a polylysine-coated surface. (**B**) Filtered photographs taken from a blank Ag colloid sample (incubated with 1 mM NaCl and no R6G analyte molecules). (**C**) and (**D**) Filtered photographs taken from a Ag colloid sample incubated with 2×10^{-11} M R6G. These images were selected to show at least one Raman scattering particle. Different areas of the cover slip were rapidly screened, and most fields of view did not contain visible particles. (**E**) Filtered photograph taken from Ag colloid incubated with 2×10^{-10} M R6G. (**F**) Filtered photograph taken from Ag colloid incubated with 2×10^{-9} M R6G. A high-performance bandpass filter was used to remove the scattered laser light and to pass Stokes-shifted Raman signals from 540 to 580 nm (920 to 2200 cm^{-1}). Continuous-wave excitation at 514.5 nm was provided by an Ar ion laser. The total laser power at the sample was 10 mW. Note the color differences between the scattered laser light in (A) and the red-shifted light in (C) through (F).

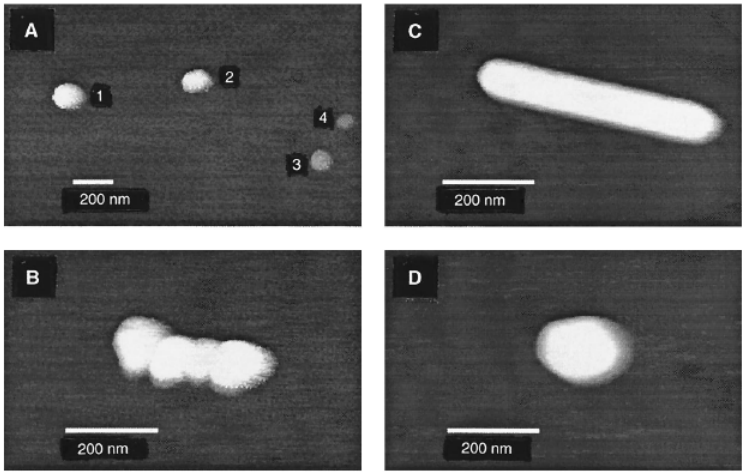

Fig. 2. Tapping-mode AFM images of screened Ag nanoparticles. (**A**) Large area survey image showing four single nanoparticles. Particles 1 and 2 were highly efficient for Raman enhancement, but particles 3 and 4 (smaller in size) were not. (**B**) Close-up image of a hot aggregate containing four linearly arranged particles. (**C**) Close-up image of a rod-shaped hot particle. (**D**) Close-up image of a faceted hot particle.

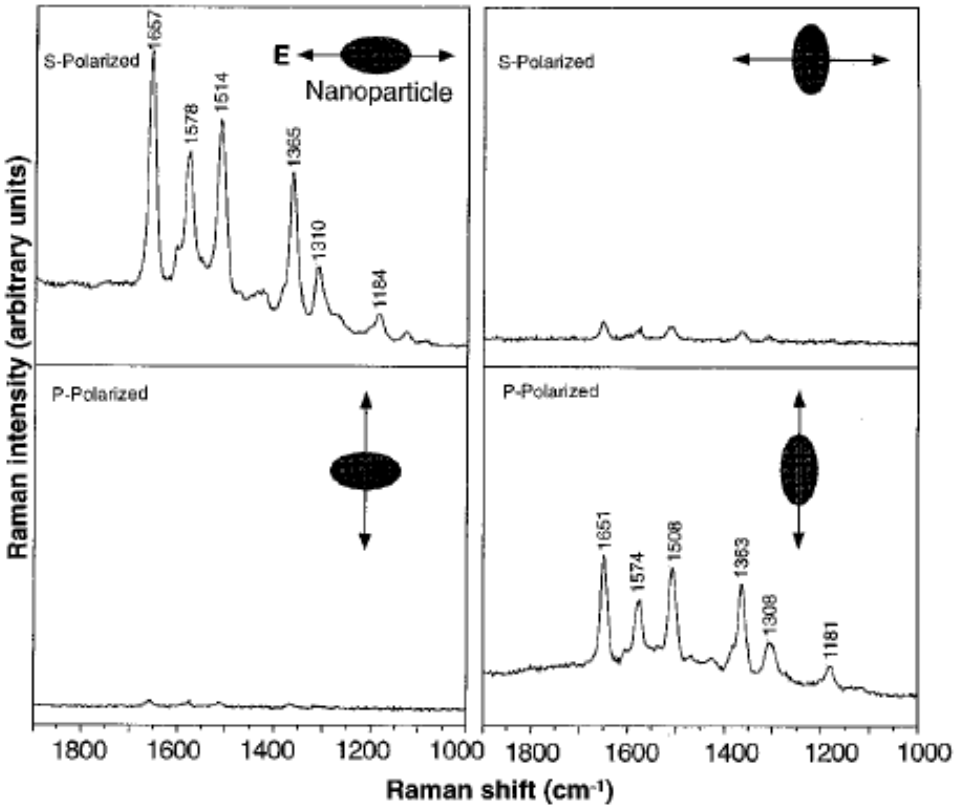

Fig. 3. Surface-enhanced Raman spectra of R6G obtained with a linearly polarized confocal laser beam from two Ag nanoparticles. The R6G concentration was 2×10^{-11} M, corresponding to an average of 0.1 analyte molecule per particle. The direction of laser polarization and the expected particle orientation are shown schematically for each spectrum. Laser wavelength, 514.5 nm; laser power, 250 nW; laser focal radius, ~250 nm; integration time, 30 s. All spectra were plotted on the same intensity scale in arbitrary units of the CCD detector readout signal.

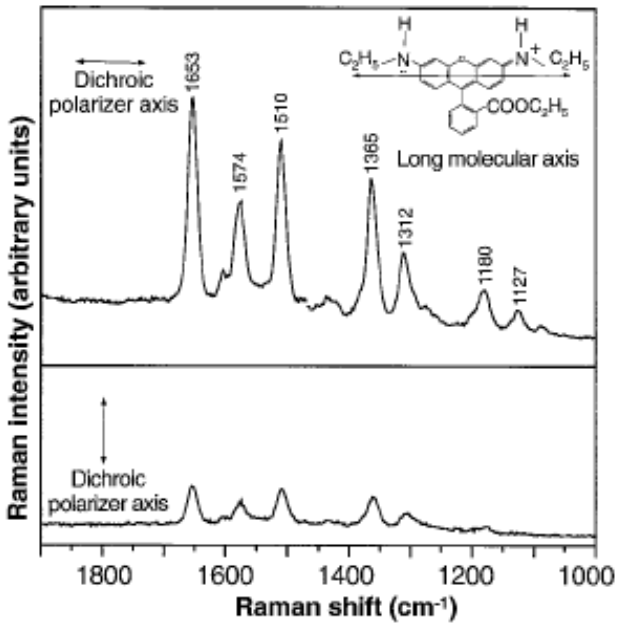

Fig. 4. Emission-polarized surface-enhanced Raman signals of R6G observed from a single Ag nanoparticle with a polarization-scrambled confocal laser beam. A dichroic sheet polarizer was rotated 90° to select Raman scattering signals polarized parallel (upper spectrum) or perpendicular (lower spectrum) to the long molecular axis of R6G. (**Inserts**) Structure of R6G, the electronic transition dipole (along the long axis when excited at 514.5 nm), and the dichroic polarizer orientations. Other conditions as in Fig. 3.

troscopic signatures of adsorbed molecules. For single rhodamine 6G molecules adsorbed on the selected nanoparticles, the intrinsic Raman enhancement factors were on the order of 10^{14} to 10^{15}, much larger than the ensemble-averaged values derived from conventional measurements. This enormous enhancement leads to vibrational Raman signals that are more intense and more stable than single-molecule fluorescence.

Electromagnetic contributions to single-molecule sensitivity in surface-enhanced Raman scattering

PRE 62 4318

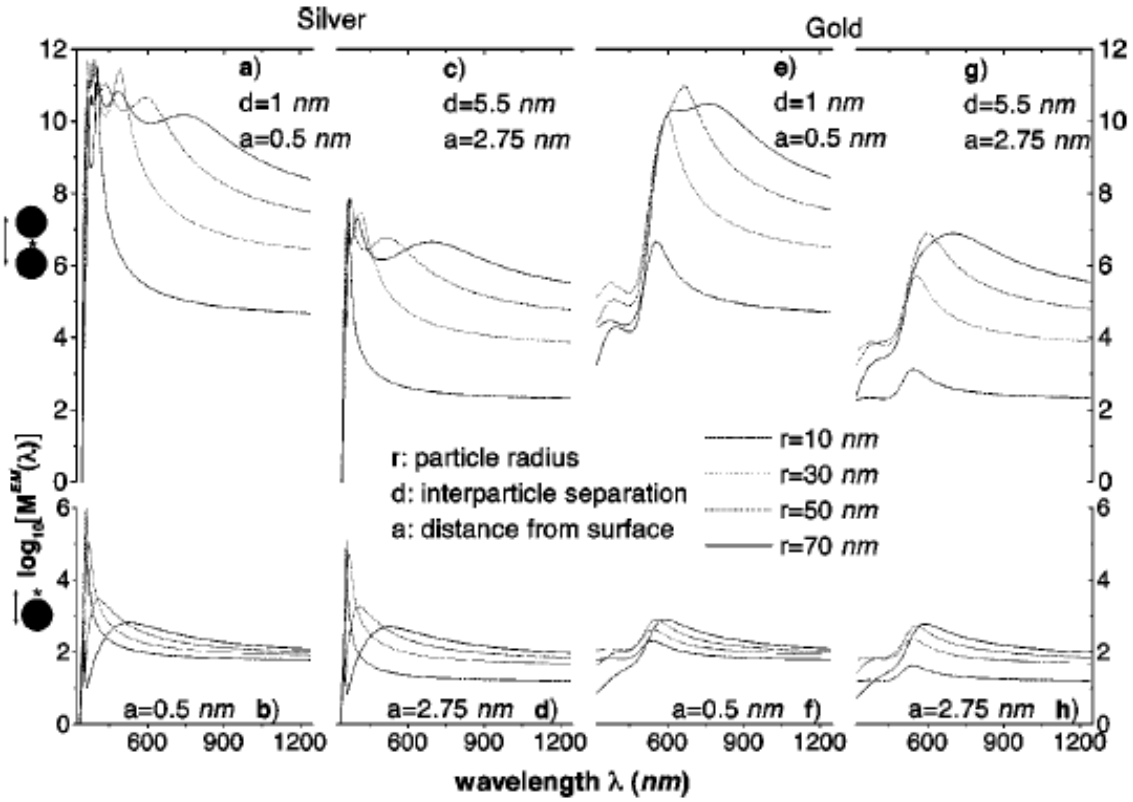

FIG. 3. (Color) EM-enhancement factor M^{EM} at a cross section through six different silver particle configurations. The wavelength of the incident field is $\lambda = 514.5$ nm with vertical polarization. The left-hand column illustrates the EM enhancement for dimer configurations of two spheres (top) and two polygons (bottom) with a separation of 1 nm. The middle column shows the same situation, but with a separation distance of 5.5 nm. The right-hand column shows the case of an isolated single particle. All particles share a common largest dimension of 90 nm. Note that the color scale from dark blue to dark red is logarithmic, covering the interval $10^0 < M^{EM} < 10^8$. Regions with enhancement outside this interval are shown in dark blue and dark red, respectively.

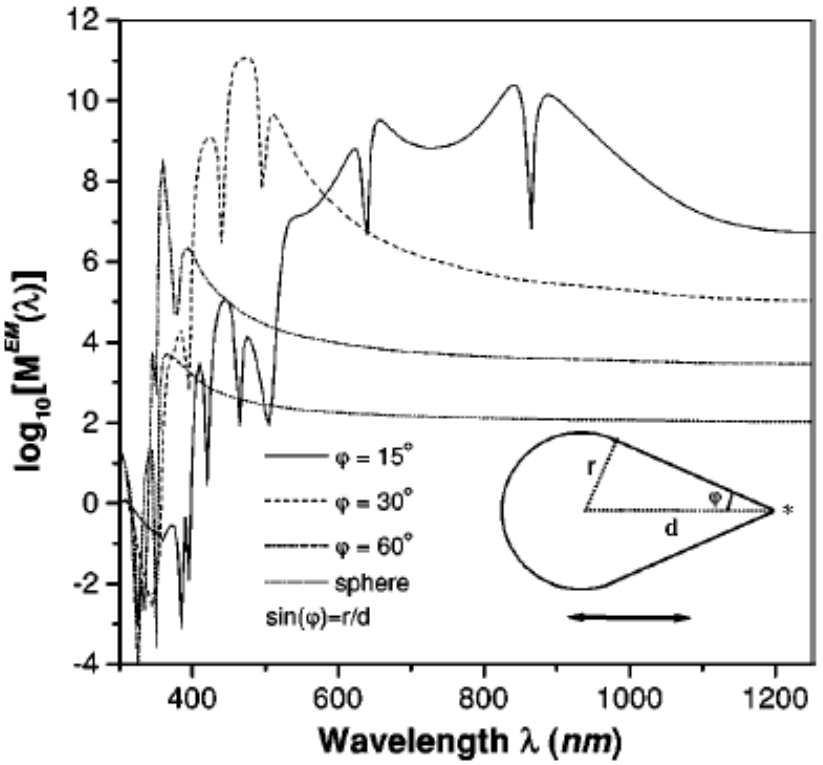

FIG. 5. EM-enhancement factor for a rotationally symmetric silver droplet as a function of the angle defining the opening edge ϕ. The field is polarized parallel to the axis of the droplet and the evaluation position (star) is located 0.5 nm outside the tip. As the droplet becomes sharper the enhancement increases several orders of magnitude.

Nanosphere Arrays with Controlled Sub-10-nm Gaps as Surface-Enhanced Raman Spectroscopy Substrates

J. AM. CHEM. SOC. 2005, *127*, 14992−14993

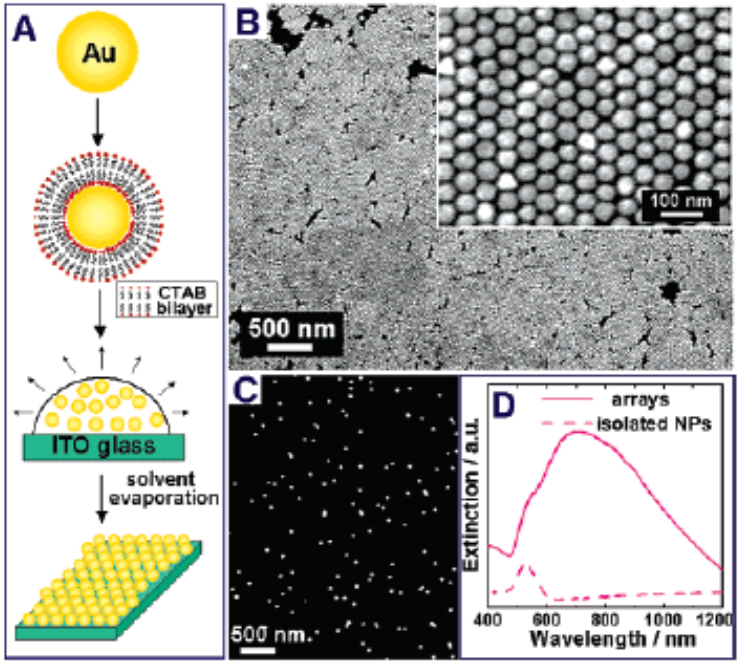

Figure 1. (A) Schematic illustration of the fabrication of sub-10-nm gap Au NP arrays. (B) SEM image of the arrays. (C) SEM image of monolayer of isolated Au NPs on ITO glass. (D) Vis−NIR extinction spectrum of the monolayer of isolated Au NPs and arrays.

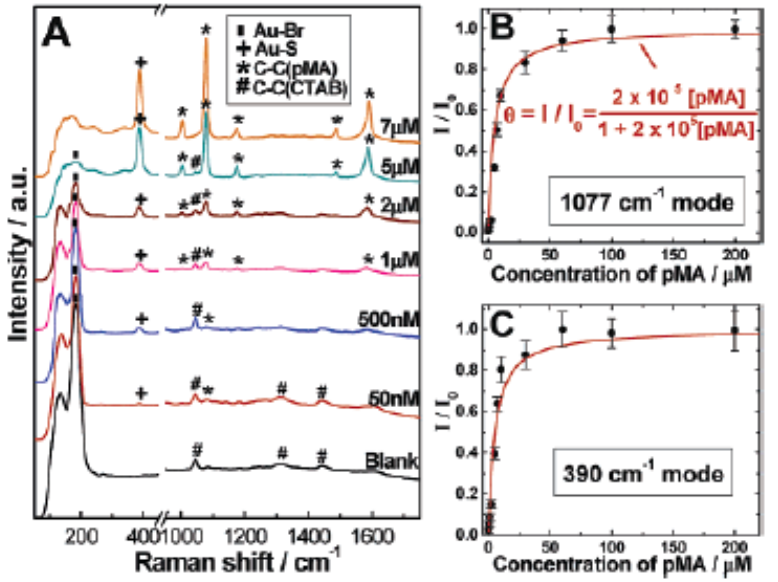

Figure 2. (A) SERS spectra of 5 μL of pMA with different concentrations deposited on the NP arrays. The excitation laser wavelength is 785 nm. Adsorption isotherm of pMA on the NP arrays obtained according to (B) 1077 and (C) 390 cm^{-1} modes in the SERS spectra. I_0 is the peak intensity of a saturated pMA monolayer.

Profiling the Near Field of a Plasmonic Nanoparticle with Raman-Based Molecular Rulers

NANO LETTERS

2006
Vol. 6, No. 10
2338−2343

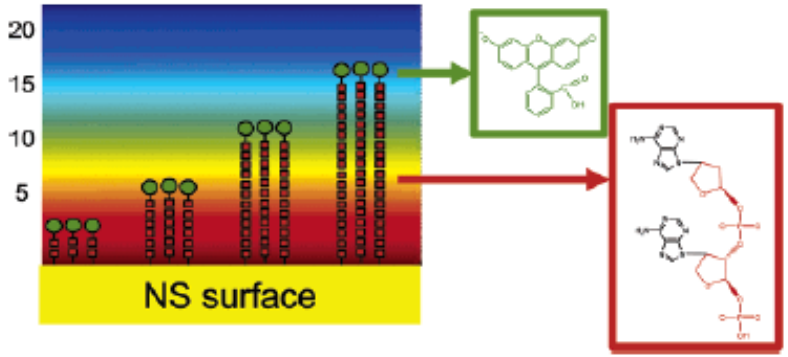

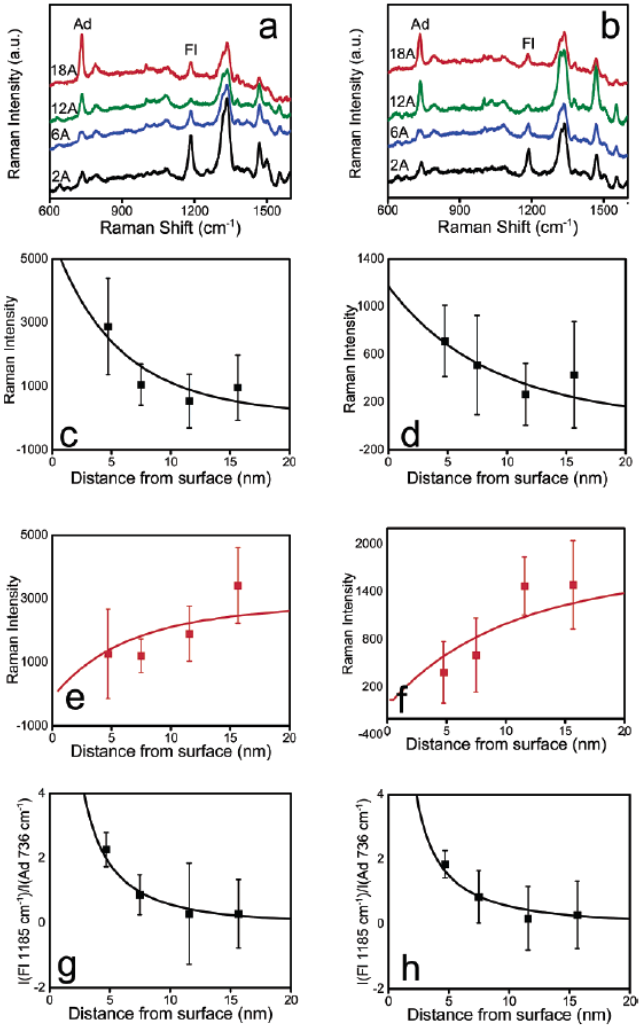

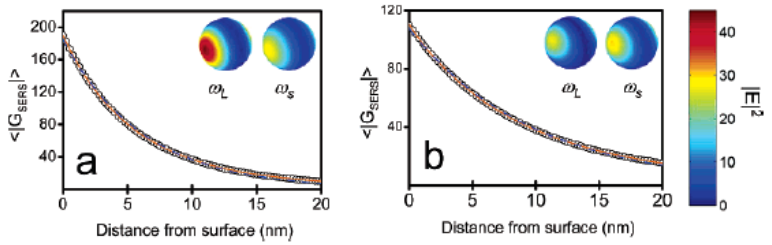

Nanomedicine

Nanomedicine is a multidisciplinary field that applies the knowledge and tools of nanotechnology to the prevention, diagnosis, and treatment of diseases. It involves the use of nanoparticles, nanostructures, and nanoscale materials to develop innovative medical therapies and diagnostic techniques.

Nanomedicine seeks to improve the effectiveness of treatments by enabling targeted drug delivery, reducing side effects, and enhancing the bioavailability of therapeutic agents. It also has the potential to revolutionize diagnostics by developing highly sensitive and accurate devices for detecting diseases at an early stage, which can significantly improve patient outcomes.

Targeted drug delivery: Nanoparticles can be engineered to carry drugs specifically to the site of a disease, improving the efficiency of the treatment and minimizing side effects.
Imaging and diagnostics: Nanoscale materials can be used as contrast agents or imaging probes, enhancing the detection of diseases and providing real-time monitoring of therapeutic responses.
Regenerative medicine: Nanotechnology can be employed to develop scaffolds or nanomaterials that promote tissue regeneration and repair.
Gene therapy: Nanocarriers can be designed to transport genetic material into cells, allowing for the correction of genetic defects or the manipulation of gene expression.
Immunotherapy: Nanoparticles can be used to modulate the immune system, either by enhancing immune responses or suppressing overactive immune reactions.

GPT-4

Nanobots

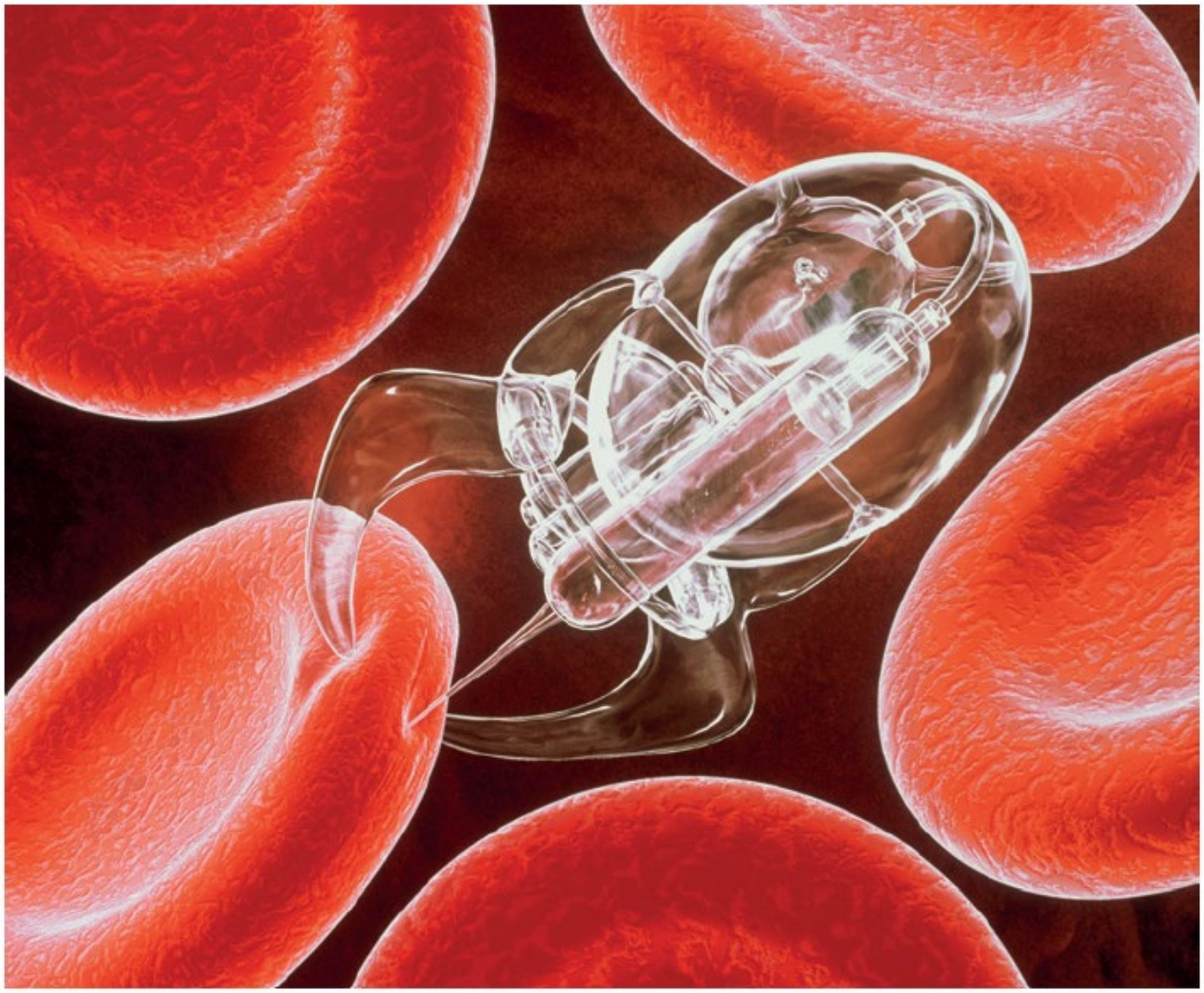

Virus Infection

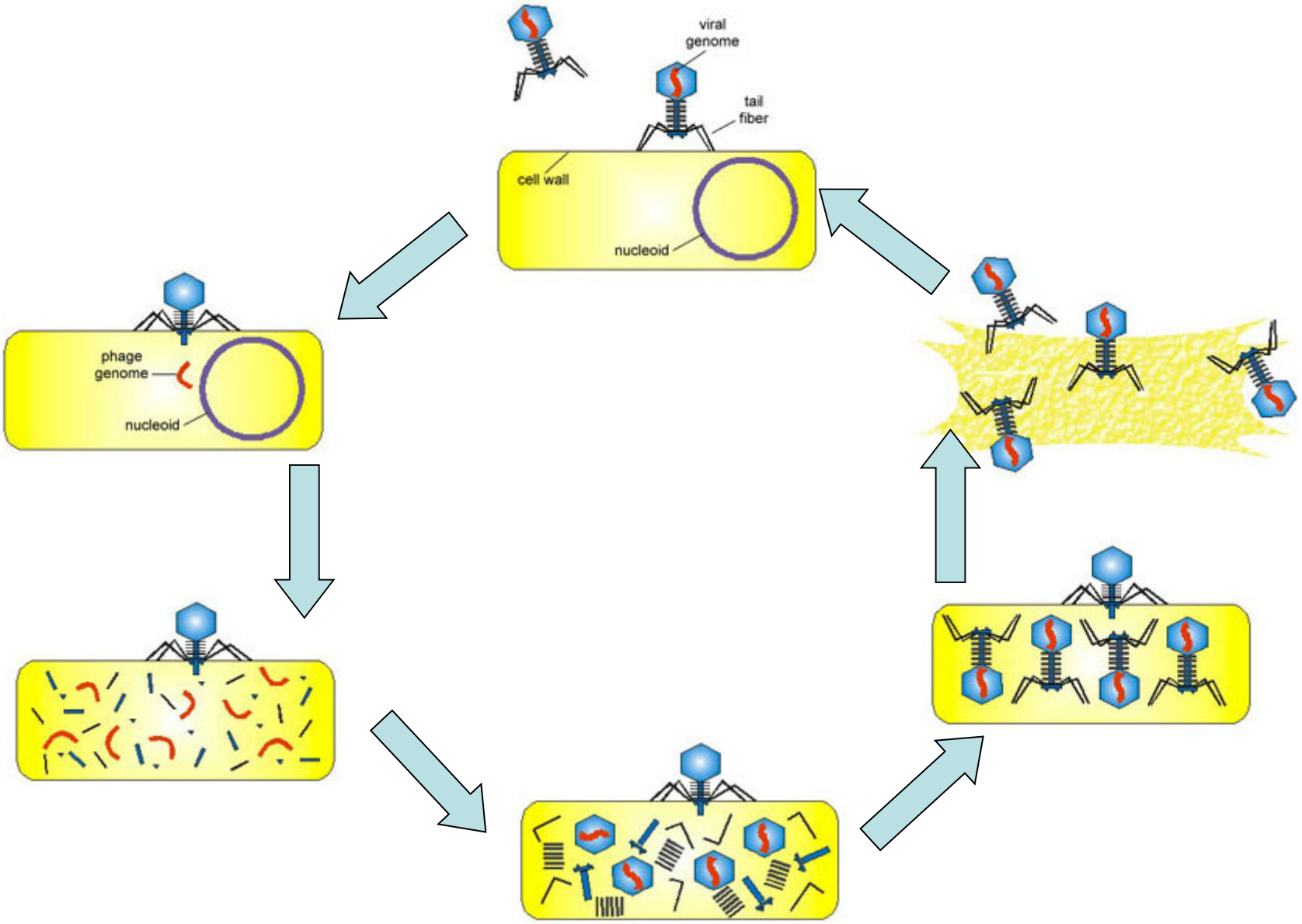

Cancer Hallmark

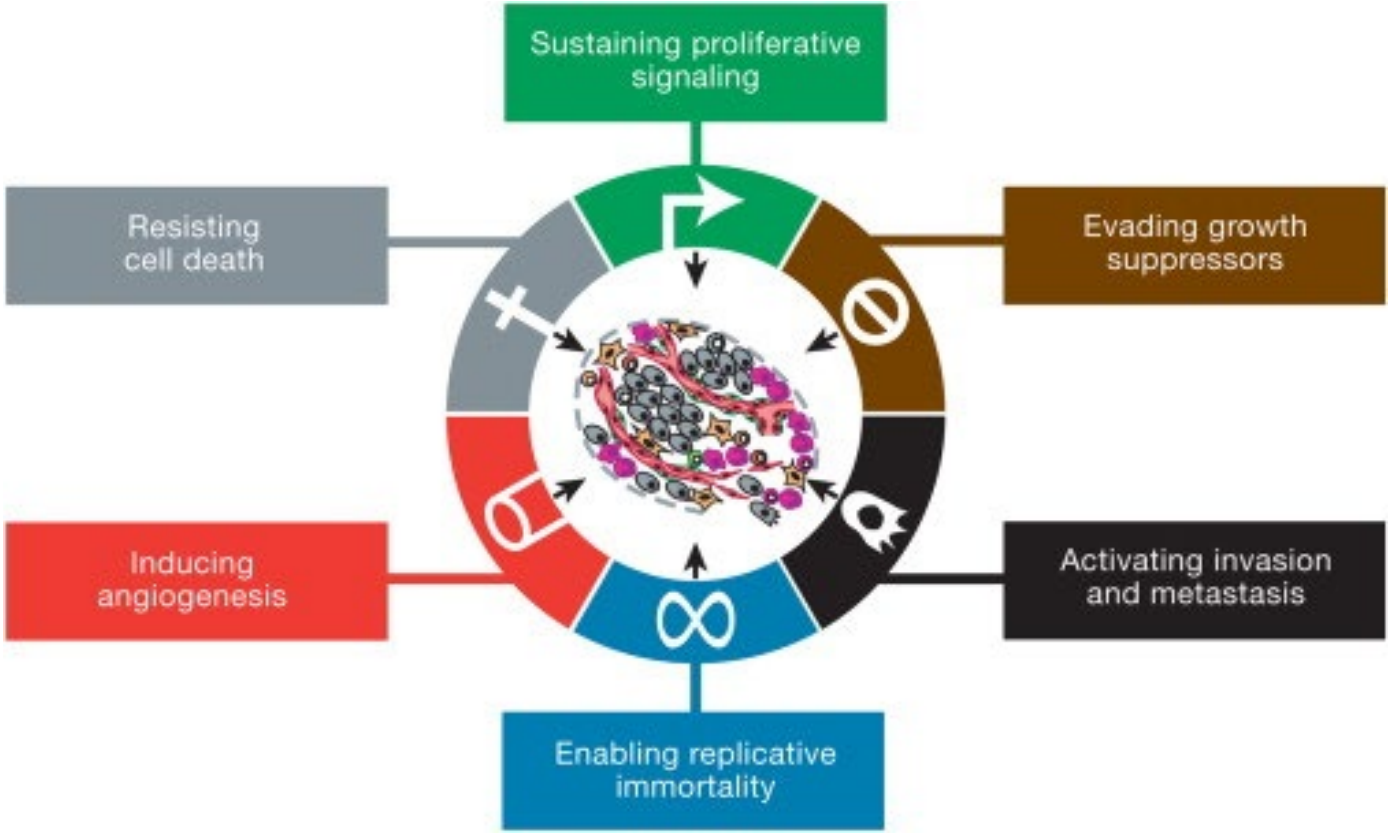

Sustained proliferative signaling: Cancer cells can stimulate their own growth by producing growth factors or by overactivating growth factor receptors.

Evasion of growth suppressors: Cancer cells can bypass cellular mechanisms that normally inhibit cell growth and division, such as tumor suppressor genes like p53 and Rb.

Resistance to cell death: Cancer cells can avoid apoptosis, the programmed cell death that occurs when cells are damaged or dysfunctional, allowing them to survive and multiply.

Replicative immortality: Cancer cells can maintain the length of their telomeres, the protective caps on the ends of chromosomes, which enables them to divide indefinitely.

Induction of angiogenesis: Cancer cells can stimulate the formation of new blood vessels (angiogenesis) to supply the growing tumor with oxygen and nutrients.

Activation of invasion and metastasis: Cancer cells can break away from the primary tumor, invade surrounding tissues, and form secondary tumors in distant sites.

Hanahan, D., & Weinberg, R. A. (2000). The hallmarks of cancer. Cell, 100(1), 57-70.

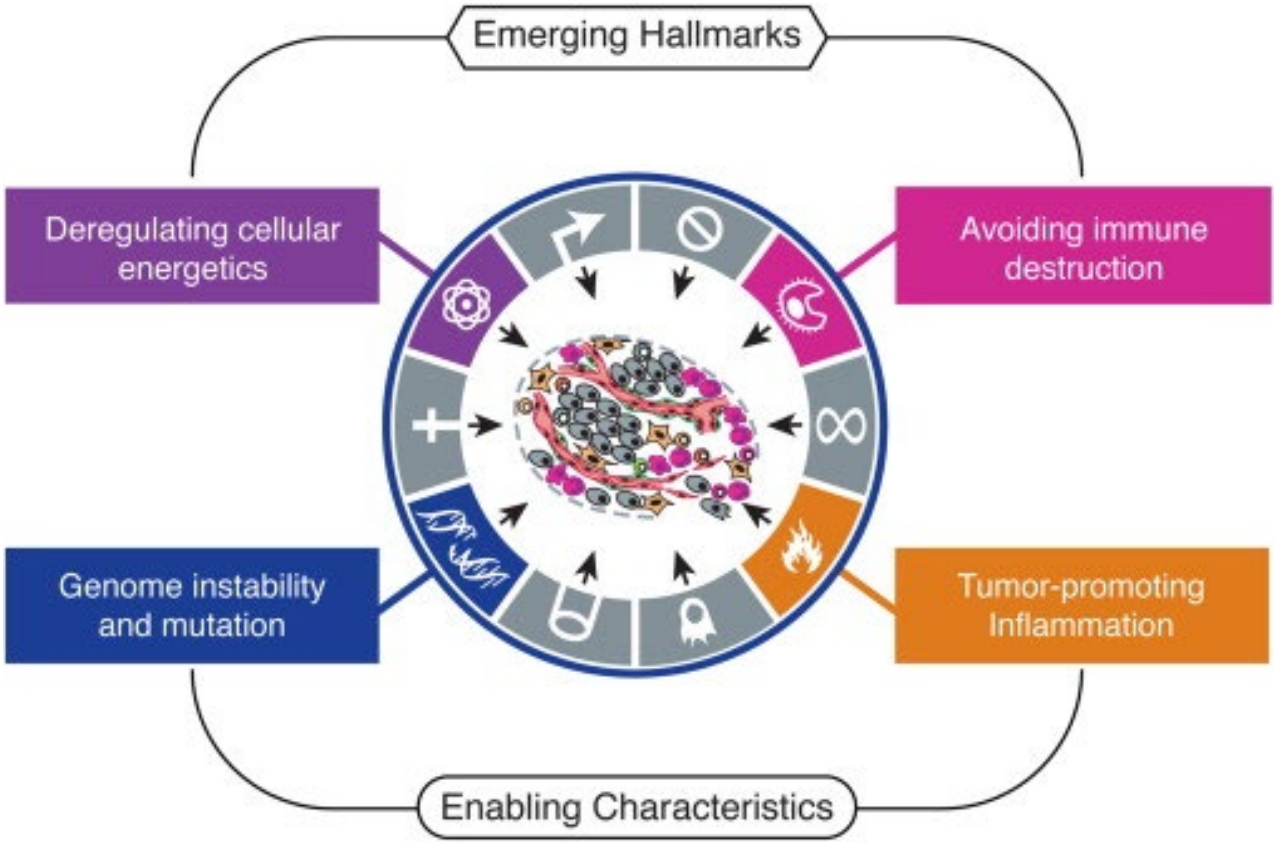

An increasing body of research suggests that two additional hallmarks of cancer are involved in the pathogenesis of some and perhaps all cancers. One involves the capability to modify, or reprogram, cellular metabolism in order to most effectively support neoplastic proliferation. The second allows cancer cells to evade immunological destruction, in particular by T and B lymphocytes, macrophages, and natural killer cells. Because neither capability is yet generalized and fully validated, they are labeled as emerging hallmarks. Additionally, two consequential characteristics of neoplasia facilitate acquisition of both core and emerging hallmarks. Genomic instability and thus mutability endow cancer cells with genetic alterations that drive tumor progression. Inflammation by innate immune cells designed to fight infections and heal wounds can instead result in their inadvertent support of multiple hallmark capabilities, thereby manifesting the now widely appreciated tumor-promoting consequences of inflammatory responses.

Deregulation of cellular energetics: Cancer cells often exhibit altered metabolism, such as increased glucose uptake and glycolysis, even in the presence of oxygen (a phenomenon known as the Warburg effect).

Avoiding immune destruction: Cancer cells can evade detection and destruction by the immune system through various mechanisms, such as the expression of immune checkpoint proteins.

(Enabling characteristic) **Genome instability and mutation**: Cancer cells often have increased genomic instability, leading to a higher rate of mutations that can drive the acquisition of the other cancer hallmarks.

(Enabling characteristic) **Tumor-promoting inflammation**: Inflammation can create a tumor-promoting environment that fosters the growth, survival, and spread of cancer cells.

Hanahan, D., & Weinberg, R. A. (2011). Hallmarks of cancer: the next generation. Cell, 144(5), 646-674.

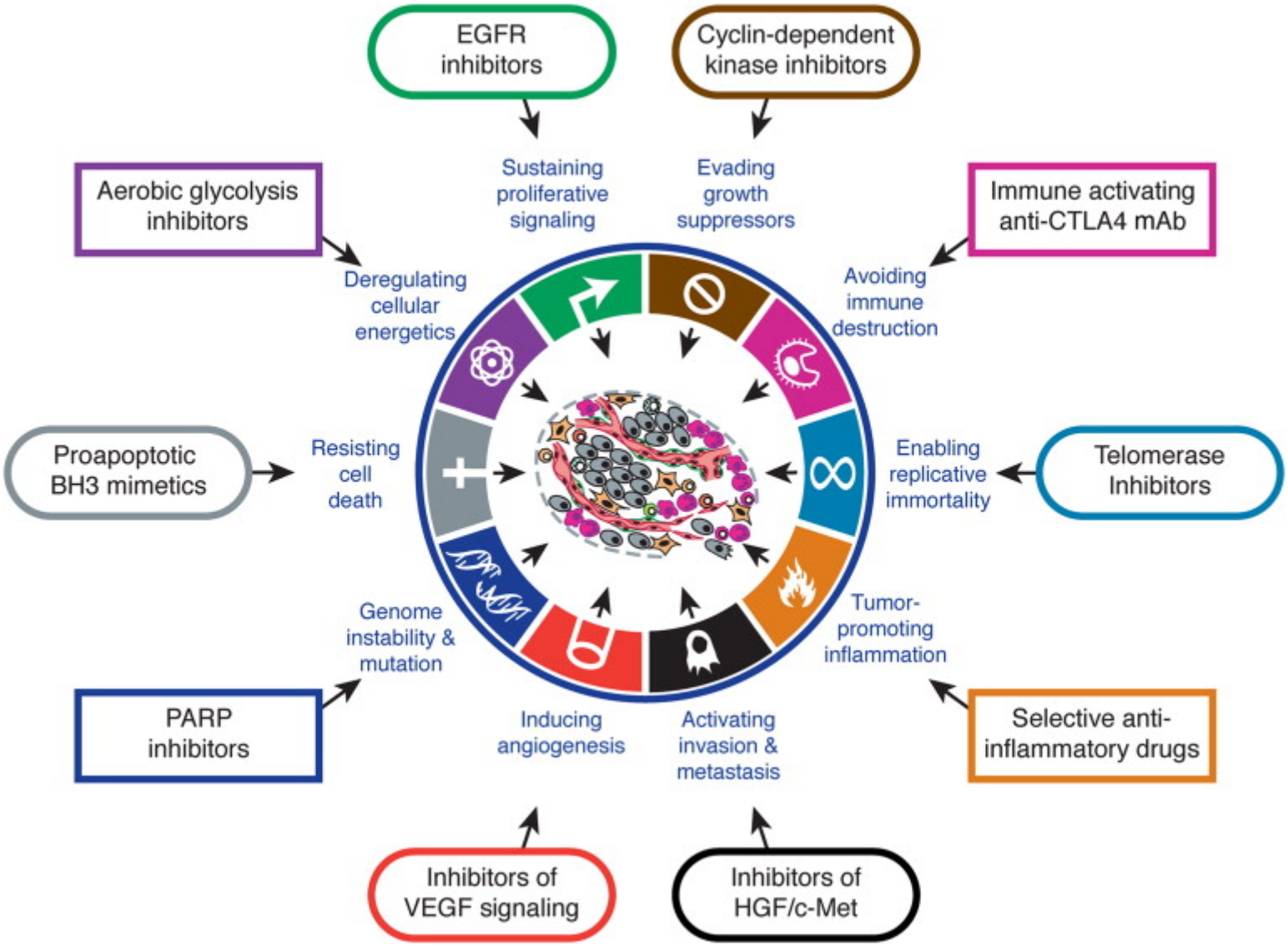
EGFR inhibitors
Cyclin-dependent kinase inhibitors
Sustaining proliferative signaling
Evading growth suppressors
Aerobic glycolysis inhibitors
Immune activating anti-CTLA4 mAb
Deregulating cellular energetics
Avoiding immune destruction
Proapoptotic BH3 mimetics
Resisting cell death
Enabling replicative immortality
Telomerase Inhibitors
Genome instability & mutation
Tumor-promoting inflammation
PARP inhibitors
Inducing angiogenesis
Activating invasion & metastasis
Selective anti-inflammatory drugs
Inhibitors of VEGF signaling
Inhibitors of HGF/c-Met

Cancer nanomedicine: progress, challenges and opportunities

Jinjun Shi[1], Philip W. Kantoff[2], Richard Wooster[3] and Omid C. Farokhzad[1,4]

Box 1 | **Distinctive features of nanotechnology in oncological applications**

- Improvement of the drug therapeutic index by increasing efficacy and/or reducing toxicities
- Targeted delivery of drugs in a tissue-, cell- or organelle-specific manner
- Enhancement of the pharmaceutical properties (for example, stability, solubility, circulating half-life and tumour accumulation) of therapeutic molecules
- Enabling of sustained or stimulus-triggered drug release
- Facilitation of the delivery of biomacromolecular drugs (for example, DNA, small interfering RNA (siRNA), mRNA and protein) to intracellular sites of action
- Co-delivery of multiple drugs to improve therapeutic efficacy and overcome drug resistance, by providing more precise control of the spatiotemporal exposure of each drug and the delivery of appropriate drug ratio to the target of interest
- Transcytosis of drugs across tight epithelial and endothelial barriers (for example, gastrointestinal tract and the blood–brain barrier)
- More sensitive cancer diagnosis and imaging
- Visualization of sites of drug delivery by combining therapeutic agents with imaging modalities, and/or real-time feedback on the *in vivo* efficacy of a therapeutic agent
- Provision of new approaches for the development of synthetic vaccines
- Miniaturized medical devices for cancer diagnosis, drug screening and delivery
- Inherent therapeutic properties of some nanomaterials (for example, gold nanoshells and nanorods, and iron oxide nanoparticles) upon stimulation

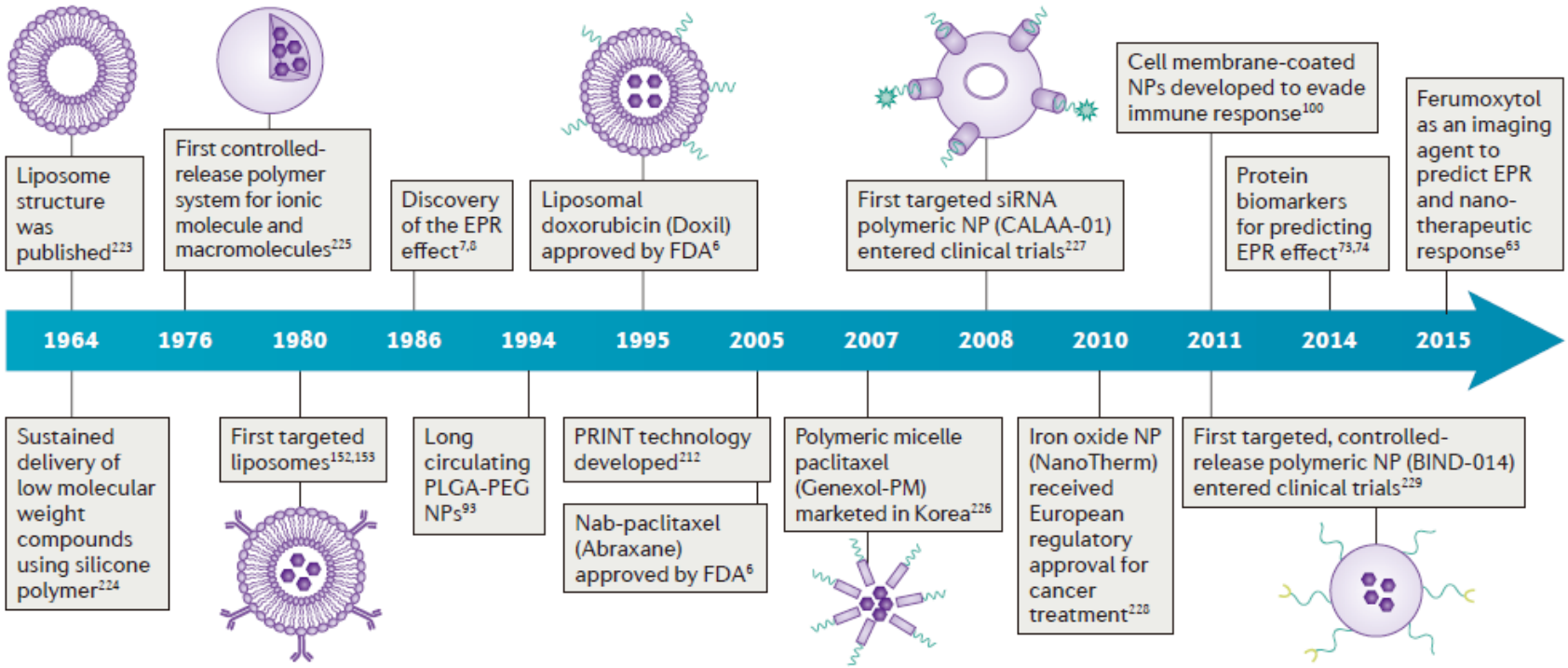

Figure 1 | **Historical timeline of major developments in the field of cancer nanomedicine.** EPR, enhanced permeability and retention; FDA, US Food and Drug Administration; nab, nanoparticle albumin-bound; NP, nanoparticle; PLGA-PEG, poly(D,L-lactic-*co*-glycolic acid)-*b*-poly(ethylene glycol); PRINT, particle replication in non-wetting template; siRNA, small interfering RNA.

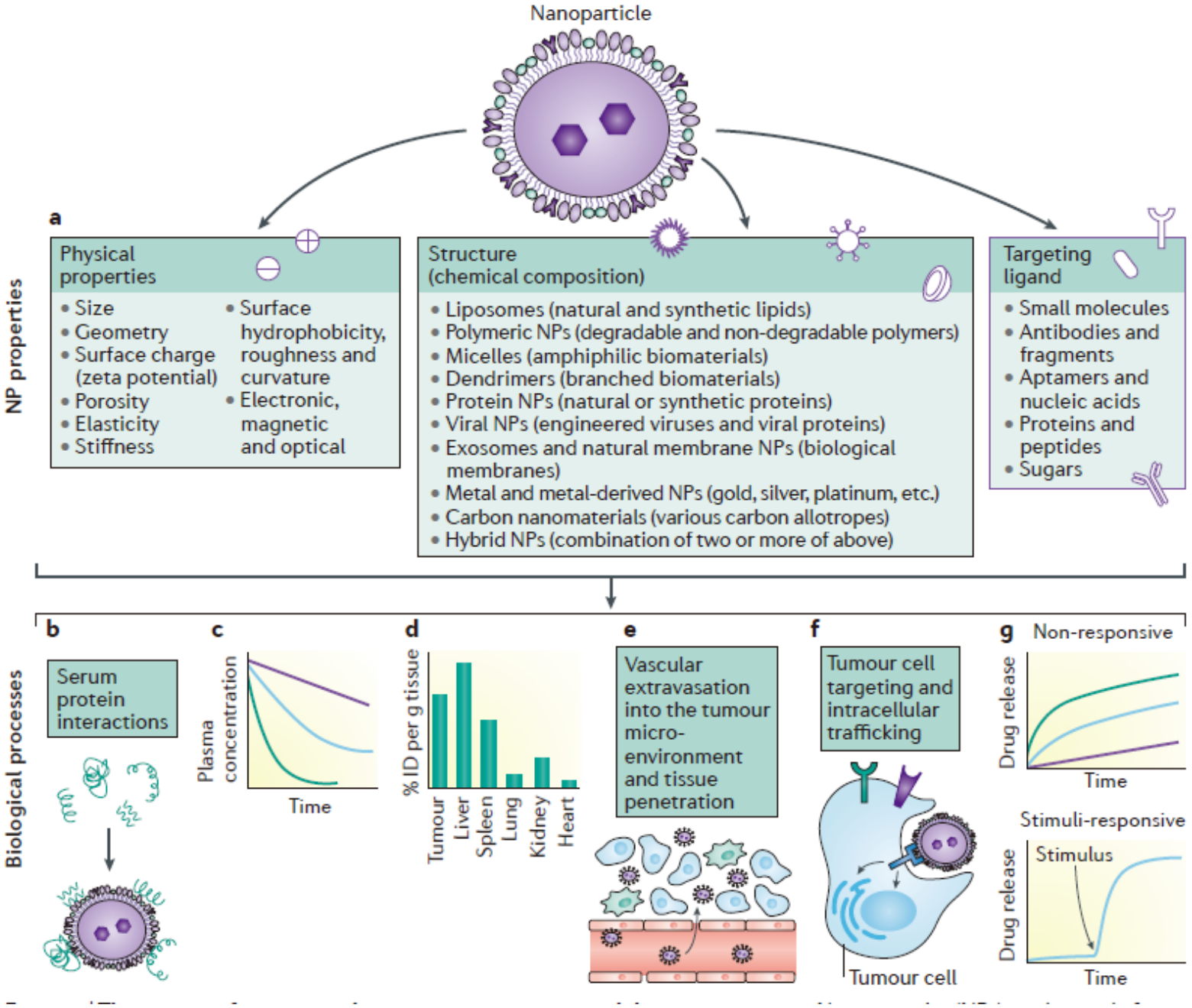
Nanoparticle
a
NP properties
Physical properties
• Size
• Geometry
• Surface charge (zeta potential)
• Porosity
• Elasticity
• Stiffness
• Surface hydrophobicity, roughness and curvature
• Electronic, magnetic and optical
Structure (chemical composition)
• Liposomes (natural and synthetic lipids)
• Polymeric NPs (degradable and non-degradable polymers)
• Micelles (amphiphilic biomaterials)
• Dendrimers (branched biomaterials)
• Protein NPs (natural or synthetic proteins)
• Viral NPs (engineered viruses and viral proteins)
• Exosomes and natural membrane NPs (biological membranes)
• Metal and metal-derived NPs (gold, silver, platinum, etc.)
• Carbon nanomaterials (various carbon allotropes)
• Hybrid NPs (combination of two or more of above)
Targeting ligand
• Small molecules
• Antibodies and fragments
• Aptamers and nucleic acids
• Proteins and peptides
• Sugars
Biological processes
b
Serum protein interactions
c
Plasma concentration
Time
d
% ID per g tissue
Tumour
Liver
Spleen
Lung
Kidney
Heart
e
Vascular extravasation into the tumour micro-environment and tissue penetration
f
Tumour cell targeting and intracellular trafficking
Tumour cell
g
Non-responsive
Drug release
Time
Stimuli-responsive
Drug release
Stimulus
Time

EPR Effect

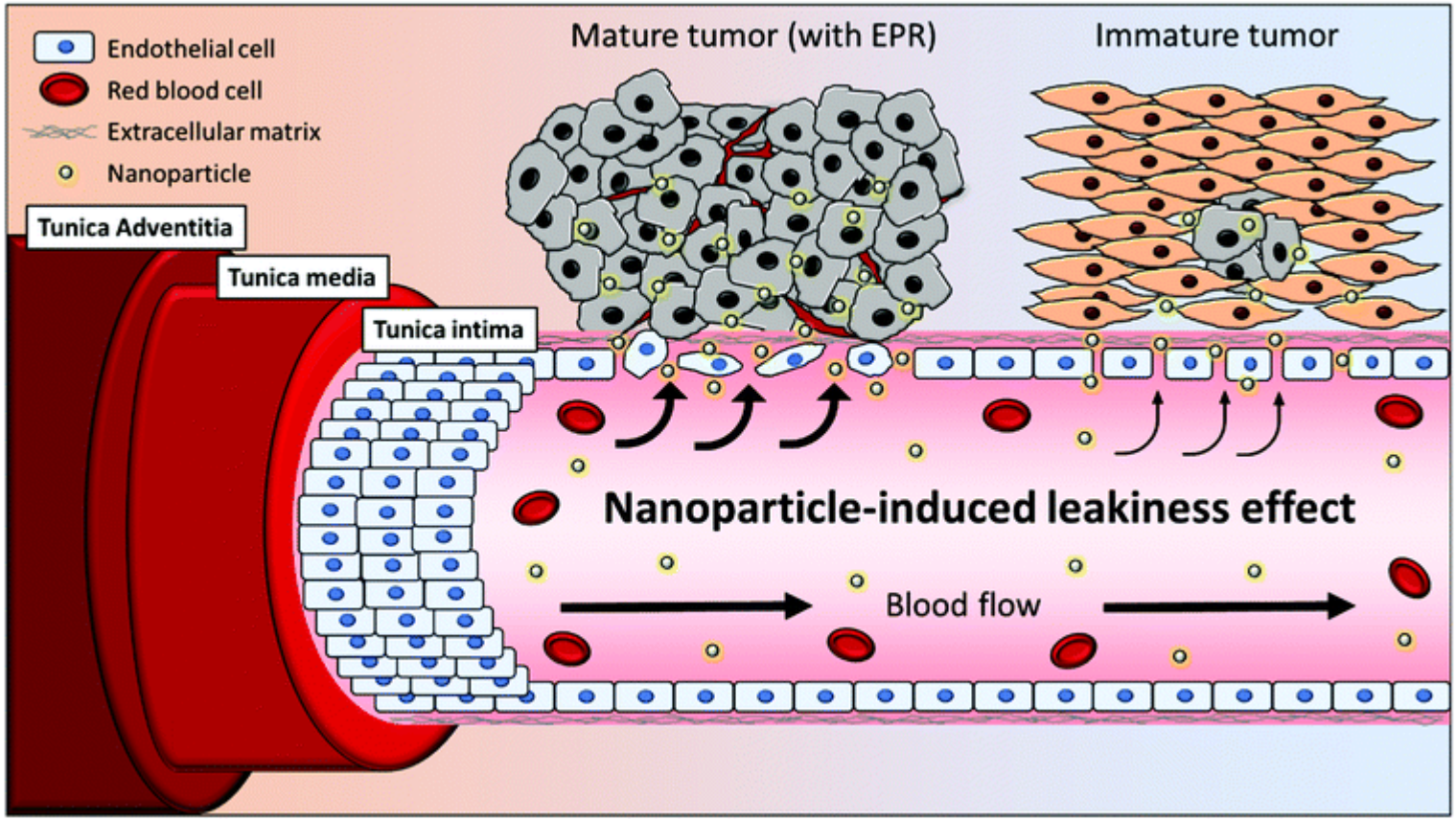
Endothelial cell
Red blood cell
Extracellular matrix
Nanoparticle
Tunica Adventitia
Tunica media
Tunica intima
Mature tumor (with EPR)
Immature tumor
Nanoparticle-induced leakiness effect
Blood flow

The Enhanced Permeability and Retention (EPR) effect is a phenomenon that is commonly exploited in nanomedicine for the passive targeting of nanoparticles to solid tumors. The EPR effect is based on the unique characteristics of the tumor microenvironment, which include leaky blood vessels and impaired lymphatic drainage.

In solid tumors, the rapid growth of cancer cells leads to the formation of new blood vessels through a process called angiogenesis. However, these newly formed blood vessels are often disorganized and have large gaps between endothelial cells, resulting in increased permeability. This enhanced permeability allows nanoparticles, which are typically in the size range of 10-200 nm, to passively accumulate in the tumor tissue more efficiently than in healthy tissues.

The second key factor contributing to the EPR effect is the impaired lymphatic drainage in the tumor microenvironment. The lymphatic system is responsible for removing excess fluids, proteins, and waste products from tissues. However, in tumors, the lymphatic vessels are often compressed or dysfunctional, which hinders their ability to efficiently drain the accumulated substances. This results in the retention of nanoparticles within the tumor tissue for extended periods, allowing them to exert their therapeutic effects.

The EPR effect provides a passive targeting mechanism for nanomedicines, enhancing their accumulation and retention within solid tumors, while reducing their distribution to healthy tissues. t.

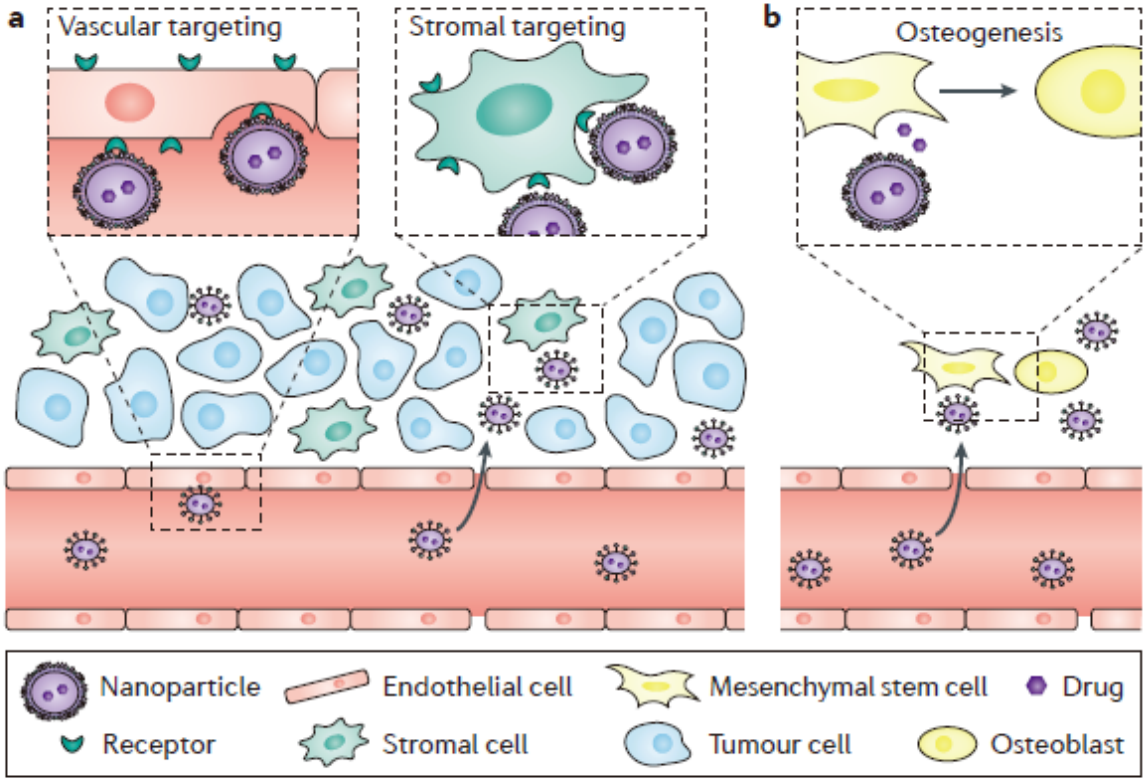

Figure 4 | **Nanoparticle targeting of the tumour microenvironment and the premetastatic niche**. Targeting of the tumour vasculature or stromal cells in the tumour microenvironment (part **a**) and the premetastatic microenvironments such as the bone marrow niche, where induction of the osteogenic differentiation of mesenchymal stem cells enhances bone strength and volume (part **b**). Cell-specific targeting can be achieved via the modification of nanoparticles (NPs) with ligands that bind to specific receptors (for example, $\alpha_v\beta_3$ integrin and mannose receptor) on the surface of tumour endothelial cells, stromal cells or other target cells. It should be noted that even without targeting ligands, NPs can be engineered for preferential cellular uptake. The payloads released from NPs localized in tumours or premetastatic tissues can also be nonspecifically taken up by these cells.

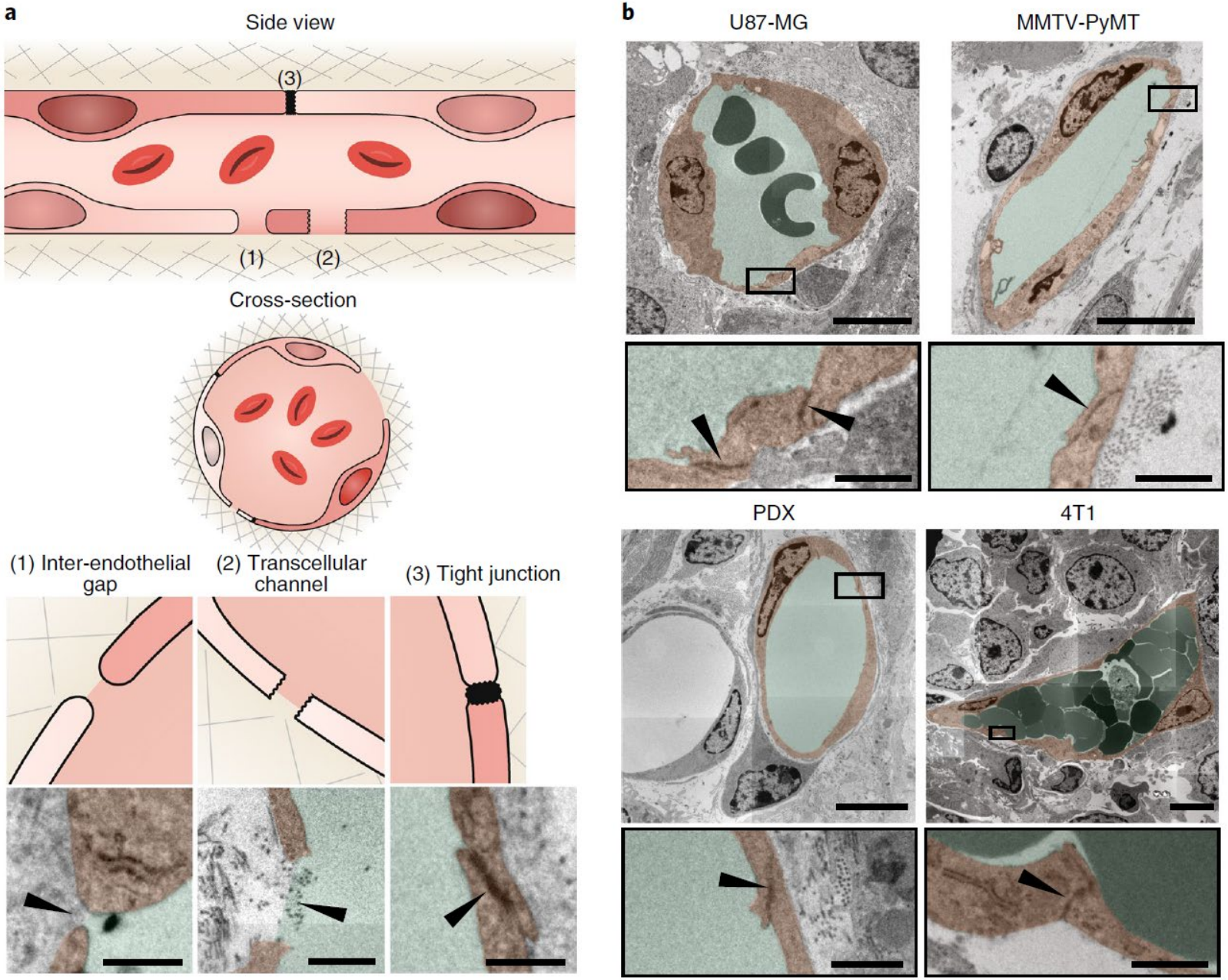
a
Side view
(3)
(1)
(2)
Cross-section
(1) Inter-endothelial gap
(2) Transcellular channel
(3) Tight junction
b
U87-MG
MMTV-PyMT
PDX
4T1

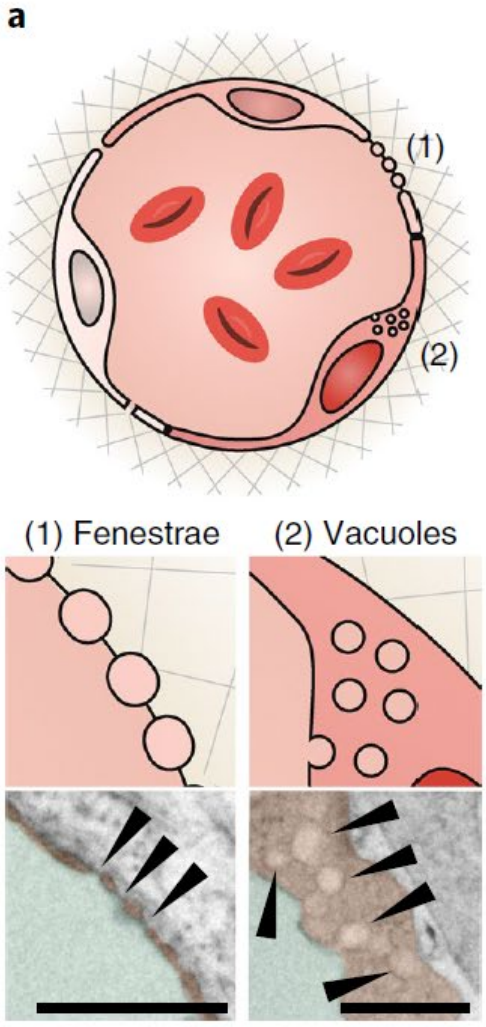
a
(1)
(2)
(1) Fenestrae
(2) Vacuoles

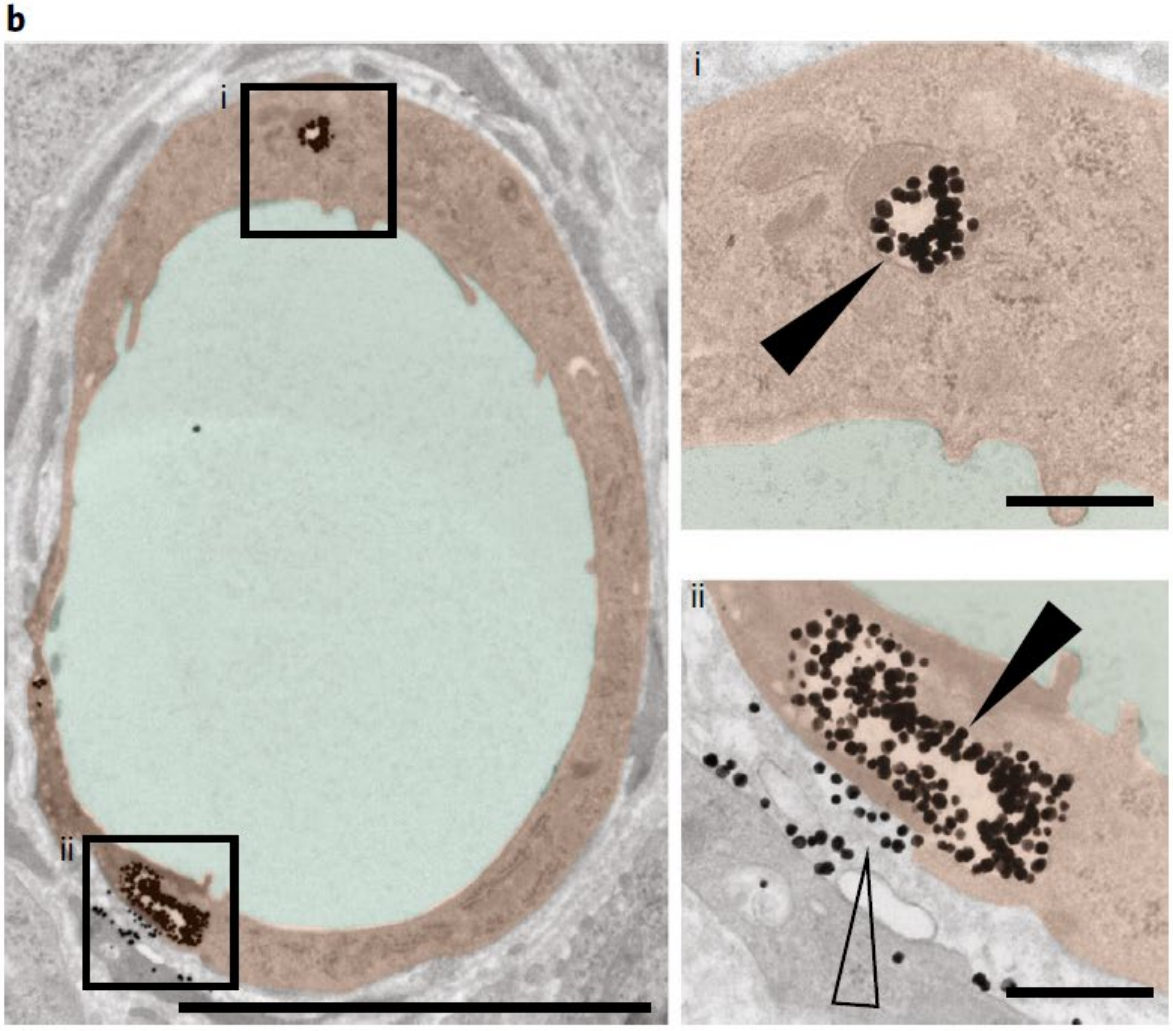
b
i
ii
i
ii

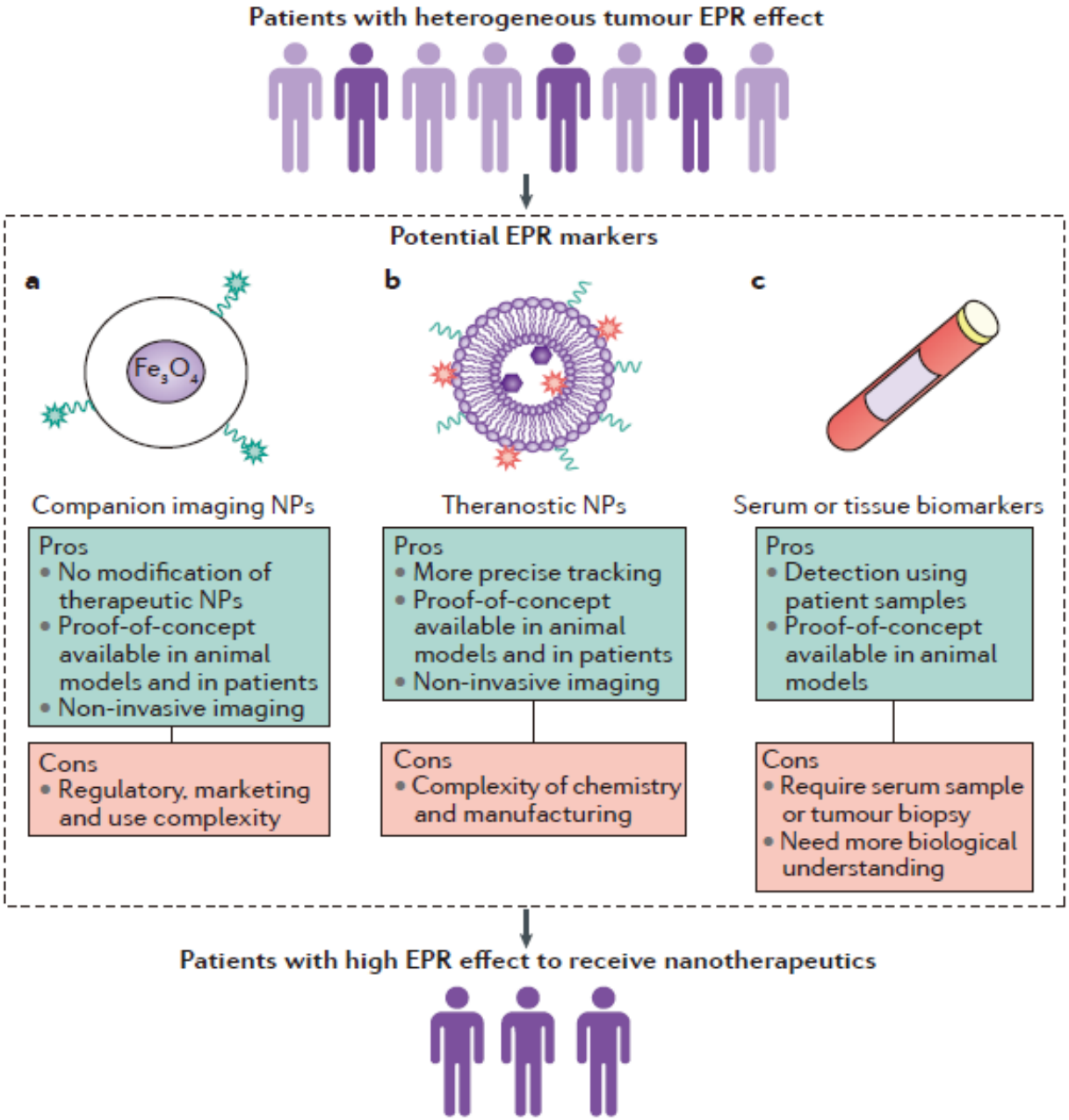
Patients with heterogeneous tumour EPR effect
Potential EPR markers
a
b
c
Fe_3O_4
Companion imaging NPs
Theranostic NPs
Serum or tissue biomarkers
Pros
• No modification of therapeutic NPs
• Proof-of-concept available in animal models and in patients
• Non-invasive imaging
Cons
• Regulatory, marketing and use complexity
Pros
• More precise tracking
• Proof-of-concept available in animal models and in patients
• Non-invasive imaging
Cons
• Complexity of chemistry and manufacturing
Pros
• Detection using patient samples
• Proof-of-concept available in animal models
Cons
• Require serum sample or tumour biopsy
• Need more biological understanding
Patients with high EPR effect to receive nanotherapeutics

Potential EPR Markers

Vascular endothelial growth factor (VEGF): VEGF is a key factor that stimulates angiogenesis in tumors, promoting the formation of disorganized and leaky blood vessels. High levels of VEGF in a tumor may suggest an increased likelihood of the EPR effect.

Angiopoietin-2 (Ang-2): Ang-2 is another angiogenic factor that contributes to the formation of leaky blood vessels in tumors. Like VEGF, elevated levels of Ang-2 may indicate a tumor microenvironment conducive to the EPR effect.

Hypoxia-inducible factors (HIFs): HIFs are transcription factors that are activated under low oxygen conditions (hypoxia), which are common in solid tumors. HIFs regulate the expression of various genes involved in angiogenesis, including VEGF, and can, therefore, serve as indirect indicators of the EPR effect.

Endoglin (CD105): Endoglin is a protein that is highly expressed on the surface of endothelial cells involved in angiogenesis. It can be used as a marker to identify newly formed blood vessels in tumors and may provide some indication of the EPR effect.

Platelet-derived growth factor (PDGF): PDGF is another factor involved in angiogenesis and blood vessel maturation. Elevated levels of PDGF may be associated with the formation of leaky blood vessels in the tumor microenvironment, which can contribute to the EPR effect.

Table 1. Examples of Nanomaterials in Clinical Use.*

Nanomaterial	Trade Name	Application	Target	Adverse Effects	Manufacturer	Current Status
Metallic						
Iron oxide	Feridex	MRI contrast	Liver	Back pain, vasodilatation	Bayer Schering	FDA approved
	Resovist	MRI contrast	Liver	None	Bayer Schering	FDA approved
	Combidex	MRI contrast	Lymph nodes	None	Advanced Magnetics	In phase 3 clinical trials
	NanoTherm	Cancer therapy	Various forms	Acute urinary retention	MagForce	In phase 3 clinical trials
Gold	Verigene	In vitro diagnostics	Genetic	Not applicable	Nanosphere	FDA approved
	Aurimmune	Cancer therapy	Various forms	Fever	CytImmune Sciences	In phase 2 clinical trials
Nanoshells	Auroshell	Cancer therapy	Head and neck	Under investigation	Nanospectra Biosciences	In phase 1 clinical trials
Semiconductor						
Quantum dot	Qdots, EviTags, semiconductor nanocrystals	Fluorescent contrast, in vitro diagnostics	Tumors, cells, tissues, and molecular sensing structures	Not applicable	Life Technologies, eBioscience, Nanoco, CrystalPlex, Cytodiagnostics	Research use only
Organic						
Protein	Abraxane	Cancer therapy	Breast	Cytopenia	Abraxis Bioscience	FDA approved
Liposome	Doxil/Caelyx	Cancer therapy	Various forms	Hand–foot syndrome, stomatitis	Ortho Biotech	FDA approved
Polymer	Oncaspar	Cancer therapy	Acute lymphoblastic leukemia	Urticaria, rash	Rhône-Poulenc Rorer	FDA approved
	CALAA-01	Cancer therapy	Various forms	Mild renal toxicity	Calando	In phase 2 clinical trials
Dendrimer	VivaGel	Microbicide	Cervicovaginal	Abdominal pain, dysuria	Starpharma	In phase 2 clinical trials
Micelle	Genexol-PM	Cancer therapy	Various forms	Peripheral sensory neuropathy, neutropenia	Samyang	For phase 4 clinical trials

* MRI denotes magnetic resonance imaging.

Doxil/Caelyx (liposomal doxorubicin): Doxil (known as Caelyx outside of the US) is a liposomal formulation of the chemotherapy drug doxorubicin. The liposomal encapsulation improves the pharmacokinetics of the drug, reduces side effects such as cardiotoxicity, and enhances its accumulation in tumors.

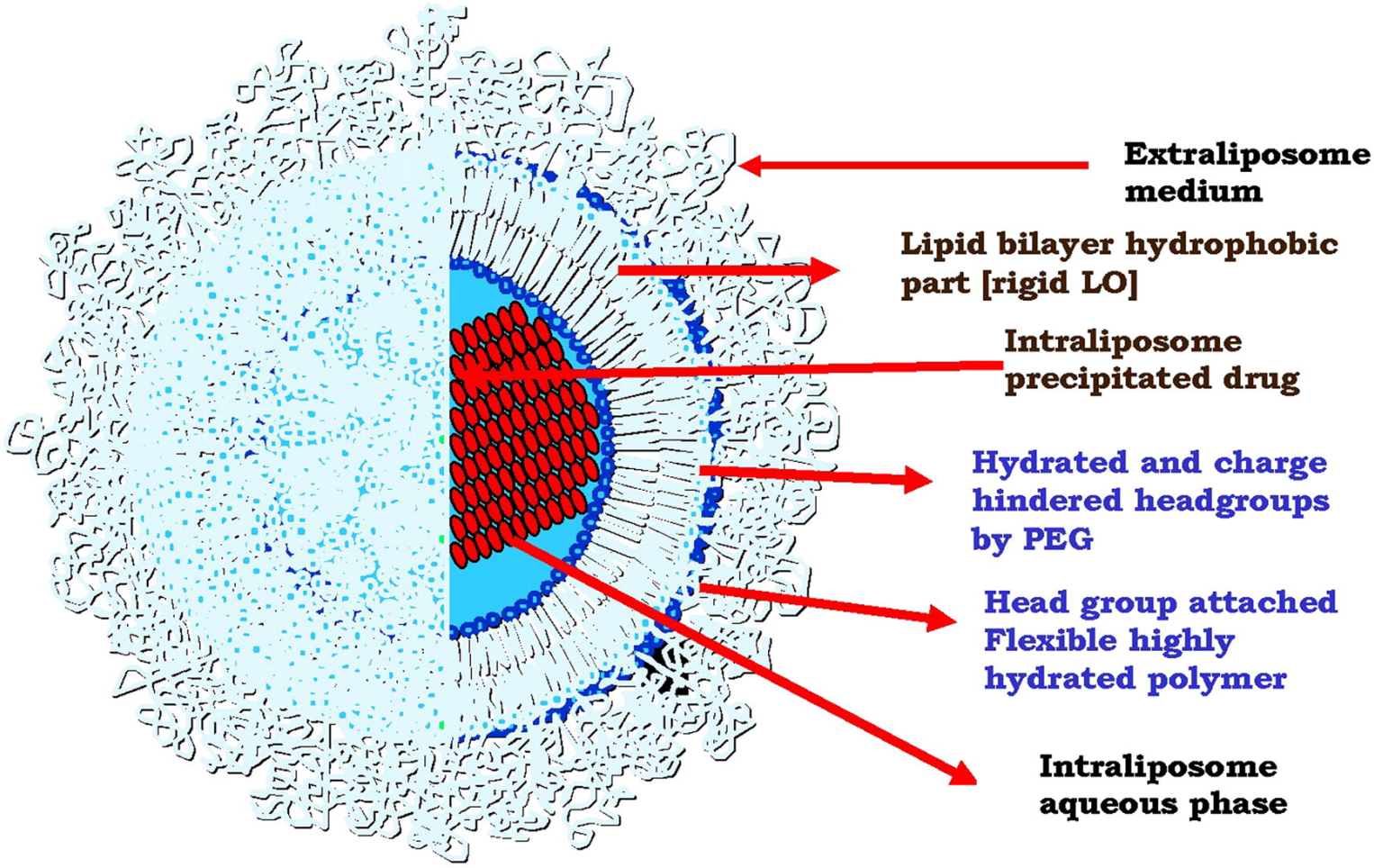

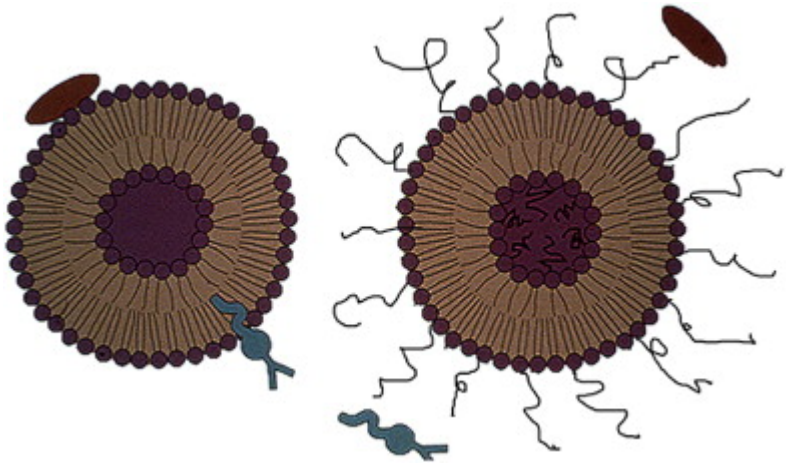

A) Doxil®

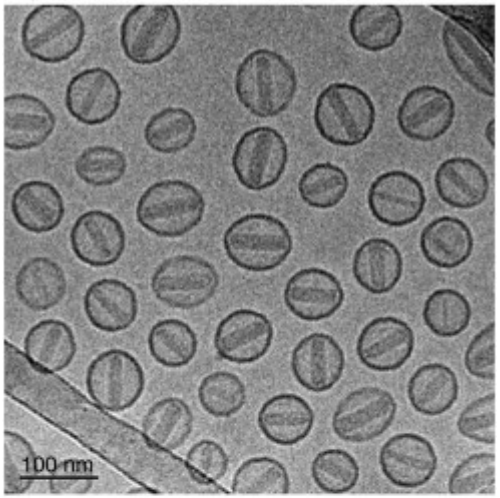

B) DOXG

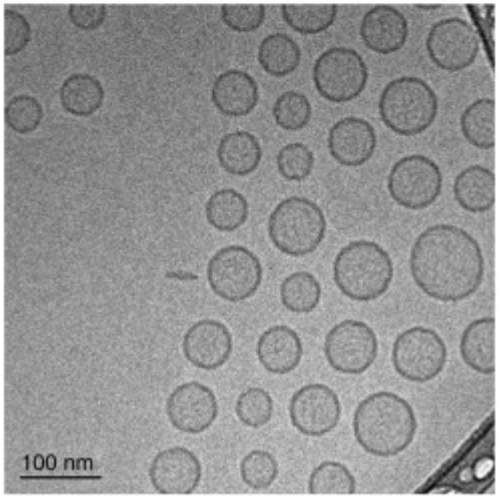

[CANCER RESEARCH 54, 987–992, February 15, 1994]

Prolonged Circulation Time and Enhanced Accumulation in Malignant Exudates of Doxorubicin Encapsulated in Polyethylene-glycol Coated Liposomes[1]

Alberto Gabizon,[2] Raphael Catane, Beatrice Uziely, Bela Kaufman, Tamar Safra, Rivka Cohen, Francis Martin, Anthony Huang, and Yechezkel Barenholz

Sharett Institute of Oncology [A. G., R. C., B. U., B. K., T. S.], Hadassah University Hospital, and Department of Membrane Biochemistry [R. C., Y. B.], Hebrew University-Hadassah Medical School, Jerusalem, Israel; and Liposome Technology, Inc., Menlo Park, California 94025 [F. M., A. H.]

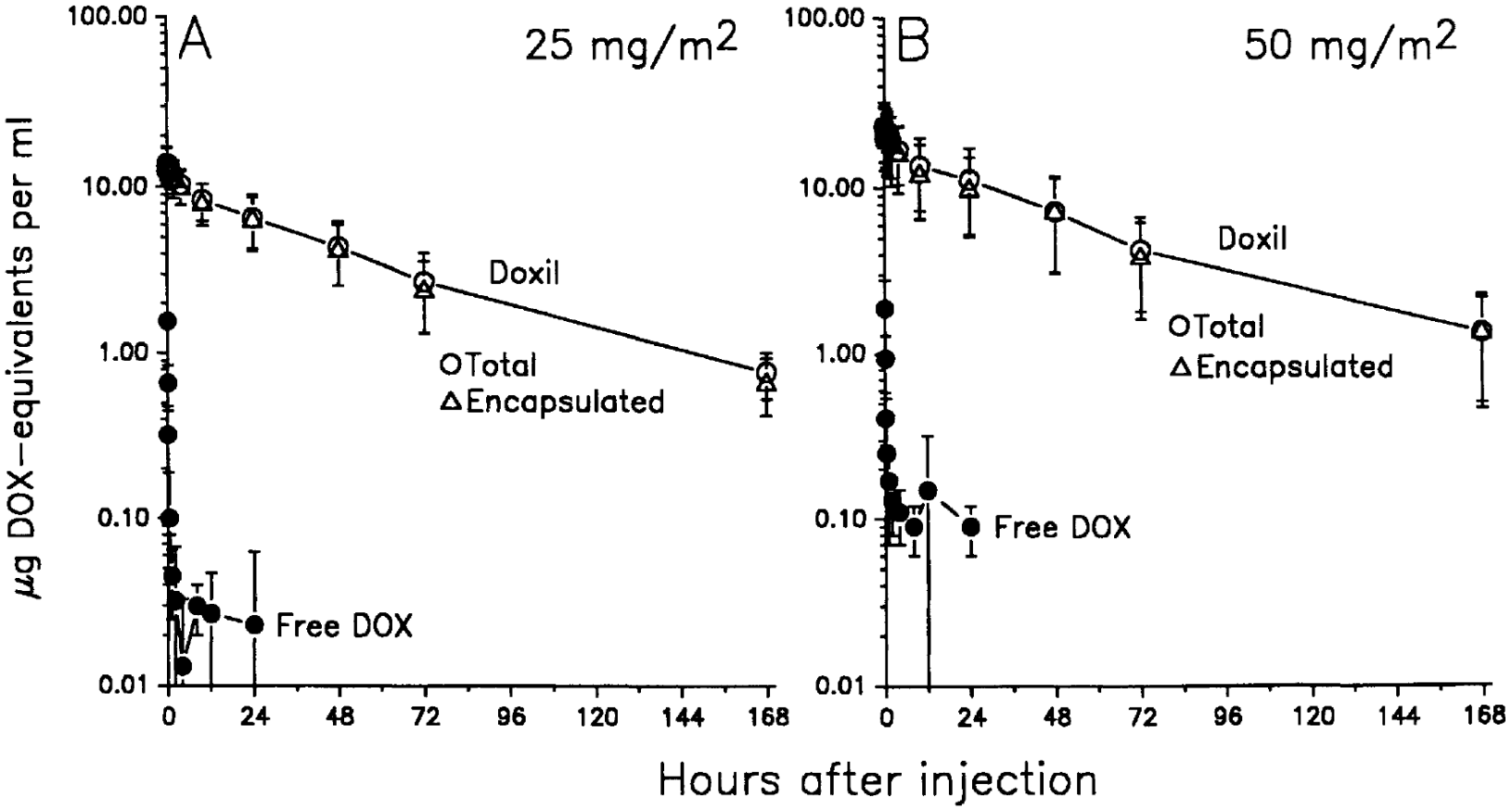

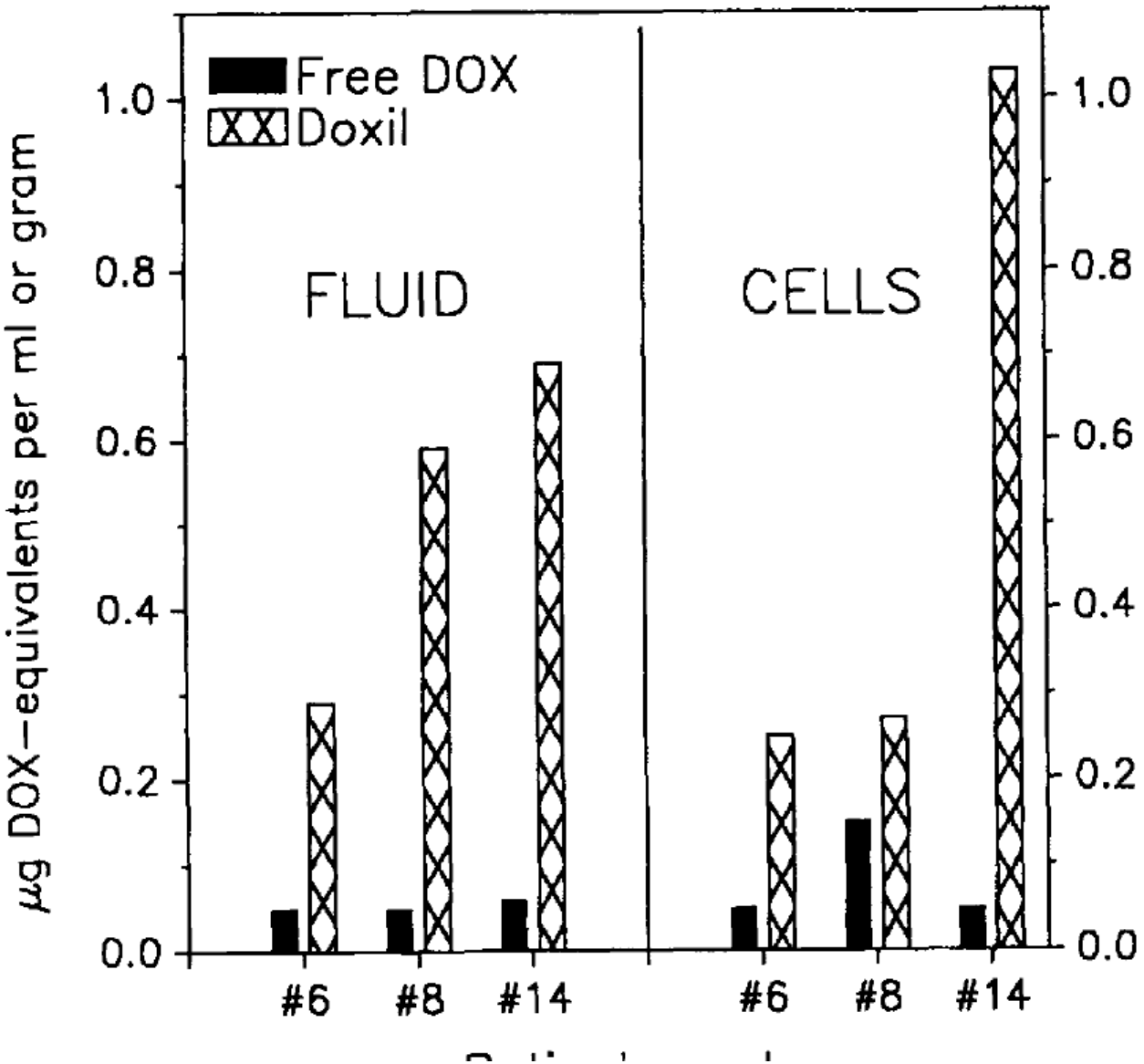
Free DOX
Doxil
FLUID
CELLS
μg DOX—equivalents per ml or gram
1.0
0.8
0.6
0.4
0.2
0.0
#6
#8
#14
#6
#8
#14

Abraxane (albumin-bound paclitaxel)

Abraxane is a nanoparticle-based formulation of the chemotherapy drug paclitaxel, bound to albumin protein. It is used for the treatment of breast cancer, non-small cell lung cancer, and pancreatic cancer. The albumin-bound formulation enhances the solubility of paclitaxel and allows for better drug delivery to tumors.
Journal of Clinical Oncology, 23(31), 7794-7803.

Phase III Trial of Nanoparticle Albumin-Bound Paclitaxel Compared With Polyethylated Castor Oil–Based Paclitaxel in Women With Breast Cancer

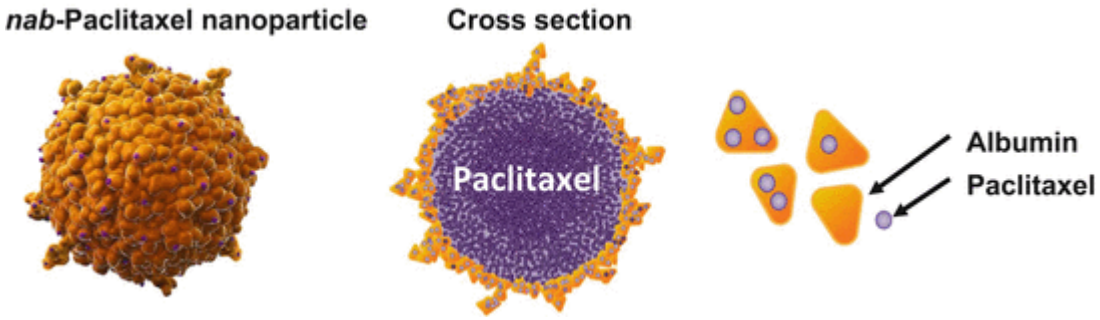

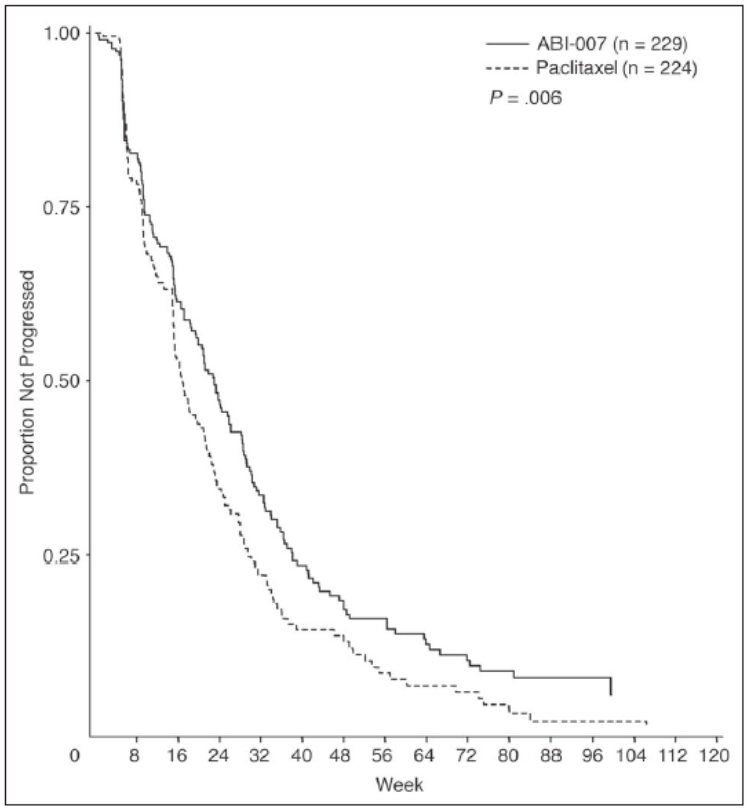

Fig 1. Median time to disease progression.

Results

ABI-007 demonstrated significantly higher response rates compared with standard paclitaxel (33% *v* 19%, respectively; $P = .001$) and significantly longer time to tumor progression (23.0 *v* 16.9 weeks, respectively; hazard ratio = 0.75; $P = .006$). The incidence of grade 4 neutropenia

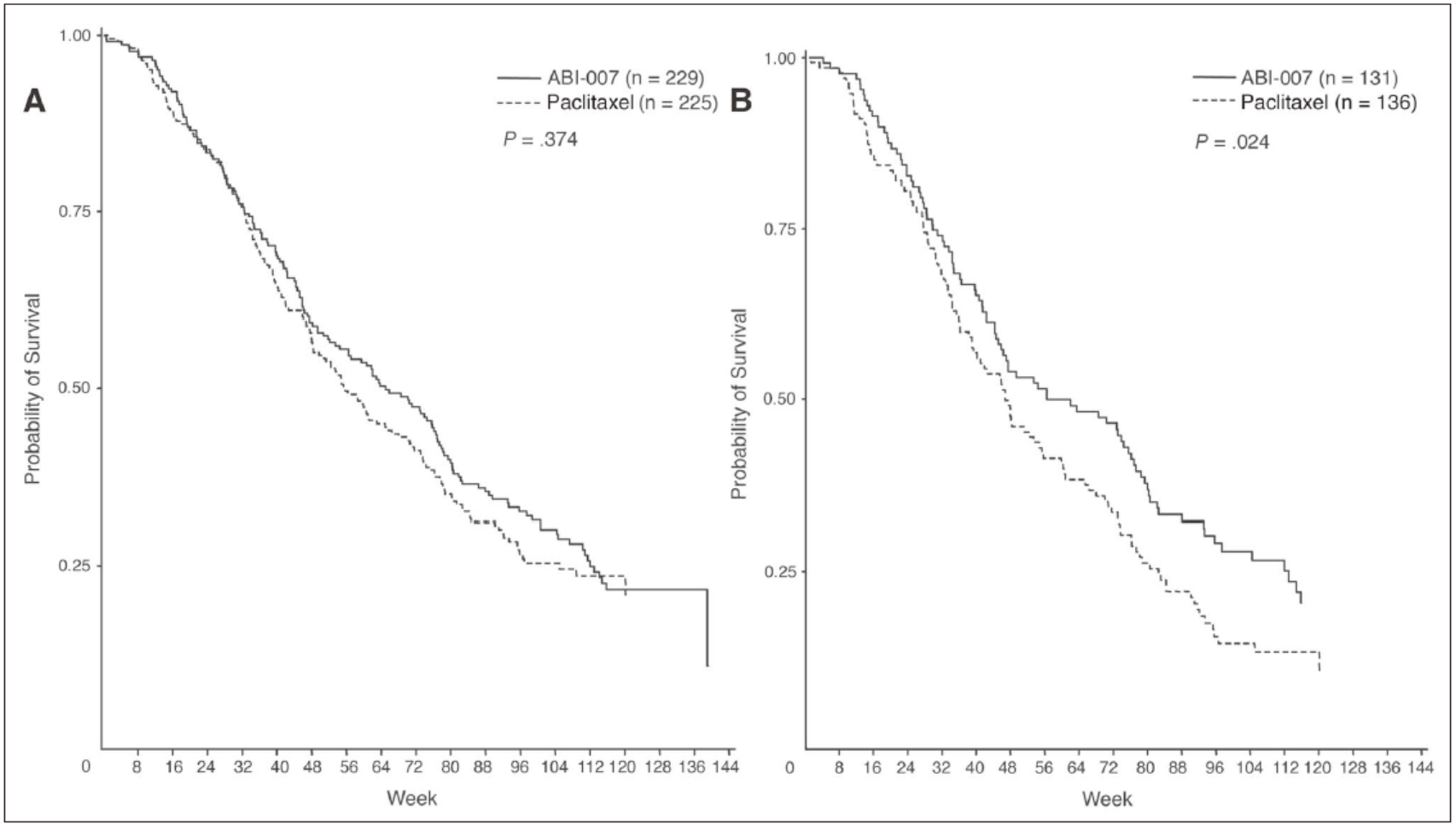

Fig 2. (A) Patient survival over time. (B) Patient survival over time in patients who received second-line or greater therapy. *P* values from log-rank test. Survival indicates time from first dose of study drug to date of death.

Onivyde (liposomal irinotecan): Onivyde is a liposomal formulation of the chemotherapy drug irinotecan, approved for use in combination with other drugs for the treatment of metastatic pancreatic cancer. The liposomal encapsulation improves the pharmacokinetics and biodistribution of irinotecan, increasing its therapeutic effect.

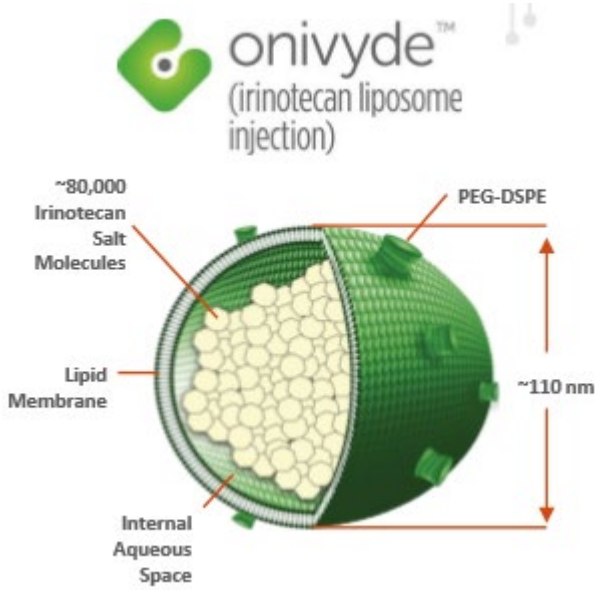

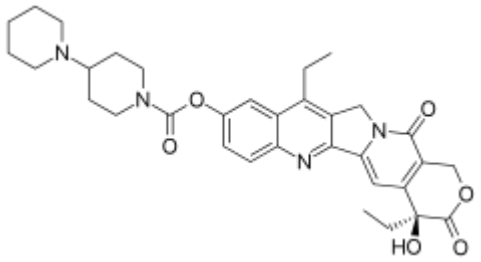

Nanoliposomal irinotecan with fluorouracil and folinic acid in metastatic pancreatic cancer after previous gemcitabine-based therapy (NAPOLI-1): a global, randomised, open-label, phase 3 trial

The Lancet, 387(10018), 545-557.

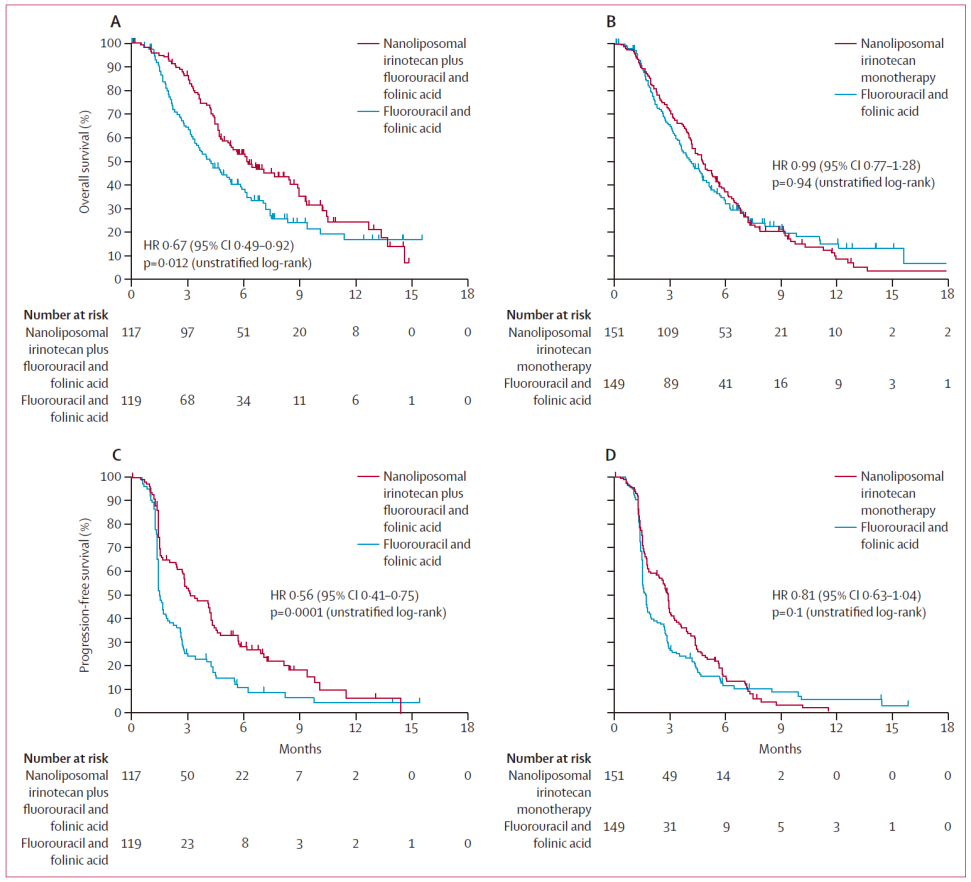

Figure 2: **Kaplan-Meier survival analyses**

HR=hazard ratio. (A) Overall survival with nanoliposomal irinotecan plus fluorouracil and folinic acid versus fluorouracil and folinic acid. (B) Overall survival with nanoliposomal irinotecan monotherapy versus fluorouracil and folinic acid. (C) Progression-free survival with nanoliposomal irinotecan plus fluorouracil and folinic acid versus fluorouracil and folinic acid. (D) Progression-free survival with nanoliposomal irinotecan monotherapy versus fluorouracil and folinic acid.

Targeted Delivery

Active targeting: Active targeting involves the functionalization of nanocarriers with ligands that specifically recognize and bind to receptors or other molecular targets overexpressed on cancer cells or tumor-associated blood vessels. This approach can enhance the selectivity and efficacy of nanomedicines.

Liposomes functionalized with antibodies: Doxil® is a PEGylated liposomal formulation of doxorubicin, an anticancer drug, that passively targets tumors through the EPR effect . Researchers have developed immunoliposomes, which are liposomes conjugated with antibodies specific to cancer cell surface antigens, such as HER2, to actively target cancer cells.

Polymeric nanoparticles: Polymeric nanoparticles have been developed to deliver chemotherapeutic agents, such as paclitaxel, to tumors. For example, Genexol-PM is a formulation of paclitaxel-loaded polymeric micelles that passively target tumors through the EPR effect. Active targeting can be achieved by conjugating ligands, such as folic acid, to polymeric nanoparticles to target cancer cells that overexpress folate receptors

Gold nanoparticles: Gold nanoparticles have been used for the targeted delivery of anticancer drugs and photothermal therapy. For example, researchers have functionalized gold nanoparticles with aptamers, which are short nucleic acid sequences that specifically bind to target molecules, to actively target cancer cells that overexpress the EpCAM antigen

Anti-HER2 Immunoliposomes: Enhanced Efficacy Attributable to Targeted Delivery[1]

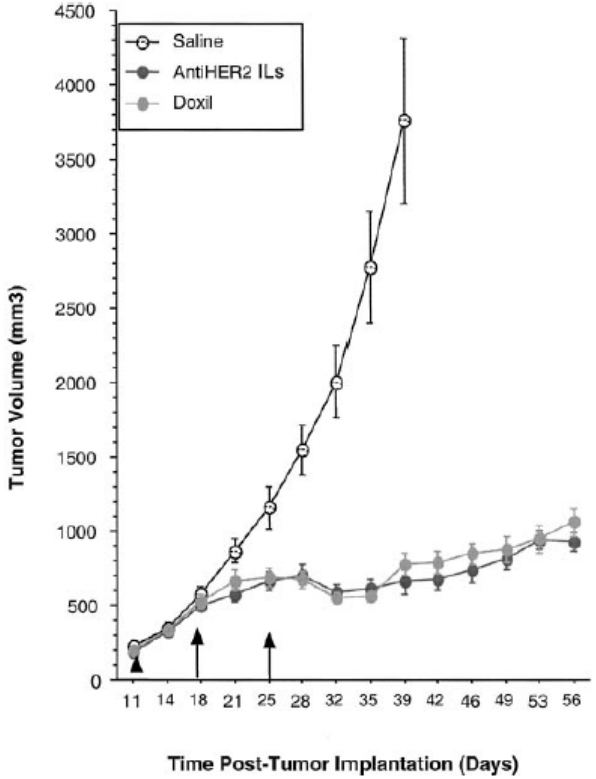

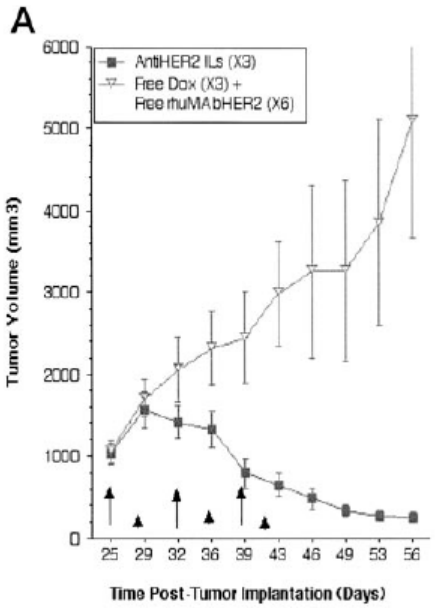

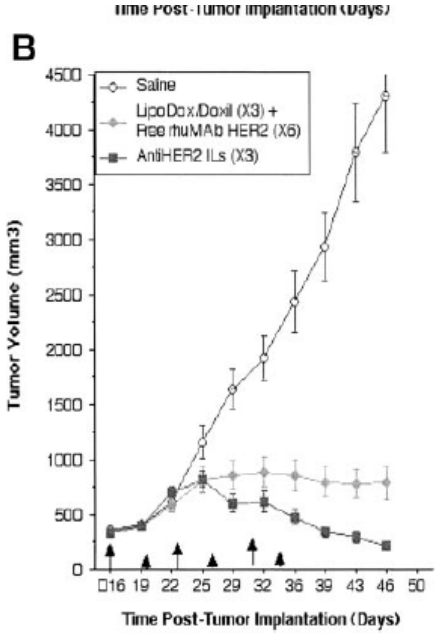

Folate decorated polymeric micelles for targeted delivery

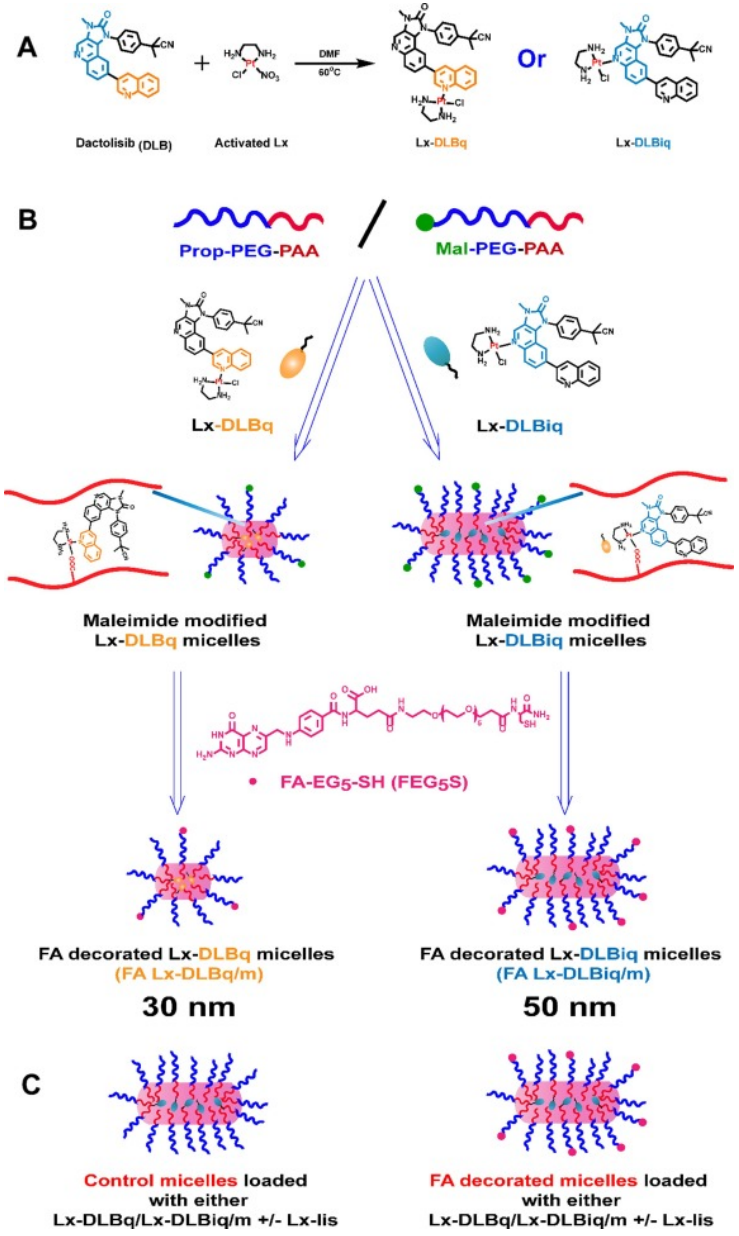

Nanomedicine Technology Development Pipeline

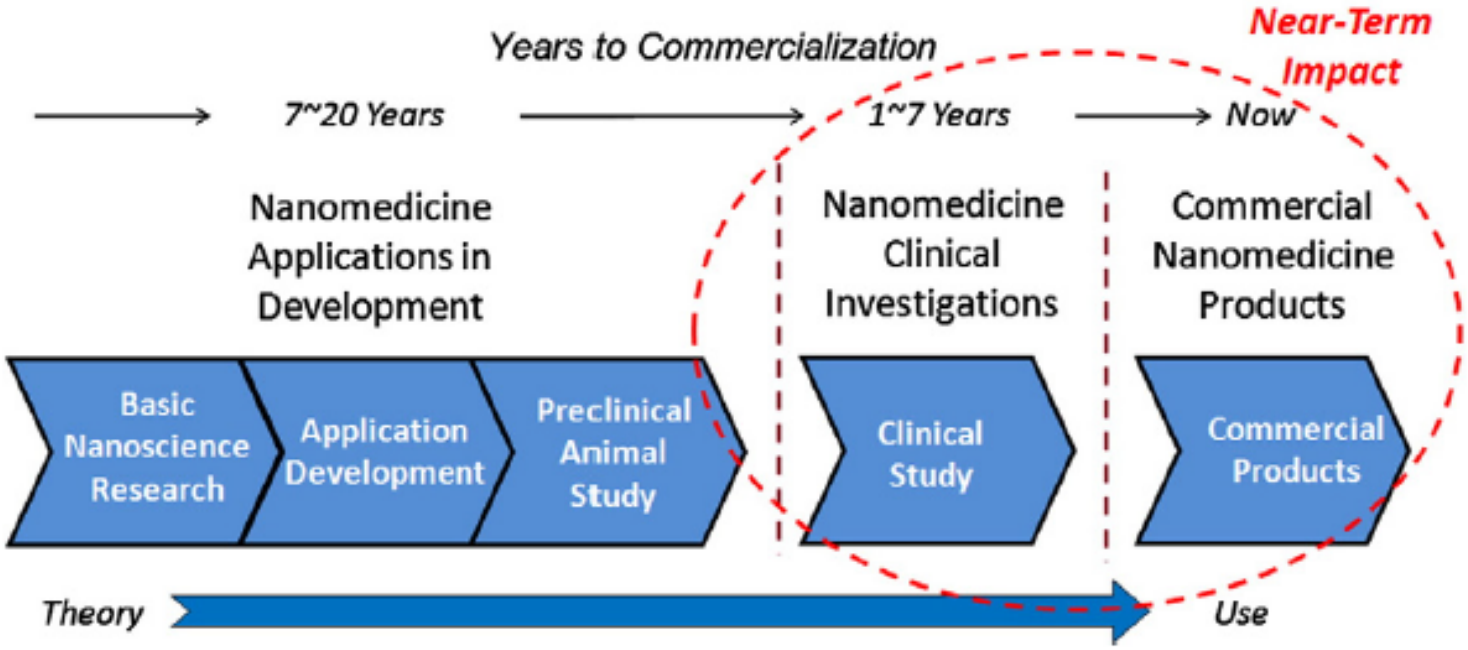

Nanomedicine: Nanotechnology, Biology, and Medicine
9 (2013) 1 – 14

Immune Cells

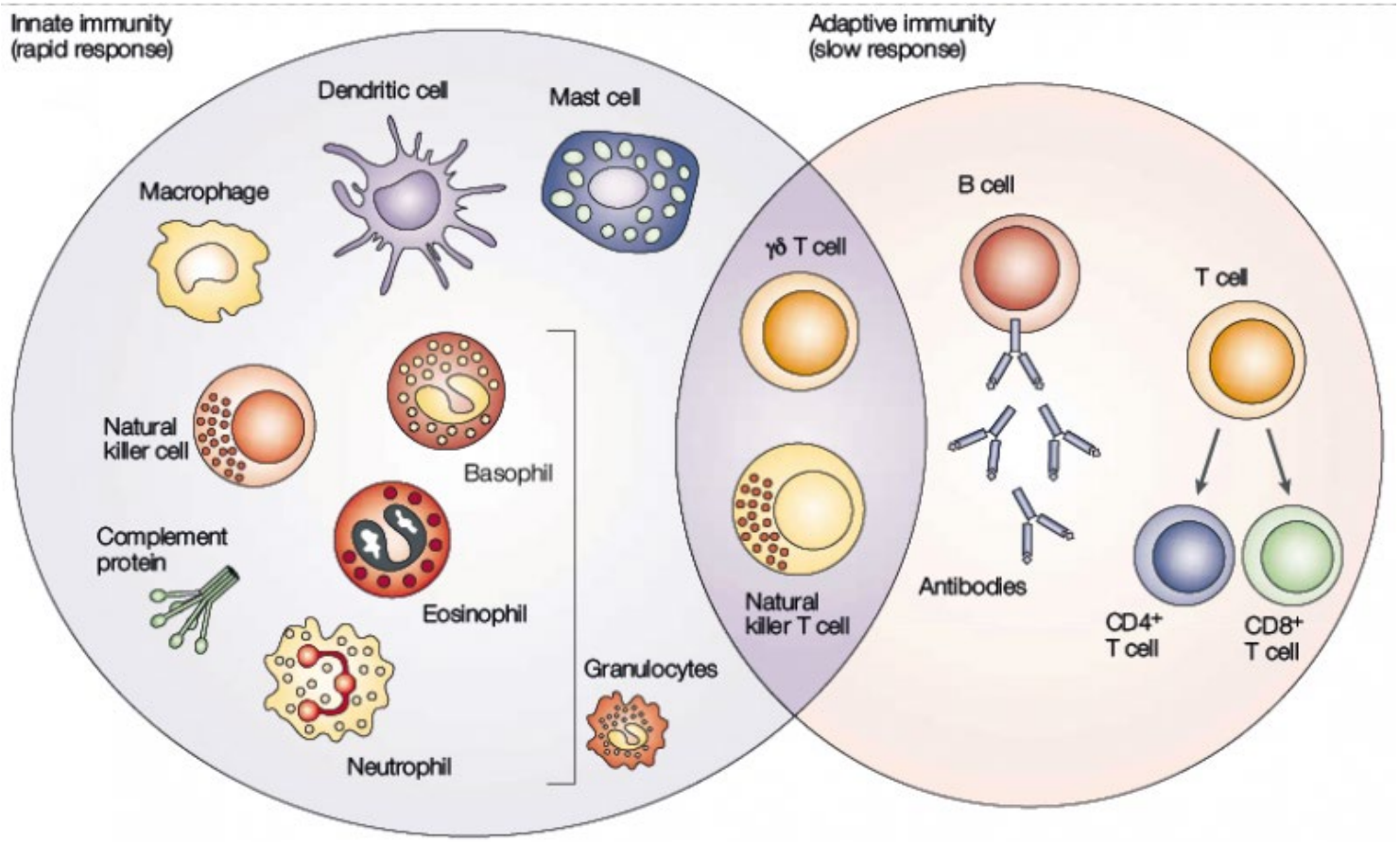

Immune System

Innate immunity: This is the first line of defense and provides a rapid, nonspecific response to harmful substances or pathogens. Innate immunity consists of various physical and chemical barriers (e.g., skin, mucous membranes, stomach acid), immune cells (e.g., **neutrophils, macrophages, dendritic cells, natural killer cells**), and proteins (e.g., complement system, cytokines). The innate immune system can recognize common molecular patterns associated with pathogens, such as lipopolysaccharides on the surface of bacteria, through pattern recognition receptors (PRRs).

Adaptive immunity: This component of the immune system provides a highly specific, targeted response to specific pathogens or antigens. It is slower to develop than innate immunity but has the advantage of immunological memory, which allows for a faster and more robust response upon subsequent encounters with the same pathogen. Adaptive immunity is mainly mediated by two types of white blood cells: **B lymphocytes (B cells) and T lymphocytes** (T cells).

Innate immune cells

Neutrophils: These are the most abundant type of white blood cells and are the first to arrive at the site of infection. They are phagocytic cells, meaning they engulf and destroy pathogens. They also release enzymes and antimicrobial peptides to kill microbes and recruit other immune cells to the site of infection.

Macrophages: These large phagocytic cells play a critical role in both innate and adaptive immunity. They engulf and destroy pathogens, remove dead cells, and secrete cytokines that regulate inflammation and recruit other immune cells. Macrophages also function as antigen-presenting cells, displaying fragments of foreign substances to T cells and initiating an adaptive immune response.

Dendritic cells: These cells act as sentinels in tissues exposed to the external environment, such as the skin and mucosal surfaces. They capture and process foreign substances and present them to T cells, thus bridging the gap between innate and adaptive immunity.

Natural killer (NK) cells: NK cells are lymphocytes that can recognize and kill virus-infected cells and cancer cells without prior sensitization. They play a crucial role in the early defense against infections and tumors.

Adaptive immune cells

B lymphocytes (B cells): B cells are responsible for producing antibodies, which are proteins that can recognize and neutralize specific pathogens or infected cells. When a B cell encounters its specific antigen, it differentiates into plasma cells that produce and secrete large amounts of antibodies, and memory B cells that provide long-lasting immunity against the same antigen.

T lymphocytes (T cells): T cells play a central role in the adaptive immune response. They can be divided into several types, including:

a. **Helper T cells (CD4+ T cells**): These cells coordinate the immune response by secreting cytokines that activate and regulate other immune cells, such as B cells, cytotoxic T cells, and macrophages.

b. **Cytotoxic T cells (CD8+ T cells**): These cells can directly kill infected or abnormal cells by releasing cytotoxic molecules, such as perforin and granzymes, that induce apoptosis (cell death).

c. **Regulatory T cells (Tregs):** These cells help maintain immune tolerance by suppressing overactive immune responses and preventing autoimmune reactions.

Memory T cells: These long-lived T cells are generated following an immune response and provide long-lasting immunity against the same antigen. They can rapidly differentiate into effector T cells upon re-exposure to the antigen, resulting in a faster and more robust immune response.

APC

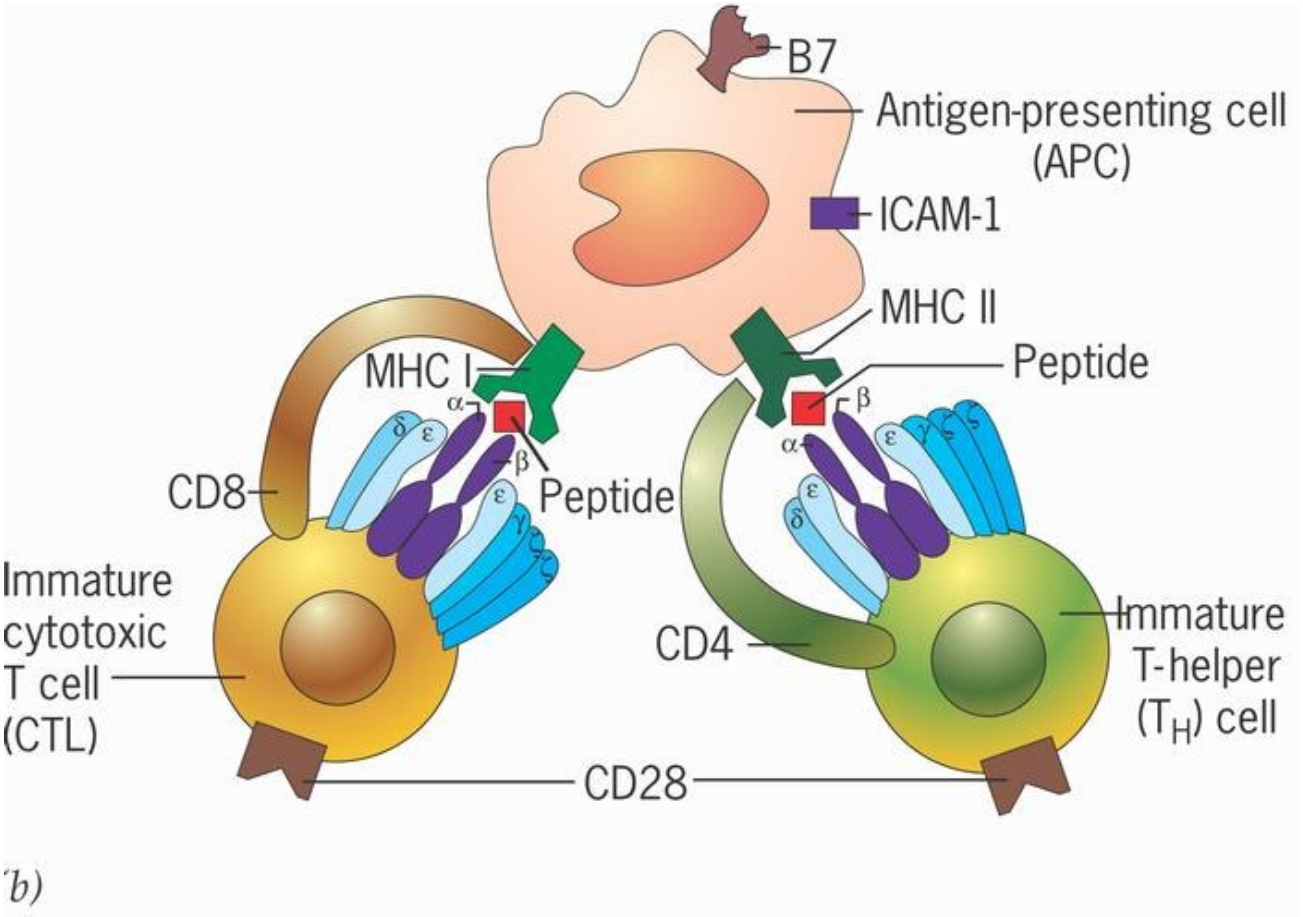
B7
Antigen-presenting cell (APC)
ICAM-1
MHC II
Peptide
MHC I
α
β
δ
ε
ε
γ
ζ
ζ
CD8
Peptide
Immature cytotoxic T cell (CTL)
CD4
Immature T-helper (T_H) cell
CD28
(b)

An **antigen-presenting cell (APC)** is a type of immune cell that plays a critical role in initiating and shaping the adaptive immune response. APCs capture, process, and present antigens—foreign substances or protein fragments derived from pathogens—on their surface in association with major **histocompatibility complex (MHC) molecules**. T cells can recognize these antigen-MHC complexes, allowing them to mount a specific immune response against the foreign substance.

Dendritic cells: These cells are often considered the most potent APCs due to their ability to initiate naive T cell responses. Dendritic cells are located in various tissues, especially those exposed to the external environment, such as the skin and mucosal surfaces. They capture and process antigens and then migrate to lymphoid organs, where they present the antigens to T cells.

Macrophages: Macrophages are phagocytic cells involved in both innate and adaptive immunity. They can engulf and destroy pathogens, as well as present antigens to T cells. Macrophages are widely distributed throughout the body and play a crucial role in the immune response against intracellular pathogens, such as bacteria and fungi.

B lymphocytes (B cells): B cells can also act as APCs, primarily in the context of the humoral immune response. When B cells encounter their specific antigen, they internalize, process, and present it to helper T cells, which in turn provide signals for B cell activation, differentiation, and antibody production.

Immunotherapy

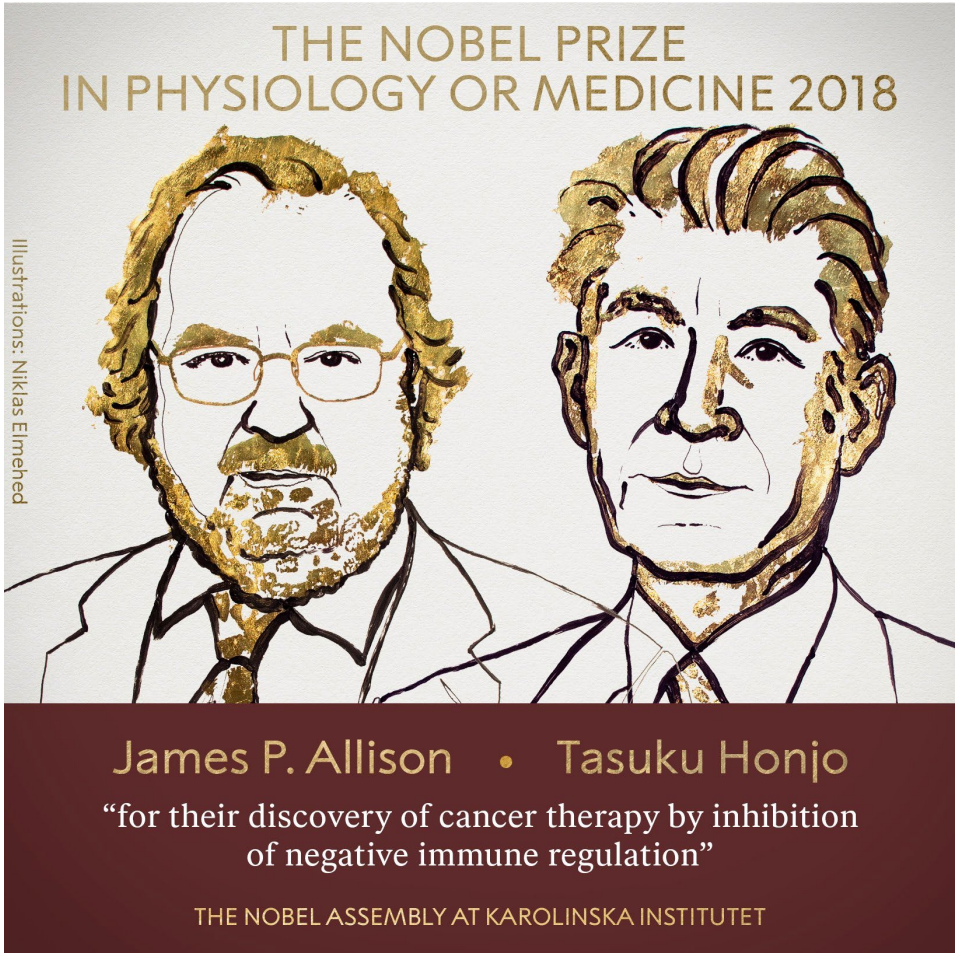

Cancer Immunotherapies

Cancer immunotherapy refers to a group of therapeutic approaches that aim to harness the power of the immune system to recognize and eliminate cancer cells. By stimulating or restoring the immune response against cancer, immunotherapies can offer a targeted and potentially long-lasting treatment for various types of cancer.

There are several types of cancer immunotherapy, including:

Immune checkpoint inhibitors:
Cancer vaccines
Adoptive cell transfer (ACT):
Oncolytic viruses:.
Cytokines:
Bispecific antibodies

Immune Checkpoint Blockade

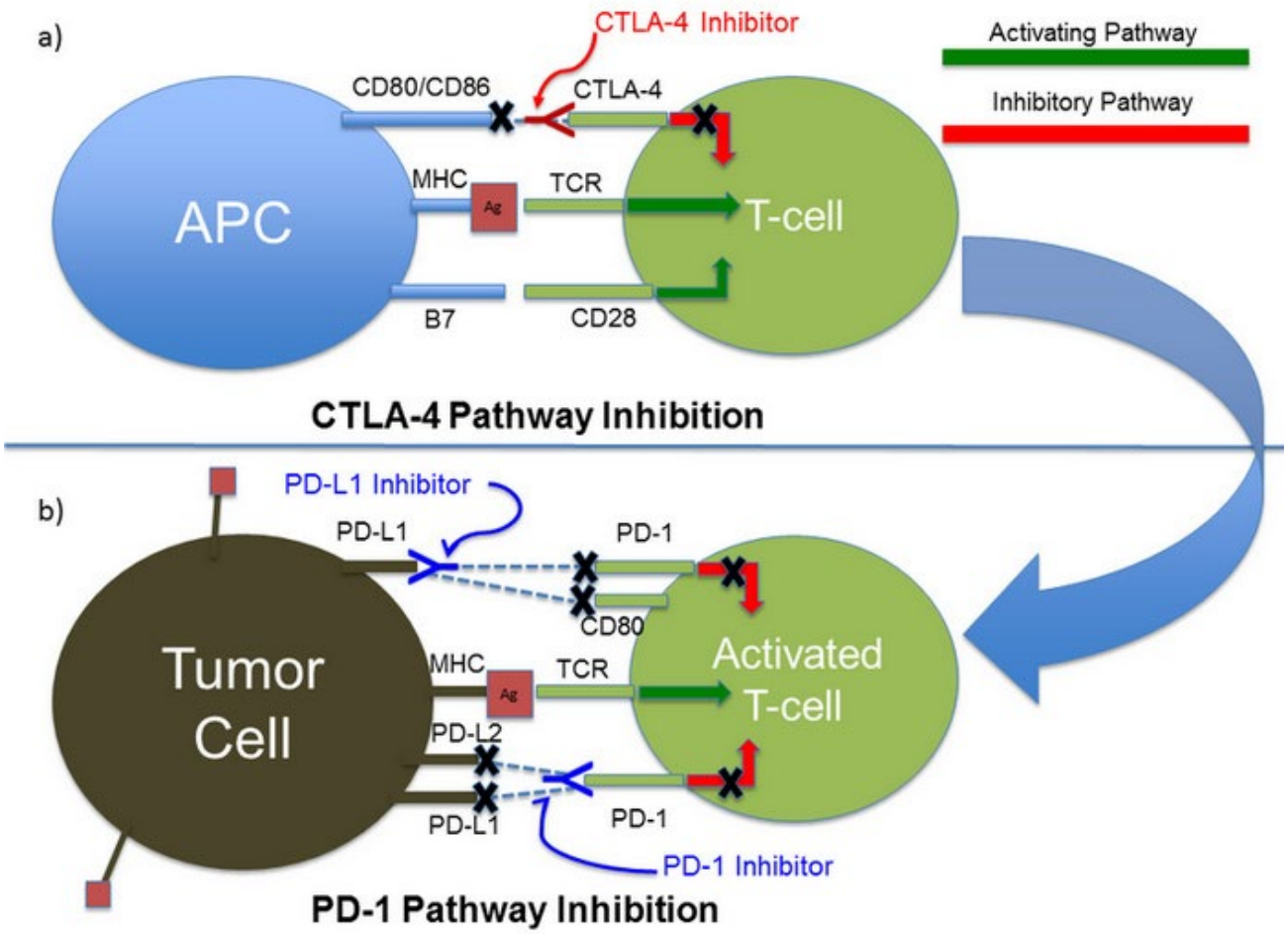

Immune checkpoint blockade involves using monoclonal antibodies that bind to and block the interaction between checkpoint proteins and their ligands, thereby "releasing the brakes" on the immune system and allowing T cells to target and kill cancer cells more effectively.

CTLA-4 (Cytotoxic T-lymphocyte-associated protein 4): CTLA-4 is an inhibitory molecule expressed on the surface of T cells. It competes with the stimulatory molecule CD28 for binding to the B7 molecules (CD80 and CD86) on antigen-presenting cells. When CTLA-4 binds to B7 molecules, it inhibits T cell activation, preventing an overactive immune response.

PD-1 (Programmed cell death protein 1): PD-1 is another inhibitory receptor found on the surface of T cells, as well as some other immune cells. It binds to its ligands, PD-L1 and PD-L2, which can be expressed on cancer cells and some immune cells in the tumor microenvironment. The interaction between PD-1 and its ligands leads to T cell exhaustion, a state of dysfunction that impairs the T cells' ability to effectively eliminate cancer cells.

PD-L1 (Programmed cell death ligand 1): PD-L1 is the primary ligand for PD-1 and is often expressed on cancer cells and some immune cells within the tumor microenvironment. Blocking PD-L1 can disrupt the inhibitory signaling pathway mediated by PD-1, leading to enhanced T cell function and anti-tumor immune response.

Partners in Immune System Signaling

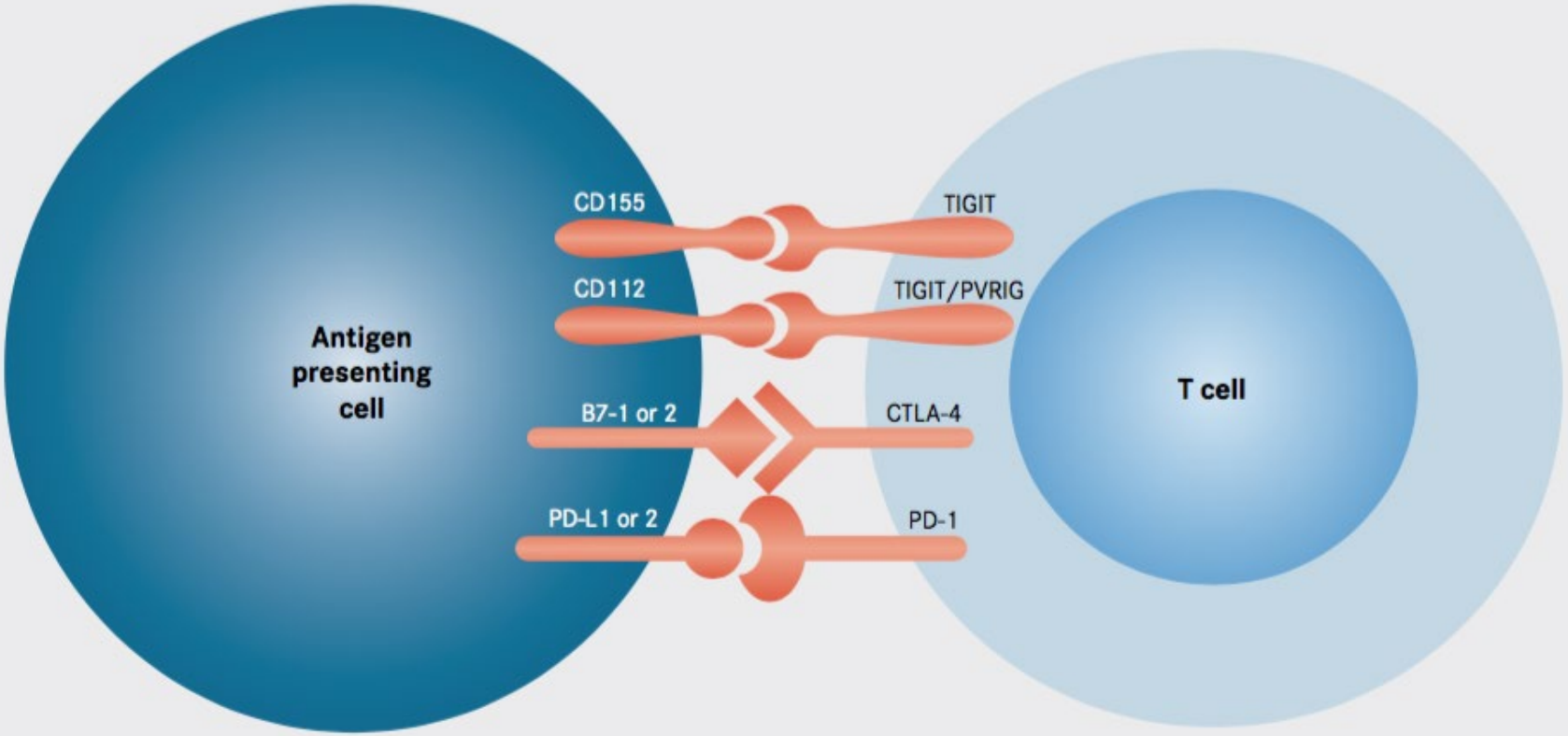

TIGIT is among the T-cell receptors that interact with proteins expressed by antigen presenting cells to send inhibitory signals to the immune system. Dysregulated interaction between TIGIT and its ligands serves to suppress immunity when under attack from cancer cells, similar to the activity of the PD-1 and CTLA-4 pathways.

Immune checkpoint inhibitors: These are drugs that target immune checkpoint proteins, such as CTLA-4, PD-1, and PD-L1, which normally act as "brakes" on the immune system to prevent overactivity and damage to healthy tissues. Cancer cells can exploit these checkpoints to evade immune recognition and destruction. By blocking these checkpoint proteins, immune checkpoint inhibitors can unleash the immune system's full potential to attack cancer cells. **Examples include ipilimumab (anti-CTLA-4), pembrolizumab (anti-PD-1), and atezolizumab (anti-PD-L1).**

Overall Survival

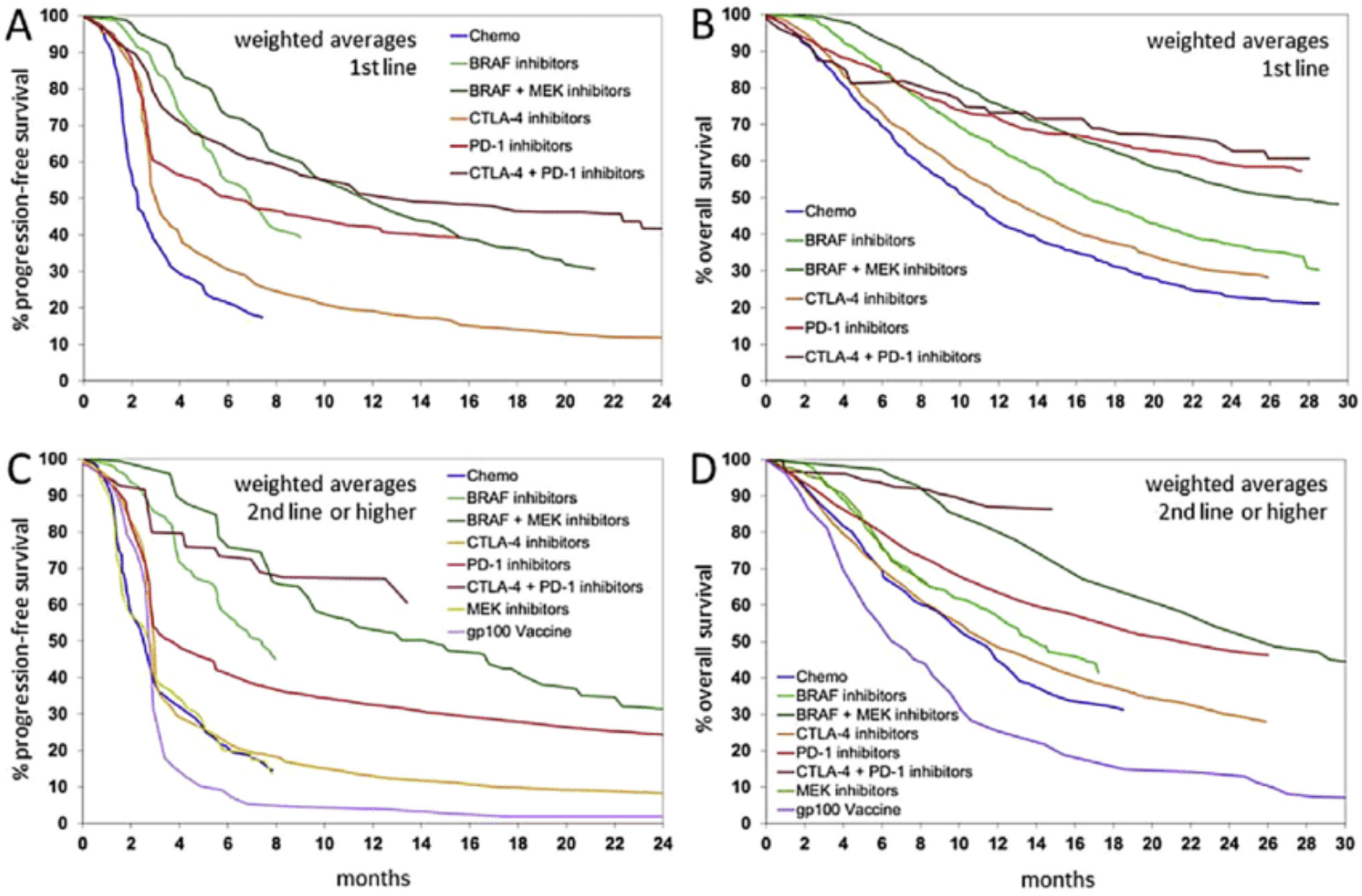

Long Term Survival

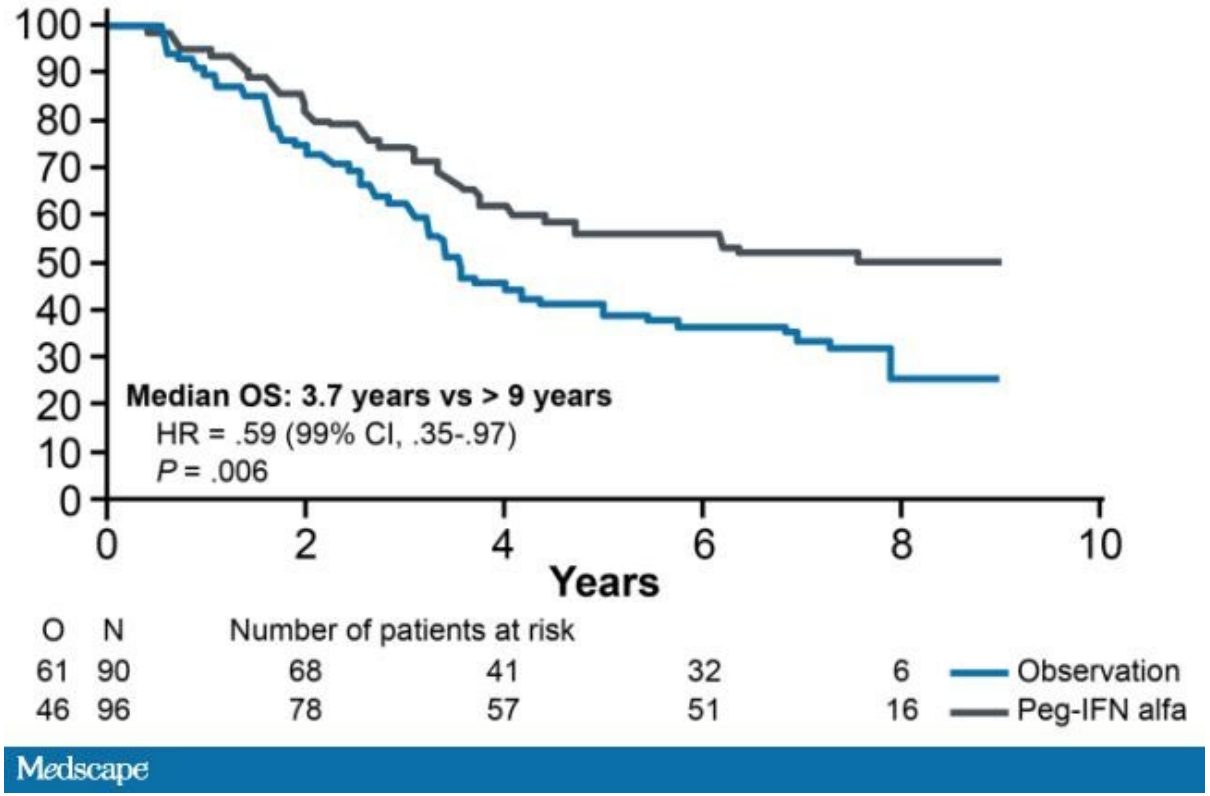

Cancer Vaccine

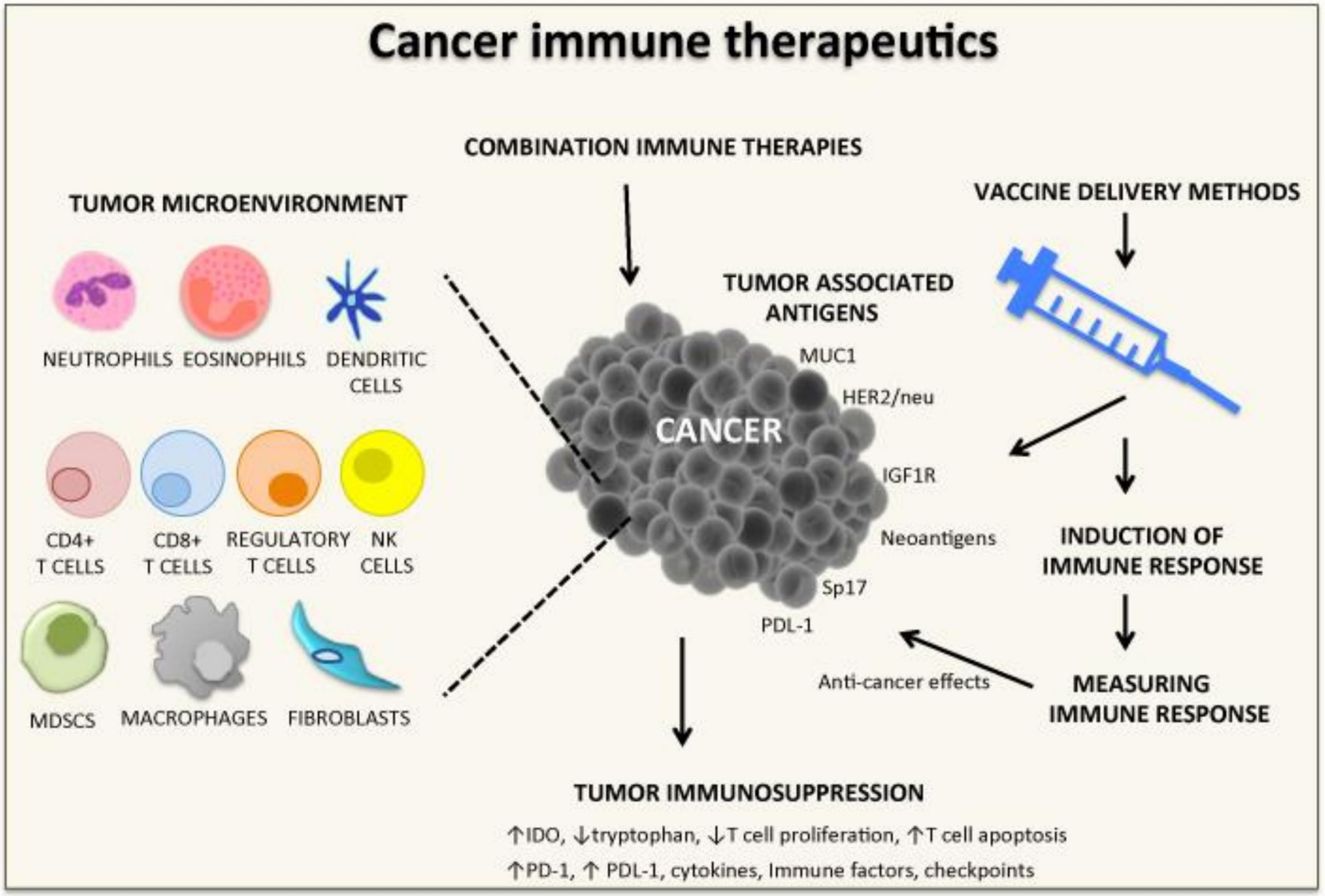

Cancer Vaccine

A cancer vaccine is a type of immunotherapy that aims to stimulate the immune system to recognize and destroy cancer cells. Cancer vaccines can be divided into two main categories: preventive vaccines and therapeutic vaccines.

Preventive vaccines: These vaccines are designed to protect against cancer-causing viruses, such as human papillomavirus (HPV) and hepatitis B virus (HBV). By preventing viral infections, these vaccines indirectly reduce the risk of developing cancers associated with these viruses, such as cervical cancer (HPV) and liver cancer (HBV). Examples of preventive cancer vaccines include Gardasil and Cervarix for HPV, and the hepatitis B vaccine.

Therapeutic vaccines: These vaccines are designed to treat existing cancers by stimulating the immune system to recognize and attack cancer cells. Therapeutic cancer vaccines usually target specific tumor-associated antigens (TAAs), which are proteins expressed by cancer cells but not (or rarely) by normal cells. By targeting these antigens, the vaccine aims to train the immune system to recognize and eliminate cancer cells without harming healthy cells.

Cancer Vaccine

There are several types of therapeutic cancer vaccines, including:

a. **Peptide-based vaccines:** These vaccines contain short fragments of proteins (peptides) derived from TAAs to stimulate an immune response against cancer cells.
b**. Tumor cell-based vaccines**: These vaccines use whole cancer cells or parts of cancer cells to provoke an immune response. The cells can be taken from the patient's own tumor (autologous) or from another individual (allogeneic).
c**. Dendritic cell-based vaccines**: These vaccines use dendritic cells, which are potent antigen-presenting cells that can activate the immune system. Dendritic cells are loaded with TAAs and then reintroduced into the patient to stimulate a targeted immune response against cancer cells.
d**. DNA/RNA-based vaccines**: These vaccines use genetic material (DNA or RNA) encoding TAAs to stimulate the production of the target antigens in the patient's own cells, leading to an immune response against the cancer cells.

One example of an FDA-approved therapeutic cancer vaccine is sipuleucel-T (Provenge), a dendritic cell-based vaccine used to treat metastatic castration-resistant prostate cancer.

How vaccines work

Weakened or dead disease bacteria introduced into the patient, often by injection

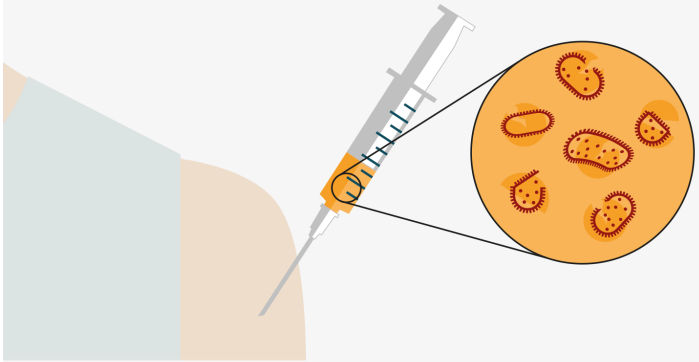

White blood cells triggered to produce antibodies to fight the disease

If patient encounters disease later, antibodies neutralise the invading cells

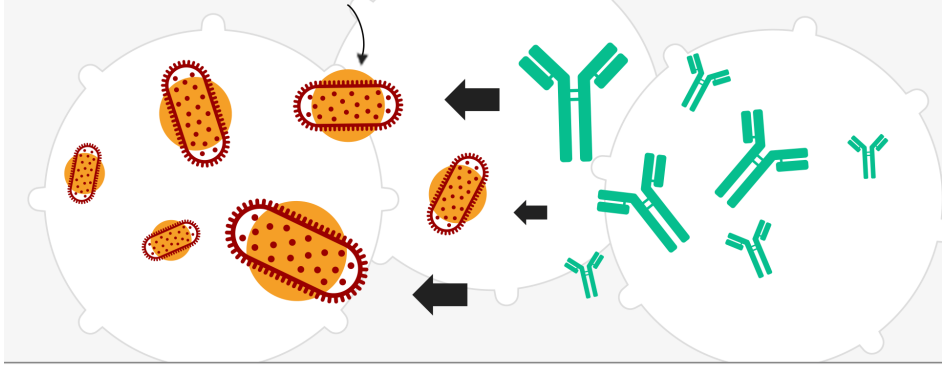

How do different Covid-19 vaccines work?

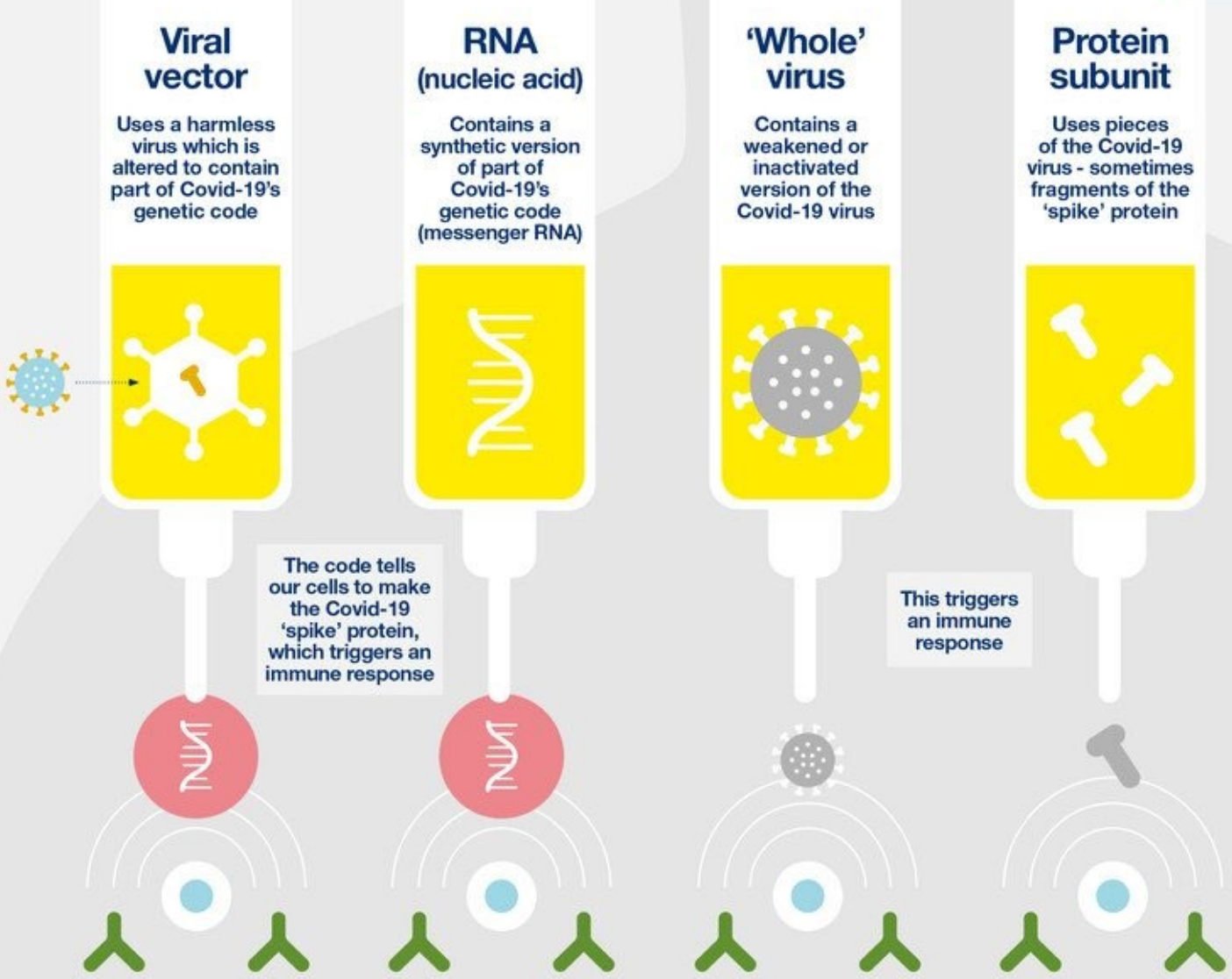

Source: Gavi https://www.gavi.org/vaccineswork/there-are-four-types-covid-19-vaccines-heres-how-they-work

Lipid Nanoparticle for Vaccine

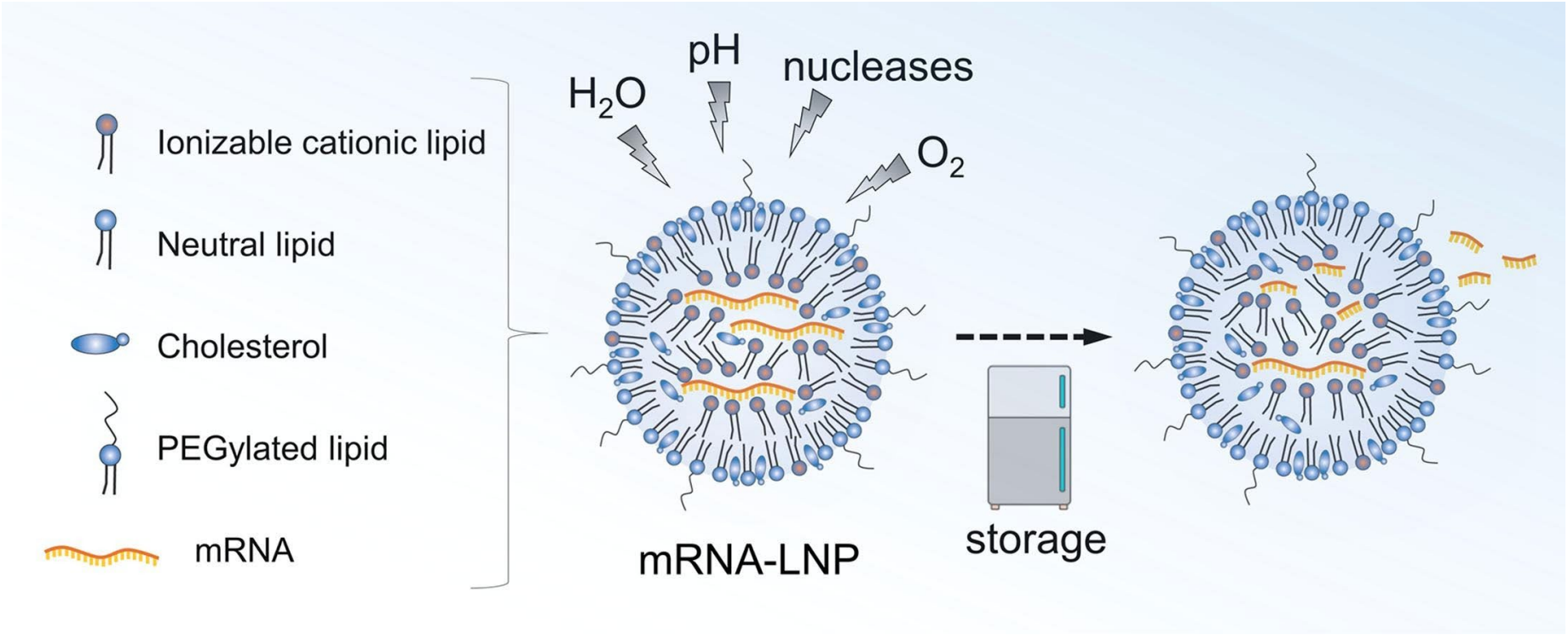

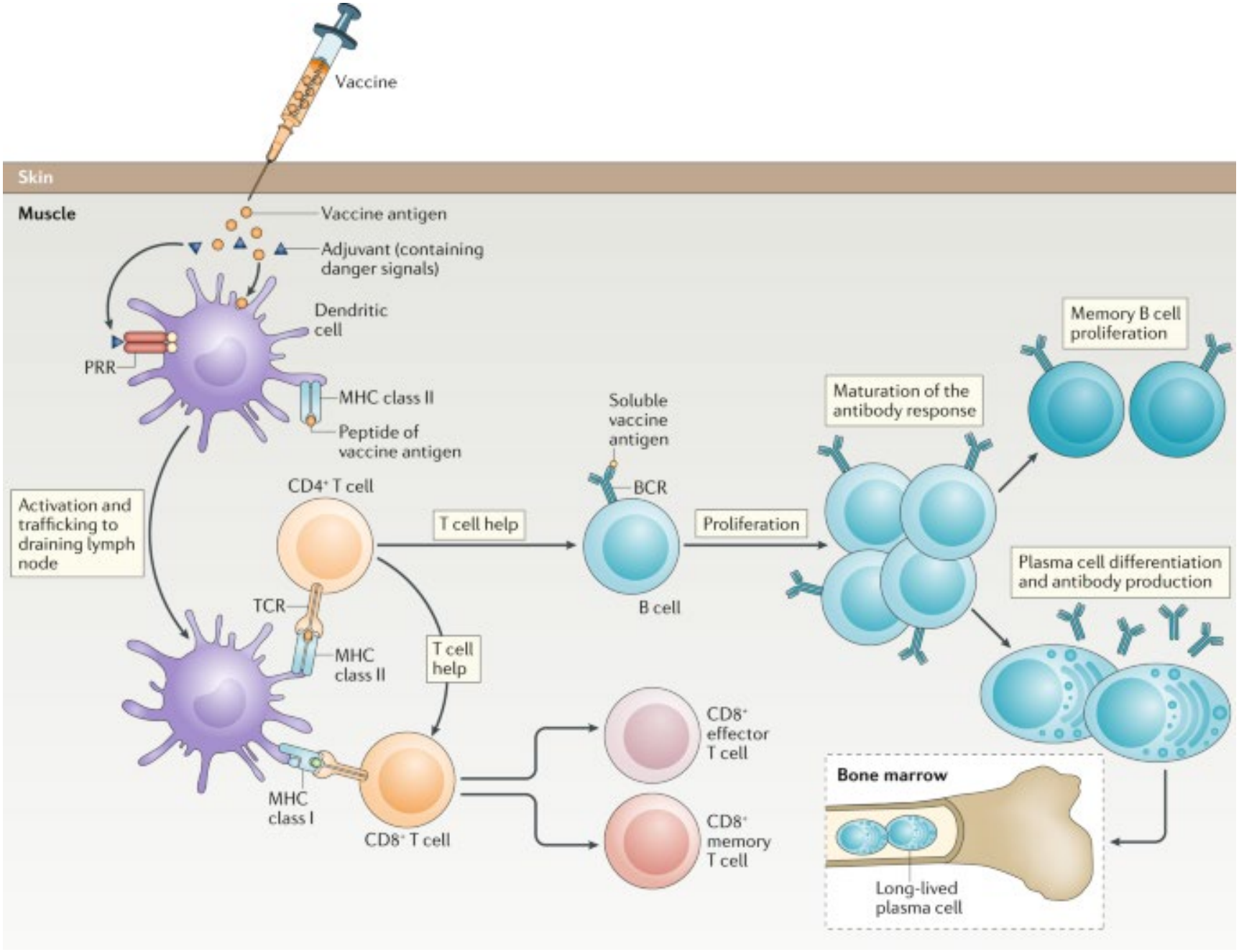
Vaccine
Skin
Muscle
Vaccine antigen
Adjuvant (containing danger signals)
Dendritic cell
PRR
MHC class II
Peptide of vaccine antigen
Activation and trafficking to draining lymph node
CD4+ T cell
T cell help
Soluble vaccine antigen
BCR
B cell
Proliferation
Maturation of the antibody response
Memory B cell proliferation
Plasma cell differentiation and antibody production
TCR
MHC class II
T cell help
MHC class I
CD8+ T cell
CD8+ effector T cell
CD8+ memory T cell
Bone marrow
Long-lived plasma cell

Adjuvants

Adjuvants play a crucial role in the development and effectiveness of cancer vaccines. They are substances added to vaccines to enhance the immune response against tumor-associated antigens (TAAs). Adjuvants work by activating and modulating the immune system in various ways, which can ultimately lead to a more robust and long-lasting anti-tumor response. Some of the roles of adjuvants in cancer vaccines include:

Activation of antigen-presenting cells (APCs).
Recruitment and activation of immune cells:
Enhanced cytokine and chemokine production:
Induction of long-lasting immunity
Modulation of the immune response

Various adjuvants are used in cancer vaccines, including aluminum salts, oil-in-water emulsions, liposomes, and TLR agonists. The choice of adjuvant depends on the specific vaccine formulation and the desired immune response. Ongoing research is focused on developing novel adjuvants and optimizing their use in cancer vaccines to improve their safety and effectiveness in stimulating anti-tumor immune responses.

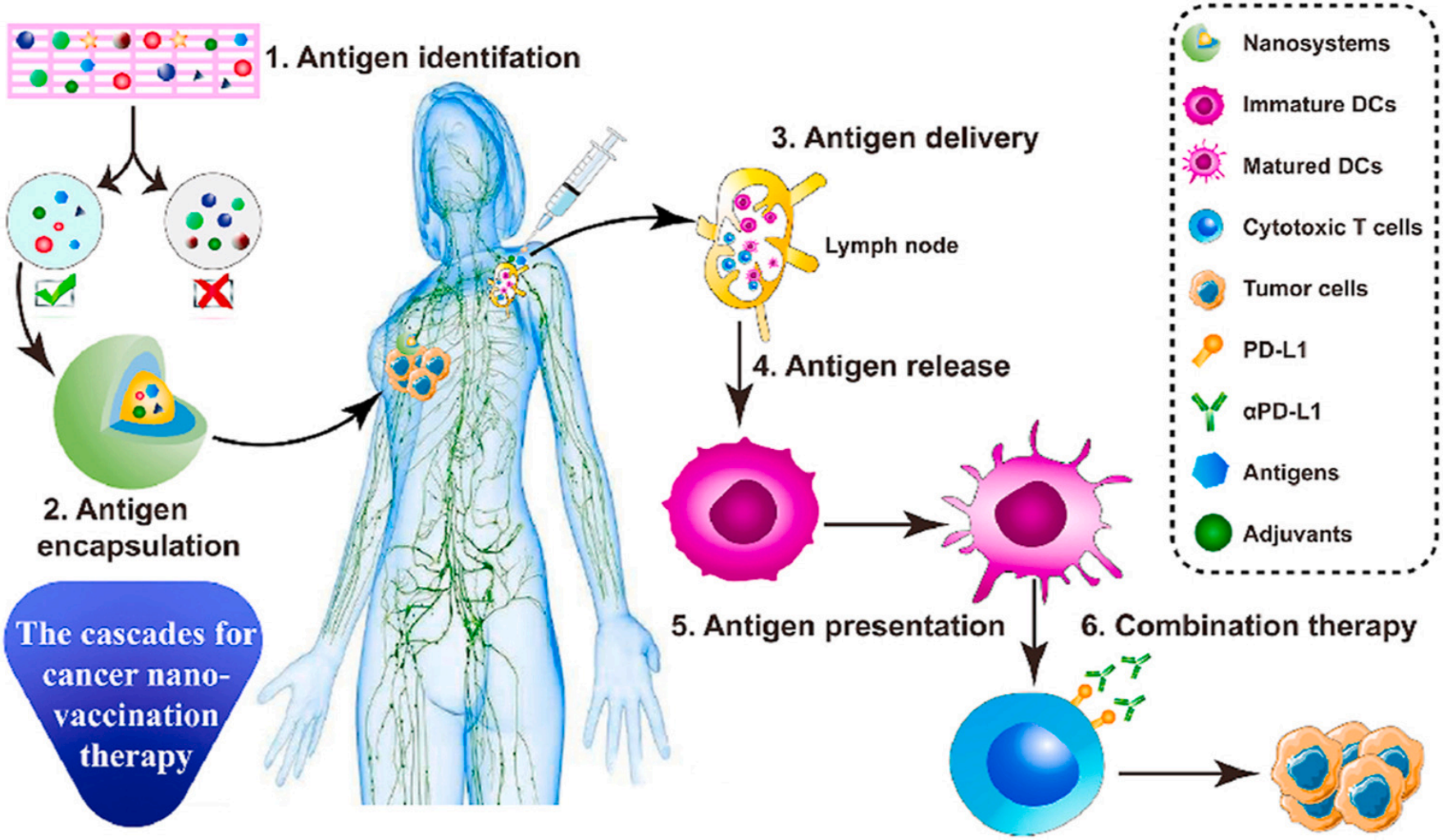
1. Antigen identifation
2. Antigen encapsulation
3. Antigen delivery
Lymph node
4. Antigen release
5. Antigen presentation
6. Combination therapy
The cascades for cancer nano-vaccination therapy
Nanosystems
Immature DCs
Matured DCs
Cytotoxic T cells
Tumor cells
PD-L1
αPD-L1
Antigens
Adjuvants

Neoantigen

Neoantigens are novel protein fragments or peptides that arise from somatic mutations within tumor cells. These mutations can result in the production of abnormal proteins that are not present in normal cells. Since neoantigens are specific to cancer cells and not found in healthy cells, they represent attractive targets for cancer immunotherapy.

The immune system can recognize neoantigens as foreign substances, which can trigger an immune response against the cancer cells expressing these neoantigens. T cells, a type of immune cell, can identify and target these neoantigens presented on the surface of cancer cells by major histocompatibility complex (MHC) molecules. This immune recognition can lead to the activation and expansion of T cells that are capable of selectively killing cancer cells while sparing healthy cells.

Neoantigens play a critical role in several cancer immunotherapy strategies, including:

Personalized cancer vaccines:
Adoptive T cell therapy:
T cell receptor (TCR)-engineered T cells.

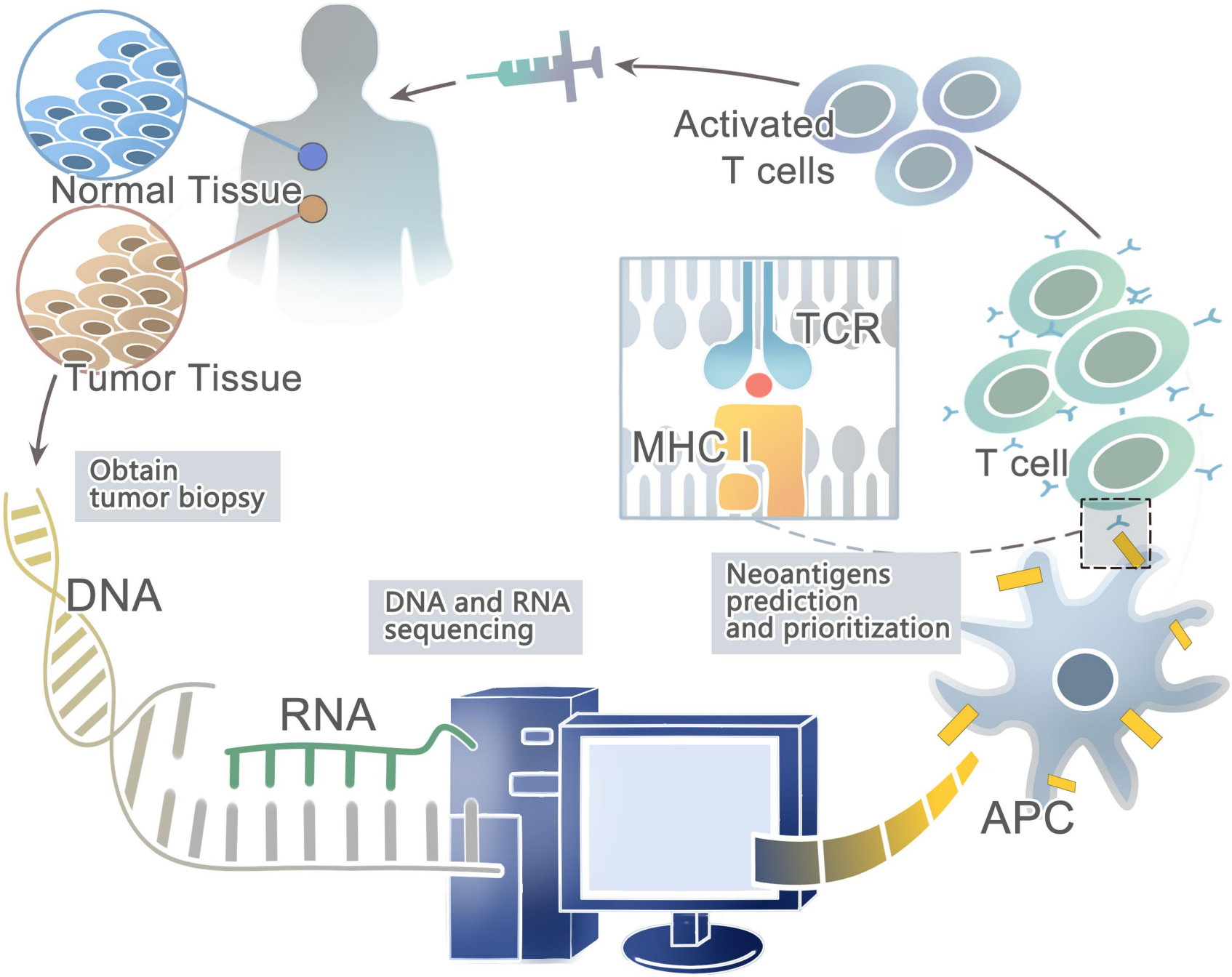
Normal Tissue
Tumor Tissue
Obtain
tumor biopsy
DNA
RNA
DNA and RNA
sequencing
Activated
T cells
TCR
MHC I
T cell
Neoantigens
prediction
and prioritization
APC

(CAR) T-cell therapy

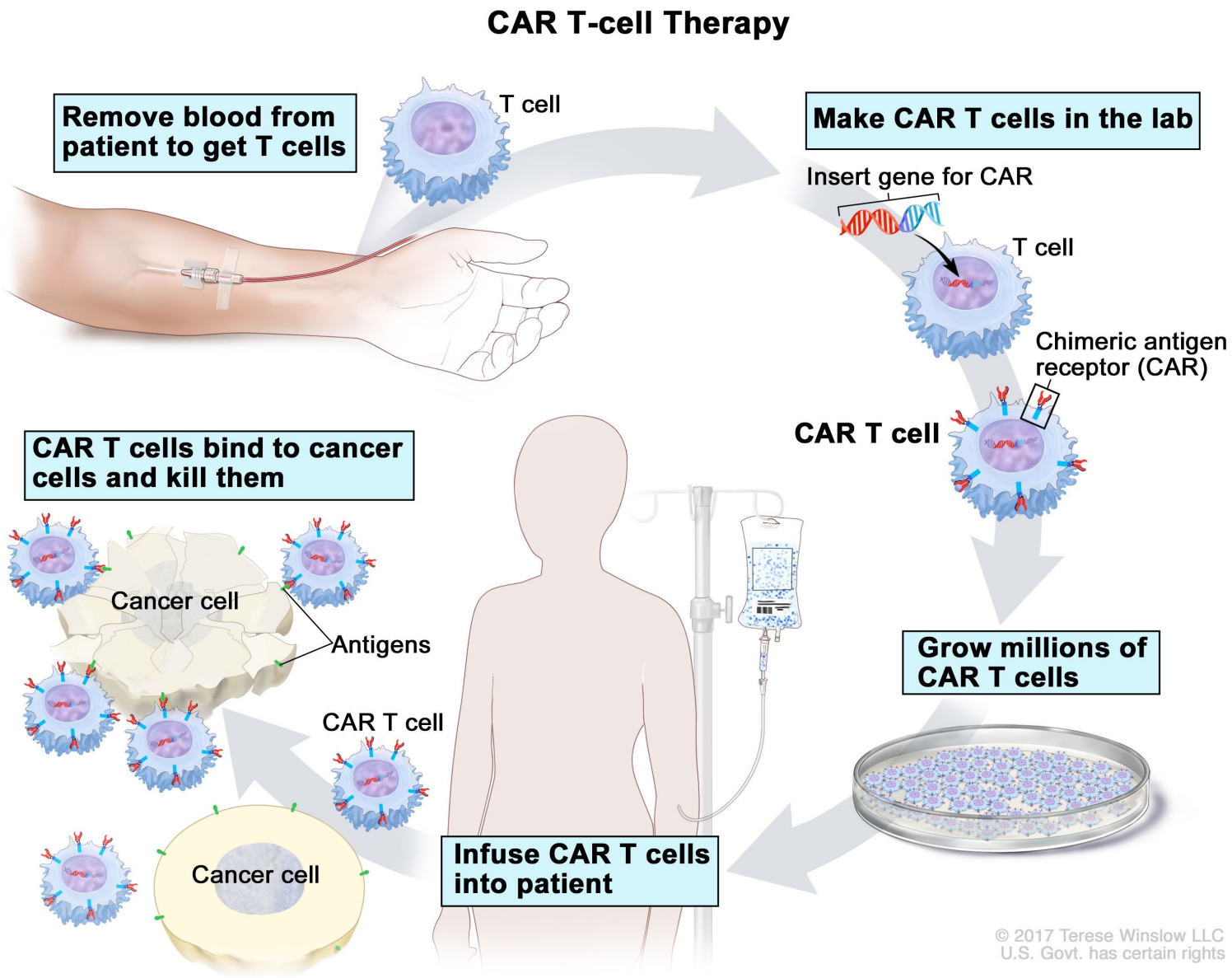

Chimeric Antigen Receptor (CAR) T-cell therapy is a type of adoptive cell therapy that harnesses the power of a patient's immune system to fight cancer. It involves the genetic engineering of a patient's T cells to express a chimeric antigen receptor (CAR) on their surface, which is designed to recognize and bind to a specific antigen expressed by cancer cells.

The principle behind CAR T-cell therapy can be broken down into several key steps:

T-cell collection:
Genetic engineering: The isolated T cells are then genetically modified, typically using viral vectors, to express a chimeric antigen receptor (CAR) on their surface. The CAR is a synthetic protein that combines an extracellular antigen-binding domain, usually derived from an antibody, with intracellular signaling domains responsible for activating the T cell upon antigen recognition.

T-cell expansion:
Patient preparation
CAR T-cell infusion

The first FDA-approved CAR T-cell therapies, Kymriah (tisagenlecleucel) and Yescarta (axicabtagene ciloleucel), target the CD19 antigen, which is commonly expressed on the surface of B-cell malignancies.

Hot Tumors and Cold Tumors

Hot Tumors:
Hot tumors are characterized by their inflamed nature, which means they contain a high number of infiltrating immune cells, such as T-cells. These tumors often express higher levels of immune checkpoint proteins and are generally more visible to the immune system due to the presence of these immune cells and the expression of neoantigens (new antigens produced by tumor mutations). Because of this immune activity, hot tumors are typically more responsive to immunotherapies such as checkpoint inhibitors. These therapies help to further activate the immune system against the tumor.

Cold Tumors:
Cold tumors, in contrast, are non-inflamed and contain few or no infiltrating immune cells. They have a lower expression of neoantigens and immune checkpoint molecules, making them less visible or even invisible to the immune system. This lack of immune activity makes cold tumors less responsive to immunotherapy, as there is minimal existing immune response to enhance. Cold tumors often require different strategies to become treatable with immunotherapy, such as combining immunotherapy with other treatments that can help to turn a cold tumor into a hot one, making it more susceptible to immune attacks.

Hot Tumors and Cold Tumors

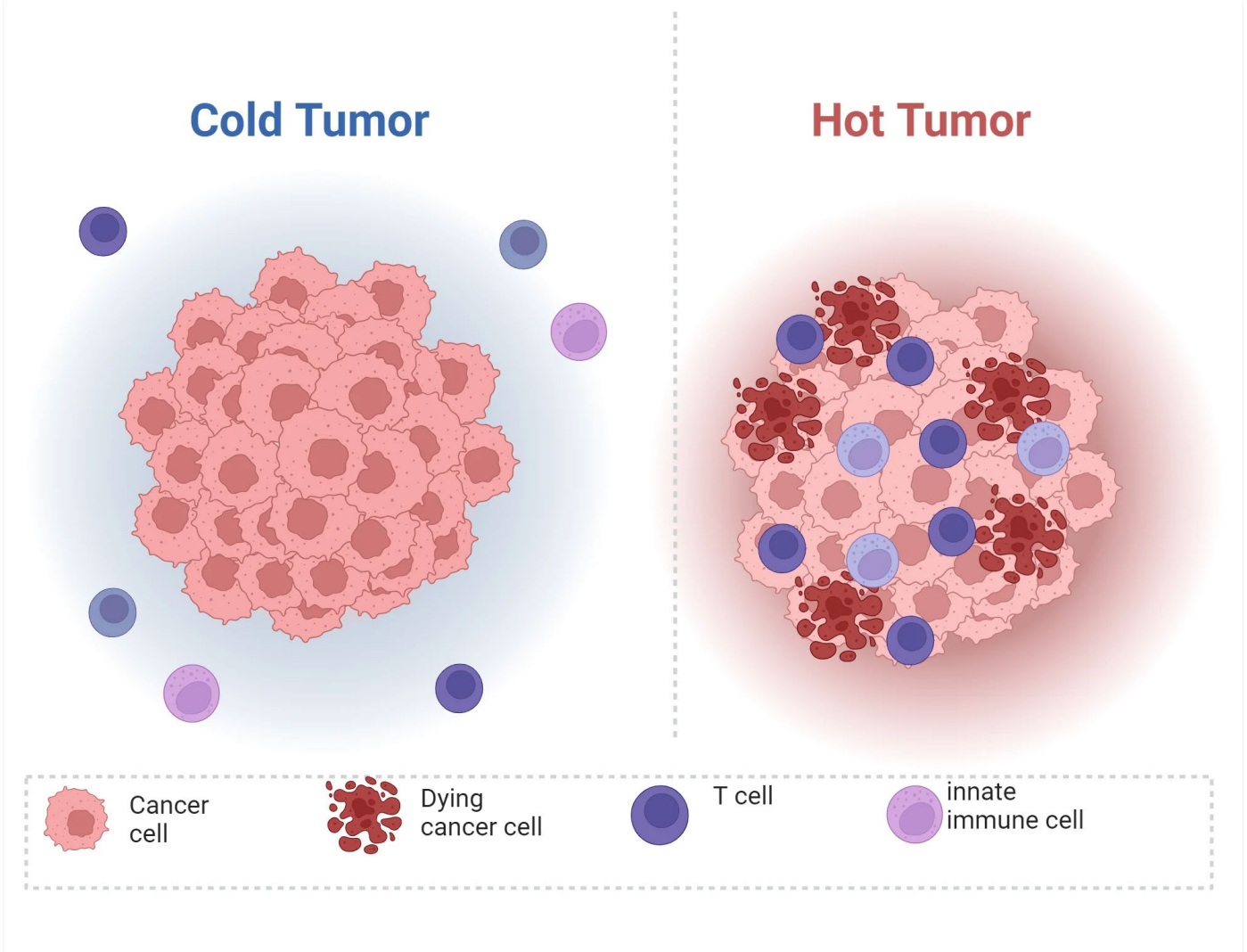

Converting Cold Tumors into Hot Tumors

Delivery of Immunomodulatory Agents:
Nanoparticles can be engineered to deliver immunostimulatory agents directly to the tumor microenvironment. These agents can include cytokines (like interleukin-2 or interleukin-12), toll-like receptor (TLR) agonists, or STING (Stimulator of Interferon Genes) agonists, which can activate immune cells and promote inflammation within the tumor.

Combination Therapy:
Combining nanomedicine with other treatments, such as chemotherapy or radiotherapy, can induce immunogenic cell death, releasing tumor antigens that attract immune cells to the tumor site. Nanoparticles can be designed to deliver chemotherapy drugs and immunotherapy agents simultaneously, allowing localized combination therapy that minimizes systemic side effects.

Checkpoint Inhibitors:
Nanoparticles can be used to deliver checkpoint inhibitors, such as PD-1 or CTLA-4 inhibitors, directly to the tumor site. This localized delivery can enhance the immune response against the tumor while reducing the immune-related adverse effects often associated with systemic administration of these drugs.

Targeting the Tumor Microenvironment:
Nanoparticles can be designed to modulate the suppressive tumor microenvironment. This can involve the delivery of agents that deplete immunosuppressive cells (like regulatory T cells or myeloid-derived suppressor cells) or reprogram the fibroblasts and other stromal cells that often support tumor growth and immune evasion.

Improving cancer immunotherapy using nanomedicines: progress, opportunities and challenges

John D. Martin, Horacio Cabral, Triantafyllos Stylianopoulos and Rakesh K. Jain

Tumor-associated antigen (TAA) refers to antigen molecules present on tumor cells or normal cells, including embryonic proteins, glycoprotein antigens, squamous cell antigens, etc., which have been widely used for treating a number of tumors.

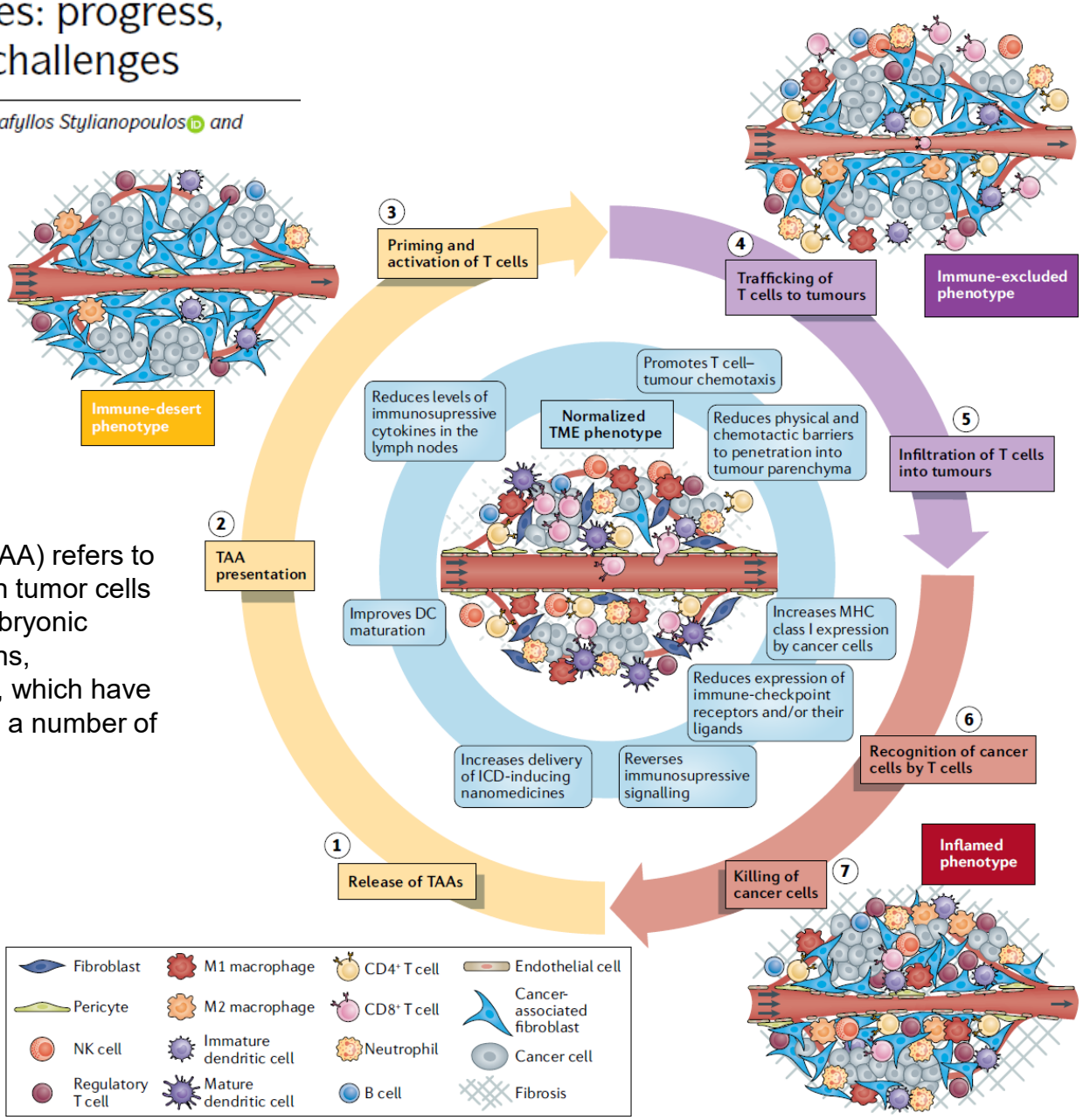

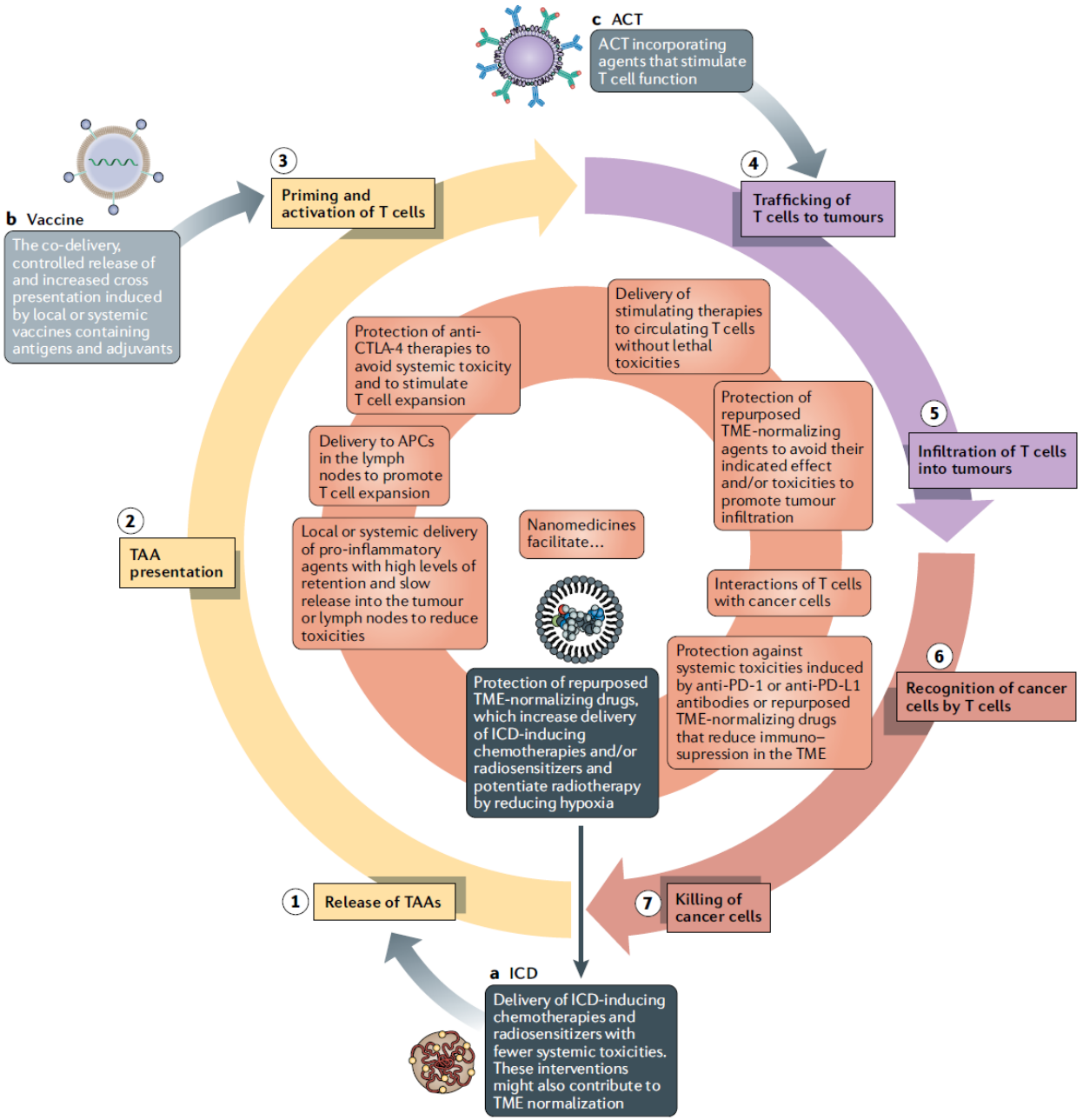

Fig. 2 | **How nanomedicines can be used to perpetuate the cancer-immunity cycle.** The goal of nanomedicine-based immunotherapy is to ensure that the cancer-immunity cycle (the seven numbered steps) perpetuates. Initially, in order to ensure that T cells are capable of attacking cancer cells, we highlight three nanomedicine-based starting points: (**a**) immunogenic cell death (ICD)-inducing therapy, (**b**) vaccines and (**c**) nanoparticle-loaded T cells.

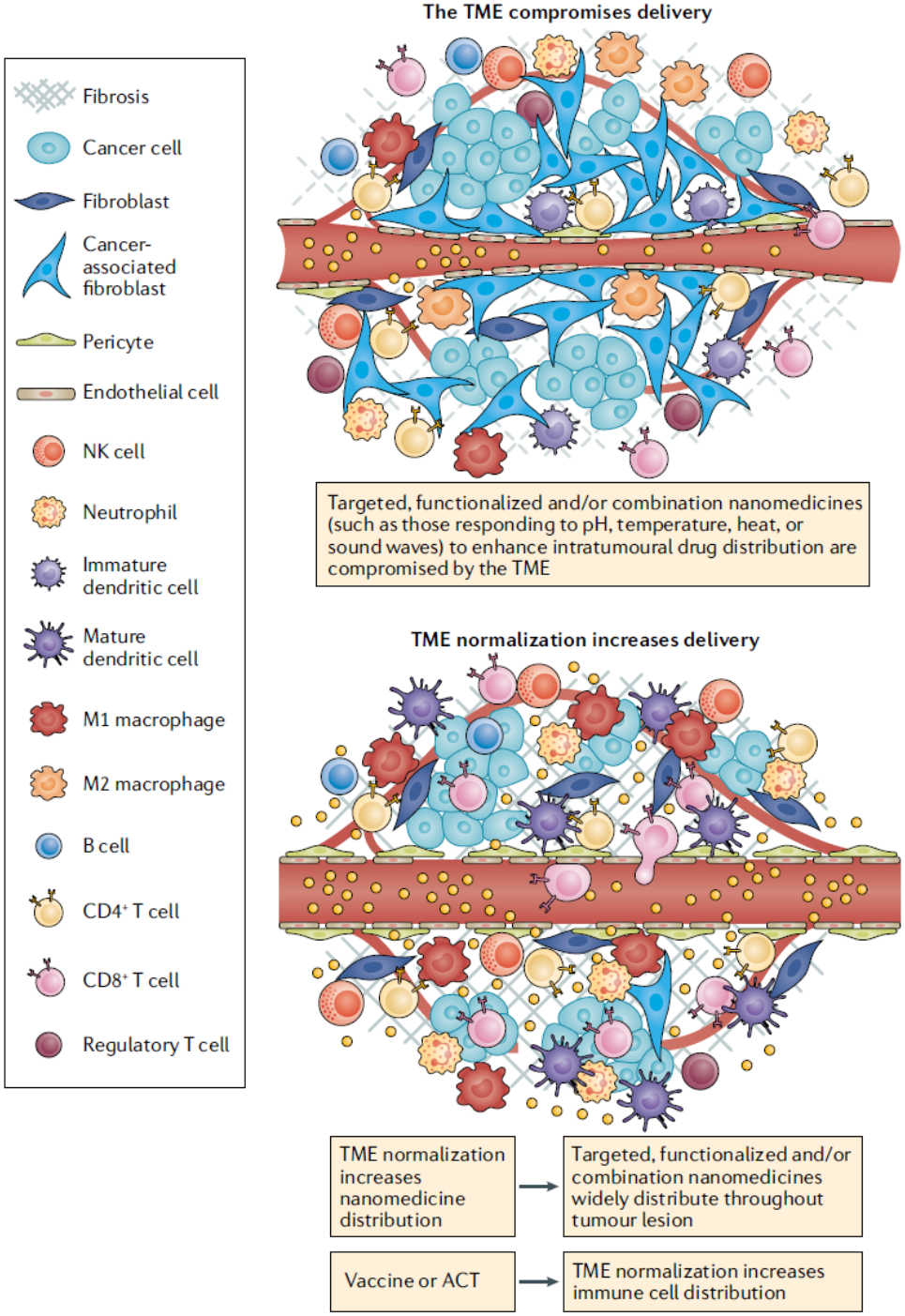
Fibrosis
Cancer cell
Fibroblast
Cancer-associated fibroblast
Pericyte
Endothelial cell
NK cell
Neutrophil
Immature dendritic cell
Mature dendritic cell
M1 macrophage
M2 macrophage
B cell
CD4+ T cell
CD8+ T cell
Regulatory T cell
The TME compromises delivery
Targeted, functionalized and/or combination nanomedicines (such as those responding to pH, temperature, heat, or sound waves) to enhance intratumoural drug distribution are compromised by the TME
TME normalization increases delivery
TME normalization increases nanomedicine distribution
Targeted, functionalized and/or combination nanomedicines widely distribute throughout tumour lesion
Vaccine or ACT
TME normalization increases immune cell distribution

Enhancing cancer immunotherapy with nanomedicine

Darrell J. Irvine[1,2,3,4,5]* *and Eric L. Dane*[1]

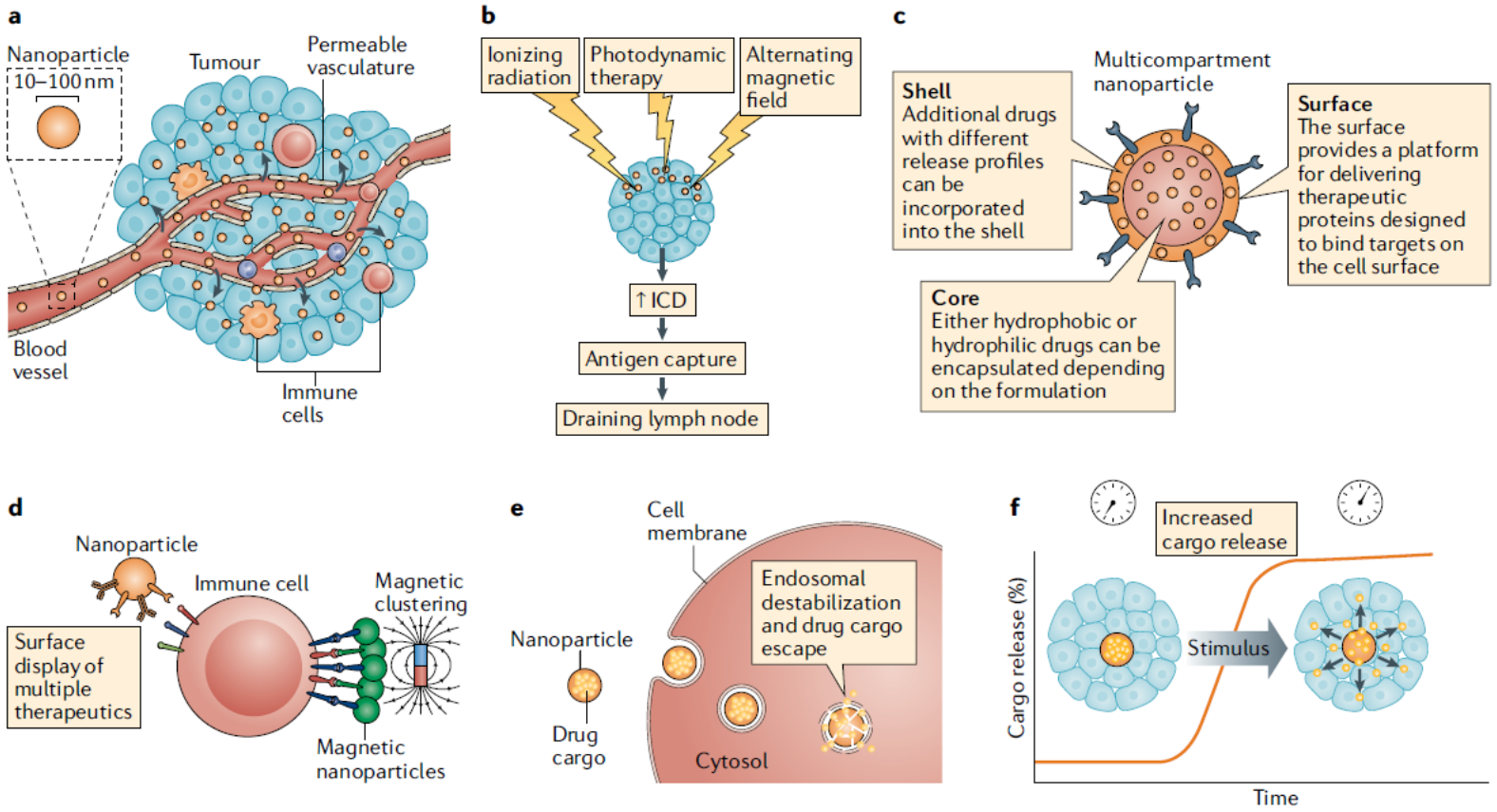

Fig. 1 | **Nanomedicines allow unique modes of action in immunotherapy. a** | Nanomedicines, such as nanoparticles, accumulate within tumours via the enhanced permeation and retention effect, concentrating the drug in tumour sites. **b** | Nanoparticles can be designed to interact with external energy sources, such as ionizing or non-ionizing radiation or magnetic fields to enhance immunogenic cell death (ICD). **c** | Nanomedicines allow combinations of therapeutics, including drugs with very different properties, to be co-delivered to tumour sites. **d** | Multiple ligands can be arrayed on the surfaces of polymers and nanoparticles to enhance engagement of immunostimulatory receptors. **e** | Nanoparticles can be formulated to destabilize endosomal membranes and promote drug delivery into the cytosol. **f** | Nanoparticles allow control of the kinetics of drug release, either preprogrammed through the particle chemistry or through responsiveness to an external stimulus such as light or heat.

Table 1 | **Clinical translation of cancer immunotherapy nanomedicines**

Developer	Concept	Indications	Clinical stage	ClinicalTrials.gov identifiers	Refs
NanoBiotix	Metal nanoparticle radioenhancers in combination with checkpoint blockade	Various solid tumours	Phase I–III	NCT03589339	25–27
Oslo University Hospital/Bristol-Myers Squibb	Pegylated liposomal doxorubicin in combination with checkpoint blockade	Metastatic breast cancer	Phase IIb	NCT03409198	16
Nektar Therapeutics	Reversibly pegylated IL-2 in combination with checkpoint blockade	Various solid tumours	Phase I, phase II	NCT02983045, NCT03138889, NCT03282344, NCT03635983, NCT03785925, NCT03729245, NCT03435640	81–83
Exicure	Intratumoural administration of TLR9 agonist-functionalized nanoparticles in combination with checkpoint blockade	Various solid tumours	Phase Ib/II	NCT03684785	49,50
Torque Therapeutics	Nanoparticle-functionalized antigen-primed T cell therapy	Various solid tumours and lymphomas	Phase I	NCT03815682	113,115,120
Rimo Therapeutics	Metal–organic framework nanoparticles as radioenhancers combined with IDO inhibitors and/or checkpoint blockade	Various solid tumours	Phase I	NCT03444714	29
Coordination Pharma	Nanoscale coordination polymer-based particles	Various solid tumours	Phase I	NCT03781362, NCT03953742	35–37
Moderna Therapeutics	Lipid nanoparticle-delivered mRNA encoding OX40L, IL-23 and IL-36γ with or without checkpoint blockade	Relapsed or refractory solid tumour malignancies or lymphoma	Phase I	NCT03739931	53
Moderna Therapeutics	Lipid nanoparticle-delivered mRNA encoding OX40L	Relapsed or refractory solid tumour malignancies or lymphoma	Phase I	NCT03323398	53
OncoNano	STING-activating polymer micelles	TBD	Phase I projected 2020–2021	NA	48,142
Tidal Therapeutics	Nanoparticles for gene transfer to macrophages and lymphocytes	TBD	Phase I projected 2020–2021	NA	127,128

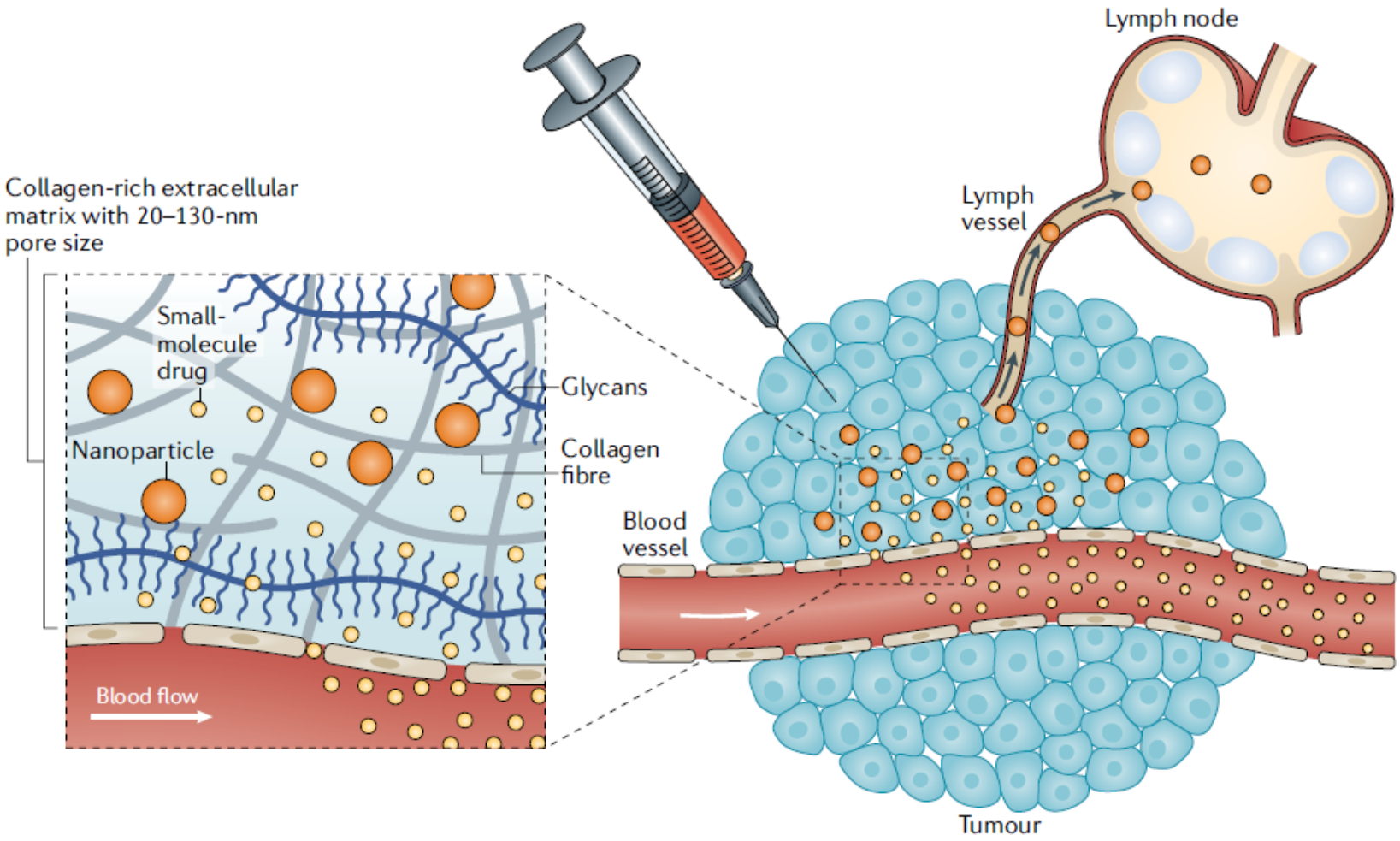

Fig. 2 | **Nanomedicines improve tumour retention and lymph node trafficking.** When nanomedicines are administered locally, the tumour's dense extracellular matrix, composed of a collagen-rich hydrogel with a pore size of 20–130 nm, preferentially retains nanomedicines and promotes their trafficking to the lymph node, whereas small-molecule drugs are rapidly cleared into the systemic circulation due to their small size and the high interstitial fluid pressure in tumours.

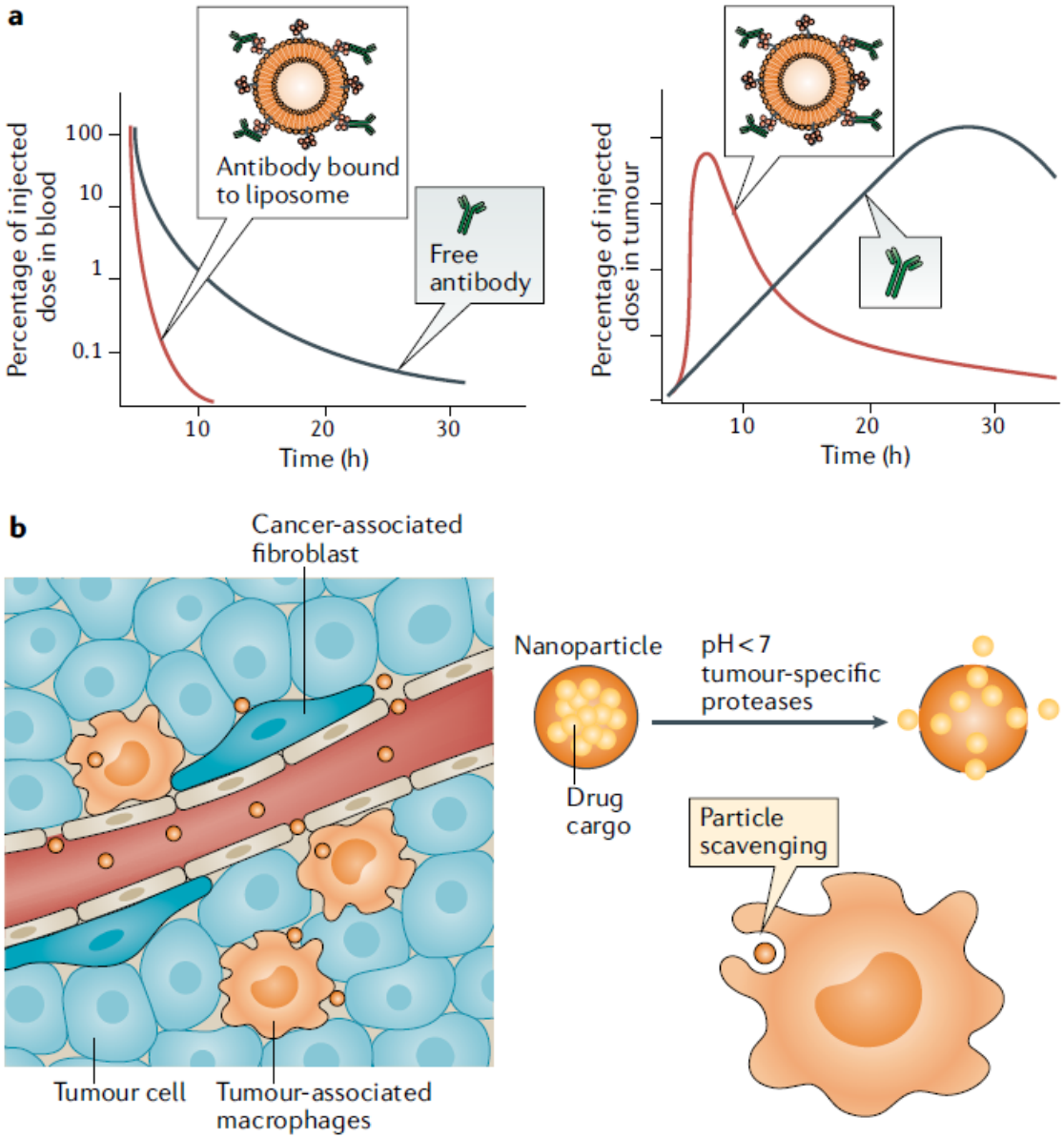

Fig. 3 | **Systemic targeting of tumours by intravenously administered nanomedicines. a** | Nanoparticles alter the pharmacokinetics of immunomodulatory drugs in a manner that can increase safety and efficacy. Illustrated is the case of an

Regulating trained immunity with nanomedicine

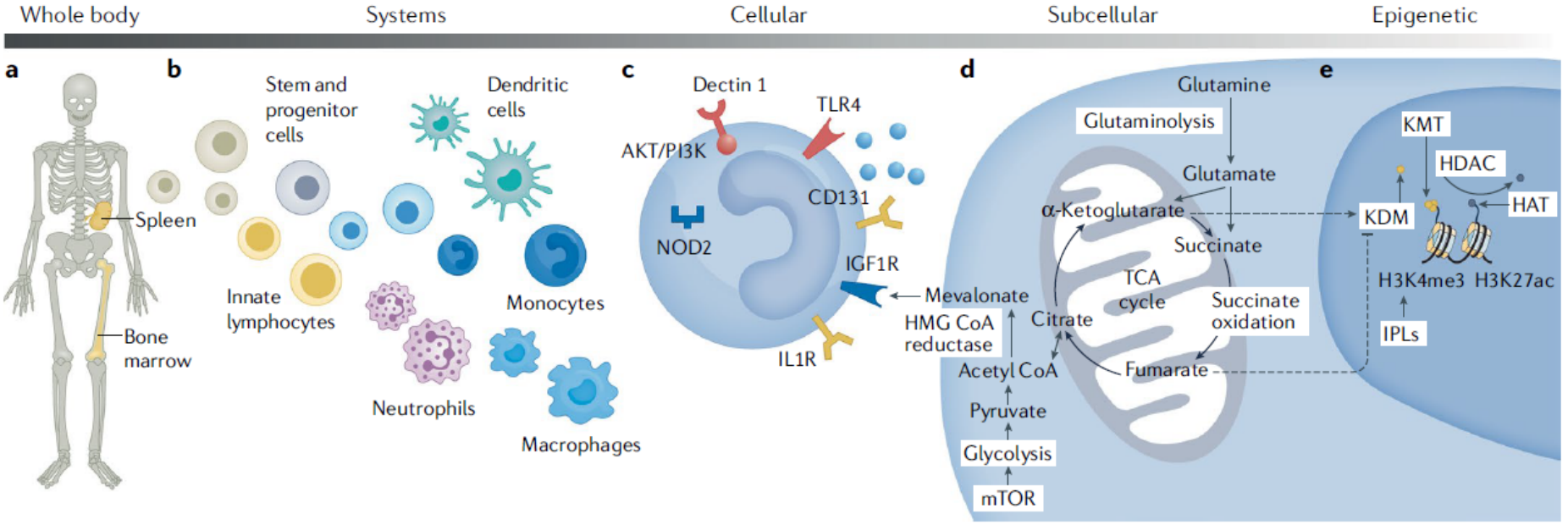

Fig. 1 | **Trained immunity targeting levels. a** | The spleen and bone marrow are important target organs, because they produce and contain large numbers of innate immune cells. **b** | Mature innate immune cells (innate lymphocytes, dendritic cells, monocytes, neutrophils and macrophages) and haematopoietic stem and progenitor cells can be targeted to prevent or enhance trained immunity. **c** | Pattern recognition receptors play an important part in trained immunity. Examples include dectin 1, Toll-like receptor 4 (TLR4) and nucleotide-binding oligomerization domain-containing protein 2 (NOD2). These receptors recognize pathogen-associated molecular patterns (PAMPs) and damage-associated molecular patterns (DAMPs). CD131 is the common β-subunit of granulocyte–macrophage colony-stimulating factor (GM-CSF) and interleukin-3 (IL-3) receptors. The IL-1 receptor (IL-1R) binds to IL-1β. Insulin-like growth factor 1 receptor (IGF1R) recognizes extracellular mevalonate. **d** | Intracellular metabolic pathways that can be targeted include glycolysis[4] (through interference with glycolytic enzymes or indirect through mechanistic target of rapamycin (mTOR) inhibition), cholesterol metabolism[54] (by targeting HMG CoA reductase), glutaminolysis[60] (through glutaminase inhibitors) and the tricarboxylic acid cycle (TCA) cycle (for example, by restricting succinate oxidation). **e** | H3K4me3 and K3K27ac are hallmark epigenetic signatures of trained immunity, which can be modified by targeting lysine demethylase (KDM), lysine methyltransferase (KMT), histone deacetylase (HDAC) and histone acetyltransferase (HAT) activity. Immune gene-priming long non-coding RNAs (IPLs) facilitate trimethylation of cytokine promotors[66]. PI3K, phosphatidylinositol 3-kinase.

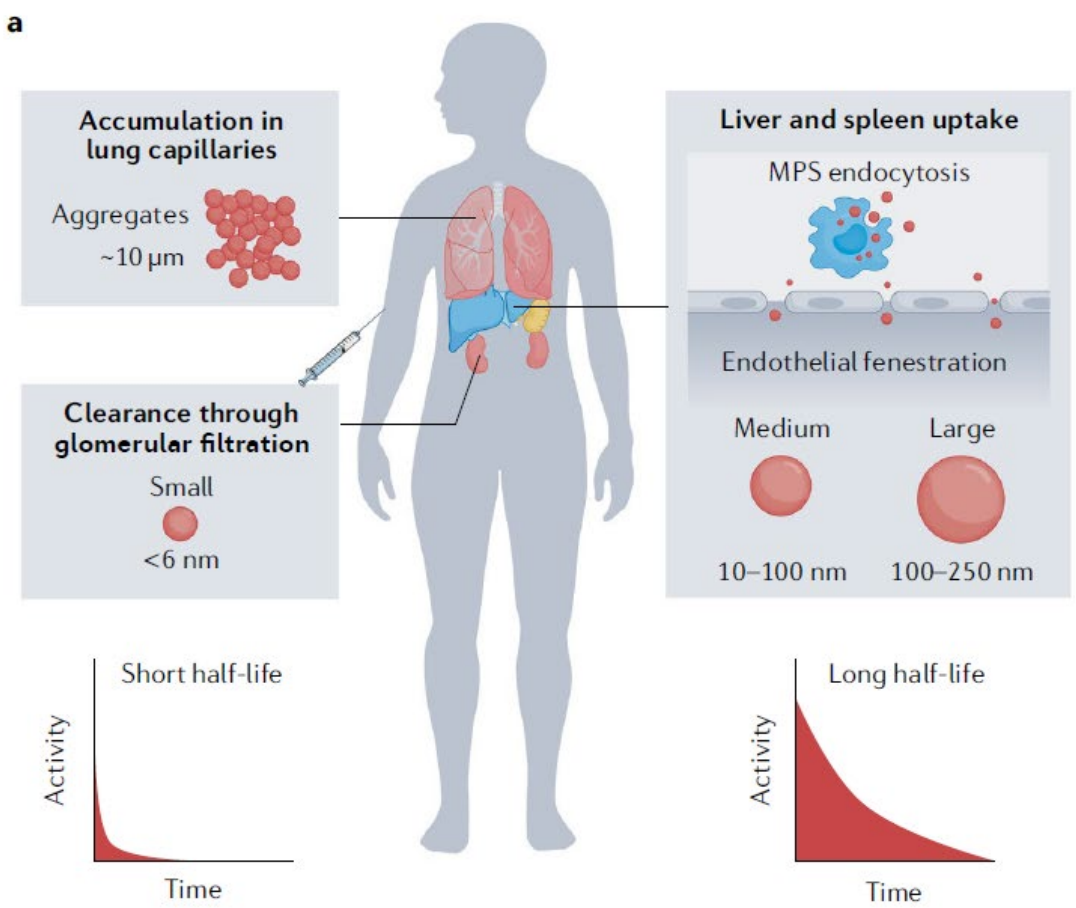
a
Accumulation in lung capillaries
Aggregates
~10 µm
Clearance through glomerular filtration
Small
<6 nm
Liver and spleen uptake
MPS endocytosis
Endothelial fenestration
Medium
Large
10–100 nm
100–250 nm
Short half-life
Activity
Time
Long half-life
Activity
Time


b
Liver
Bone marrow
Spleen
48 hours

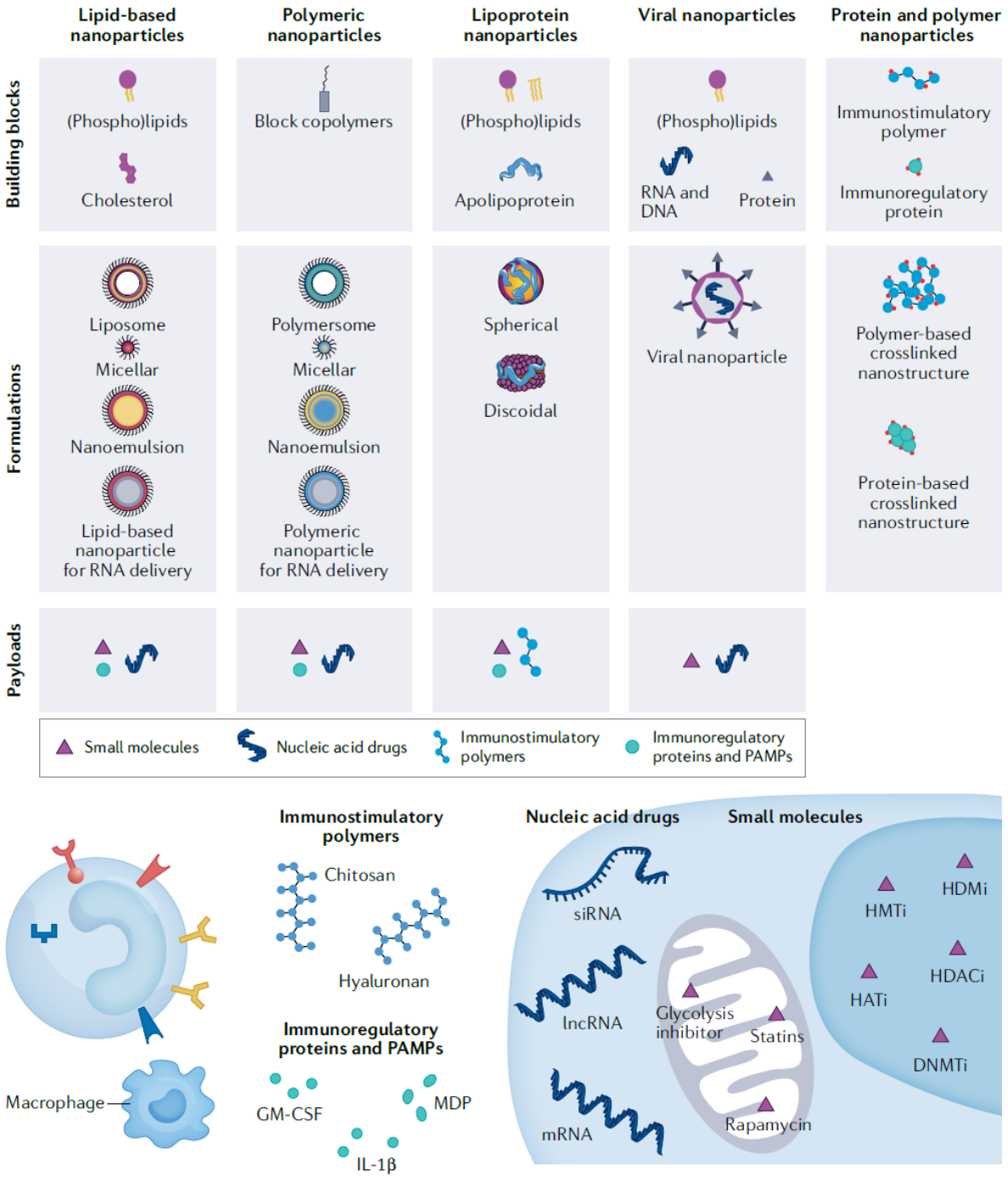
Lipid-based nanoparticles
Polymeric nanoparticles
Lipoprotein nanoparticles
Viral nanoparticles
Protein and polymer nanoparticles
Building blocks
(Phospho)lipids
Cholesterol
Block copolymers
(Phospho)lipids
Apolipoprotein
(Phospho)lipids
RNA and DNA
Protein
Immunostimulatory polymer
Immunoregulatory protein
Formulations
Liposome
Micellar
Nanoemulsion
Lipid-based nanoparticle for RNA delivery
Polymersome
Micellar
Nanoemulsion
Polymeric nanoparticle for RNA delivery
Spherical
Discoidal
Viral nanoparticle
Polymer-based crosslinked nanostructure
Protein-based crosslinked nanostructure
Payloads
Small molecules
Nucleic acid drugs
Immunostimulatory polymers
Immunoregulatory proteins and PAMPs
Macrophage
Immunostimulatory polymers
Chitosan
Hyaluronan
Immunoregulatory proteins and PAMPs
GM-CSF
MDP
IL-1β
Nucleic acid drugs
Small molecules
siRNA
lncRNA
mRNA
Glycolysis inhibitor
Statins
Rapamycin
HMTi
HDMi
HATi
HDACi
DNMTi

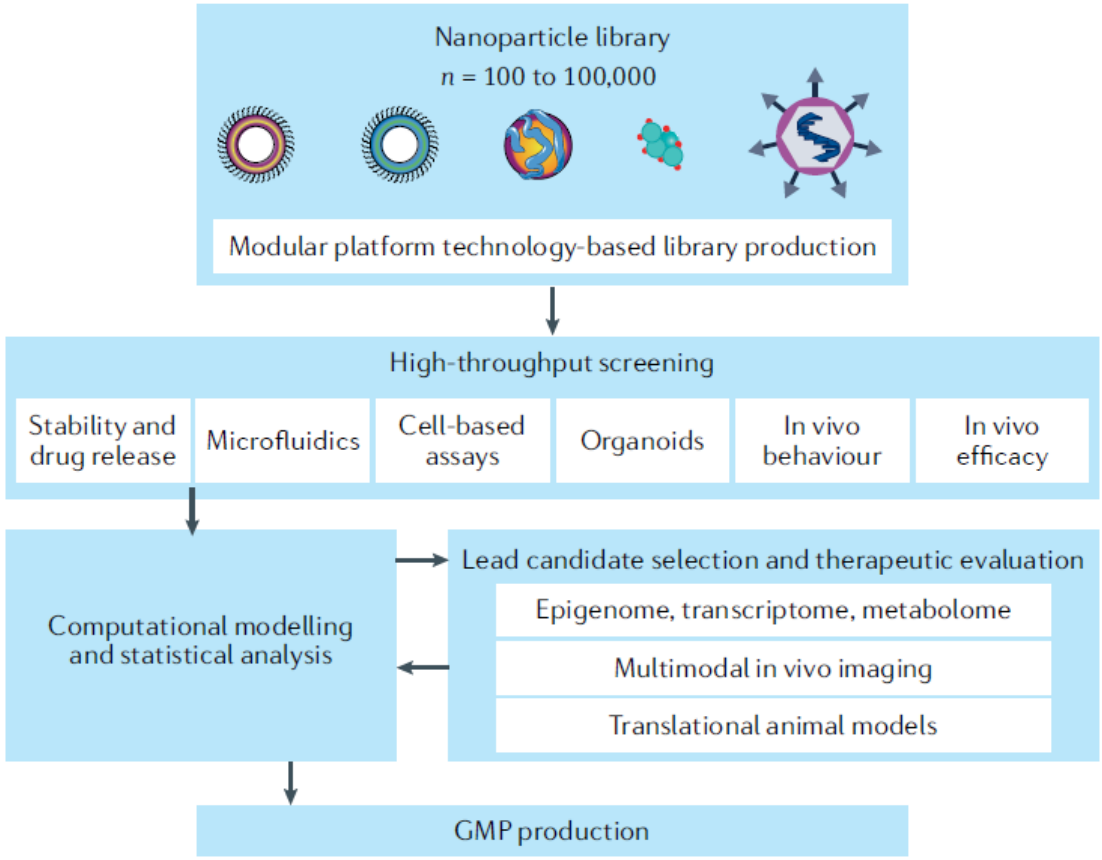
Nanoparticle library
n = 100 to 100,000
Modular platform technology-based library production
High-throughput screening
Stability and drug release
Microfluidics
Cell-based assays
Organoids
In vivo behaviour
In vivo efficacy
Computational modelling and statistical analysis
Lead candidate selection and therapeutic evaluation
Epigenome, transcriptome, metabolome
Multimodal in vivo imaging
Translational animal models
GMP production

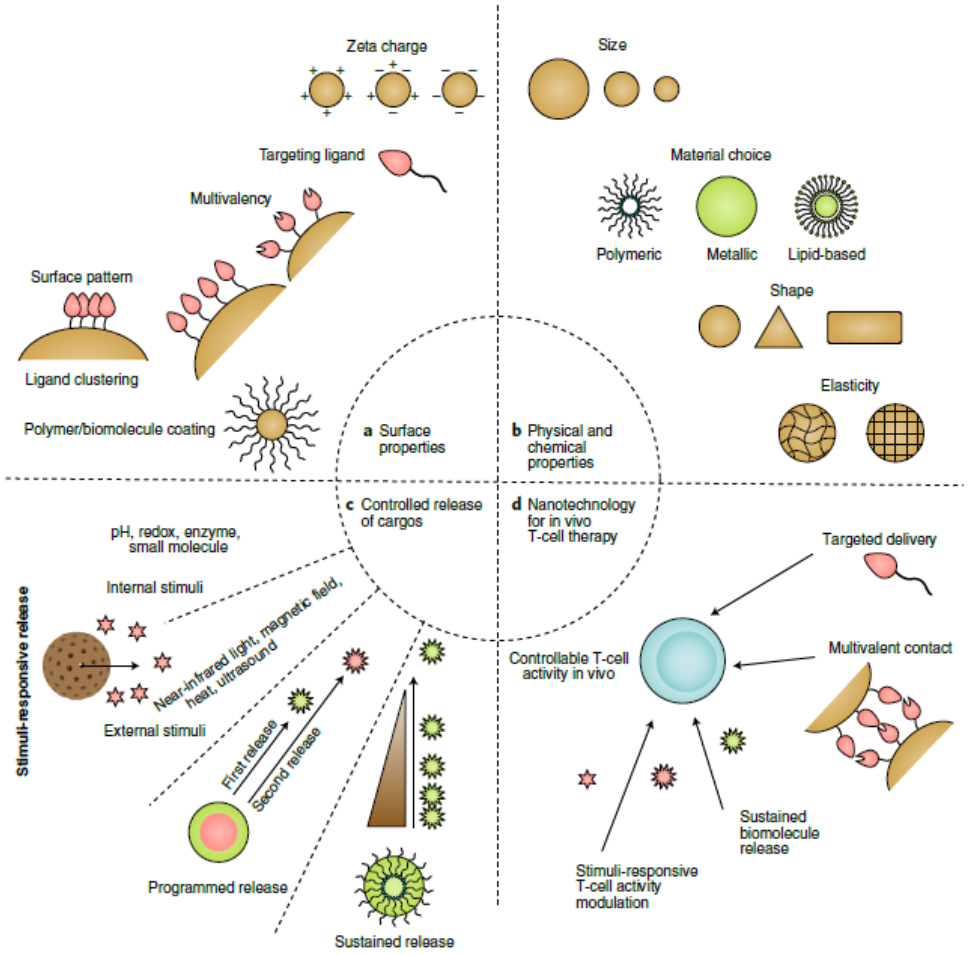

Fig. 2 | The current nanomaterial toolbox can be applied to in vivo T-cell therapies. a–c, Current strategies for expanding the functionalities of nanotechnologies include surface characteristics (**a**), physicochemical properties (**b**) and encapsulation and release features (**c**) of nanomaterials. **d**, Nanomaterials with optimized features could greatly benefit future T-cell cancer immunotherapies in vivo.

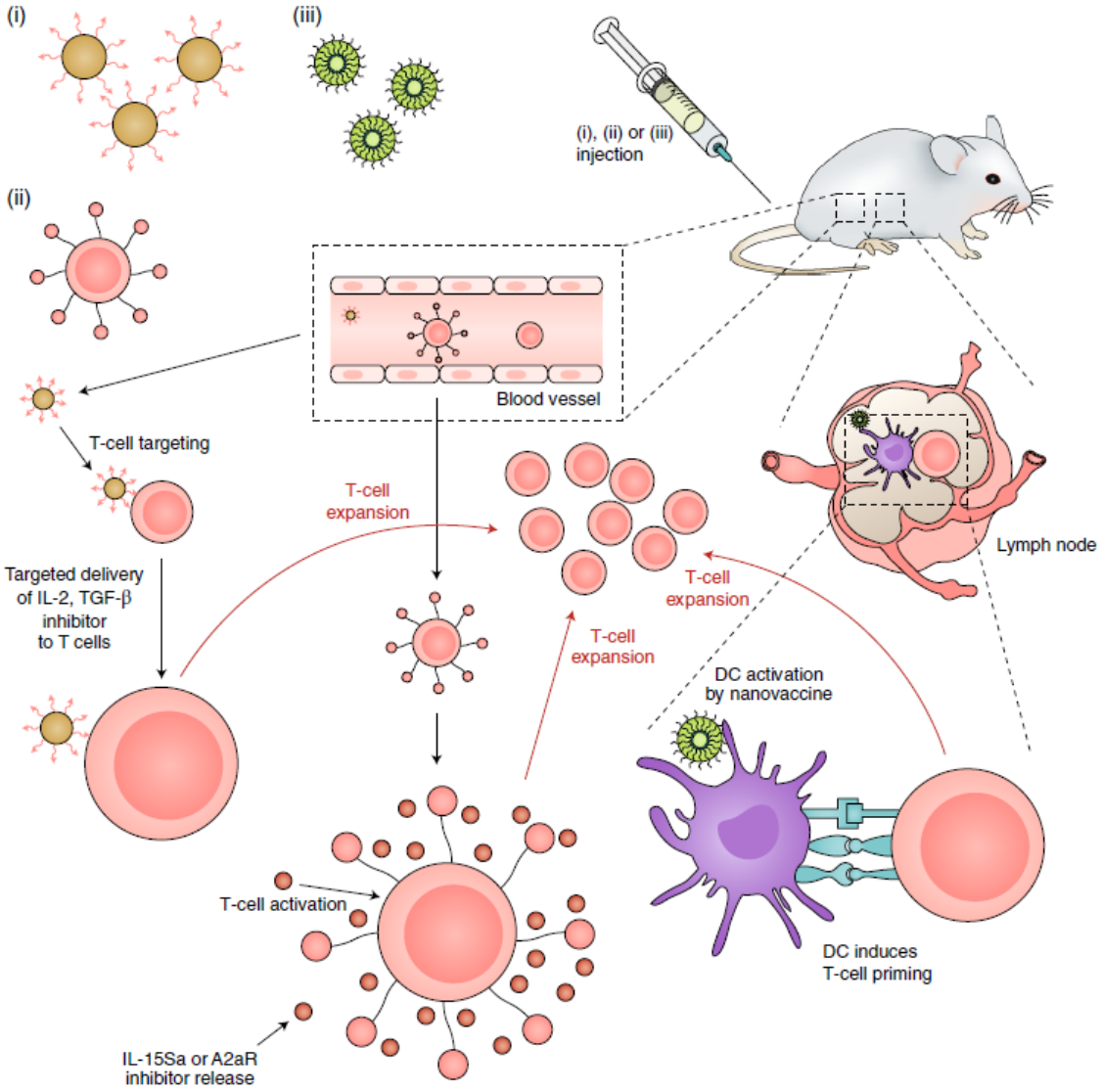

Fig. 3 | Nanomaterials for in vivo T-cell expansion. Nanomaterials can be designed for targeted delivery to T cells and induce T-cell activation and expansion in vivo (i). Backpacking nanoparticles are attached to the T-cell surface and release their cargo of stimulatory cues in response to environmental or applied stimuli, leading to precise control over the expansion of T cells in vivo (ii). Vaccine nanoparticles that target antigen-presenting cells, such as DCs, can activate these cells and induce T-cell expansion in vivo (iii).

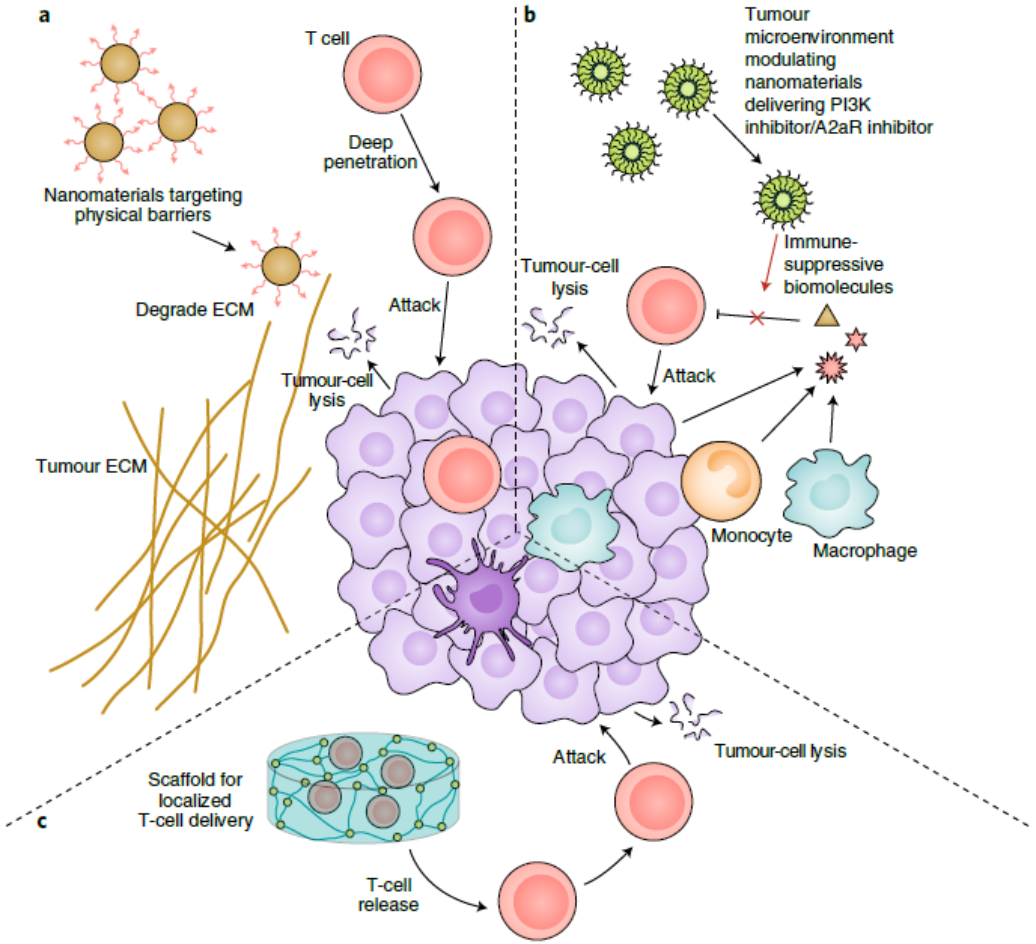

Fig. 4 | Nanomaterials overcome physical barriers and immune-suppressive environments for T-cell therapy. a, Nanomaterials can be designed to target the ECM and degrade the physical barriers inhibiting T-cell penetration and tumour cell targeting. **b**, Nanomaterials targeting the tumour microenvironment can deliver stimulatory cues to the tumour tissue and reverse the suppressive tumour microenvironment (immunological barrier), thus activating T-cell activity. **c**, Nanomaterials can locally deliver T cells directly to the tumour tissue with sustained release, which enhances tumour cell killing.

Table 2 | Preclinical and clinical studies of nanomaterials-based T-cell cancer immunotherapies

Nanomaterials		Cargo molecules	Model/indication	Stage
Nanomaterials for T-cell expansion in vivo	**T-cell-targeted delivery**			
	Poly(beta-amino ester)-based nanomaterial	Plasmids encoding a 194-1BBz CAR and a piggyBac transposase	TBD	Phase 1 projected 2020–2021
	Liposome	IL-2–Fc fusion protein	Mouse melanoma	Preclinical
	Liposome	TGF-β inhibitor (SB525334)	Mouse melanoma	Preclinical
	PLGA–PEG nanomaterial	TGF-β receptor inhibitor (SD-208)	Mouse colon cancer	Preclinical
	T-cell (Treg)-targeted hybrid nanomaterial	STAT3/STAT5 pathway inhibitor (imatinib)	Mouse melanoma	Preclinical
	Iron nanomaterial	Anti-CD137 and anti-PD-L1	Mouse melanoma	Preclinical
	Liposome-coated polymeric gel	Mouse IL-2 and a TGF-β inhibitor (SB505124)	Mouse melanoma	Preclinical
	Backpacking nanomaterials			
	IL-15 superagonist complex nanogel	IL-15 superagonist complex	Various solid tumours and lymphomas	Phase 1
	Multilamellar liposomal vesicles	A2a adenosine receptor inhibitor (SCH-58261)	Mouse model of human ovarian cancer	Preclinical
	Nanomaterials-based vaccines			
	Amphiphile ligands (EGFRvIII peptide-conjugated DSPE–PEG)	NA	Mouse glioma expressing EGFRvIII^{+}	Preclinical
	Lipid nanomaterial	mRNA encoding the tight junction protein claudin 6 (CLDN6)	Mouse melanoma expressing CLDN6	Preclinical

		junction protein claudin 6 (CLDN6)	expressing CLDN6		
Nanomaterials overcome physical barriers and hostile tumour microenvironments	**Nanomaterials that target physical barriers**				
	PLGA nanomaterial	Photothermal agent indocyanine green	Mouse melanoma	Preclinical	104
	Calcium phosphate nanomaterials with lipid bilayer coating	An antifibrotic compound α-mangostin and a plasmid encoding the stimulatory cytokine LIGHT	Mouse pancreatic cancer	Preclinical	59
	Nanomaterials that reverse the immune-suppressive environment				
	Lipid nanomaterial	A PI3K inhibitor (PI-3065) and a T-cell stimulator (7DW8-5)	Mouse breast cancer	Preclinical	61
	Multilamellar liposomal vesicles	A2a adenosine receptor inhibitor (SCH-58261)	Mouse model of human ovarian cancer	Preclinical	93
	Nanomaterials for local T-cell delivery				
	Macroporous alginate scaffolds	IL-15 superagonists, antibodies for CD3, CD28 and CD137	Mouse breast cancer, mouse ovarian cancer	Preclinical	60
	Nickel–titanium alloys	Antibodies for CD3, CD28, CD137	Mouse model of human pancreatic cancer expressing receptor tyrosine kinase-like orphan receptor (ROR1)	Preclinical	111
Nanomaterials as NBiTEs	Liposome	Human epidermal growth factor receptor 2 (HER2) and CD20 antibodies	Mouse breast cancer	Preclinical	131
	Polystyrene nanomaterial	Antibodies for HER2 and calreticulin protein	Mouse breast cancer	Preclinical	132
	Exosome	Exosome expressing antibodies for CD3 and epidermal growth factor receptor (EGFR)	Mouse breast cancer	Preclinical	58

TBD, to be determined; NA, not applicable; LIGHT, tumour necrosis factor superfamily 14.

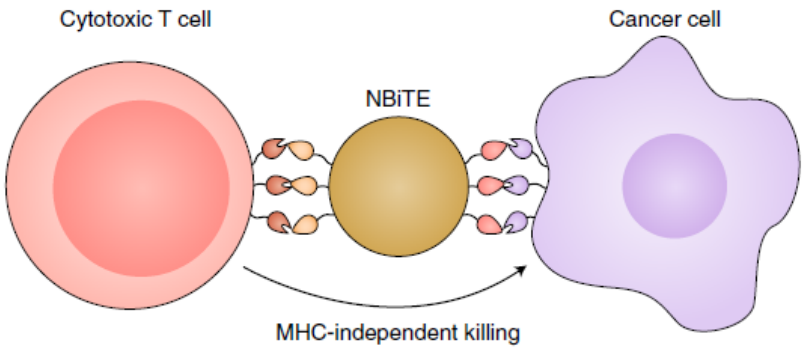

Fig. 5 | NBiTEs for cancer immunotherapy. A typical NBiTE is developed by adding two scFvs on the nanoparticle surface, with one scFv targeting a T-cell-specific antigen while the other targets a tumour-specific antigen. The multivalent contact at the nanomaterial/cell interfaces makes NBiTEs bridge T cells and tumour cells more effectively than traditional BiTEs and induces potent tumour cell killing.

Gene Delivery

- Transfection- the delivery of foreign molecules such as DNA and RNA into eukaryotic cells
- Naked DNA is not suitable for in-vivo transport of genetic materials-> degradation by serum nucleases
- Ideal gene delivery system
  - Biocompatible
  - Non-immunogenic
  - Stable in blood stream
  - Protect DNA during transport
  - Small enough to extravagate
  - Cell and tissue specific

Endocytosis

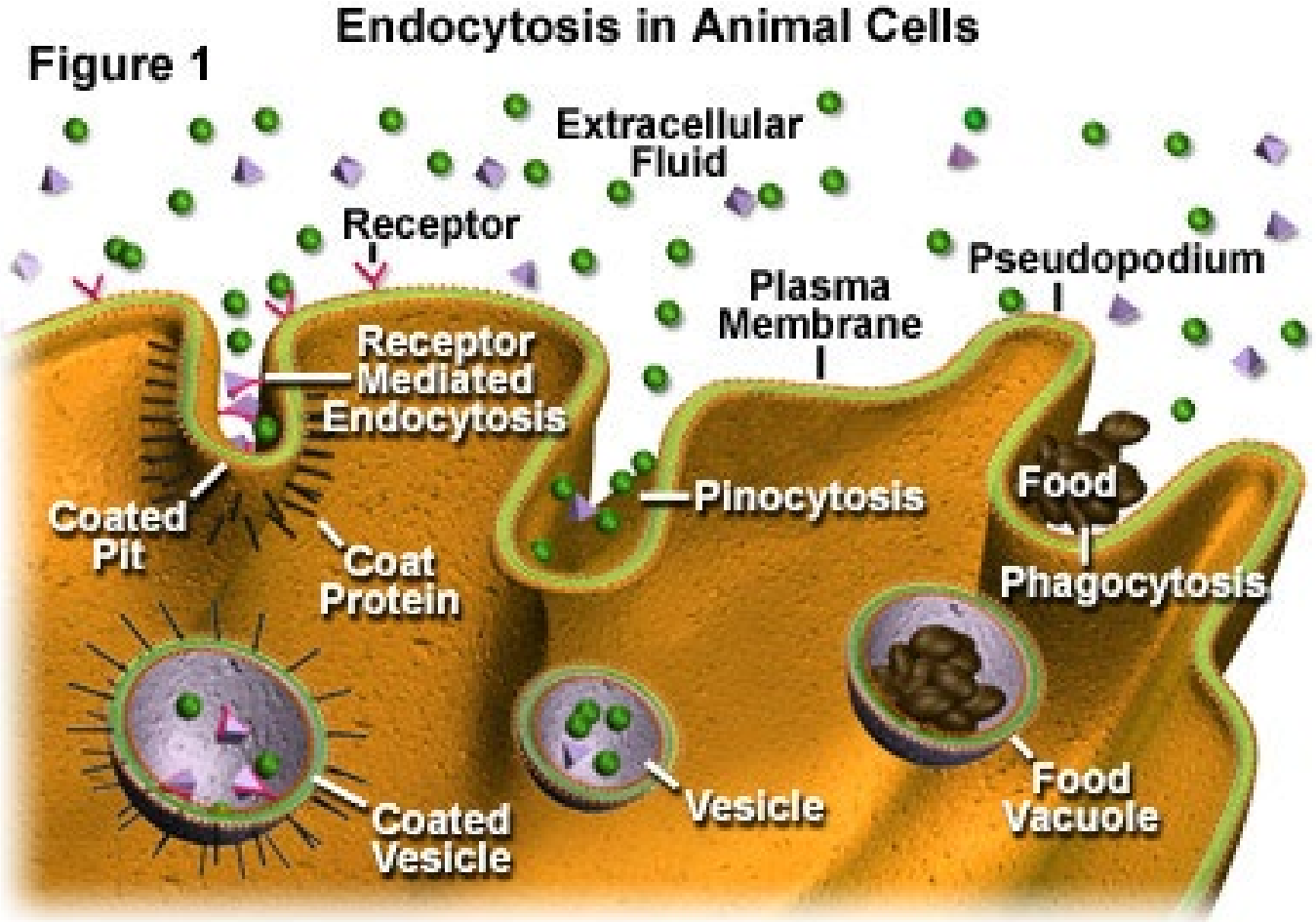

Endocytic pathway in mammalian cells

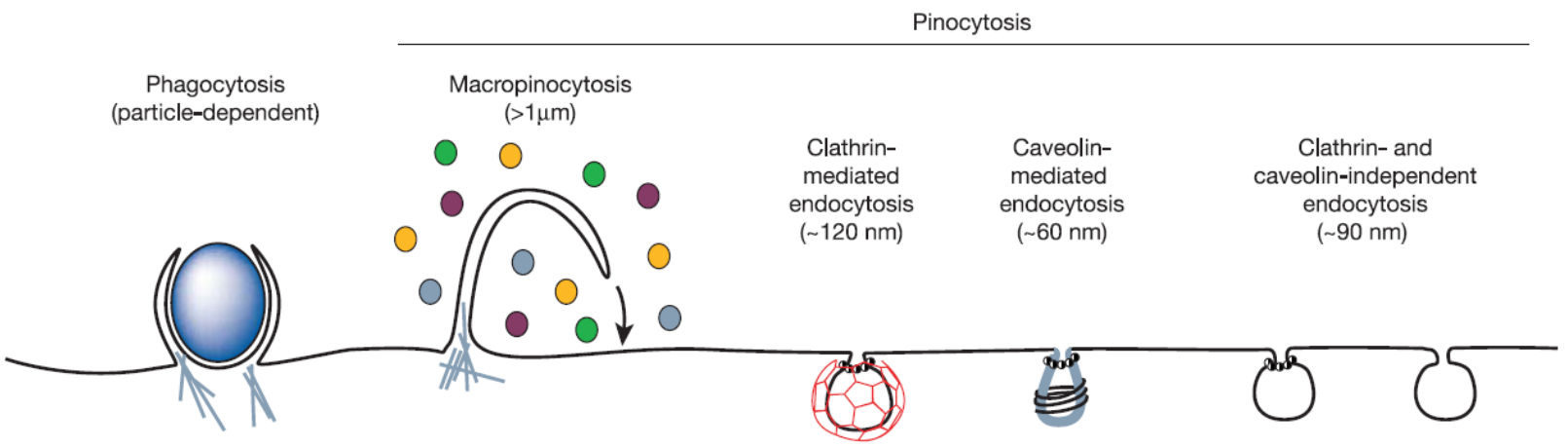

Figure 1 Multiple portals of entry into the mammalian cell. The endocytic pathways differ with regard to the size of the endocytic vesicle, the nature of the cargo (ligands, receptors and lipids) and the mechanism of vesicle formation.

Barrier to non-viral gene delivery

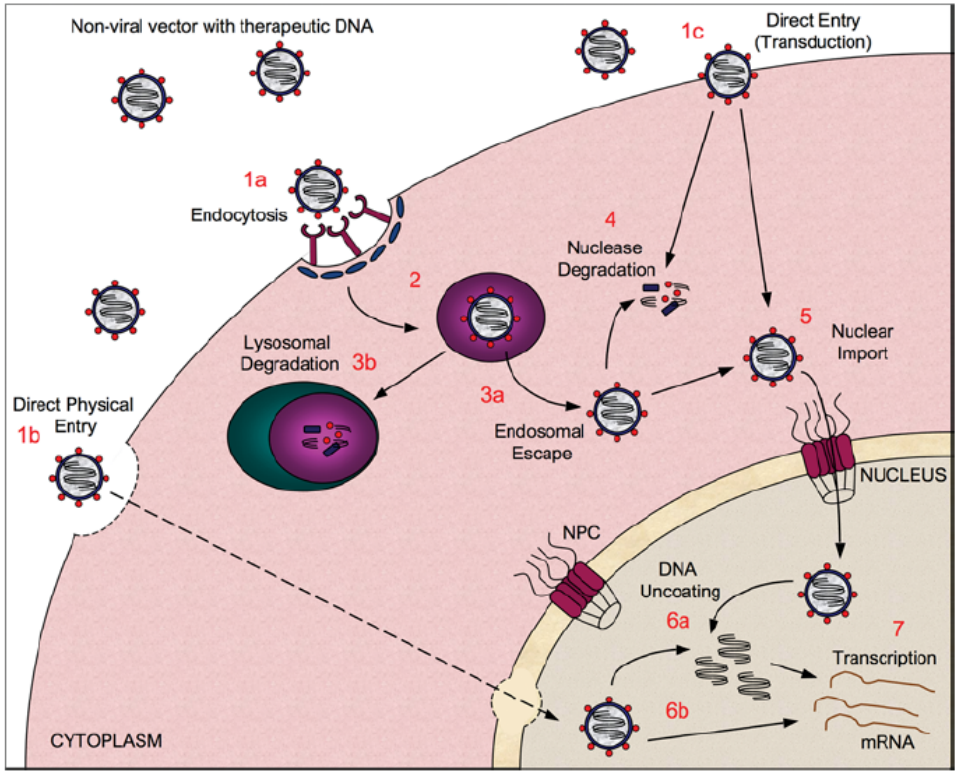

Figure 1 Barriers to non-viral gene delivery

Representation of the route travelled by a non-viral gene-delivery vector carrying therapeutic DNA to the nucleus. A non-viral vector, formed by interaction of the DNA with a carrier compound, must cross the plasma membrane to enter the cell. This can be via several routes, including endocytosis-based entry (1a), direct physical entry routes, such as electroporation or ballistic delivery (1b), or direct entry via protein transduction (1c). Depending on the mode of cellular entry, the vector may become encapsulated in an endosome (2), from which it must escape (3a) or it will become degraded when the endosome fuses with a lysosome (3b). The DNA will at some point be subjected to degradation by cytosolic nucleases (4), as it traverses through the cytoplasm to reach the nucleus. Finally, the vector must undergo nuclear transport (5) through NPCs embedded in the NE in order to gain access to the nucleoplasm. Once in the nucleus, the DNA may (6a) or may not (6b) need to be uncoated, depending upon the vector used, before it can ultimately be transcribed (7).

Biochem. J. (2007) **406**, 185–202 (Printed in Great Britain) doi:10.1042/BJ20070505

NLS-mediated nuclear import

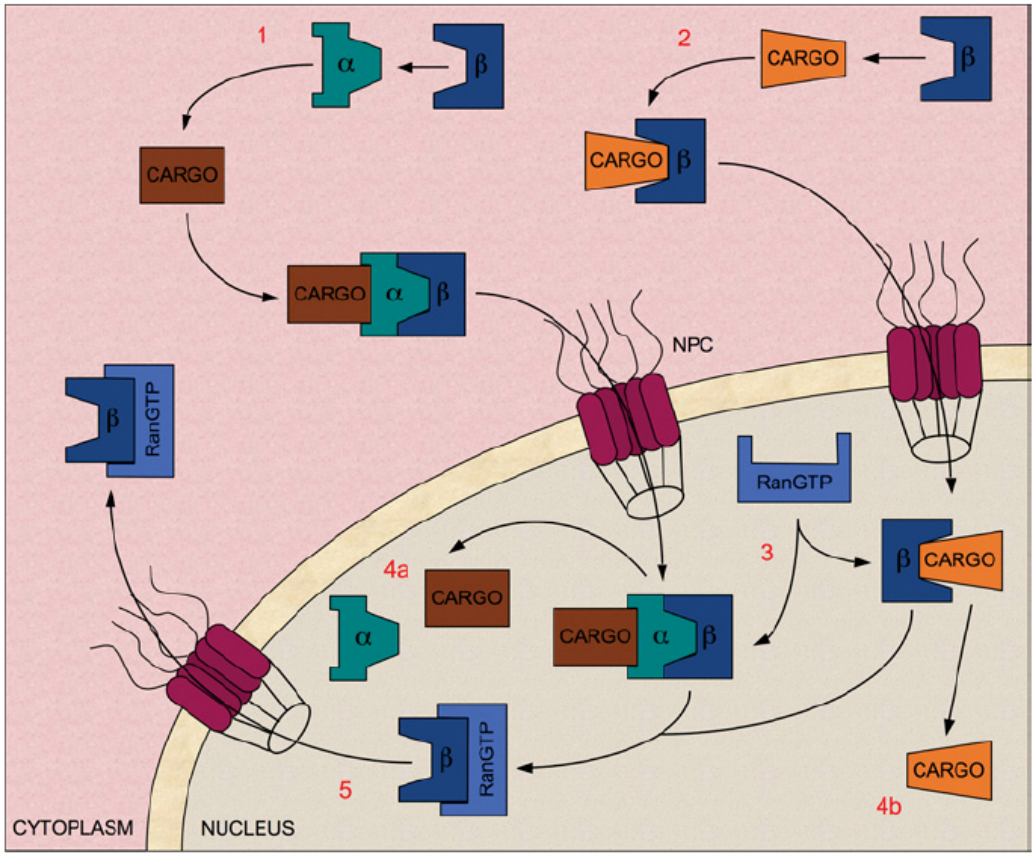

Figure 2 NLS-mediated nuclear import pathways

In classical nuclear import, the NLS found in cargo bound for the nucleus is recognized by the Imp α subunit of the Imp α/β heterodimer (1). However, there are also many examples where Imp β or one of its many homologues can mediate nuclear import or cargo proteins independently of Imp α (2). In both cases, transient interactions between the Imp β and the nucleoporin proteins that line the NE-embedded NPCs mediate translocation into the nucleus. Once inside, RanGTP binds to Imp β (3), releasing Imp α and the cargo into the nucleoplasm (4a and 4b). RanGTP itself is then recycled back to the cytoplasm (5), where it is converted into its RanGDP state (not shown). An animated version of this Figure can be found at http://www.BiochemJ.org/bj/406/0185/bj4060185add.htm

Barriers to DNA Delivery

BOX 1

A number of challenges and barriers face the successful delivery of therapeutic DNA to target cells in the body. Physicochemical, economic and sterilization challenges complicate formulation; the complex environment of the human body hinders its successful transport to the target cell population; and endocytic pathway barriers hinder its successful transport to the nucleus of the cell (the site of action). Each known and major barrier is listed in Fig. B1, using nanoscale DNA-delivery systems as representative examples. Each barrier exists independent of length scale. L = lysosome. A number of clever systems have been devised to overcome these barriers, the general design criteria of which are given in Tables B1 and B2.

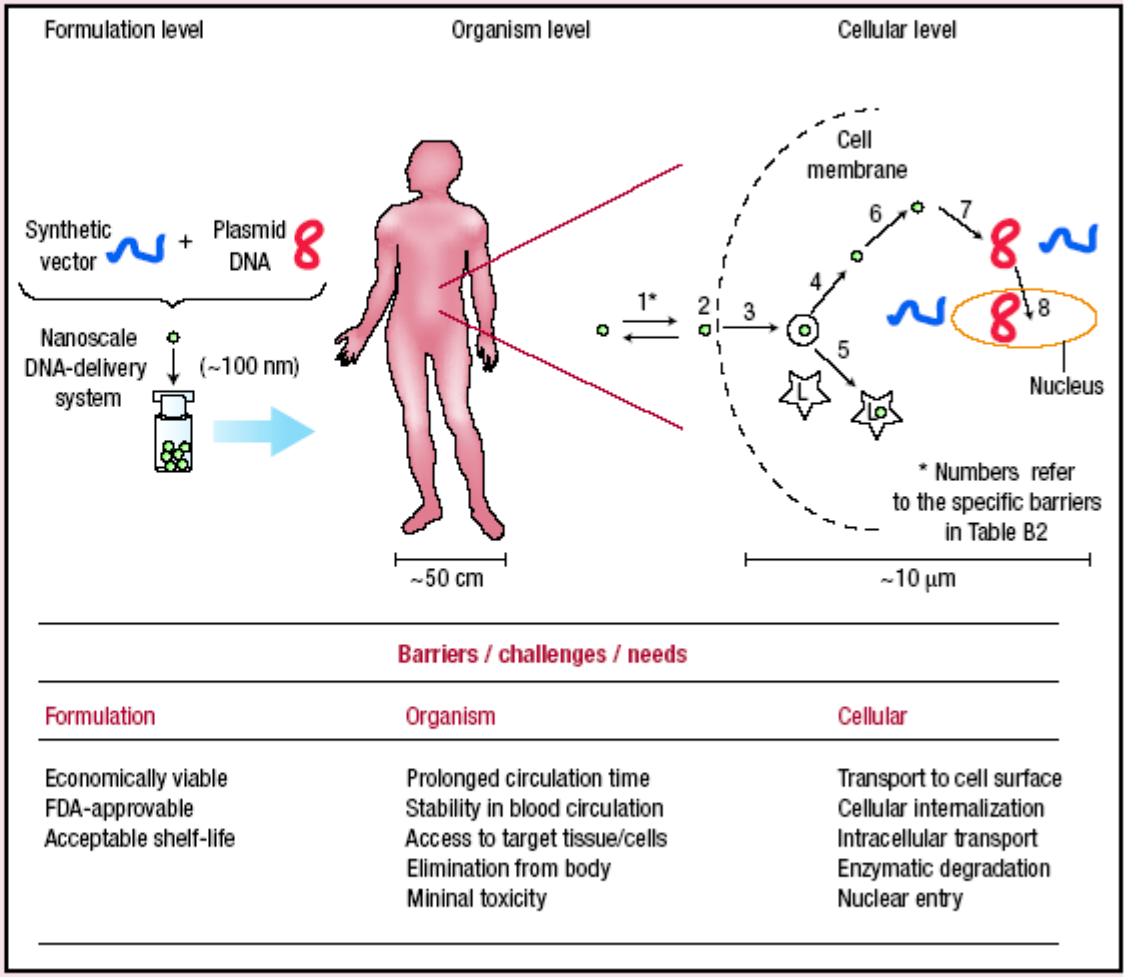

Barriers / challenges / needs

Formulation	Organism	Cellular
Economically viable	Prolonged circulation time	Transport to cell surface
FDA-approvable	Stability in blood circulation	Cellular internalization
Acceptable shelf-life	Access to target tissue/cells	Intracellular transport
	Elimination from body	Enzymatic degradation
	Mininal toxicity	Nuclear entry

Figure B1 Barriers to DNA delivery.

Organism Level			
Barrier/challenge/need	**Rationale**	**Example approaches**	**Materials design criteria**
Prolonged circulation time	Maximize total flux past target cell type	PEG conjugates to minimize interaction with serum proteins	Hydrophilic Uncharged
Stability within blood circulation	Maintenance of designed functionality	Crosslinking to maximize overall stability	Stable crosslinks within bloodstream, but reversible upon entry into target cell
Access to target tissue/cells	Transport from capillary lumen to extracellular space to reach target cell surface	Vaso-active protein conjugates (for example, vascular endothelial growth factor)	Retention of protein activity post conjugation
		Targeting restricted to 'leaky' vessel tissues (for example, tumour, liver, spleen).	Small diameter delivery system (for example, <100 nm)
Elimination from body	Minimal build-up of delivery vector over time	Control over molecular weight	Filterable through kidneys
		Engineered biodegradation sites	Biodegradable
Minimal toxicity and immunogenicity	Safety over treatment duration and beyond that required for FDA-approval	Minimize cation density	Non-cytotoxic
		Avoid protein-based materials/conjugates	Non-immunogenic

Cellular Level

Barrier number (from Fig. B1)	Barrier/challenge/need	Example approaches	Materials design criteria
1, 2 and 3	Transport to cell surface, association with cell membrane, internalization	Receptor/ligand interaction (for example, antibody/polymer conjugates, recombinant protein–polymer fusions, carbohydrate conjugates)	Cell-type specificity, low cross reactivity, if desired
			Promiscuous attachment, high cross reactivity, if desired (for example, positive zeta potential, lipid conjugation)
		Non-specific interaction with cell surface (for example, positive zeta potential, lipid conjugates)	
			Endocytic pathway trigger (for example, clathrin-dependent, clathrin-independent, caveolin-dependent)
4 and 5	Escape endosomal vesicle and avoid transport to lysosome	Buffering capacity between pH ~7.2 and ~5.0	Ability to disrupt endosomal membrane and/or fusion of endosome with lysosome
		Fusogenic peptide conjugate	
6	Transport through cytosol to perinuclear space with minimal degradation	'Higher' molecular weight to maintain complex stability within cytosol	Thermodynamic and kinetic stability of complex within cytosol
			Minimize DNA degradation within cytosol
7	Separation of complex to allow nuclear translocation	Hydrolytically or reductively degradable polymers to reduce molecular weight	'Triggered' degradation of polymer to reduce thermodynamic and kinetic stability of complex. Release of intact DNA at or near nuclear envelope
8	Nuclear entry	Nuclear localization sequence conjugates	Facilitate nuclear uptake of DNA using virus-derived signals
		Mitosis	Facilitate nuclear uptake during mitosis when the nuclear envelope is dissolved.

CANCER NANOTECHNOLOGY: OPPORTUNITIES AND CHALLENGES

NATURE REVIEWS | CANCER VOLUME 5 | MARCH 2005 | 161

Summary

- Nanotechnology concerns the study of devices that are themselves or have essential components in the 1–1,000 nm dimensional range (that is, from a few atoms to subcellular size).
- Two main subfields of nanotechnology are nanovectors — for the administration of targeted therapeutic and imaging moieties — and the precise patterning of surfaces.
- Nanotechnology is no stranger to oncology: liposomes are early examples of cancer nanotherapeutics, and nanoscale-targeted magnetic resonance imaging contrast agents illustrate the application of nanotechnology to diagnostics.
- Photolithography is a light-directed surface-patterning method, which is the technological foundation of microarrays and the surface-enhanced laser desorption/ionization time-of-flight approach to proteomics. Nanoscale resolution is now possible with photolithography, and will give rise to instruments that can pack a much greater density of information than current biochips.
- The ability of nanotechnology to yield advances in early detection, diagnostics, prognostics and the selection of therapeutic strategies is predicated based on its ability to 'multiplex' — that is, to detect a broad multiplicity of molecular signals and biomarkers in real time. Prime examples of multiplexing detection nanotechnologies are arrays of nanocantilevers, nanowires and nanotubes.
- Multifunctionality is the fundamental advantage of nanovectors for the cancer-specific delivery of therapeutic and imaging agents. Primary functionalities include the avoidance of biobarriers and biomarker-based targeting, and the reporting of therapeutic efficacy.
- Thousands of nanovectors are currently under study. By systematically combining them with preferred therapeutic and biological targeting moieties it might be possible to obtain a very large number of novel, personalized therapeutic agents.
- Novel mathematical models are needed, in order to secure the full import of nanotechnology into oncology.

Protein Corona

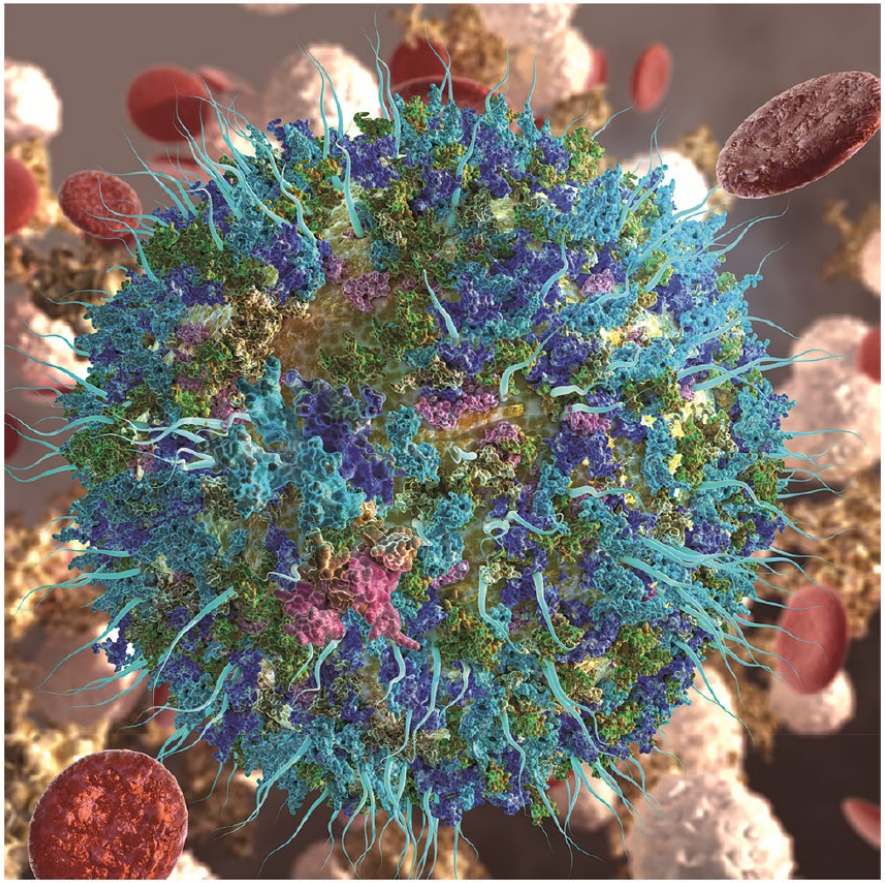

Figure 1. A nanoparticle gains a new biological identity upon its dynamic interactions with biological fluids, giving rise to a protein corona (shown as adsorbed green, blue, and cyan globules), which consequently influences drug delivery and targeting of the functionalized nanoparticle (illustrated as aqua blue fibrils).

DOI: 10.1021/acsnano.7b08008
ACS Nano 2017, 11, 11773−11776

The protein corona effect refers to the phenomenon that occurs when nanoparticles are introduced into a biological environment, such as blood or tissue fluids. Upon exposure to these environments, proteins and other biomolecules in the fluid can adsorb onto the surface of the nanoparticles, forming a layer or "corona" around them. This protein corona can significantly impact the physicochemical properties, biological interactions, and the overall fate of the nanoparticles in the body.

Altered physicochemical properties: The protein corona can change the size, shape, and surface charge of the nanoparticles, which may affect their stability, aggregation, and circulation half-life in the body.

Impact on cellular uptake and targeting: The protein corona can influence how nanoparticles interact with cells, as it may mask the surface ligands or functional groups on the nanoparticles that are intended for targeted delivery. This can lead to a reduced targeting efficiency and unintended uptake by other cells, including immune cells.

Immunogenicity and toxicity: The presence of a protein corona can potentially trigger an immune response, leading to the clearance of the nanoparticles from the body or causing adverse side effects. The composition of the protein corona may also influence the potential toxicity of the nanoparticles.

Biodistribution and clearance: The protein corona can affect the biodistribution of nanoparticles in the body and their subsequent clearance by altering the recognition and interaction of nanoparticles with various organs and tissues.

Vroman Effect

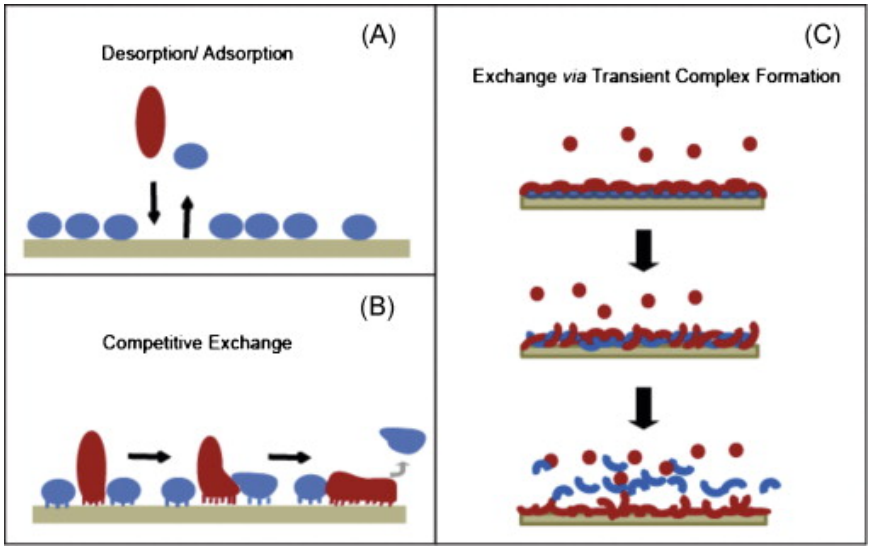

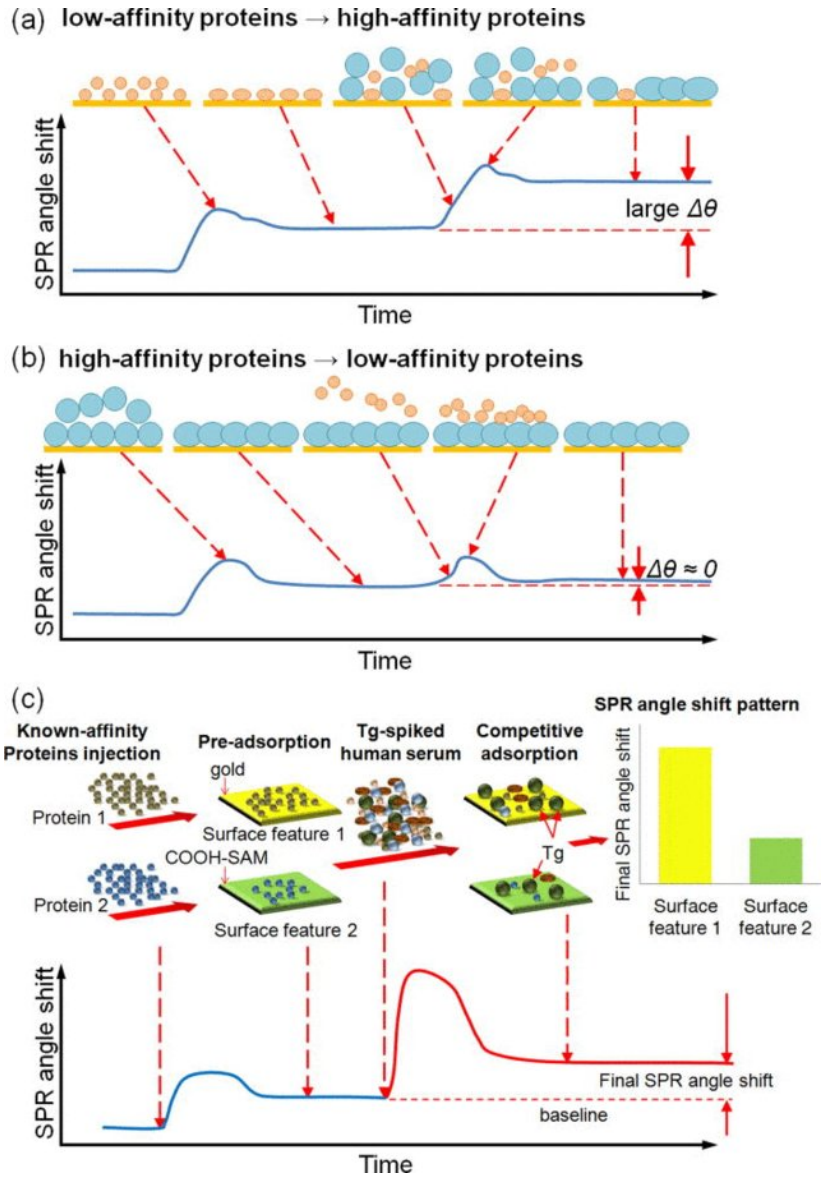

Vroman Effect

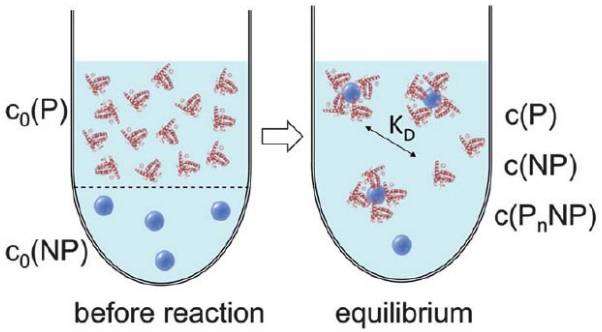

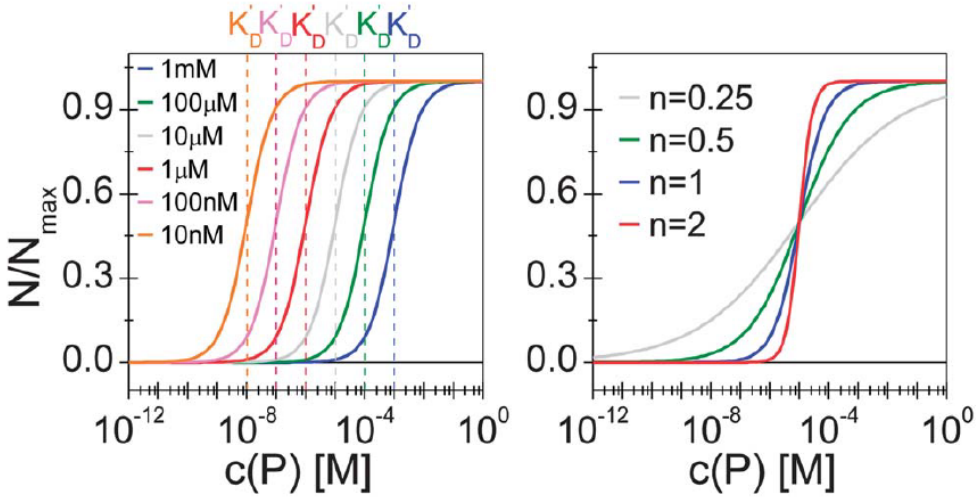

$$NP + nP \leftrightarrow P_nNP$$

$$K_D = \frac{c(NP)c^n(P)}{c(P_nNP)} = \frac{k_{off}}{k_{on}}$$

The Vroman effect, also known as the Vroman's adsorption-desorption principle, is a phenomenon named after Dr. Leo Vroman, who first described the process in the context of blood-material interactions in the 1960s. The Vroman effect refers to the dynamic exchange of proteins adsorbing onto and desorbing from a surface over time, with higher affinity proteins displacing those with lower affinities. In the context of nanoparticles, the Vroman effect has important implications for understanding the protein corona that forms around nanoparticles in biological fluids.
When nanoparticles are introduced into biological fluids, they rapidly interact with proteins and other biomolecules present in the fluid. Initially, high-abundance proteins with relatively low affinity for the nanoparticle surface may adsorb quickly due to their higher concentration. However, over time, these proteins can be replaced by lower-abundance proteins that have higher affinity for the nanoparticle surface. This dynamic exchange of proteins can lead to changes in the composition of the protein corona over time.

Cellular uptake and targeting: Changes in the protein corona composition can affect the targeting efficiency and cellular uptake of nanoparticles, potentially leading to off-target effects and unintended interactions with immune cells.
Immunogenicity and toxicity: The Vroman effect can influence the immunogenicity and potential toxicity of nanoparticles, as different proteins in the corona can trigger immune responses or cause adverse side effects.
Biodistribution and clearance: The dynamic nature of the protein corona can affect the biodistribution of nanoparticles in the body and their subsequent clearance by altering the recognition and interaction of nanoparticles with various organs and tissues.

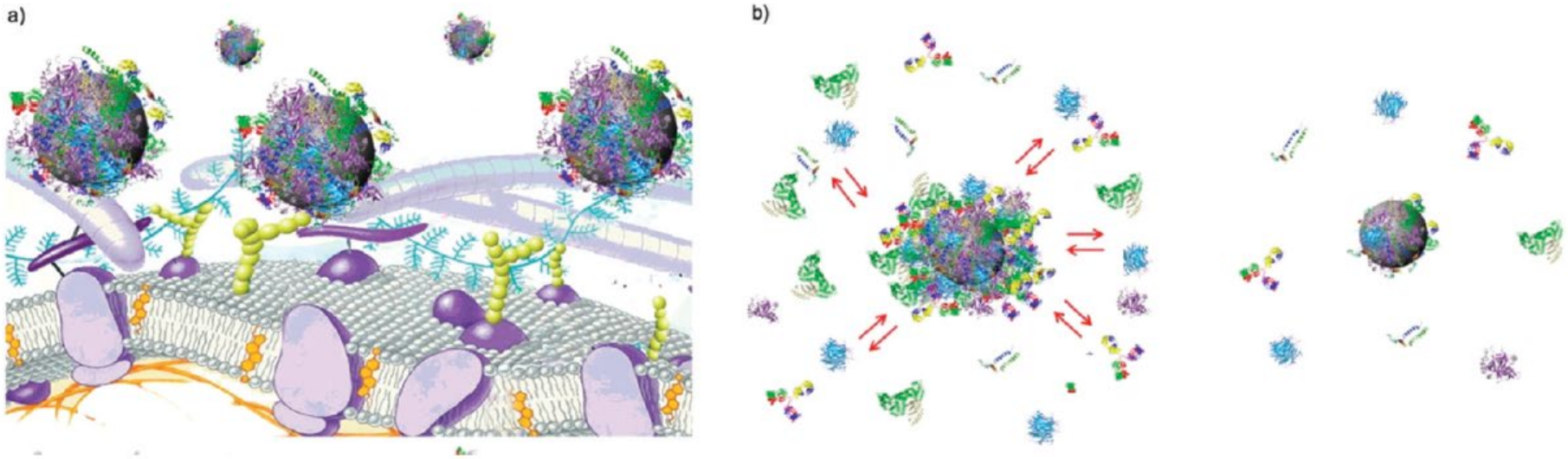

Figure 1. (a) Cartoon representation of the possible exchange/interaction scenarios at the bionanointerface at the cellular level. (b) Schematic drawing of the structure of NP−protein complexes in plasma: the "core" nanoparticle is surrounded by the protein corona composed of an outer weakly interacting layer of protein (left, full red arrows) rapidly exchanging with a collection of free proteins and a "hard" slowly exchanging corona of proteins (right). Diagram is not to scale in representing the proportions of the different objects.

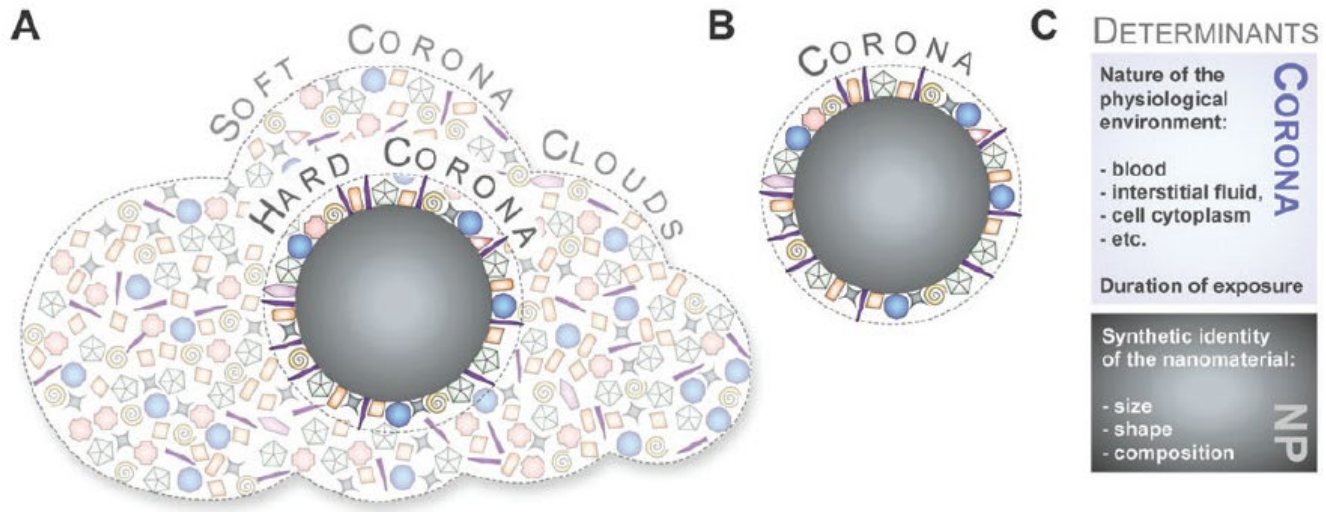

Fig. 3 Illustration of the old and new models referring to the description and determinants of the protein corona. (A) Hard and soft coronas, as well as protein clouds. (B) Coronas as analytically accessible NP–protein complexes. (C) Determinants of corona formation include not only the synthetic identity of the nanomaterial, but also the nature of the physiological environment.

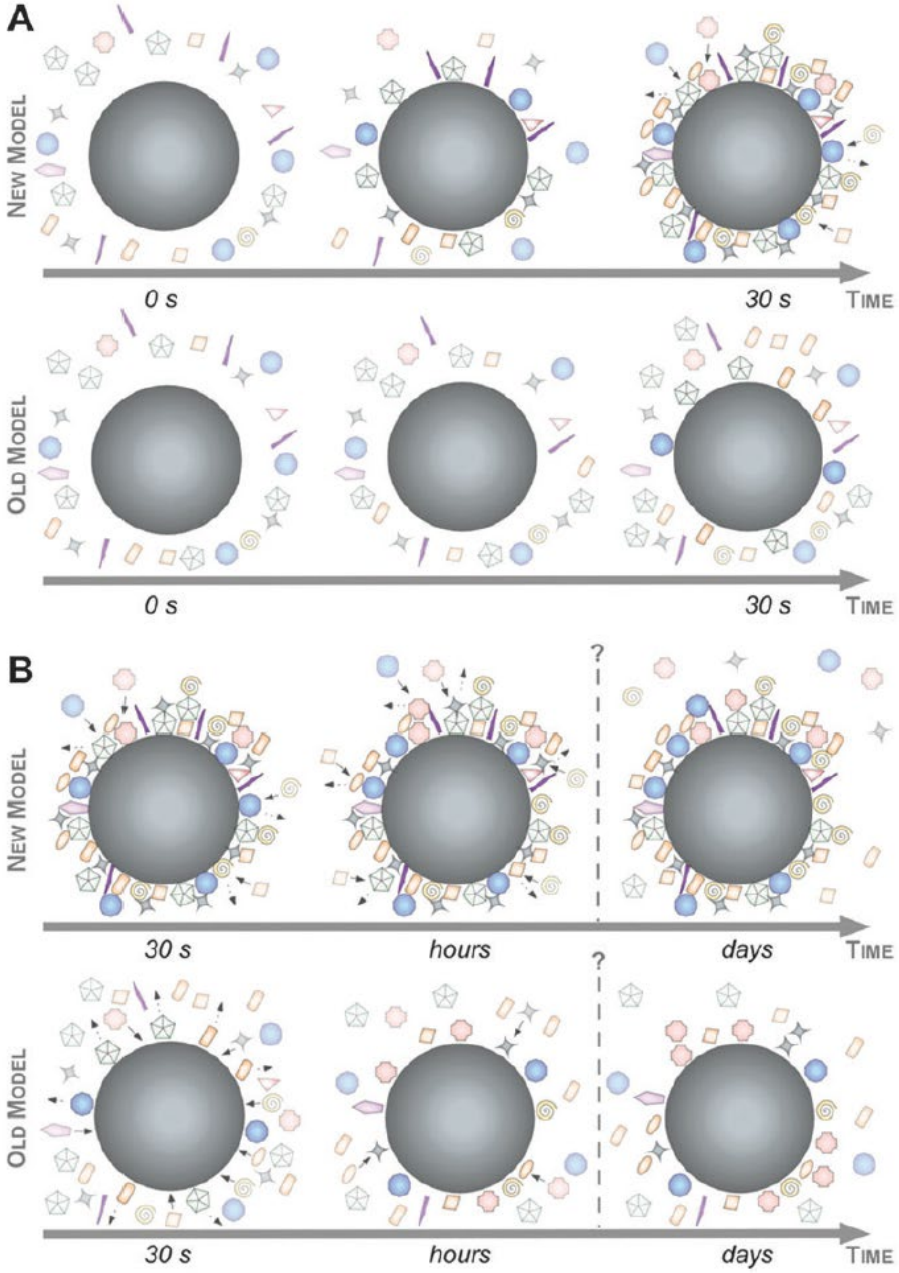

Fig. 6 Complexity and evolution of the biomolecule corona – the old *versus* the new model. (A) The early phase: a highly complex corona is established already in 30 sec, which may be composed of multiple core–shell structures ('new'). A corona of low complexity evolves slowly ('old'). (B) The late phase: corona composition *ex situ* remains stable and changes predominantly quantitatively rather than qualitatively over time with Vroman-effect dependent and independent binding kinetics ('new'). A highly dynamic protein corona, changes significantly over time, controlled by the 'Vroman-effect' ('old'). Note that the objects are not drawn to scale.

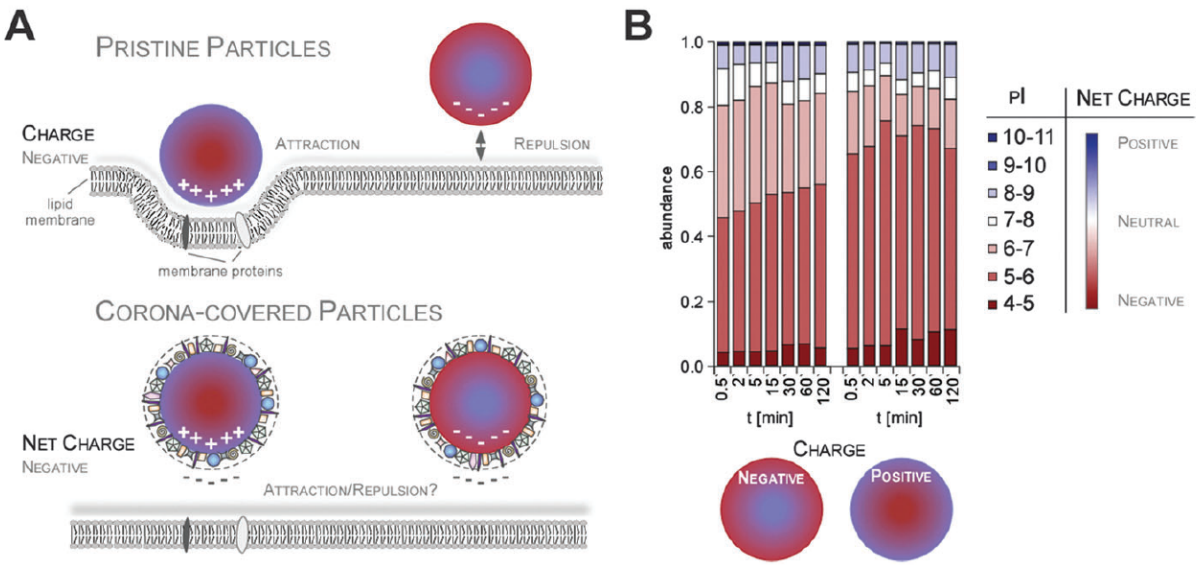

Fig. 7 Impact of NP charge on cellular uptake in the absence or presence of the protein corona. (A) Improved cellular uptake of positively charged NPs may be mediated by enhanced interaction with the negatively charged cell membrane only for pristine NPs (upper panel). In contrast, plasma corona covered NPs are overall negatively charged *in situ*, probably preventing NP-charge driven cell membrane interaction. (B) Plasma corona covered NPs are overall negatively charged, irrespective of the NPs' negative or positive surface functionalization.

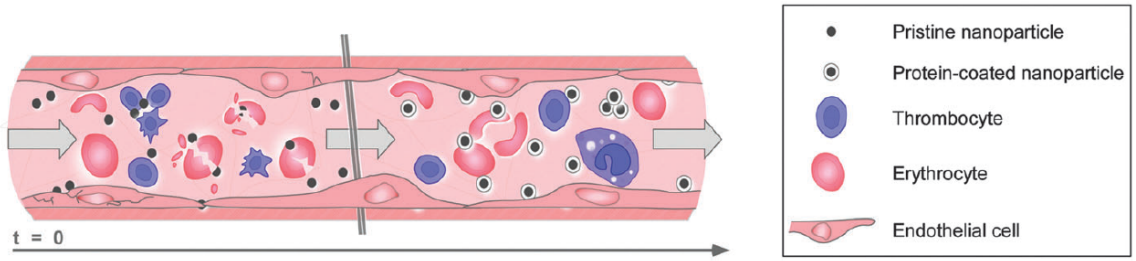

Fig. 8 Illustration of how rapid corona formation kinetically impacts early nanopathology in the human blood system. Upon entry or parenteral application, pristine NPs only exist for a short period of time, but are still capable of immediately affecting the vitality of endothelial cells, triggering thrombocyte activation and aggregation, and may also induce hemolysis. Formation of the biomolecule corona rapidly modulates the NPs' decoration with bioactive proteins protecting the cells of the blood system against nanoparticle-induced (patho)biological processes, and can also promote cellular uptake. Note, the elements are not drawn to scale.

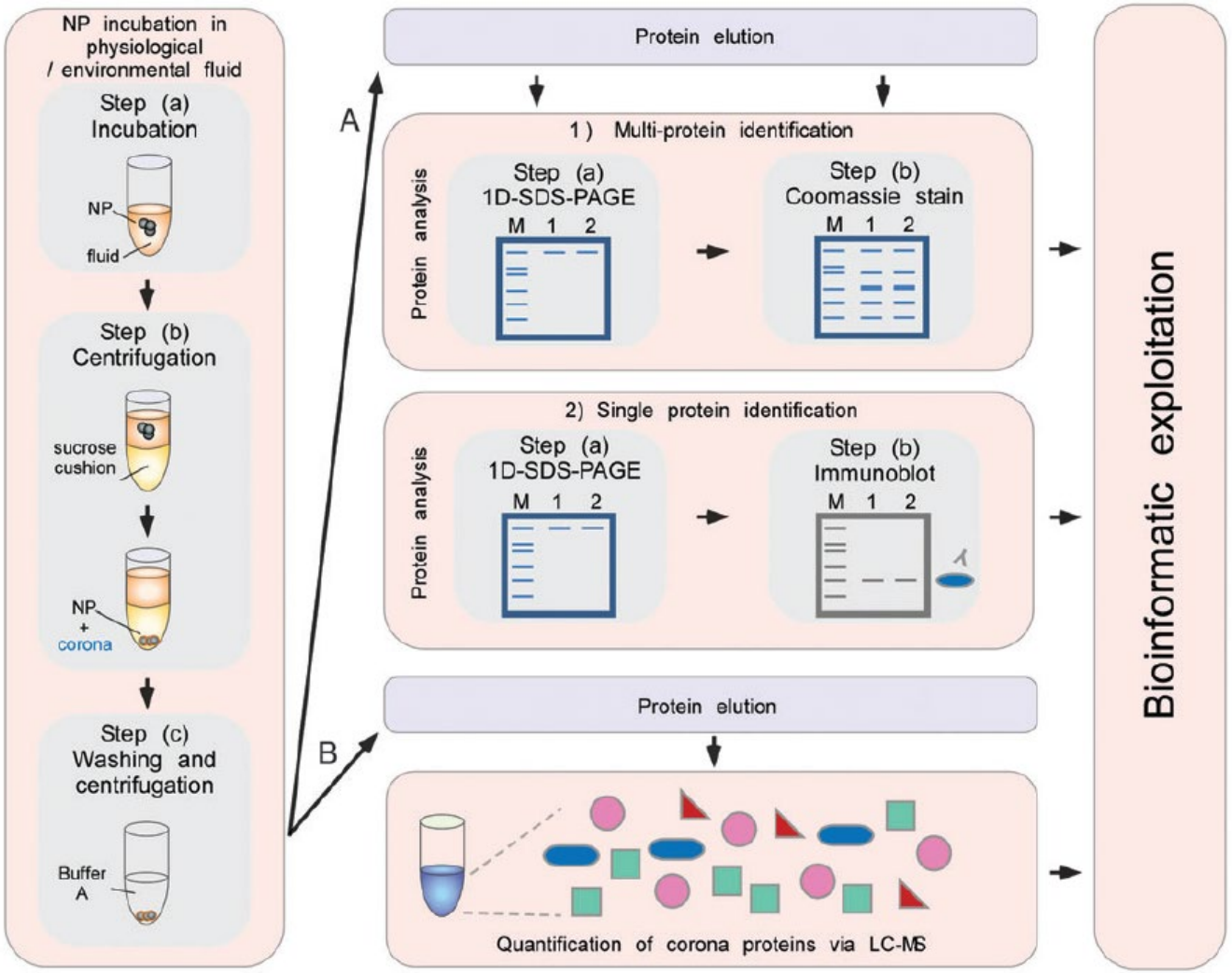
NP incubation in physiological / environmental fluid
Step (a) Incubation
NP
fluid
Step (b) Centrifugation
sucrose cushion
NP + corona
Step (c) Washing and centrifugation
Buffer A
A
B
Protein elution
1) Multi-protein identification
Protein analysis
Step (a) 1D-SDS-PAGE
M 1 2
Step (b) Coomassie stain
M 1 2
2) Single protein identification
Protein analysis
Step (a) 1D-SDS-PAGE
M 1 2
Step (b) Immunoblot
M 1 2
Protein elution
Quantification of corona proteins via LC-MS
Bioinformatic exploitation

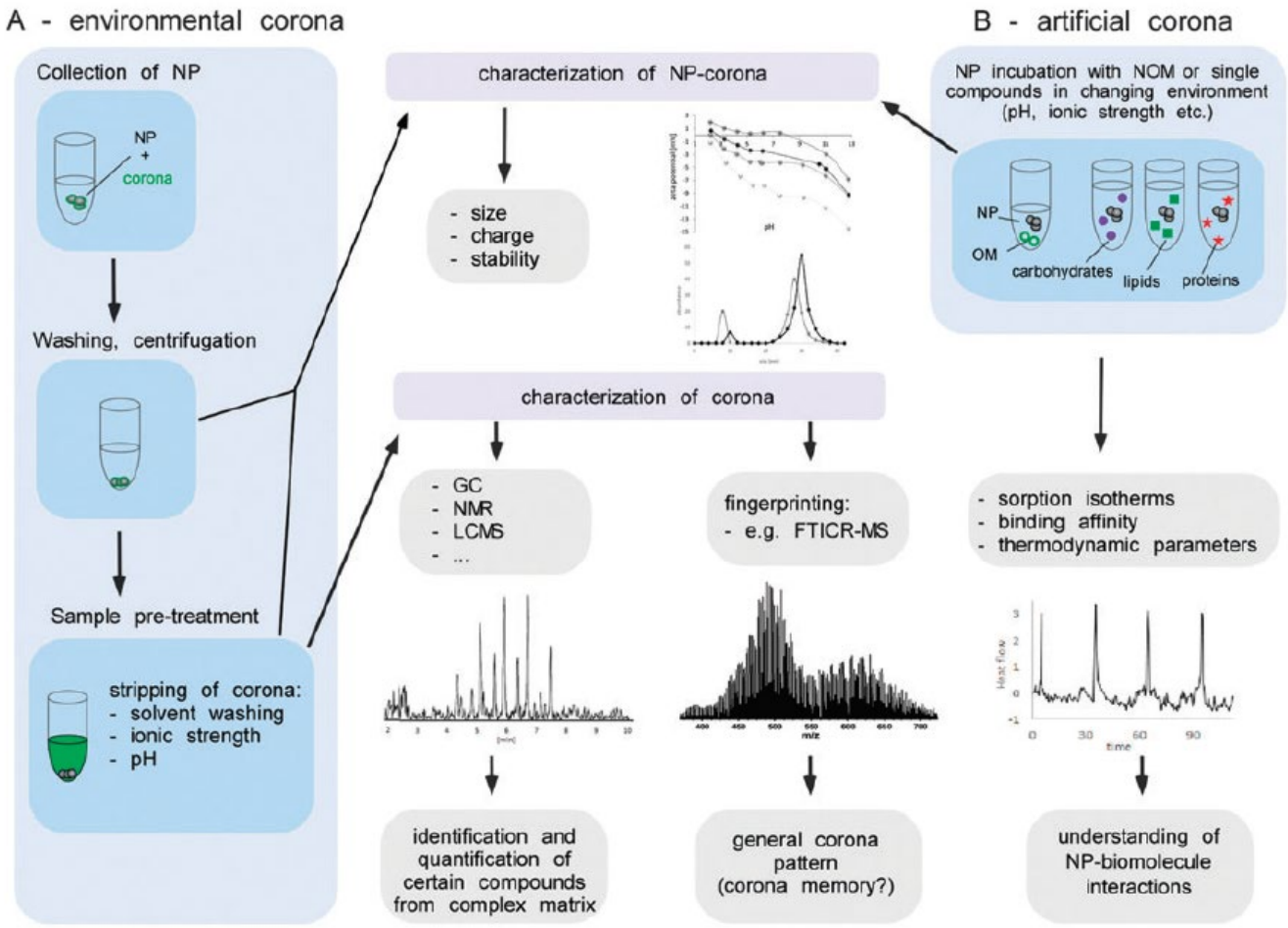
A - environmental corona
B - artificial corona
Collection of NP
NP
+
corona
Washing, centrifugation
Sample pre-treatment
stripping of corona:
- solvent washing
- ionic strength
- pH
characterization of NP-corona
- size
- charge
- stability
characterization of corona
- GC
- NMR
- LCMS
- ...
fingerprinting:
- e.g. FTICR-MS
identification and quantification of certain compounds from complex matrix
general corona pattern (corona memory?)
NP incubation with NOM or single compounds in changing environment (pH, ionic strength etc.)
NP
OM
carbohydrates
lipids
proteins
- sorption isotherms
- binding affinity
- thermodynamic parameters
understanding of NP-biomolecule interactions

Delivery Efficiency

< 1%ID

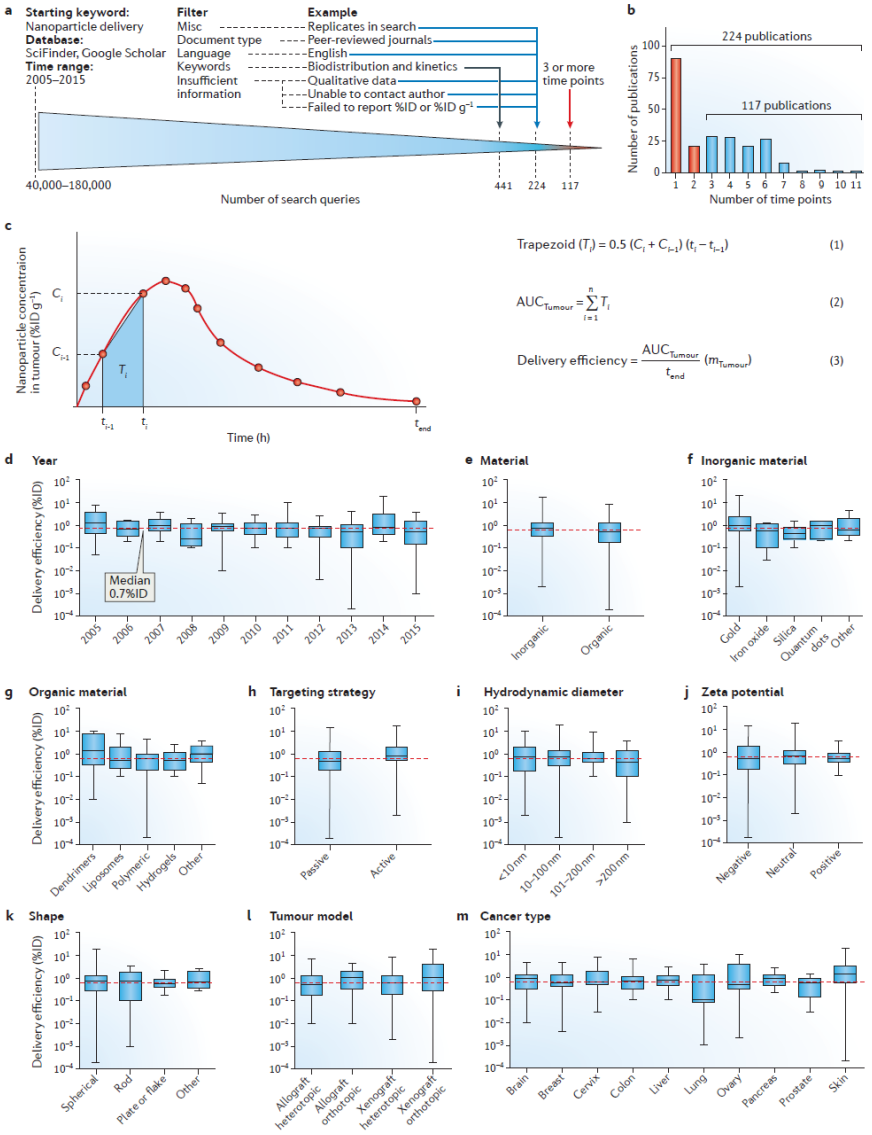

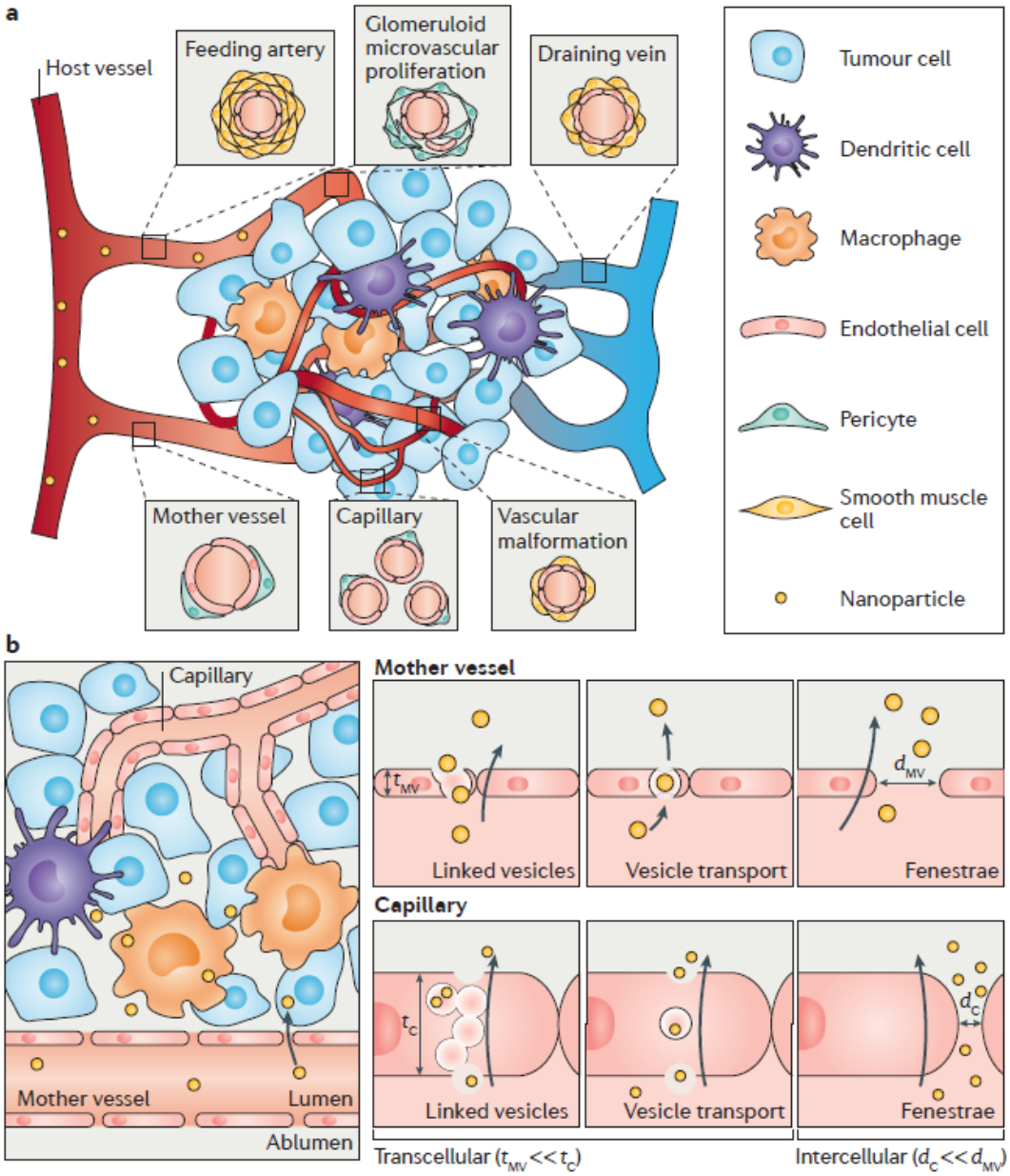
a
Host vessel
Feeding artery
Glomeruloid microvascular proliferation
Draining vein
Mother vessel
Capillary
Vascular malformation
Tumour cell
Dendritic cell
Macrophage
Endothelial cell
Pericyte
Smooth muscle cell
Nanoparticle
b
Capillary
Mother vessel
Lumen
Ablumen
Mother vessel
t_{MV}
Linked vesicles
Vesicle transport
d_{MV}
Fenestrae
Capillary
t_C
Linked vesicles
Vesicle transport
d_C
Fenestrae
Transcellular ($t_{MV} << t_C$)
Intercellular ($d_C << d_{MV}$)

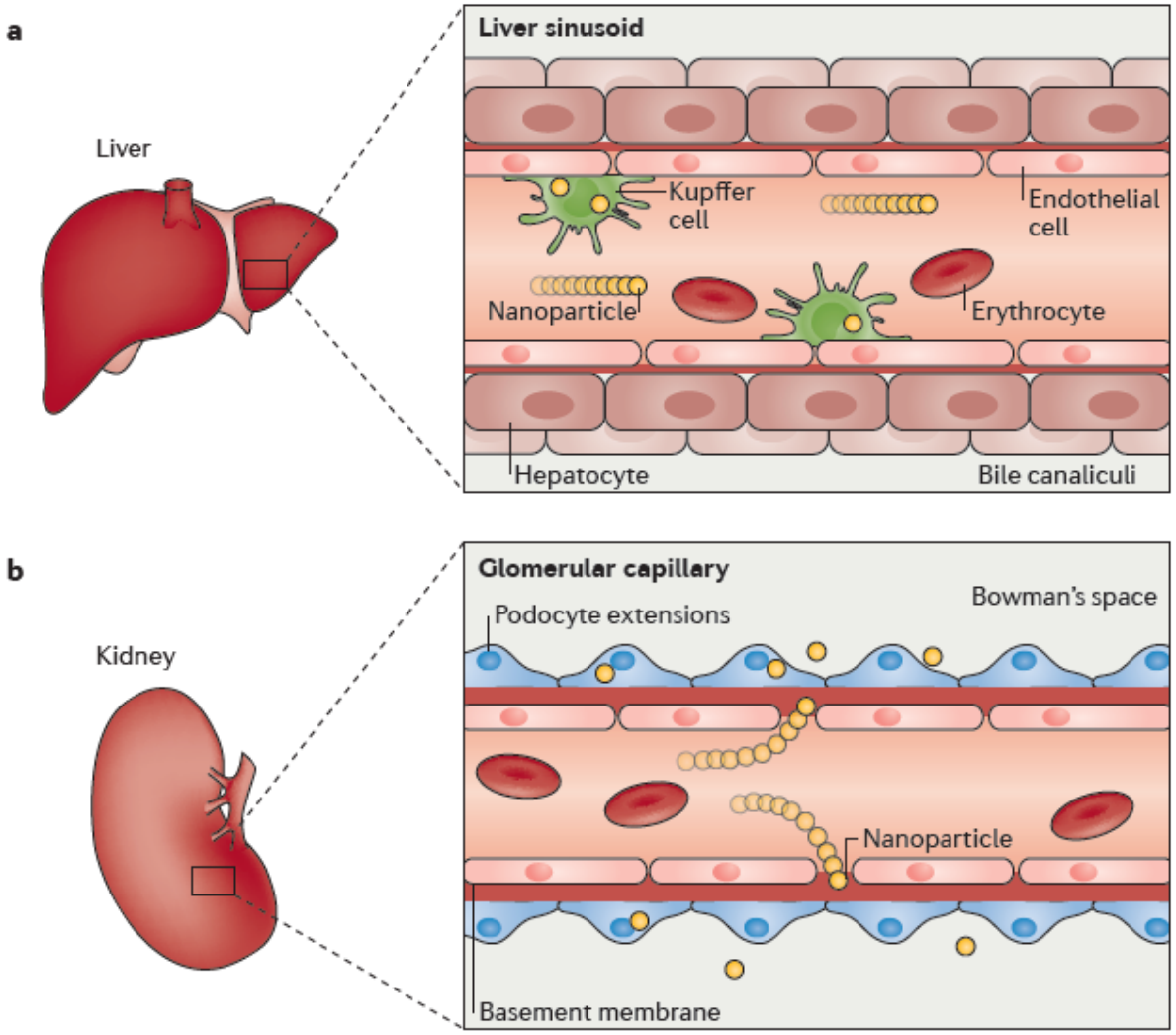

Figure 4 | **Mechanisms for nanoparticle elimination from the bloodstream. a** | The liver is the primary organ of the mononuclear phagocytic system that entraps a vast majority of the administered nanoparticle dose. Phagocytic cells, such as Kupffer cells, line the liver sinusoid. **b** | If the hydrodynamic diameter of a nanoparticle is smaller than 5.5 nm, it may be filtered from the blood via the kidneys and excreted in urine. Other major organs that are involved in the removal of nanoparticles from the bloodstream include the spleen, lymph nodes and the skin.

(A)

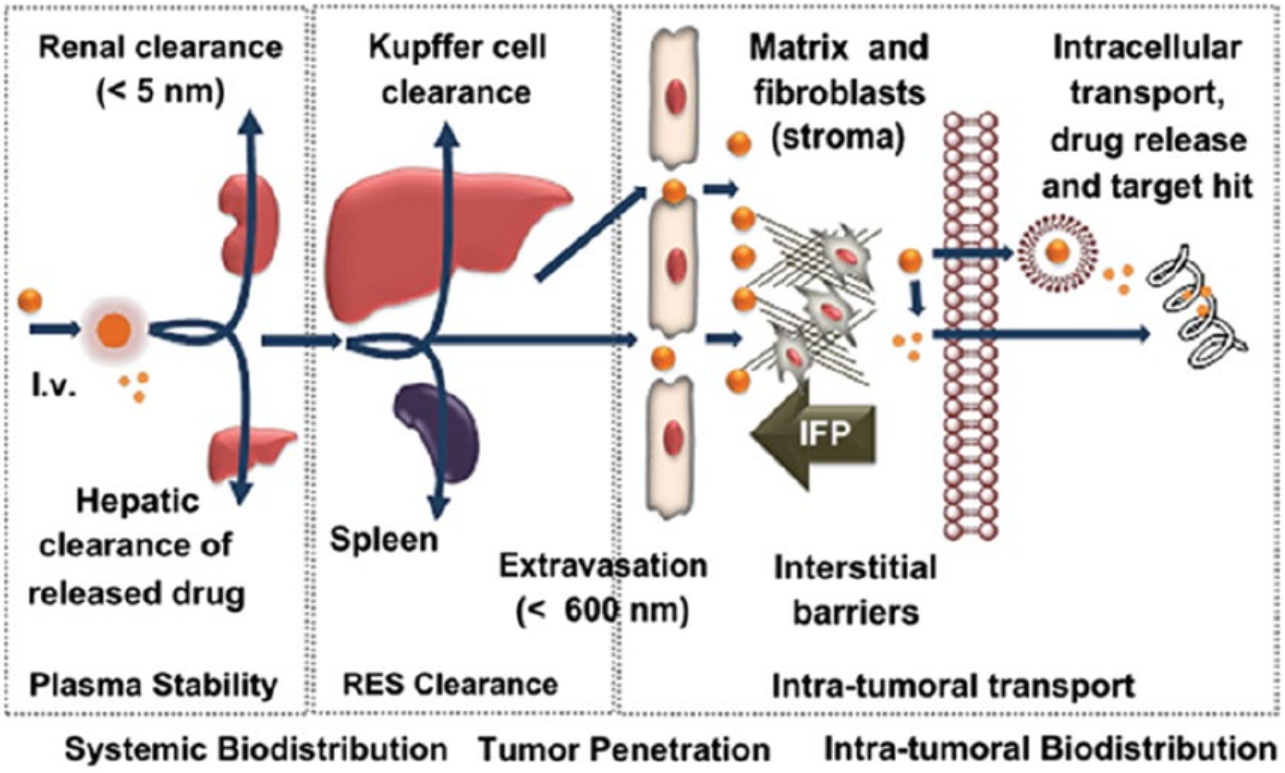
Renal clearance
(< 5 nm)
Kupffer cell
clearance
Matrix and
fibroblasts
(stroma)
Intracellular
transport,
drug release
and target hit
I.v.
IFP
Hepatic
clearance of
released drug
Spleen
Extravasation
(< 600 nm)
Interstitial
barriers
Plasma Stability
RES Clearance
Intra-tumoral transport
Systemic Biodistribution
Tumor Penetration
Intra-tumoral Biodistribution

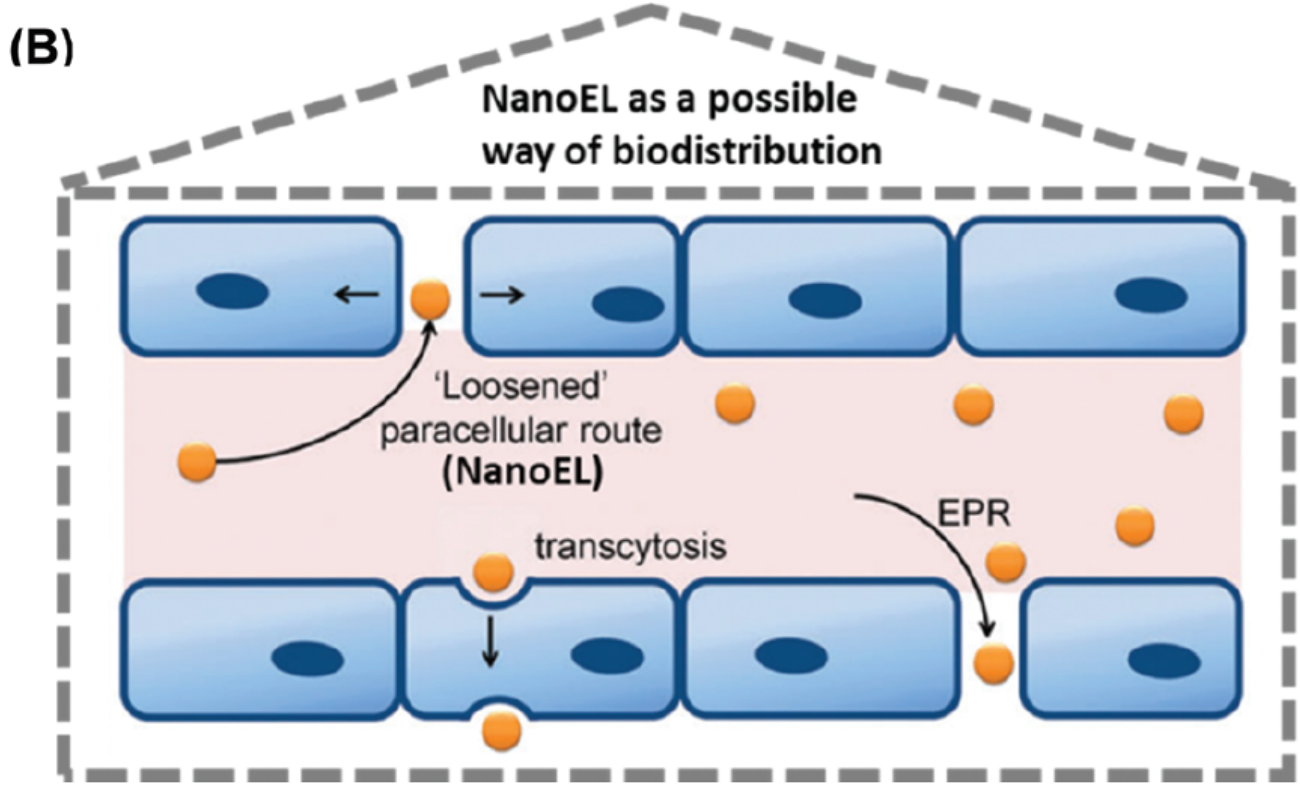

Fig. 1 Drug delivery by NPs are subjected to various factors that limit the overall dose of drugs reaching the target site. (A) These factors can be classified into three separate phases, namely, systemic biodistribution, tumor penetration and intra-tumoral biodistribution. Reproduced with permission from Ernsting *et al.*[24] Copyright 2013 Elsevier. (B) Nanomaterial-induced endothelial leakiness (NanoEL) may be viewed as an emerging strategy to improve the biodistribution of nanomedicine to target sites. Adapted from Setyawati *et al.*[25] with permission from the Royal Society of Chemistry 2015. IFP, interstitial fluid pressure.

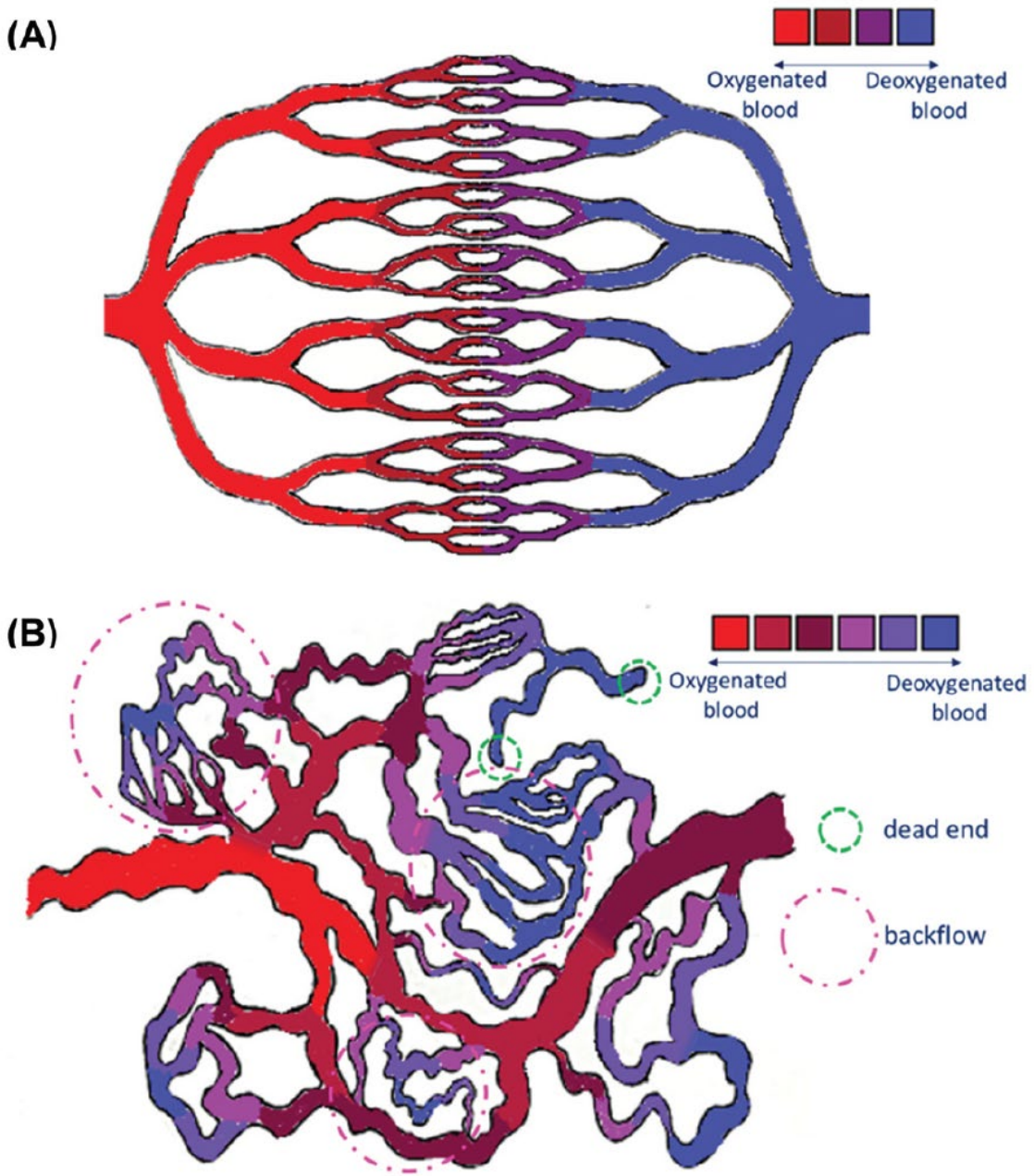
(A)
Oxygenated blood
Deoxygenated blood
(B)
Oxygenated blood
Deoxygenated blood
dead end
backflow

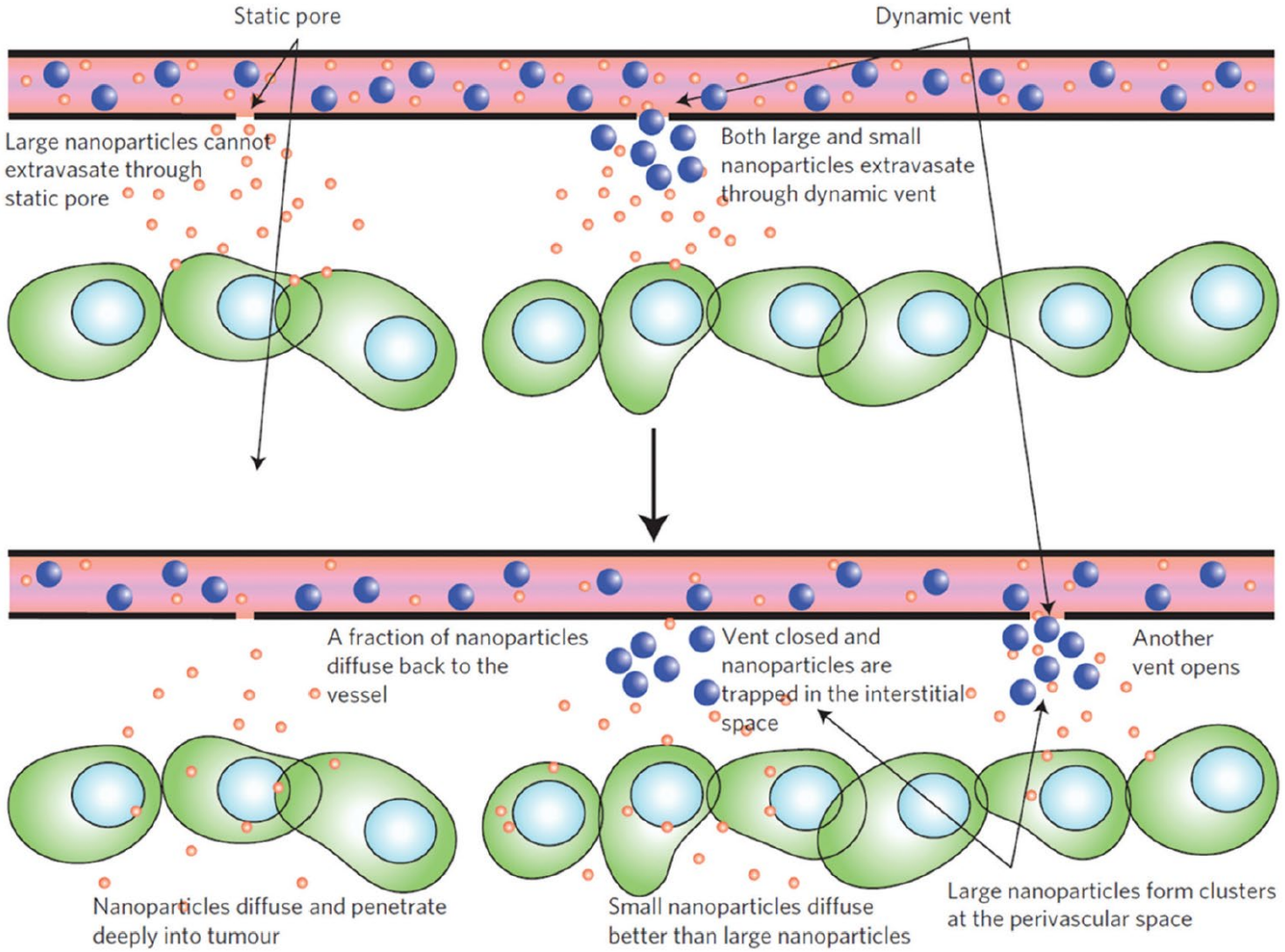

Fig. 3 Presence of static pores and dynamic vents in tumor vessels allows for NPs of differential permeability of NPs to penetrate through the vessel walls to reach the tumor sites. Predominantly for small NPs, static pores promote a deeper penetration of these NPs for a longer period of time. On the other hand, dynamic vents form transient openings which allow both small and large NPs to diffuse across the vessel walls, but over a shorter period of time. Reproduced with permission from Matsumoto *et al.*[107] Copyright 2016 Springer Nature.

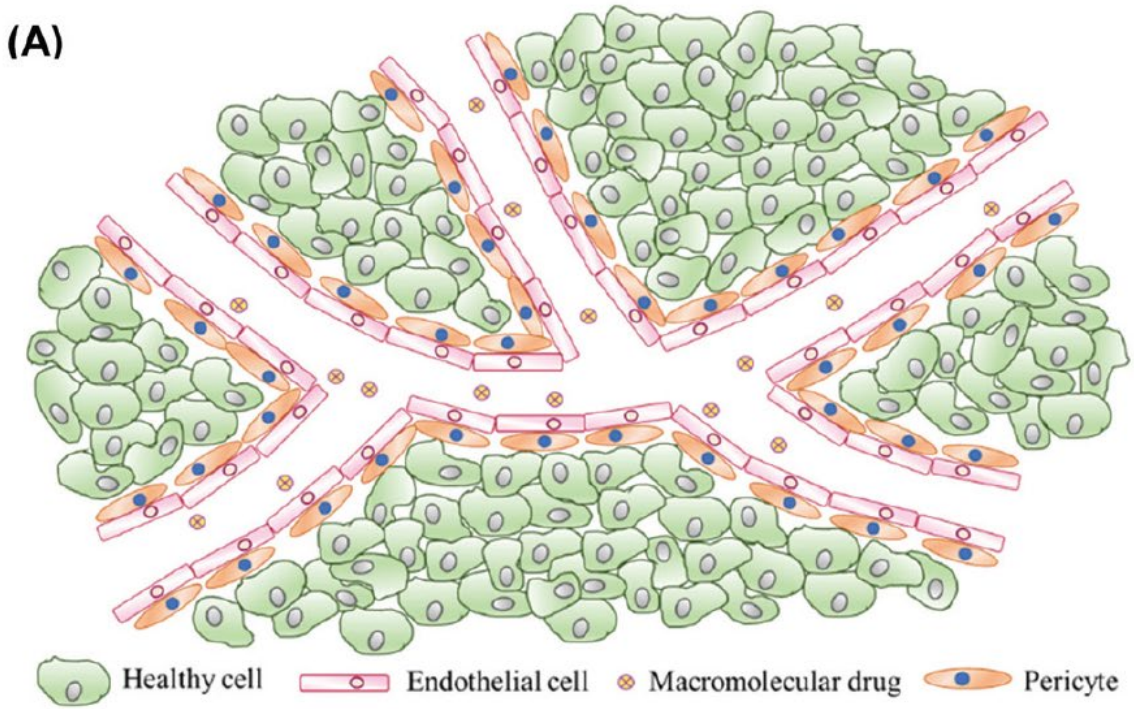
(A)
Healthy cell
Endothelial cell
Macromolecular drug
Pericyte

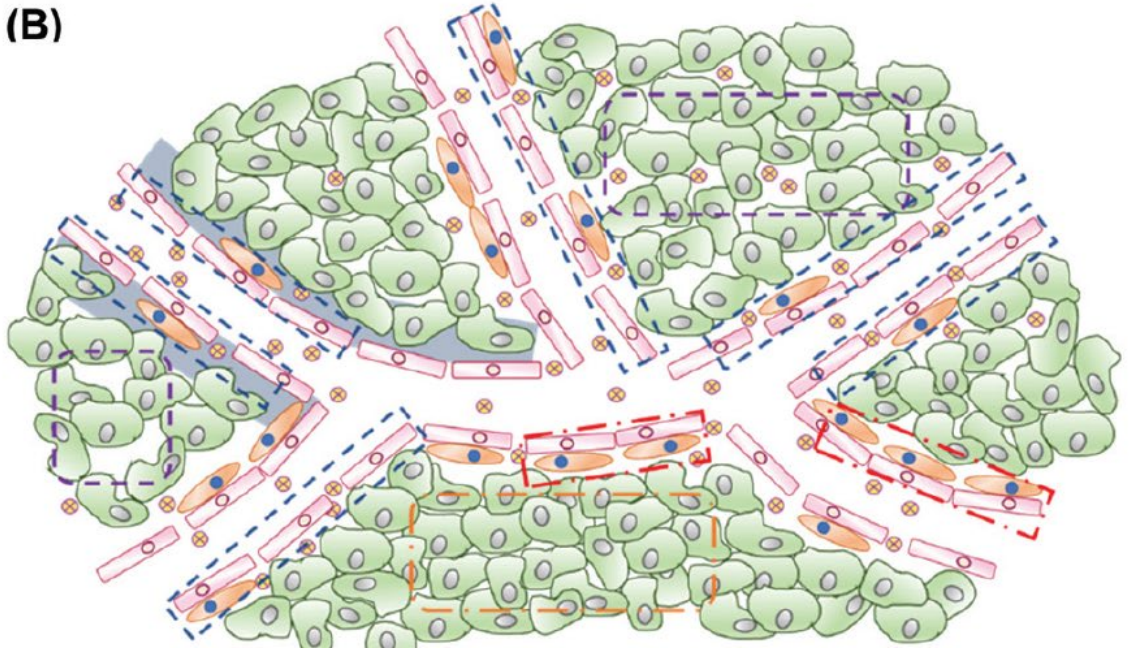
(B)

Renal clearance of quantum dots

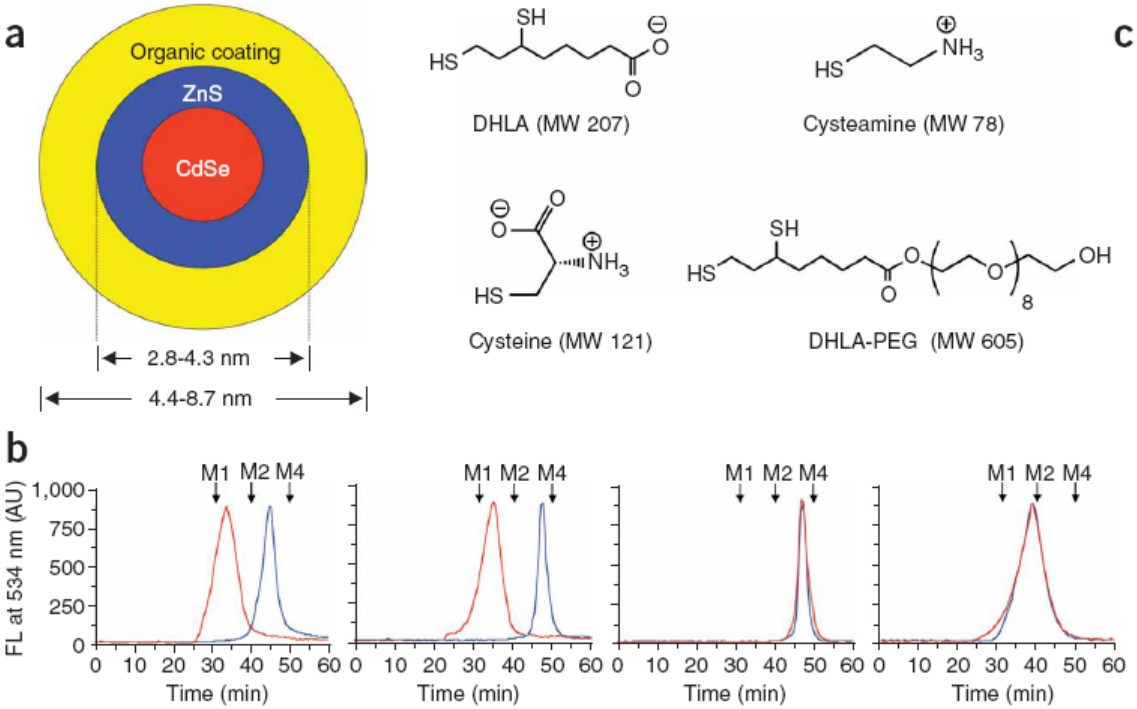

QD-Cys	Em Max (nm)	TEM Diameter (nm)	DLS		GFC
			HD (nm)	%PD	HD (nm)
QD515	515	2.85 ± 0.18	4.64 ± 0.08	20.9	4.36 ± 0.09
QD534	534	3.02 ± 0.20	4.91 ± 0.05	25.9	4.99 ± 0.18
QD554	554	3.30 ± 0.25	5.64 ± 0.01	13.1	5.52 ± 0.14
QD564	574	3.80 ± 0.20	6.40 ± 0.02	24.7	6.70 ± 0.33
QD574	584	4.31 ± 0.46	7.22 ± 0.20	24.8	8.65 ± 0.52

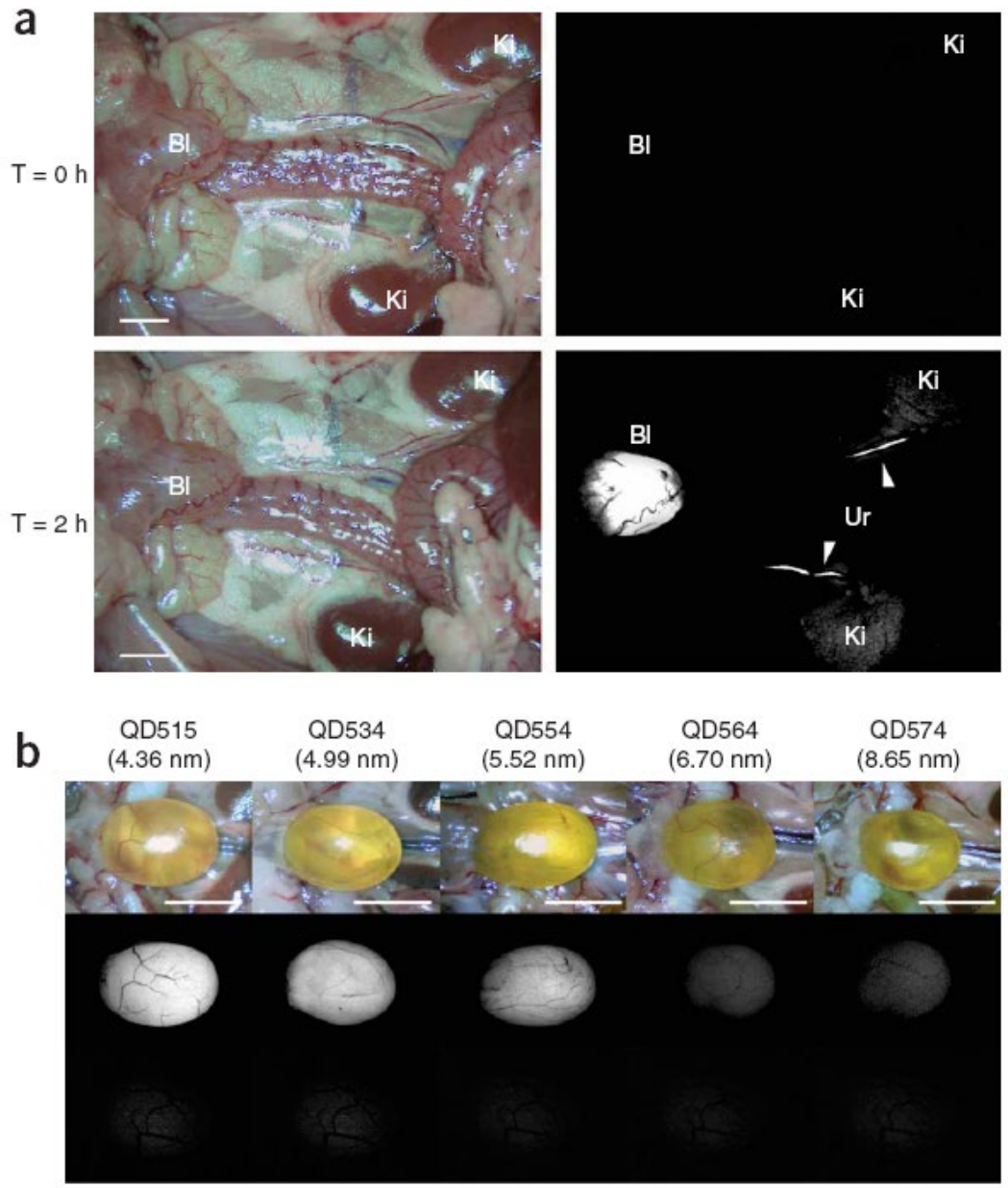

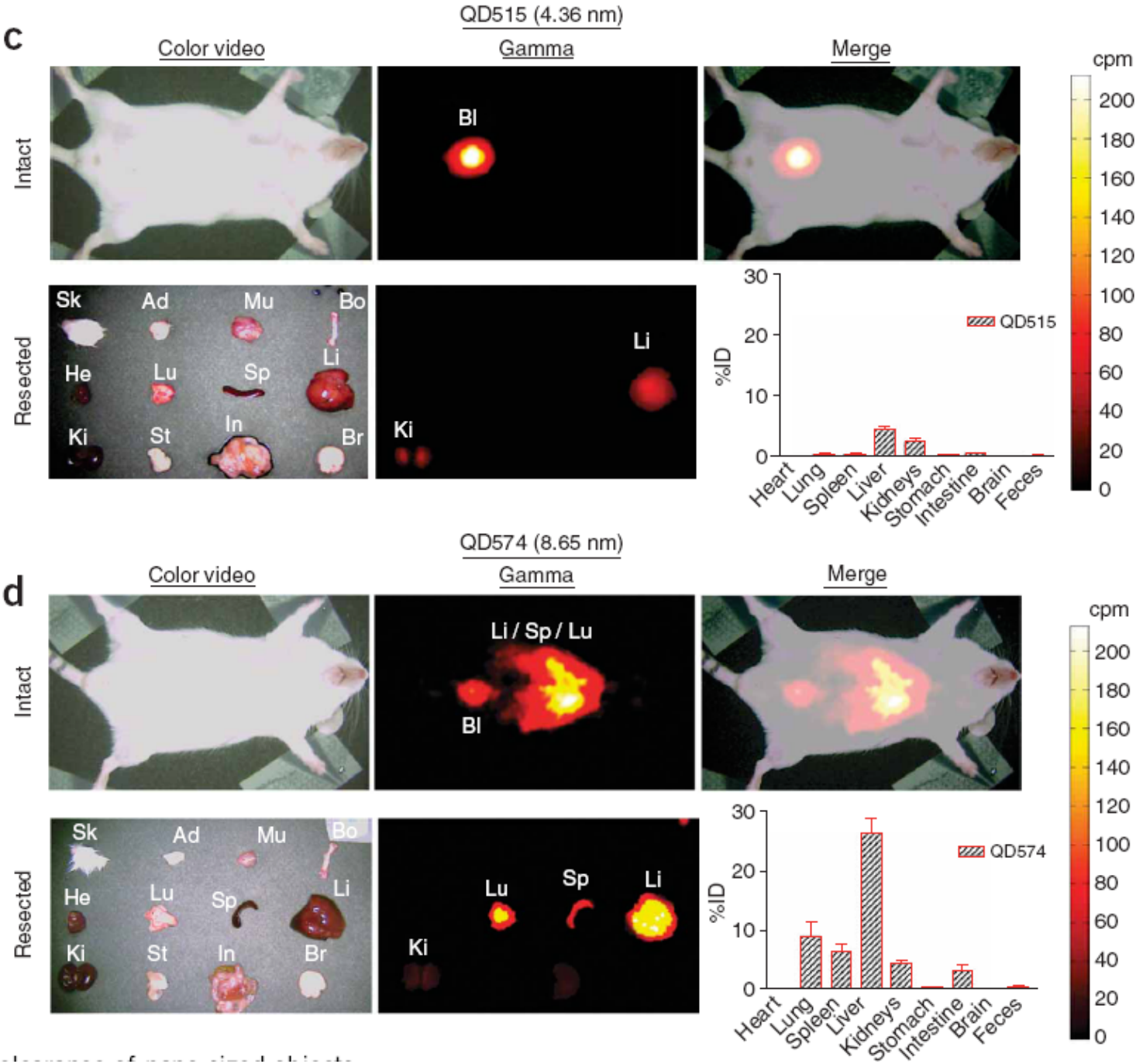
c
QD515 (4.36 nm)
Color video
Gamma
Merge
Intact
Resected
Bl
Sk
Ad
Mu
Bo
He
Lu
Sp
Li
Ki
St
In
Br
Li
Ki
%ID
30
20
10
0
QD515
Heart
Lung
Spleen
Liver
Kidneys
Stomach
Intestine
Brain
Feces
cpm
200
180
160
140
120
100
80
60
40
20
0
d
QD574 (8.65 nm)
Color video
Gamma
Merge
Intact
Resected
Li / Sp / Lu
Bl
Sk
Ad
Mu
Bo
He
Lu
Sp
Li
Ki
St
In
Br
Lu
Sp
Li
Ki
%ID
30
20
10
0
QD574
Heart
Lung
Spleen
Liver
Kidneys
Stomach
Intestine
Brain
Feces
cpm
200
180
160
140
120
100
80
60
40
20
0

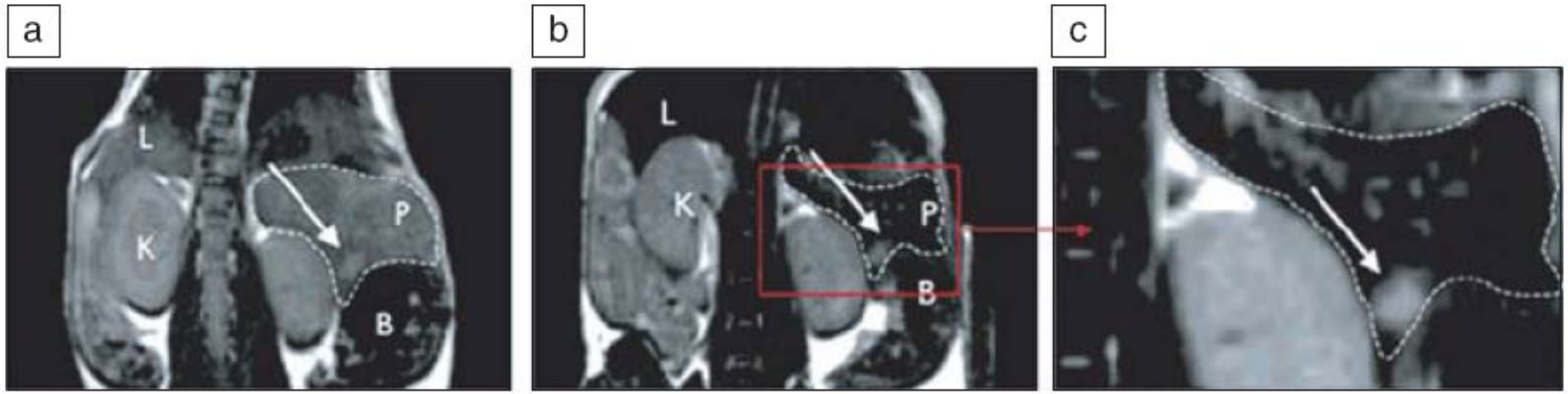

Figure 1. Cross-linked iron oxide (CLIO) nanoparticles for T_2-weighted images of rodent pancreatic cancer: (a) preinjection of CLIO, (b) postinjection of CLIO, and (c) higher magnification of postinjection image with the arrow indicating tumor. L, liver; P, pancreas; K, kidney; B, bowel.[16]

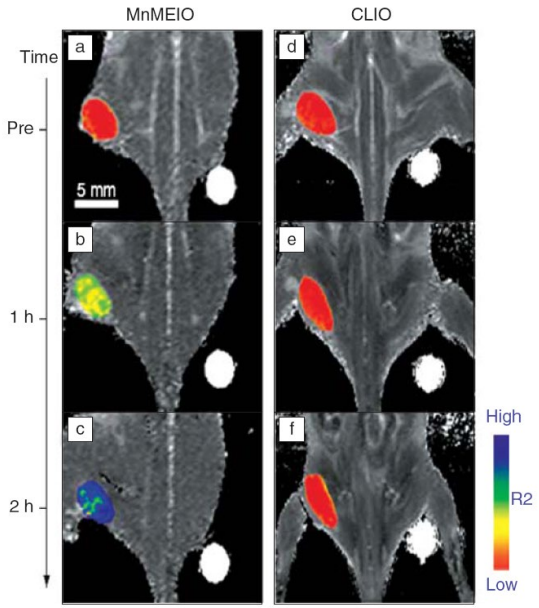

Figure 2. *In vivo* magnetic resonance detection of cancer after administration of magnetic nanoparticles Herceptin conjugates. $MnFe_2O_4$ nanoparticles (MnMEIO) (a–c) show higher signal enhancement than cross-linked iron oxide (CLIO) (d–f).[24] R2, inverse of transverse relaxation time.

Liposome

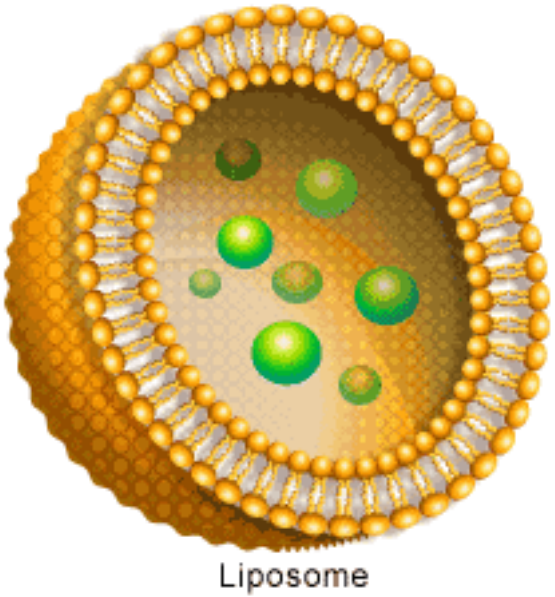

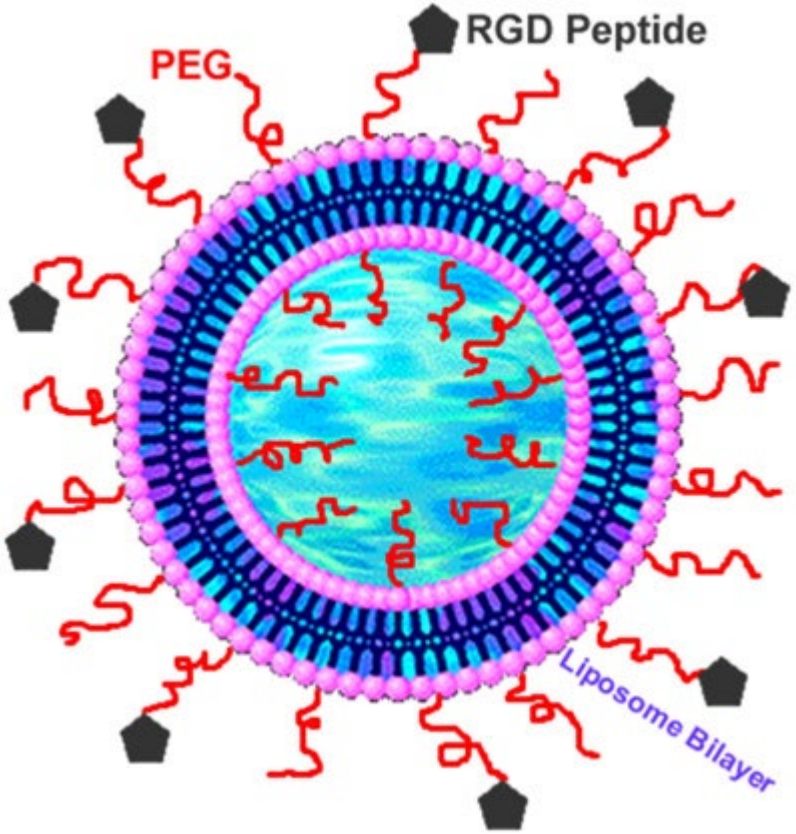

Cationic Lipids

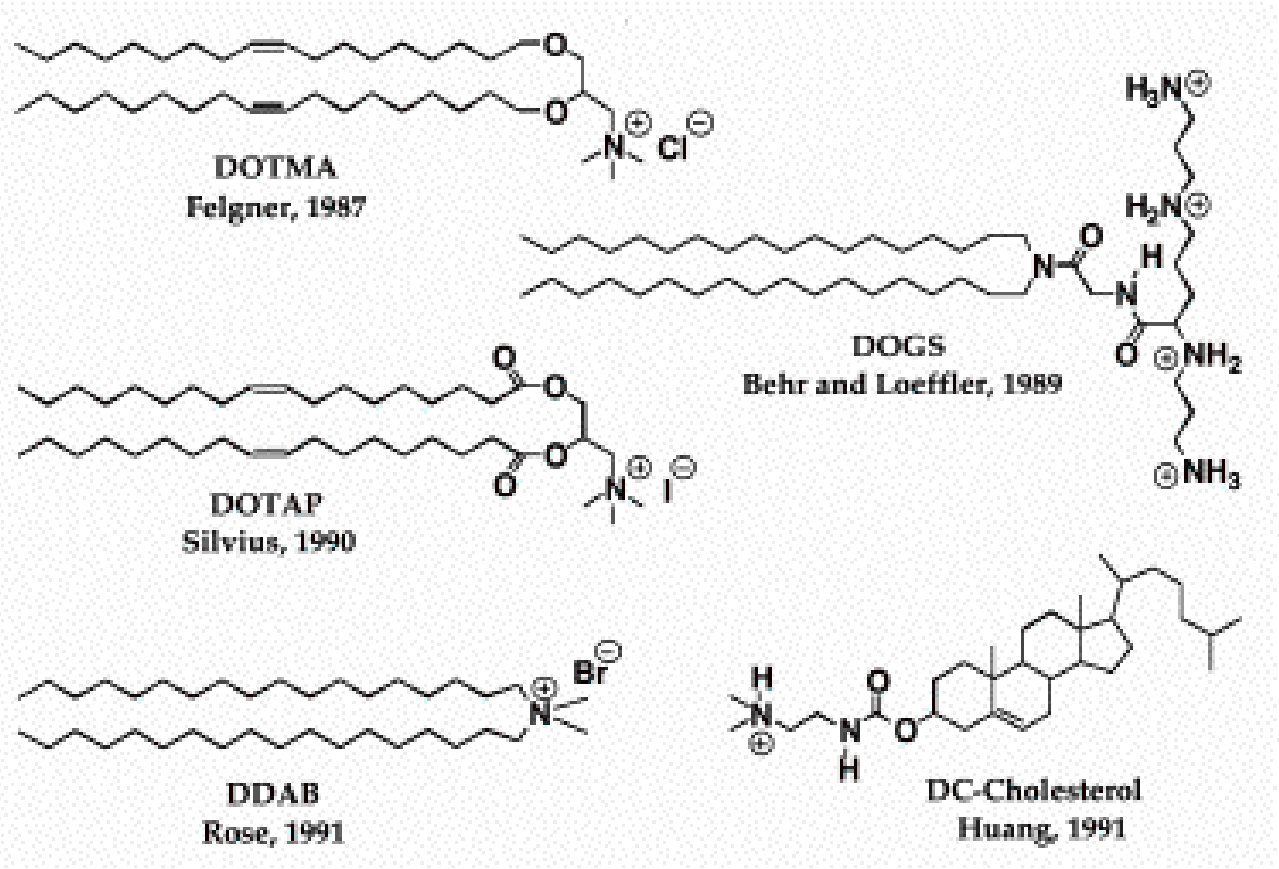

Lipid Nanoparticle for Vaccine

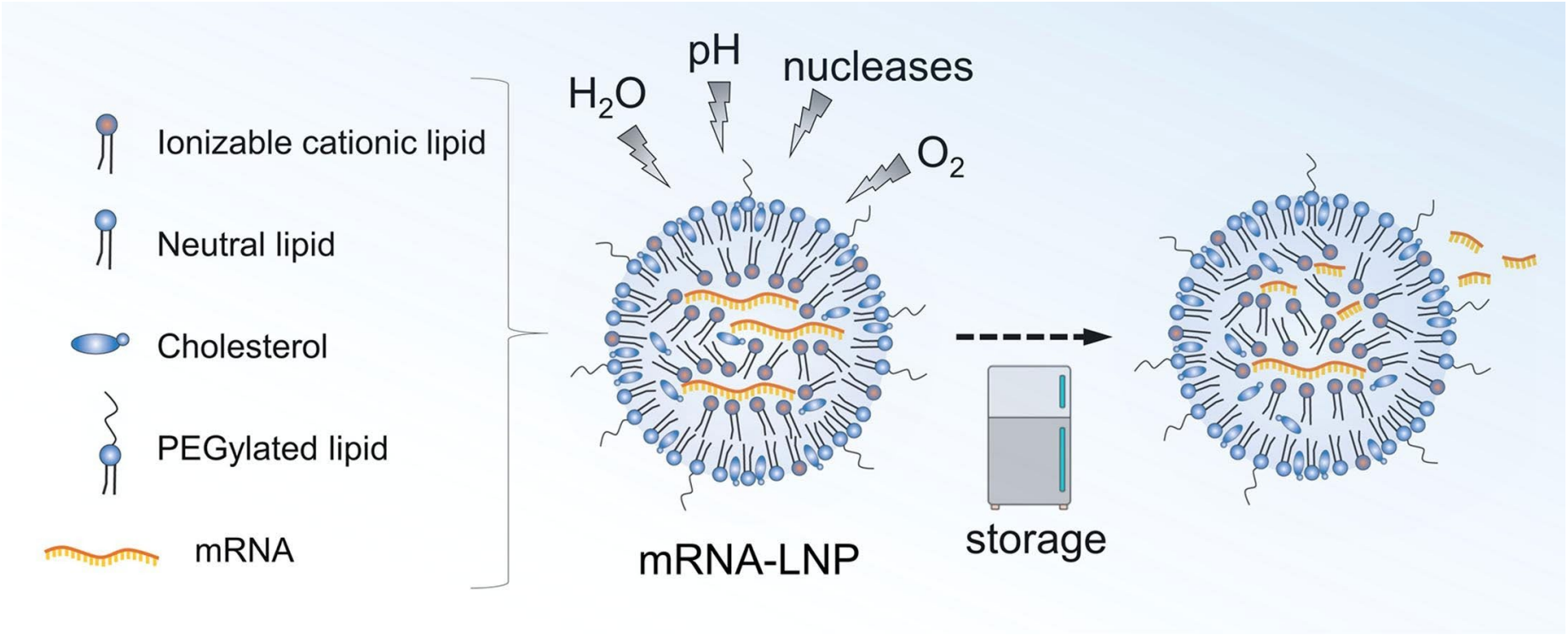

nature nanotechnology

REVIEW ARTICLE

https://doi.org/10.1038/s41565-020-0759-5

Check for updates

A framework for designing delivery systems

Wilson Poon[1,2,7], Benjamin R. Kingston[1,2,7], Ben Ouyang[1,2,3], Wayne Ngo[1,2] and Warren C. W. Chan[1,2,4,5,6] ✉

NATURE NANOTECHNOLOGY | VOL 15 | OCTOBER 2020 | 819–829

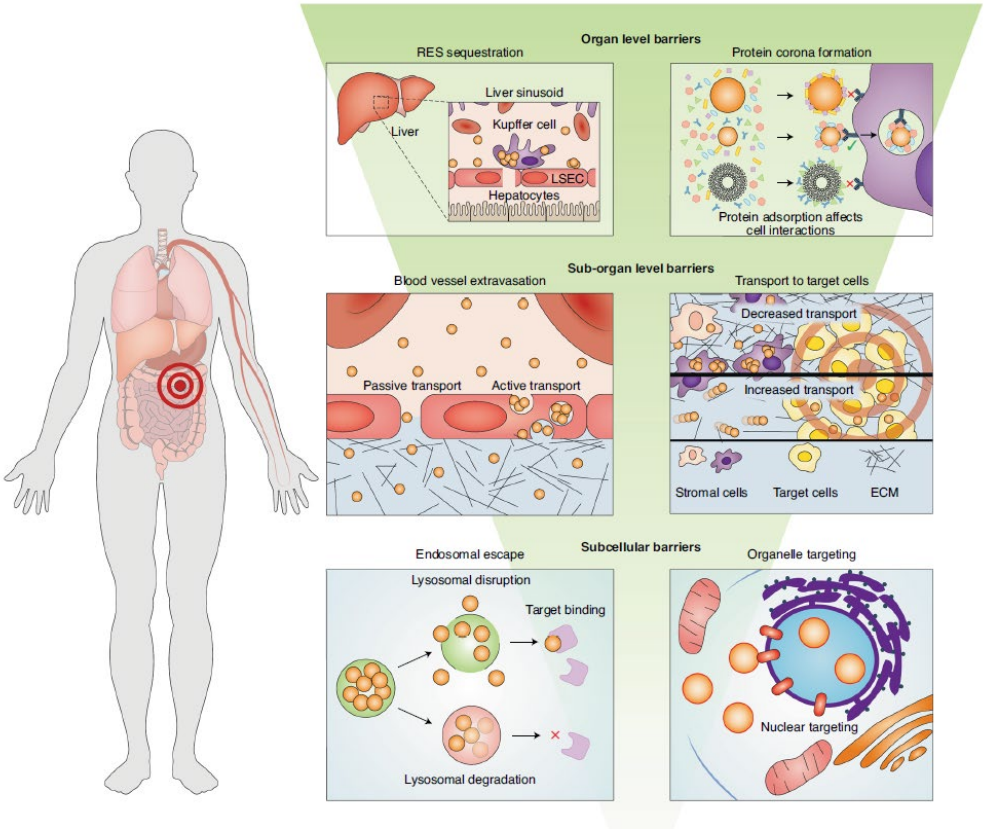

a

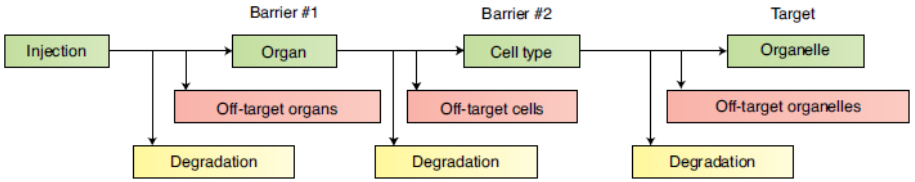

b

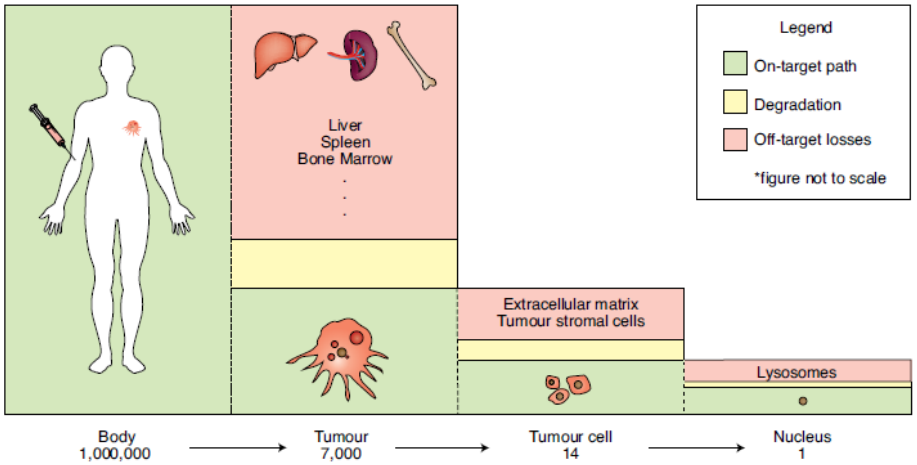

c

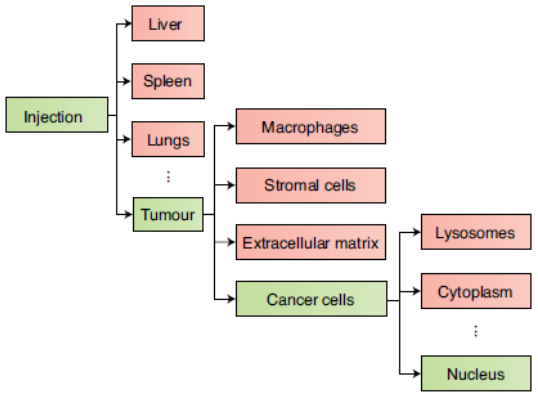

Barriers needed to be overcome

Therapeutic target	Therapeutic example	Blood	RES organs	Tumour endothelium	Tumour ECM	Tumour stromal cells	Tumour cell lysosomes	Tumour cell nucleus
Tumour endothelium	P-selectin for anti-metastases	×	×					
Tumour ECM	Hyaluronidase/MMP treatment	×	×	×				
Cancer cell surface	Herceptin/Bi-specific T cell engagers	×	×	×	×	×		
Cancer cell cytoplasm	RNA interference	×	×	×	×	×	×	
Cancer cell DNA	Doxorubicin	×	×	×	×	×	×	×

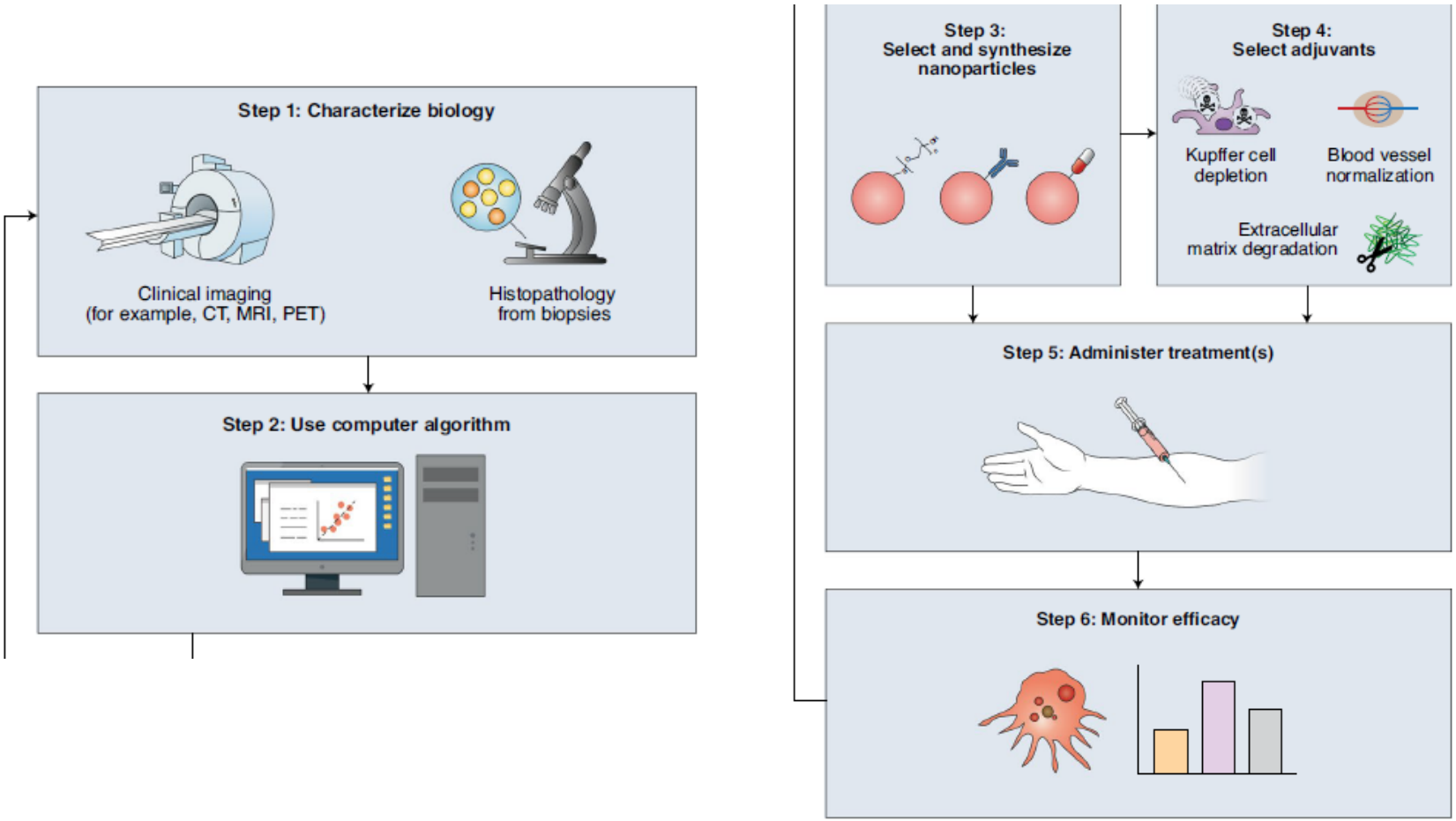
Step 1: Characterize biology
Clinical imaging
(for example, CT, MRI, PET)
Histopathology
from biopsies
Step 2: Use computer algorithm
Step 3:
Select and synthesize
nanoparticles
Step 4:
Select adjuvants
Kupffer cell
depletion
Blood vessel
normalization
Extracellular
matrix degradation
Step 5: Administer treatment(s)
Step 6: Monitor efficacy

Table 1 | Critical questions for designing nanoparticle delivery systems

Question	Rationale for the question
(1) Where is the delivery target?	The specific biological target (organ or tissue, cell type and subcellular location) defines design of the nanoparticle strategy.
(2) What is the cargo or active agent that needs to be delivered to the target location?	This defines the chemistry for incorporating the agents into the nanoparticle for delivery.
(3) Where is the site of administration?	The location of administration and the delivery target location define the delivery pathway.
(4) What are the specific organs, tissues and cells encountered along the delivery pathway?	This defines the barriers that the nanoparticle will encounter.
(5) What are the interactions between the nanoparticle carrier and the body in each of these biological environments along the delivery pathway?	These interactions will determine if the formulation is degraded or sequestered before it can reach its intended target location.
(6) What strategies are available to overcome the barriers at each step in the delivery pathway?	This allows the development of specific strategies to overcome the barriers.
(7) How will any administered components leave the disease site and be excreted from the body?	This helps to define locations of toxicity and elimination routes.

nature nanotechnology

PERSPECTIVE

https://doi.org/10.1038/s41565-019-0567-y

Smart cancer nanomedicine

NATURE NANOTECHNOLOGY | VOL 14 | NOVEMBER 2019 | 1007–1017 |

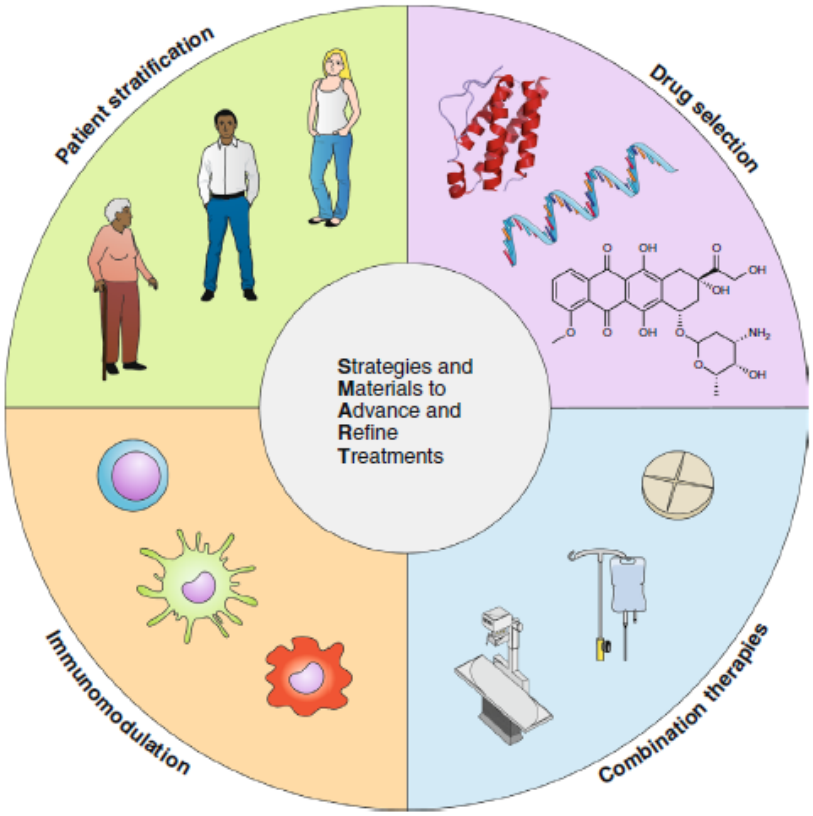

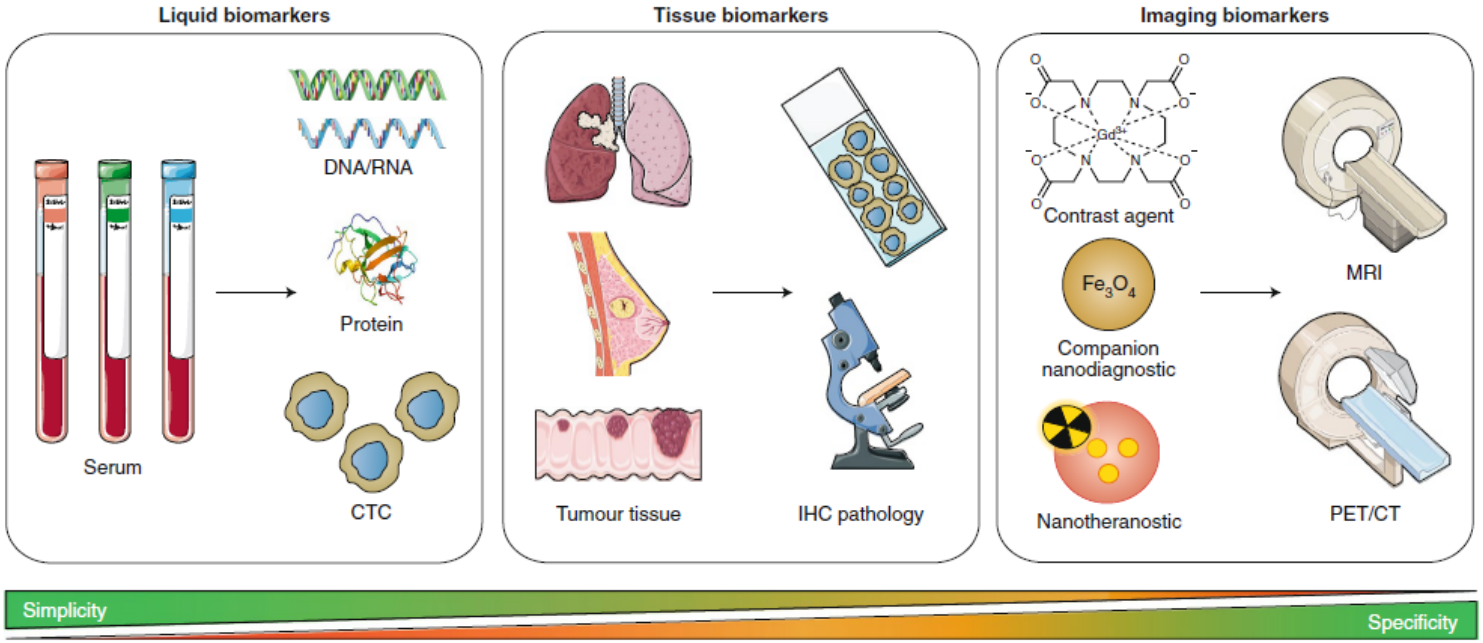
Liquid biomarkers
DNA/RNA
Protein
Serum
CTC
Tissue biomarkers
Tumour tissue
IHC pathology
Imaging biomarkers
Contrast agent
MRI
Fe_3O_4
Companion nanodiagnostic
Nanotheranostic
PET/CT
Simplicity
Specificity

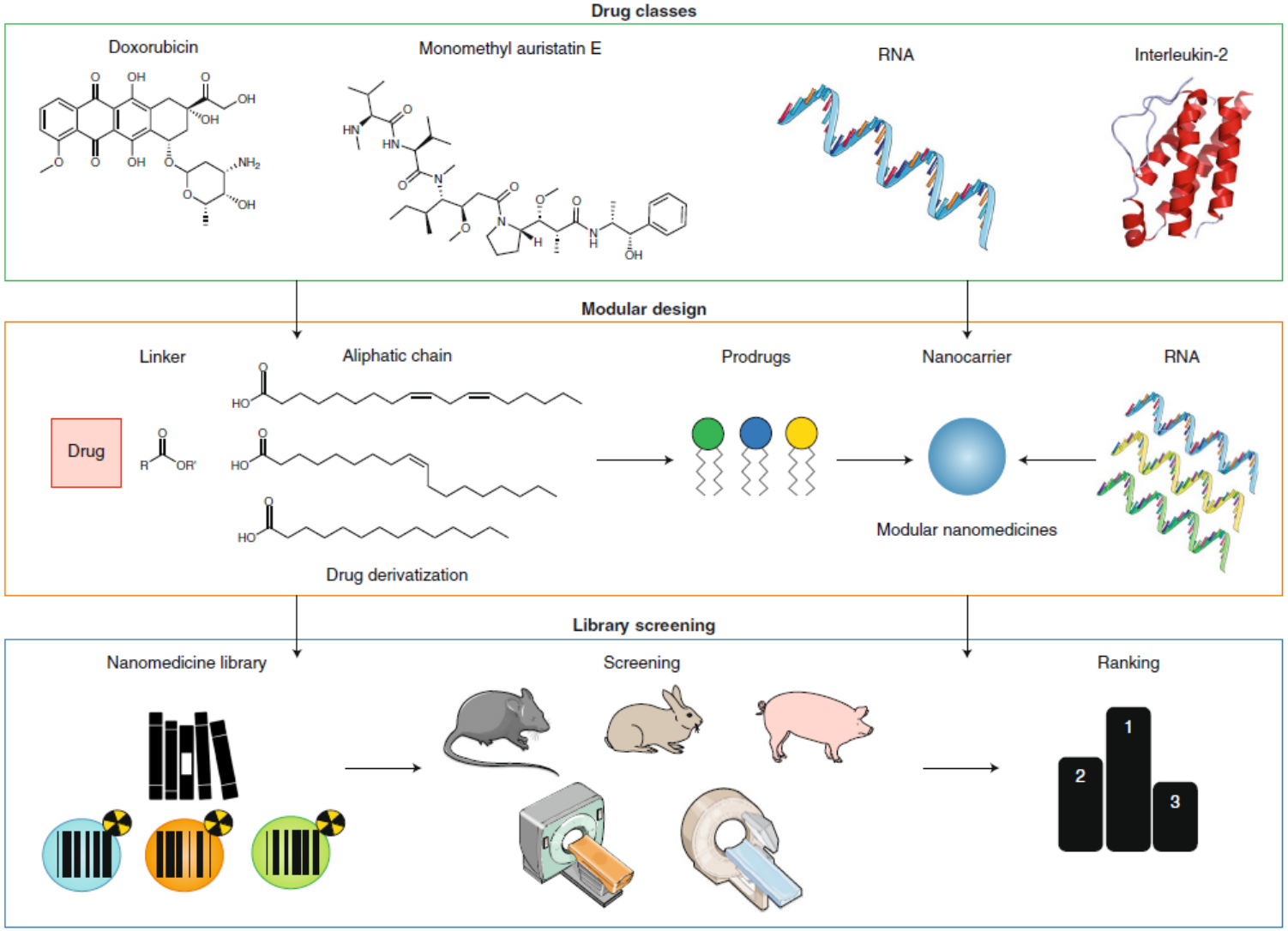
Drug classes
Doxorubicin
Monomethyl auristatin E
RNA
Interleukin-2
Modular design
Linker
Aliphatic chain
Prodrugs
Nanocarrier
RNA
Drug
Drug derivatization
Modular nanomedicines
Library screening
Nanomedicine library
Screening
Ranking
1
2
3

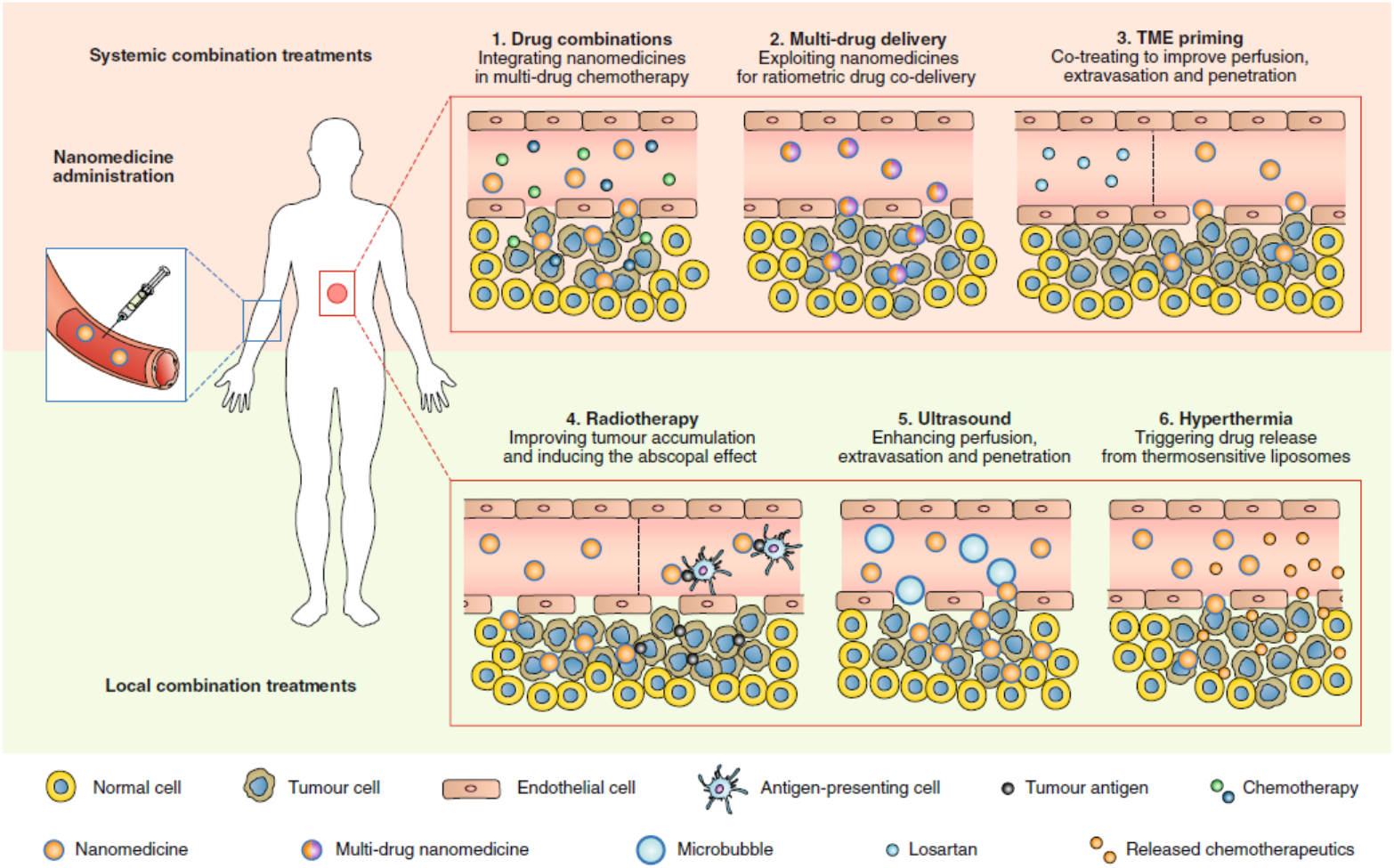
Systemic combination treatments
Nanomedicine administration
1. Drug combinations
Integrating nanomedicines in multi-drug chemotherapy
2. Multi-drug delivery
Exploiting nanomedicines for ratiometric drug co-delivery
3. TME priming
Co-treating to improve perfusion, extravasation and penetration
4. Radiotherapy
Improving tumour accumulation and inducing the abscopal effect
5. Ultrasound
Enhancing perfusion, extravasation and penetration
6. Hyperthermia
Triggering drug release from thermosensitive liposomes
Local combination treatments
Normal cell
Tumour cell
Endothelial cell
Antigen-presenting cell
Tumour antigen
Chemotherapy
Nanomedicine
Multi-drug nanomedicine
Microbubble
Losartan
Released chemotherapeutics

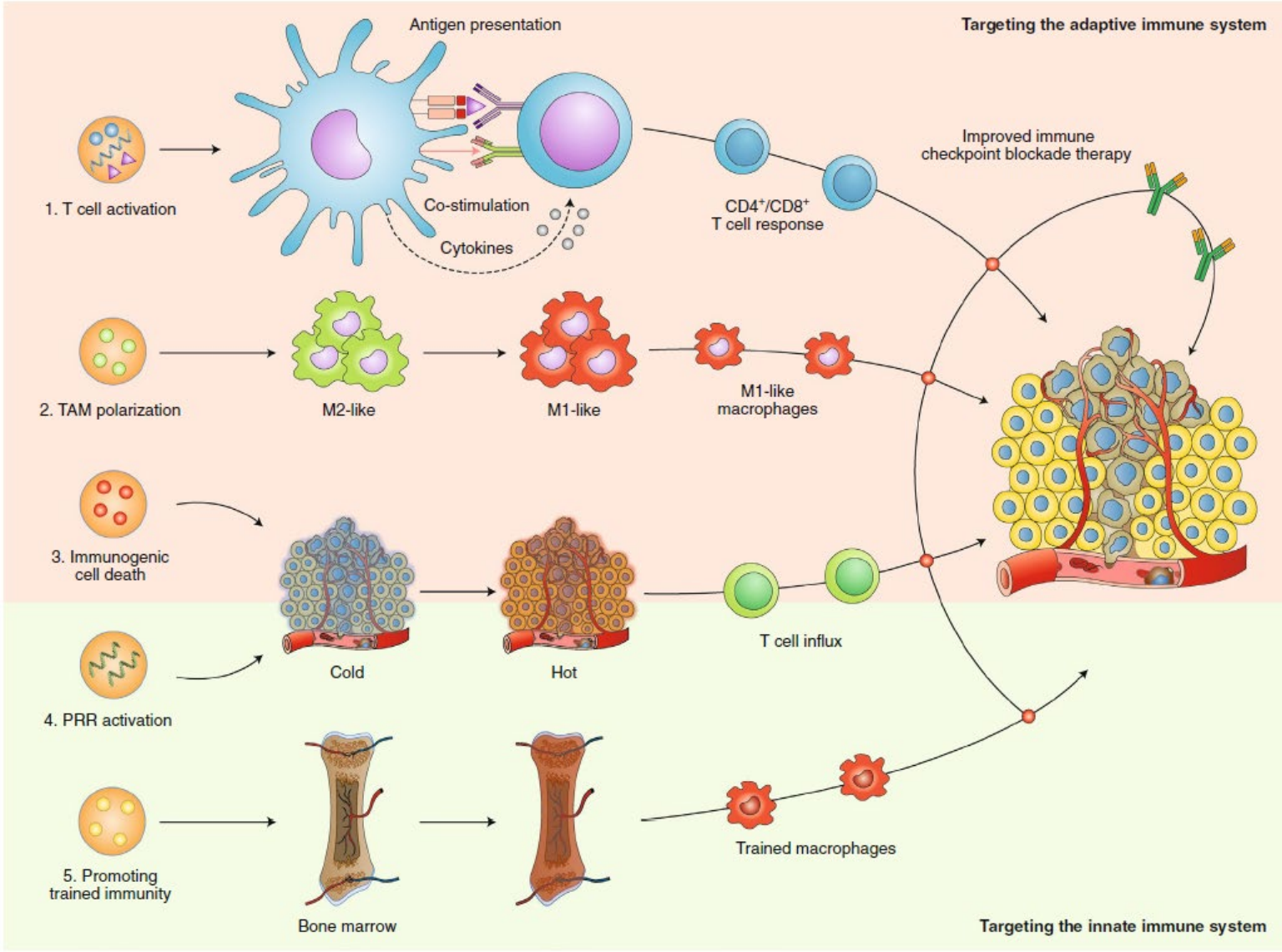
Antigen presentation
Targeting the adaptive immune system
1. T cell activation
Co-stimulation
Cytokines
CD4+/CD8+
T cell response
Improved immune
checkpoint blockade therapy
2. TAM polarization
M2-like
M1-like
M1-like
macrophages
3. Immunogenic
cell death
Cold
Hot
T cell influx
4. PRR activation
5. Promoting
trained immunity
Bone marrow
Trained macrophages
Targeting the innate immune system